306318855$

# Investigating the Mechanisms Responsible for DNA Double-Strand Break-Induced Loss of Heterozygosity in Fission Yeast.

A thesis presented for the degree of
Doctor of Philosophy (D. Phil).
University of Oxford.

Jason Kingsley Cullen
MRC, Radiation and Oncobiology Unit, Harwell
and
Wolfson College, University of Oxford.







**Trinity Term, 2007**



**ACKNOWLEDGEMENTS.** ..... **6**
**ABSTRACT** ..... **7**
**NOMENCLATURE** ..... **8**
**ABBREVIATIONS** ..... **9**
**LIST OF TABLES.** ..... **11**
**LIST OF FIGURES.** ..... **13**

**1. INTRODUCTION** .....

**1.1. GENOME INSTABILITY AND CANCER.** ..... **17**
1.1.1. Loss of heterozygosity (LOH) and cancer. ..... 19
**1.2. DNA DOUBLE-STRAND BREAK FORMATION** ..... **20**
1.2.1. Endogenous and exogenous causes of DSBs. ..... 20
1.2.2. Enzymatically induced DSBs. ..... 24
**1.3. MECHANISMS OF DSB REPAIR.** ..... **26**
1.3.1. HOMOLOGOUS RECOMBINATION (HR) REPAIR. ..... 26
1.3.1.1. Gene conversion (GC). ..... 27
1.3.1.2. Single-strand annealing (SSA) ..... 32
1.3.1.3. Break-induced replication (BIR) ..... 34
1.3.2. GENES AND PROTEINS INVOLVED IN HR. ..... 37
1.3.2.1. The MRX(N) complex and Exo1 ..... 37
1.3.2.2. The *RAD51*, *RAD52*, *RAD54*, *RDH54*, *RAD55*, *RAD57*, *RAD59* subfamily and RPA. ..... 42
1.3.2.3. Srs2/RecQ helicases. ..... 51
1.3.3. NON-HOMOLOGOUS END JOINING (NHEJ) ..... 53
1.3.4. GENES AND PROTEINS INVOLVED IN NHEJ. ..... 54
**1.4. THE DNA INTEGRITY CHECKPOINTS.** ..... **57**
**1.5. CELL CYCLE REGULATION OF REPAIR MECHANISM** ..... **58**
**1.6. TELOMERES, TELOMERASE AND DSBS.** ..... **62**
1.6.1. Telomere structure and maintenance. ..... 62
1.6.2. *De novo* telomere addition. ..... 65
**1.7. THE CH$^{16}$-MGH SYSTEM** ..... **69**
**1.8. AIM OF WORK** ..... **71**

**2. MATERIALS AND METHODS.** .....

**2.1. GENERAL LABORATORY SUPPLIES.** ..... **73**
2.1.1. Chemical reagents, kits and equipment. ..... 73
2.1.2. Buffers and solutions. ..... 73
**2.2. MEDIA.** ..... **75**
2.2.1. Escherichia coli (E. coli) media. ..... 75
2.2.2. Schizosaccharomyces pombe (*S. pombe*) media and solutions. ..... 75
**2.3. PLASMIDS.** ..... **77**
**2.4. STRAINS.** ..... **77**
2.4.1. *E. coli.* ..... 77
2.4.2. *S. pombe.* ..... 77
**2.5. EXPERIMENTAL PROCEDURES.** ..... **79**
**2.5.1. Growth, storage and manipulation of strains.** ..... 79
2.5.1.1. Growth of *E. coli* strains. ..... 79

2.5.1.2. Storage of *E. coli* strains. ..... 79
2.5.1.3. Growth of *S. pombe* strains. ..... 79
2.5.1.4. Storage of *S. pombe* strains. ..... 83
2.5.1.5. Genetic manipulation of *S. pombe* strains ..... 83
2.5.1.6. Sensitivity of *S. pombe* strains to DNA damaging agents. ..... 84
2.5.1.7. Light microscopy. ..... 85
**2.5.2. Transformation of Strains.** ..... 85
2.5.2.1. Transformation of *E. coli* with DNA. ..... 85
2.5.2.2. Transformation of *S.pombe* with DNA (Electroporation method). ..... 86
2.5.2.3. Transformation of *S.pombe* with DNA (Lithium acetate method). ..... 86
**2.5.3. Isolation of DNA.** ..... 87
2.5.3.1. Small scale plasmid DNA isolation from *E. coli.* ..... 87
2.5.3.2. Large scale plasmid DNA isolation from *E. coli.* ..... 88
2.5.3.3. Isolation of genomic DNA from *S. pombe.* ..... 88
2.5.3.4. Isolation of DNA from agarose gels. ..... 89
2.5.3.5. Isolation of DNA from solution. ..... 89
**2.5.4. Manipulation and analysis of DNA.** ..... 89
2.5.4.1. Enzymatic restriction of DNA. ..... 89
2.5.4.2. Phosphatase treatment of linearised DNA. ..... 90
2.5.4.3. Klenow and T4 DNA polymerase extension/resection of DNA ..... 90
2.5.4.4. Ligation of DNA. ..... 91
2.5.4.5. The Polymerase Chain Reaction (PCR) ..... 91
2.5.4.6. Sequencing of DNA. ..... 93
2.5.4.7. Quantification of DNA samples ..... 94
**2.5.5. Analysis of DNA by gel electrophoresis.** ..... 94
2.5.5.1. Agarose gel electrophoresis. ..... 94
2.5.5.2. Preparation of chromosomal DNA for Pulsed-Field Gel Electrophoresis (PFGE). ..... 95
2.5.5.3. Running and visualisation of pulsed-field gels. ..... 96
**2.5.6. Southern blot analysis.** ..... 97
2.5.6.1. Transfer of chromosomal/genomic DNA to nitrocellulose. ..... 97
2.5.6.2. Radioactive marker/probe compilation. ..... 98
2.5.6.3. Southern probing ..... 99
2.5.6.4. Stripping the blot ..... 99
**2.5.7. Analysing cellular responses to a site-specific DNA double-strand break.** ..... 100
2.5.7.1. A genetic assay for investigating DSB-induced loss of heterozygosity (LOH) – The LOH assay ..... 100
2.5.7.3. An assay to investigate strain viability in response to a DSB ..... 103
2.5.7.4. *De-novo* telomere addition assay. ..... 103
2.5.7.5. Minichromosome loss assay. ..... 104
**2.5.8. Plasmid Construction.** ..... 105
2.5.8.1. Construction of pREP82X-HO. ..... 105

**3. INVESTIGATING THE GENETIC REQUIREMENTS OF EXTENSIVE DSB-INDUCED LOH VIA TRANSLOCATIONS.** .....

**3.1. INTRODUCTION** ..... **107**
**3.2. ALLELIC CROSSOVERS AND BIR REQUIRE THE MRN COMPLEX, *RAD11*$^+$ AND *RAD22*$^+$.** ..... **113**
3.2.1. DSB repair and extensive LOH in MRN complex mutants ..... 113

3.2.2. $Ch^X$ formation requires *rad32*$^+$, *rad50*$^+$ and *nbs1*$^+$ ..... 117
3.2.3. DSB repair and extensive LOH in *rad11D223Y* ..... 117
3.2.4. $Ch^X$ is not observed in *rad11D223Y*. ..... 119
3.2.5. DSB repair and extensive LOH in *rad22Δ*. ..... 121
3.2.6. Isolation and analysis of non-suppressed *rad22Δ* $Ch^{16}$-MHH ..... 121
3.2.7. $Ch^X$ formation requires *rad22*$^+$. ..... 124
**3.3. DISCUSSION. ..... 125**

**4. HR PREVENTS EXTENSIVE DSB-INDUCED LOH VIA *DE NOVO* TELOMERE ADDITION. .....**

**4.1. INTRODUCTION ..... 134**
**4.2. DSB-INDUCED LOH OCCURS VIA *DE NOVO* TELOMERE ADDITION IN HR MUTANTS. ..... 135**
4.2.1. DSB-induced LOH in *rhp51Δ* occurs predominantly from truncation of $Ch^{16}$. ..... 135
4.2.2. Truncated $Ch^{16}$ is genetically stable with telomeric sequence at the HO break site. ..... 138
4.2.3. Extensive DSB-induced LOH in *rhp51Δ* occurs predominantly via telomere addition. ..... 139
4.2.3. *rad22*$^+$, *rhp55*$^+$, *rhp54*$^+$ and *mus81*$^+$ also prevent break-induced telomere addition. ..... 142
4.2.4. Telomere addition is observed in *rad11D223Y*. ..... 146
4.2.5. A role for the MRN complex and *exo1*$^+$ in break-induced telomere addition. ..... 147
**4.4. DISCUSSION. ..... 152**
4.4.1. HR prevents *de novo* telomere addition at DSB sites. ..... 152
4.3.3. Telomere addition is associated with an allelic crossover in *rad32Δ* and *rad50Δ* cells. ..... 159
4.3.4. Summary. ..... 161

**5. HR COMPETES WITH TELOMERE ADDITION FOR THE REPAIR OF RESECTED DSB ENDS. .....**

**5.1. INTRODUCTION ..... 163**
**5.2. INVESTIGATING A ROLE FOR DSB END PROCESSING IN *DE-NOVO* TELOMERE ADDITION. ..... 163**
5.2.1. DSB repair and extensive LOH in *exo1Δ rhp55Δ* . ..... 163
5.2.2. Deletion of *exo1*$^+$ does not affect telomere addition in *rhp55Δ*. ..... 166
5.2.3. DSB repair and extensive LOH in *ku70Δ rhp55Δ* and *lig4Δ rhp55Δ* ..... 167
5.2.4. *ku70*$^+$ represses break-induced *de-novo* telomere addition in *rhp55Δ* cells. ..... 170
**5.3. HOMOLOGOUS RECOMBINATION COMPETES WITH TELOMERE ADDITION FOR RESECTED DNA ENDS ..... 172**
5.3.1. DSB repair and extensive LOH in *rhp55Δ* $Ch^{16}$-MGH + pIRT3/pIRT3-*rhp51*. ..... 173
5.3.2. Overexpression of *rhp51* reduces break-induced *de novo* telomere addition in *rhp55Δ* cells. ..... 175

**5.4. INVESTIGATING THE ROLE OF THE MRN COMPLEX IN *DE-NOVO* TELOMERE ADDITION. ..... 177**
5.4.1. DSB repair and extensive LOH in *rad32Δ rhp55Δ*, *rad50Δ rhp55Δ* and *nbs1Δ rhp55Δ*. ..... 177
5.4.2. *rad32*$^{+}$, *rad50*$^{+}$ and *nbs1*$^{+}$ repress *de-novo* telomere addition in *rhp55Δ*. .. 178
**5.5. OVEREXPRESSION OF *RHP51* MAY PROMOTE CROSSOVERS IN *RHP55Δ* CELLS. ..... 182**
**5.6. DISCUSSION. ..... 186**
5.6.1. Investigating repair in *rhp55Δ* Ch$^{16}$-MGH. ..... 186
5.6.2. HR competes with telomere addition for the repair of ssDNA overhangs. . 192
5.6.3. Summary. ..... 198

**6. GENERAL DISCUSSION. ..... 200**

**7. REFERENCES. ..... 207**

**8. APPENDICIES. ..... 227**

# ACKNOWLEDGEMENTS.

First, I would like to thank the Medical Research Council for kindly funding this research. Huge thanks also go to my supervisor, Dr. Tim Humphrey, for his guidance and support during my D. Phil studies. There have been plenty of times during the course of my time at Harwell where I've been worried about certain aspects of the work (sometimes unnecessarily!) and I thank him for his patience and calming influence during those bouts of anxiety.

I'd also like to thanks all members of the Cell Cycle Group and RAGSU, past and present, who have helped me over the last 4 years. A very special thanks also goes to Carol Walker for her help with pulsed-field gels and various other aspects related to work. Many thanks also go to the cleaning ladies, Angela and Sue.

There are a few people outside of the science world who I'd also like to mention. First, my brothers Richard and Marc. Both of you are great in your own way. Secondly, Jimmy, Ben and Glenn. I told you I'd get you in here somehow! Although I can't really talk about the half man half monkey like you'd want me too! Thanks for showing me how to enjoy life again. Thirdly, anyone I've lived with (at Imperial, Lake Street and the Gunnersbury Palace), and of course, my beautiful fiancé, Abby, for her understanding and support during the past 8 months. It's been a hard slog and I thank you from the bottom of my heart for your patience.

Finally, but by no means least, I'd like to thank my parents, Richard and Geraldine. I really appreciate everything you've done and taught me during the course of my life. There is no-one else like you in the world. It is to you that I dedicate this Thesis.

# Analysing the mechanisms responsible for DNA double-strand break-induced loss of heterozygosity in fission yeast.

**Jason Kingsley Cullen**

**Wolfson College**
**Department of Zoology**

**Doctor of Philosophy (D.Phil.)**

**University of Oxford**
**Trinity Term, 2007**

## ABSTRACT.

Loss of heterozygosity (LOH) is considered a causal event in the formation of many cancers, with increasing evidence suggesting that DNA double-strand breaks (DSBs) play a major role in its occurrence. Despite its prominence in cancer, however, the precise molecular mechanisms responsible for extensive LOH and how such events are suppressed in normal cells is poorly understood.

To investigate the mechanisms responsible for extensive break-induced LOH in eukaryotes, this study took advantage of an assay system in which such events could be identified through screening for loss of an auxotrophic *his3*$^{+}$ marker, found ~25kb distal to an HO-endonuclease cut site in a non-essential minichromosome in *Schizosaccharomyces pombe.*

Studies using this system had previously shown that extensive break-induced LOH in wild-type background, whilst infrequent, was predominantly associated with large translocations resulting from both allelic crossovers during G2 phase and break-induced replication (BIR). Such extensive loss of allele specific information was also found to require *rhp55*$^{+}$, *rhp51*$^{+}$, *rhp54*$^{+}$ and *mus81*$^{+}$. This study has identified an additional role for the MRN complex, Rad22 and RPA in such break-induced translocations, suggesting that both allelic crossovers and BIR require homologous recombination (HR) in fission yeast. Surprisingly, break-induced extensive LOH was still observed in HR mutants. In contrast to wild-type cells, however, such extensive LOH was found to arise predominantly through *de novo* telomere addition at, or near, the break-site. Interestingly, telomere addition was most frequently observed in a *rad22Δ* background that disrupts HR following end resection. Further analysis demonstrated that *de novo* telomere addition was also significantly increased in *ku70Δ rhp55Δ* cells. Moreover, overexpression of *rhp51* in *rhp55Δ* cells led to a substantial reduction in break-induced *de novo* telomere addition. Together, these findings support a model in which HR prevents *de novo* telomere addition at DSBs by competing for resected ssDNA ends.

In addition to providing information on break-induced LOH this study has identified a requirement for the MRN complex in efficient repair in *rhp55Δ* cells, which was previously found to occur via sister chromatid recombination (SCR) or a HR-dependent end-joining pathway (EJ). Interestingly, deletion of MRN components also resulted in an increase in telomere addition, providing further evidence that HR competes with telomere addition for the repair of DSBs.

Overall, these findings shed light on the competitive relationships between pathways of DSB repair/misrepair in *S. pombe* and how such mechanisms contribute to the prevention or promotion of genome instability.

# NOMENCLATURE.

***S. pombe***

Genes: Denoted by lower-case letters in italics.
Wild type genes are given the suffix $^{+}$ (e.g. *rad22*$^{+}$); mutant alleles are designated by letters and numbers (e.g. *ade6-210*); deletion/null mutants are given the symbol Δ (e.g. *rad22*Δ).

Proteins: Denoted by lower-case letters with a capital initial (e.g. Rad22).

***S. cerevisiae.***

Genes: Wild type genes are denoted by capital letters in italics (e.g. *RAD52*); mutant alleles are denoted in lower-case letters and numbers (e.g. *srs2-7AV*); deletion/null mutants are denoted in lower-case letters with a Δ symbol (e.g. *srs2*Δ).

Proteins: Denoted by lower-case letters with a capital initial (e.g. Srs2).

**Mammalian and humans.**

Genes: Genes are denoted by capital letters in italics (e.g. *BRCA1*); in knockout animals or mutant cell lines, genetic homozygosity is given the prefix $^{-/-}$ or $^{+/+}$ while heterozygosity is given $^{+/-}$ (e.g. *BRCA1*$^{+/+}$).

Proteins: Denoted by capital letters (e.g. ATM) or lower-case letters with a capital initial (e.g. Cdc25A).

# ABBREVIATIONS.

| | |
|---|---|
| BIR | break-induced replication |
| bp | base pair |
| Ch | chromosome |
| $Ch^{16}$ | minichromosome 16 |
| CPT | Camptothecin |
| $dH_2O$ | distilled $H_2O$ |
| DNA | deoxyribonucleic acid |
| DSB | double-strand break |
| EJ/SCR | end joining/sister chromatid recombination |
| EtBr | ethidium bromide |
| EtOH | ethanol |
| g | gram or relative centrifugal force (x g) |
| G418 | geneticin |
| GC | gene conversion |
| hr | hour |
| HR | homologous recombination repair |
| HJ | Holliday junction |
| kb | kilobase |
| l | litre |
| LOH | loss of heterozygosity |
| LTGC | long-tract GC |
| M | molar |
| Mb | megabase |
| mg | milligram |
| ml | millilitre |
| mM | millimolar |
| MRN | Mre11/Rad32-Rad50-Nbs1 complex |
| NHEJ | non-homologous end-joining |
| PCR | polymerase chain reaction |
| PFGE | pulsed-field gel electrophoresis |
| *S. pombe* | *Schizosaccharomyces pombe* |
| *S. cerevisiae* | *Saccharomyces cerevisiae* |
| wt | wild-type |

| | |
|---|---|
| w/v | weight per volume |
| Δ | gene disruption |
| °C | degree Celcius |
| µg | microgram |
| µl | microlitre |
| µM | micromolar |
| O/N | overnight |

# LIST OF TABLES.

**Table 1.1.** Checkpoint and DSB repair proteins identified in cancer-related disorders.....p18

**Table 1.2.** HR repair proteins identified in *S. cerevisiae*, *S. pombe* and humans.....p38

**Table 1.3.** Evidence of direct roles for checkpoint factors in DSB repair and apoptosis.....p59

**Table 2.1.** Buffers and solutions used during this study.....p74

**Table 2.2.** *E. coli* media.....p76

**Table 2.3.** *S. pombe* media.....p78

**Table 2.4.** *S. pombe* strains used during this study.....p80

**Table 3.1.** DSB-induced marker loss in wt and HR mutants.....p114

**Table 3.2.** PFGE analysis of *ade*$^{+}$ G418$^{S}$/Hyg$^{S}$ *his*$^{-}$ colonies from wt and HR mutants .....p115

**Table 4.1.** Mechanisms of break-induced LOH in wt and HR mutants .....p141

**Table 4.2.** Break-point telomere junctions in HR mutants.....p151

**Table 5.1.** DSB-induced marker loss in wt, NHEJ and *rhp55Δ* mutants.....p164

**Table 5.2.** Mechanisms of break-induced LOH in wt, NHEJ and *rhp55Δ* mutants.....p165

**Table 5.3.** Effect of *rhp51* overexpression on DSB-induced marker loss in *rhp55Δ*.....p174

**Table 5.4.** PFGE analysis of EJ/SCR and GC populations from wt and *rhp55Δ* mutant cells.....p183

# LIST OF FIGURES.

**Figure 1.1.** Double Strand Break Repair (DSBR) model.....p28

**Figure 1.2.** Synthesis Dependent Strand Annealing (SDSA) models.....p29

**Figure 1.3.** Single-Strand Annealing (SSA).....p33

**Figure 1.4.** Possible mechanisms of BIR.....p36

**Figure 1.5a.** Model of upstream events during DSB repair in eukaryotes.....p44

**Figure 1.5b.** Model of downstream events during DSB repair in eukaryotes.....p45

**Figure 1.6.** Model of NHEJ in eukaryotes.....p56

**Figure 1.7.** Checkpoint response pathways in yeast and humans.....p61

**Figure 1.8.** Telomere binding proteins in eukaryotes.....p67

**Figure 1.9.** $Ch^{16}$-MGH/MHH LOH assay (Phenotypic outcomes following DSB induction).....p70

**Figure 2.1.** LOH assay (Schematic of assay procedure).....p102

**Figure 3.1.** DSB-induced LOH results from large translocations in wild-type background.....p108

**Figure 3.2.** Schematic of $Ch^{X}$ formation via allelic crossovers and BIR.....p110

**Figure 3.3.** Possible mechanisms of $Ch^{XY}$ formation in *ade*$^{+}$ $G418^{S}$/$Hyg^{S}$ *his*$^{-}$ cells from various HR mutants.....p111

**Figure 3.4.** $Ch^{X}$ is absent from *rhp51Δ* and *rhp55Δ ade*$^{+}$ $G418^{S}$ *his*$^{-}$ colonies....p112

**Figure 3.5.** $Ch^X$ is absent from *rad32Δ*, *rad50Δ* and *nbs1Δ ade*$^+$ $G418^S/Hyg^S$ *his*$^-$ colonies.....p118

**Figure 3.6.** $Ch^X$ is absent from *rad11D223Y* and *rad22Δ ade*$^+$ $G418^S/Hyg^S$ *his*$^-$ colonies.....p120

**Figure 3.7.** Isolation of non-suppressed *rad22Δ* $Ch^{16}$-MHH.....p122

**Figure 3.8.** Working model of DSB-induced repair and extensive LOH in wild-type backgrounds (1).....p127

**Figure 3.9.** Working model of DSB-induced repair and extensive LOH in HR mutant backgrounds (1).....p128

**Figure 4.1.** DSB-induced LOH in *rhp51Δ* cells result from $Ch^{16}$ truncations.....p136

**Figure 4.2.** Break-induced LOH results from *de novo* telomere addition in *rhp51Δ* cells.....p140

**Figure 4.3.** HR prevents LOH from *de novo* telomere addition at break-sites.....p144

**Figure 4.4.** Telomere addition is responsible for DSB-induced LOH in *rad11D223Y* .....p148

**Figure 4.5.** Working model of DSB-induced repair and LOH in wild-type background (2).....p153

**Figure 4.6.** Working model of DSB-induced repair and LOH in HR mutant backgrounds (2).....p154

**Figure 4.7.** Possible mechanism to describe telomere addition with an allelic crossover in HR mutants.....p160

**Figure 5.1.** PFGE analysis of LOH colonies from various *rhp55Δ* mutants.....p168

**Figure 5.2.** HR competes with telomere addition for the repair of ssDNA ends...p169

**Figure 5.3.** PFGE analysis of LOH colonies from various *rhp55Δ* and MRN double mutants.....p179

**Figure 5.4.** The MRN complex prevents telomere addition in the absence of *rhp55*$^{+}$.....p180

**Figure 5.5.** Overexpression of *rhp51* promotes EJ/SCR, interchromosomal GC and possibly crossover formation in *rhp55Δ*.....p184

**Figure 5.6.** Model of DSB-induced repair in wt, *rhp55Δ*, *rad32Δ/rad50Δ/nbs1Δ* *rhp55Δ* and *ku70Δ rhp55Δ*.....p187

**Figure 5.7.** Model depicting dual roles for HR in extensive DSB-induced LOH.....p194

# 1. INTRODUCTION.

## 1.1. GENOME INSTABILITY AND CANCER.

Maintaining genome stability is a crucial function critical to normal cellular growth and survival. Although it is unclear whether genome instability is an initiating event and thus a driving force behind tumourigenesis, a strong correlation between loss of genome integrity and the development and progression of cancer has been observed in nearly all solid tumours (Lengauer et al., 1998). Indeed, deficiencies in DNA repair and chromosomal integrity pathways which maintain genome stability cause inherited cancer syndromes (Table 1.1). Preneoplastic lesions from sporadic colorectal tumours lack any observable genome instability, however, suggesting that such a phenomenon is not an initiating factor (Sieber et al., 2003; Rajagopalan et al., 2003). The progressive nature of genome instability in cancers has led to the proposal of the mutator hypothesis. This suggests that tumour heterogeneity and progression is a consequence of ongoing mutations/rearrangements that promote changes in gene dosage/expression of various oncogenes/tumour suppressor genes. The resultant outcome of such events is further instability which iteratively promotes a growth advantage (Loeb, 2001). Indeed, a phenomenon known as loss of heterozygosity (LOH) is a possible cause or effect of such instability and may contribute to either the initiation of tumourigenesis or the mutator phenotype through the inactivation of tumour suppressor genes (discussed in Section 1.2.1). Not all cancers exhibit ongoing genome instability, however; for example, a single chromosome translocation is responsible for the progression of chronic myelogenous leukaemia (Sattler and Griffin, 2001). Furthermore, genome rearrangements are not only observed in cancers. Genetically stable rearrangements have been described as inherited mutations that cause a variety of other human diseases (Deininger and Batzer, 1999).

**Table 1.1. Checkpoint and DSB repair proteins identified in cancer-related disorders.**

| Protein | Protein function and associated disorder | Reference |
|---|---|---|
| ATM | Checkpoint kinase. Mutated ATM causes the condition Ataxia Telangiectasia (A-T), leading to increased susceptibility to the formation of cancers. A-T is characterised by chromosomal and telomeric instability, radiosensitivity, radioresistant DNA synthesis and defective cell cycle checkpoint activation. | Savitsky *et al.*, 1995 |
| MRE11 | DNA repair protein with roles in checkpoint activation. Mutated in A-T like disorder (ATLD), with similar clinical features to those seen in A-T and NBS patients, including cancer predisposition. | Stewart *et al.*, 1999 |
| NBS1 | DNA repair protein with roles in S-phase checkpoint activation. Mutated in Nijmegan Breakage Syndrome (NBS) patients. Similar clinical features to those seen in A-T and ATLD. | Carney *et al.*, 1998 |
| BLM | RecQ-like DNA helicase involved in DNA repair. Mutation results in Bloom's syndrome, characterised by stunted growth, sensitivity to UV and predisposition to cancer. | Ellis *et al.*, 1995<br>Mohagegh and Hickson, 2001 |
| WRN | RecQ-like DNA helicase. Mutation results in Werner's syndromeCancer predisposition is largely associated with soft tissue sarcomas. | Yu *et al.*, 1996 |
| RECQL4 | RecQ-like DNA helicase. Mutation is associated with Rothmund-Thomson Syndrome (RTS), characterised by genomic instability. | Kitao *et al.*, 1999<br>Mohagegh and Hickson., 2001 |
| BRCA1<br>BRCA2 | Checkpoint and DNA repair proteins. Mutation predisposes individuals to breast and ovarian cancers. | Futreal *et al.*, 1994<br>Wooster *et al.*, 1995 |
| CHK2 | Checkpoint kinase. Mutations in *CHK2* have been found in Li-Fraumeni patients. | Bell *et al.*, 1999 |

### 1.1.1. Loss of heterozygosity (LOH) and cancer.

Diploid cells carrying two functional copies of a gene on homologous chromosomes usually require two genetic events to acquire a phenotypic change (except in the case of haploinsufficiency). This is termed the 'two hit hypothesis' (Knudson, 1971). The first 'hit' could be a sporadic point mutation or the inheritance of a mutant allele, whilst the second 'hit' could be any genetic event that functionally inactivates the remaining allele and thus leads to homozygosis, a process called loss of heterozygosity (LOH). As previously described, LOH is thought to contribute to tumourigenesis through the functional inactivation of tumour suppressor genes (Knudson, 1993). LOH often extends several megabases to encompass multiple genetic loci or even whole chromosome arms, thus leading to extensive loss of allele-specific information. It is generally observed in all solid tumour types and has been detected at specific tumour suppressor loci in familial cancers at high frequencies (Borgdorff et al., 2005; Lasko et al., 1991; Nadège Presneau, 2005). In sporadic cancers up to half of all chromosomes undergo extensive LOH, although not all of these regions are linked to tumour suppressor genes (Kinzler and Vogelstein, 1997). Despite its prominence in cancer there has been little progress, however, in determining the precise molecular mechanisms responsible for extensive LOH and how such events are regulated in normal cells.

A number of possible mechanisms responsible for LOH have been inferred from karyotype and polymorphic marker analysis in tumour cells. It appears from these studies that LOH can arise from several pathways, including chromosomal loss, epigenetic silencing, chromatin condensation, gross rearrangement of chromosomes (GCRs) e.g. interstitial deletions, truncations, reciprocal and non-reciprocal translocations, and allelic recombination between distinct alleles (Hiraoka et al., 2000;

Lasko et al., 1991; Jasin, 2000; Baylin and Chen, 2005; Richard L. Momparler, 2000). Recent evidence suggests that these pathways may also interact with one another to promote LOH. For example, chromosomal truncations which lead to loss of allele specific information in a region without tumour suppressor genes have recently been found to contribute to colorectal cancer through promoting the epigenetic suppression of the α-catenin tumour suppressor (Liu et al., 2007). There is a wealth of experimental evidence to suggest that DNA double strand breaks are an important initiating lesion in the formation of chromosomal rearrangements and therefore play a central role in LOH and thus tumourigenesis.

## 1.2. DNA DOUBLE STRAND BREAK FORMATION.

### 1.2.1. Endogenous and exogenous causes of DSBs.

Surprisingly, as little as one DSB is sufficient to kill a cell if it disrupts an essential gene or triggers apoptosis (Khanna and Jackson, 2001). Despite their threat to cell survival and genome stability not all DSBs are unscheduled events. Indeed, many physiologically relevant processes such as V(D)J recombination in higher eukaryotes, mating type switching in yeast and meiosis require the ordered formation and repair of DSBs (Gellert, 2002; Haber, 1998; Richardson et al., 2004). Free radicals generated during endogenous metabolic processes can also cause DSBs (Wallace, 1998).

DSBs and one-ended breaks are also thought to arise spontaneously during normal DNA metabolism through the action of topoisomerases or when a migrating replication fork stalls and collapses or meets a nick in the DNA template (Hayatu

Raji, 2006). Spontaneously generated one-ended breaks have also been observed in vertebrate cells in the absence of the RAD51 recombinase (see Section 1.3.3.2), where they were found to arise during normal S-phase (Sonoda et al., 1998). The view that these lesions represent the majority of spontaneous damage during DNA replication has recently been called into question, however, with work in budding yeast. Lettier *et al.* have shown that cells carrying distinct alleles of a HR repair gene (*RAD52*; see Section 1.3.3.2), whilst unable to repair enzymatically induced DSBs and CPT induced one-ended DSBs, are as proficient as a wild-type strain in inter- and intra-chromosomal mitotic repair events that occur spontaneously (Lettier *et al.*, 2006). One-ended DSBs may still be important factor in tumourigenesis. For example, it was recently demonstrated in budding yeast that replication stress, induced using a temperature sensitive allele of a replicative polymerase, can generate breaks at fragile sites and promote chromosomal rearrangements analogous to those commonly observed in cancer (Lemoine et al., 2005). Thus, whilst breaks may not form spontaneously during normal DNA S-phase, replication stress or the absence of repair pathways may promote the conversion of such damage to DSB ends, an event which can lead to chromosomal rearrangements that promote LOH and ultimately cancer. One-ended DSBs can also form at degraded telomeres. Such structures are recognised by DNA damage checkpoint proteins to prevent rearrangements and promote senescence, although a subset of cells can escape the arrest using recombination in both yeast and mammalian cancers (Section 1.6.1).

A number of exogenous and chemical agents are also capable of inducing DSBs. Since investigating the repair of spontaneously occurring DSBs is not possible, owing to their low frequency of occurrence, DNA damaging agents have played an important role in determining how DSB repair is accomplished and co-coordinated

within cells. UV irradiation results in the formation of pyrimidine dimers and adducts that are usually processed to single-stranded nicks and gaps by the nucleotide and base excision repair pathways (for a review see Sinha and Hader, 2002). A one-ended DSB may be formed if such nicks are encountered by a replicative polymerase during DNA replication (Sinha and Hader, 2002). Indeed, other DNA damaging agents are thought to induce one-ended DSB formation during DNA replication in a similar fashion, albeit via slightly different mechanisms. CPT is known to stabilize the covalent DNA-Topoisomerase 1 (Top1) intermediate that forms during the catalytic DNA nicking-closing cycle required for DNA replication to progress (Hsiang et al., 1985; Hsiang and Liu, 1988). This has been shown to promote the formation of stable nicks in genomic DNA which are then converted into one-ended DSBs when replicated (Hsiang et al., 1989).

Methylmethanosulfonate (MMS) is a potent alkylating agent known to modify both adenine (to 3-methyladenine) and guanine (to 7-methylguanine) to cause base-mispairing and replication blocks, respectively (Beranek, 1990). At low concentrations (0.03%) MMS was originally believed to cause DSBs *in vivo* (Choy and Kron, 2002). This view is supported by the fact that several HR mutants in yeast and humans are highly sensitive to MMS within this range (Krogh and Symington, 2004). One-ended DSBs were thought to arise by a nick-repair-replication type mechanism similar to that proposed for UV damage (Sobol et al., 2003; Pascucci et al., 2005), but it has recently been shown that DSBs do not form in either yeast or human cells after treatment with low concentrations of MMS (Lundin et al., 2005). The study goes on to show that the breaks observed in previous experiments were an experimental artefact generated by the experimental conditions used. The sensitivity of DSB repair mutants to low concentrations of MMS may therefore reflect an

inability to repair stalled forks or ssDNA gaps distal to the replication fork, rather than that of one-ended DSBs. At higher doses, some of these agents are capable of producing *bona fide* DSBs in cells. Indeed, both UV irradiation and MMS have been shown to induce DSBs at higher doses (e.g. 0.5% MMS) as a result of clustered nicks and gaps (Rapp and Greulich, 2004; Chlebowicz and Jachymczyk, 1979). Even though the mode of action of some of these agents is still ill-defined, both CPT and MMS have been shown to induce genome instability, far above the level of spontaneous events observed in wild-type yeast (Myung and Kolodner, 2003). The fact that CPT treatment increases the rate at which chromosomal rearrangements form suggests that one-ended DSBs are indeed an important lesion in the etiology of genome instability and LOH.

Ionising radiation (IR) e.g. γ-radiation and X-rays, and radiomimetic drugs such as bleomycin are potent inducers of DSBs and have also been widely used to investigate the co-ordination and control of DSB repair in both yeast and mammalian systems (Olive, 1998; Povirk et al., 1977; Povirk, 1996). IR is known to produce free radicals and to cause a spectrum of other lesions in addition to DSBs including single-strand breaks and base or nucleotide damage which can further promote DSB formation (Olive, 1998). As a result, the DSBs produced by IR are generally more complex in terms of breakpoint structure (so called 'dirty' breaks; also reviewed in Goodhead, 1994). Like other inducers of DNA damage, IR promotes a significant elevation in chromosomal rearrangements compared to spontaneous damage in both yeast and mammalian cell systems, again emphasising an important role for DSBs in promoting genome instability and LOH (Morgan et al., 1996; Myung and Kolodner, 2003).

### 1.2.2. Enzymatically induced DSBs.

Enzymatic DSB production has several advantages over the use of IR and other DNA damaging agents for the induction and analysis of DSB repair and LOH. Firstly, since IR produces a spectrum of DNA lesions and cytosolic free radicals in addition to DSBs it can be difficult to decipher whether the cellular response to irradiation is DSB-dependent. Indeed, an enzymatic DSB produces a 'clean' break circumventing this issue. A disadvantage of this approach, however, is that a 'clean' DSB may be processed differently from a more physiologically relevant 'dirty' break. Secondly, an enzymatically induced DSB can also be targeted to any location within the genome to help aid studies of break-induced marker loss. Finally, if the enzyme required to induce the break is placed under control of an inducible promoter, DSB induction can be synchronously and temporally regulated such that repair may be monitored in large populations at distinct cell cycle phases, for example.

There are a number of strategies that have been used to enzymatically induce DSBs in yeast and human cells e.g. the use of *EcoR*I in *S. cerevisiae* (Lewis et al., 1998) or the transient transfection of rare cutting endonucleases in mammalian cell lines (Thacker, 1994). However, the two most common endonucleases used to induce DSBs are: The HO (homothallism) endonuclease of *S. cerevisiae* that recognises a 22bp sequence within the *MAT*a (mating-type) locus (Strathern et al., 1982); and the I-*Sce*I endonuclease (intron-encoded endonuclease I of *S. cerevisiae*) which has an 18 bp non-symmetrical recognition sequence (Colleaux et al., 1988). Both I-*Sce*I and HO endonucleases produce a 4 bp 3'-ssDNA overhang within their respective restriction site. HO-induced breaks have been extensively used in *S. cerevisiae* to analyse the requirements and co-ordination of DSB repair by various mechanisms (Paques and Haber, 1999). Such studies have been conducted in the context of the original *MAT*

locus (Raveh et al., 1989; White and Haber, 1990) as well as in other chromosomal loci (Parket et al., 1995; Inbar and Kupiec, 1999). HO-induced breaks have also been used to direct chromosomal rearrangements *in vivo* (Schulz and Zakian, 1994; Bosco and Haber, 1998). HO expression is typically under the transcriptional control of the inducible *GAL1* promoter, which is activated once cells are transferred to galactose containing medium (White and Haber, 1990). The *MAT*a target site has also been used to investigate DSB repair in *S. pombe.* Indeed, HO-induced DSBs were found to be unique, site-specific and increase intra-chromosomal recombination in *S. pombe* 2,000 fold over spontaneous levels (Osman et al., 1996). The HO system was also recently used to examine the genetic requirements of DSB repair in a non-essential setting, a system which was modified and used in this study (Prudden et al., 2003; See Section 1.7).

The I-*Sce*I system, whilst having been used in several yeast based studies (Storici et al., 2003; Lisby et al., 2004), has more frequently been used to investigate DSB repair in mammalian systems (Liang et al., 1998b; Richardson et al., 1998). Interestingly, this system has been used to identify a requirement for a *RAD51* like gene, *XRCC2*, in HR repair (Johnson et al., 1999). Furthermore, I-*Sce*I induced DSBs have been used to show that HR may be more prominent in mammalian systems than once thought, accounting for ~40% of all DSB repair events in an asynchronous population (Johnson and Jasin, 2001).

Thus, it appears that DSBs represent a major threat to genome stability. Indeed, this suggests that the appropriate repair of such lesions is of paramount importance in protecting against chromosomal abnormalities and potentially LOH.

## 1.3. MECHANISMS OF DSB REPAIR.

Two mechanisms are responsible for the majority of DSB repair events in eukaryotes: Non-homologous end joining (NHEJ) and homologous recombination (HR) repair (Kanaar et al., 1998). These pathways have been highly conserved throughout the course of evolution although their usage varies greatly in different organisms. As outlined above, compromising DSB repair can result in chromosomal loss or rearrangements leading to cell death or genomic instability and tumourigenesis (Khanna and Jackson, 2001). NHEJ is the predominant mechanism of DSB repair in higher eukaryotes whilst single-celled organisms such as yeast rely to a greater extent on HR (Jeggo, 1990). This is presumably due to differences in growth, developmental stage and the cell cycle dependency of repair mechanism choice (Section 1.5). HR repair requires extensive sequence homology from a donor and is generally believed to be error free. This depends ultimately on the donor sequence, typically a sister chromatid during vegetative growth, although repair can occur less frequently using a homologous chromosome or even an ectopic site with sequence homology on a non-homologous chromosome (Aylon and Kupiec, 2004). As a result, repair via HR is usually restricted to S and G2 cell cycle phases where a suitable donor is present. NHEJ requires little or no homology and is considered error prone, although this ultimately depends on the nature of the broken ends. Indeed, the direct rejoining of DSB ends via NHEJ is the predominant repair mechanism in G1 phase when a homologous chromatid is absent.

### 1.3.1. HOMOLOGOUS RECOMBINATION (HR) REPAIR.

Much of our understanding of HR in eukaryotes has originated from studies using *S. cerevisiae*. There are several types of HR repair: Gene conversion (GC); Single-strand

annealing (SSA); and Break-induced replication (BIR). All are thought to begin in the same way i.e. DSB ends are first resected, either by a set of redundant 5'-3' exonucleases or through the action of a DNA helicase and endonuclease, to produce ssDNA structures with a 3' overhang capable of invading homologous sequence (See below). All deviate substantially from this point, however (Paques and Haber, 1999).

### 1.3.1.1. Gene conversion (GC).

Gene conversion is defined as the non-reciprocal transfer of genetic information, usually between alleles of the same gene, from one DNA molecule to its homologue. Models to describe HR via GC are primarily based on studies from meiotic cells in *S. cerevisiae*, where recombination is pre-programmed and essential (Aylon and Kupiec, 2004). Here, the majority of GC events (30-50%) are associated with a reciprocal exchange of flanking sequence from a homologue, a phenomenon known as 'crossing-over' (Inbar et al., 2000). The model proposed by Szostak *et al.* (1983) to account for this observation was based on concepts previously described by Holliday (1964), and Meselson and Radding (1975). In its simplest form, the DSB repair (DSBR) model (Figure 1.1) proposes that one of the 3'-ssDNA tails from a resected DSB end invades a homologous chromosome (single-ended invasion) to generate a displacement loop (D-loop) structure. The region of heteroduplex DNA (hDNA) created by the invading strand serves as a primer for DNA synthesis, which extends the D-loop such that the second end of the break can base pair and anneal to it (second end capture). Following further DNA synthesis, ligation of discontinuous strands occurs leading to the formation of a joint molecule intermediate containing a double-Holliday junction (dHJ). dHJs may or may not undergo extensive branch migration, after which they are cleaved by a resolvase that cuts the crossed or non-crossed strands resulting in either crossover or non-crossover products. Resolution of this

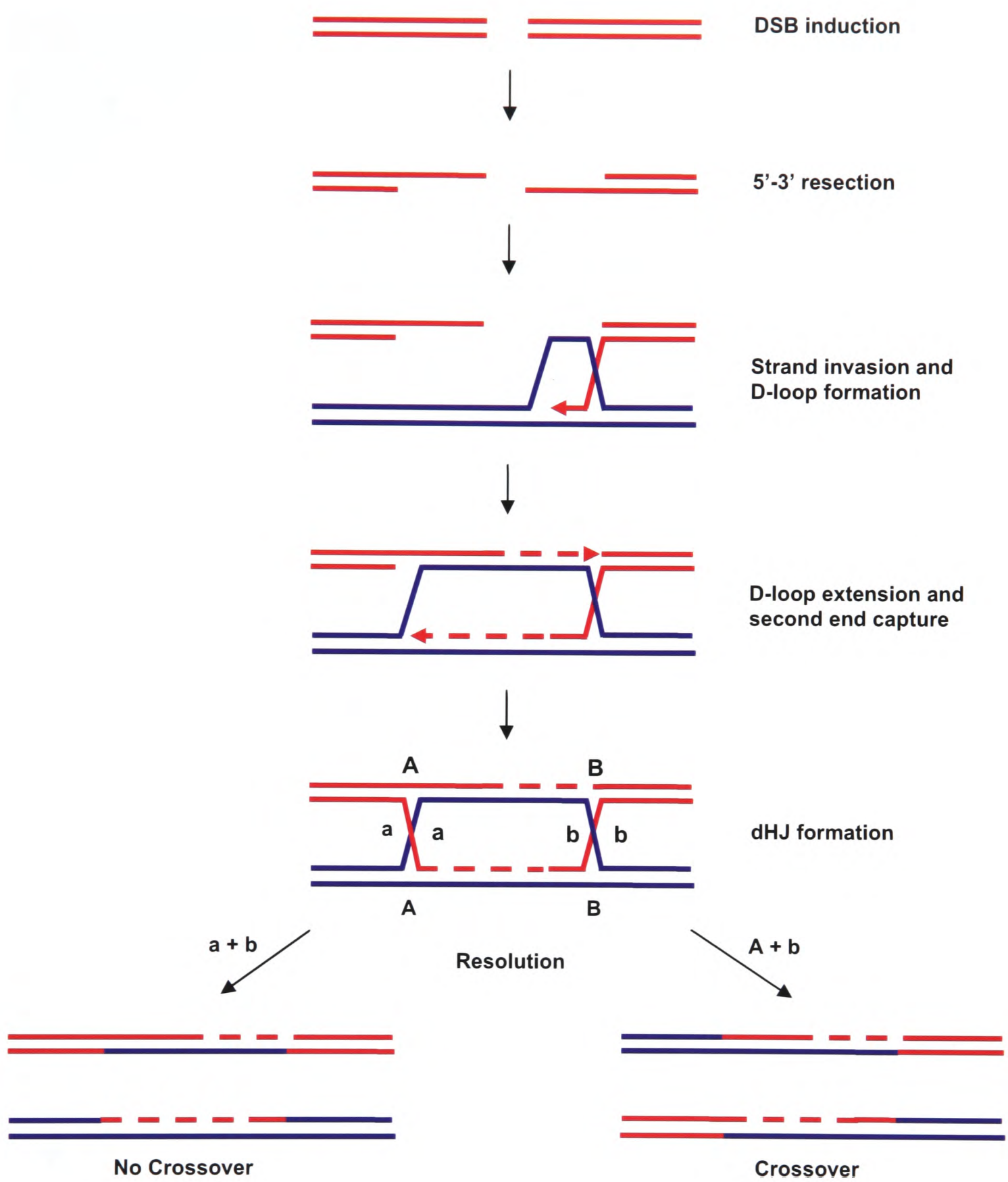



**Figure 1.1. Double Strand Break Repair (DSBR) model.** DSB ends undergo 5'-3' resection. The 3'-ssDNA tails generated from this process invade a homologous template and initiate new DNA synthesis. A dHJ structure is subsequently formed through second end capture, and is resolved as shown to produce non-crossover or crossover products. Adapted from Paques and Haber, 1999.

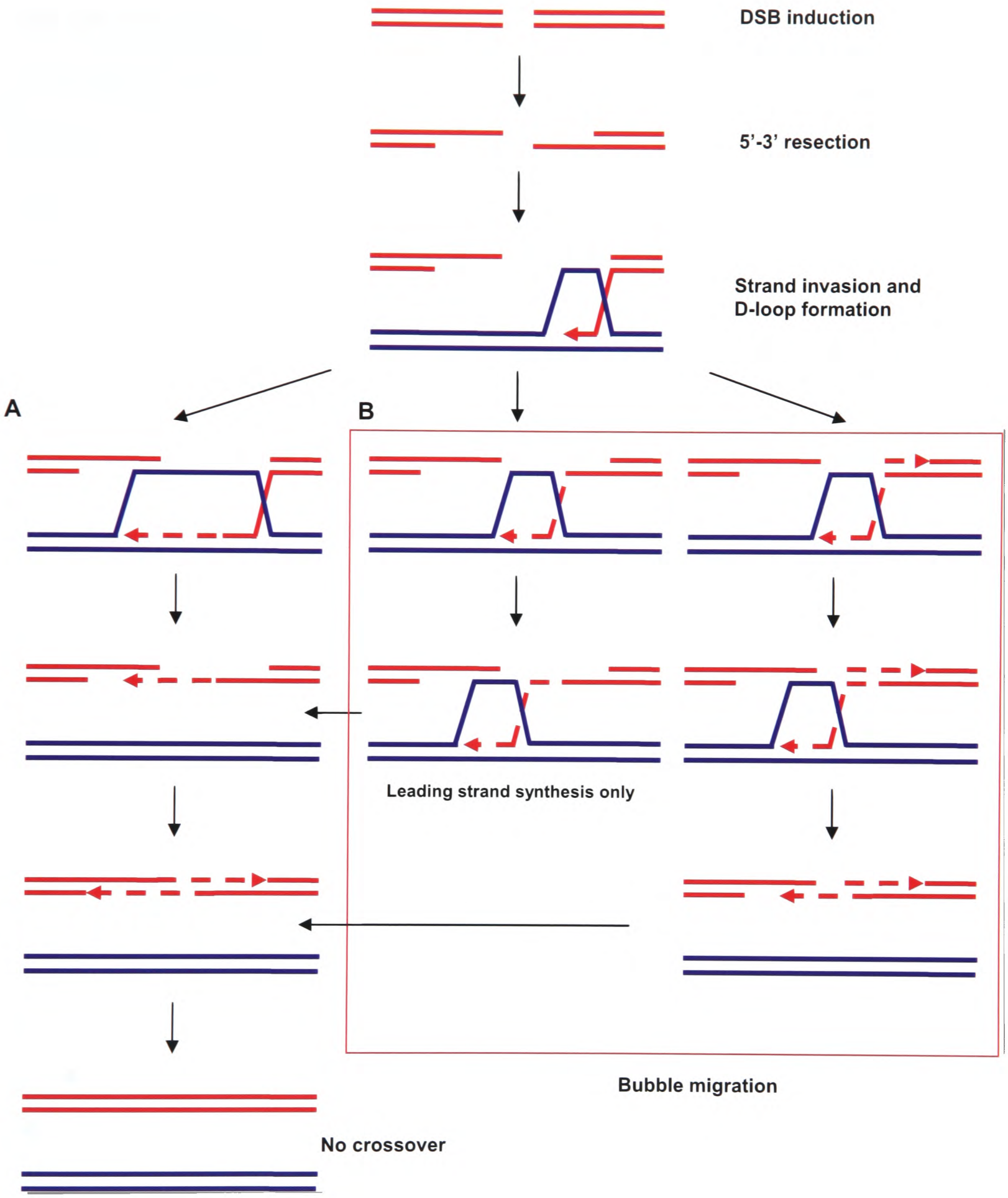



**Figure 1.2. Synthesis Dependent Strand Annealing (SDSA) models.** After strand invasion and D-loop formation, leading strand DNA replication either extends the D-loop (**A**) or promotes its migration (**B**) to facilitate second end capture. Strand invasion may initiate both leading and lagging strand synthesis in the 'bubble migration model' of SDSA. Adapted from Paques and Haber, 1999.

intermediate may also occur through dHJ dissolution (see Section 1.3.2.3). Many of the key intermediates proposed by the DSBR model have been experimentally observed, at least in *S. cerevisiae* i.e. 5'-3' resected DSBs, single-ended invasions and dHJs (Lorenz and Whitby, 2006). However, the resolution of dHJs is a step that is still poorly characterised. This is primarily due to the fact that the putative HJ resolvase has yet to be identified. It is interesting to note that dHJs may not form in all organisms during HR repair. For example, it has recently been shown in *S. pombe* that meiotic crossovers occur from the cleavage of a single Holliday junction by Mus81 (Cromie et al., 2006). Whilst 30-50% of meiotic GC events are associated with a reciprocal crossover between homologous chromosomes in *S. cerevisiae*, the processes of allelic recombination and crossing over are suppressed in mitotic cells (Paques and Haber, 1999; Stark and Jasin, 2003). It has also been shown that crossovers and non-crossovers stem from distinct pathways in budding yeast (Lorenz and Whitby, 2006). Indeed, evidence for a non-crossover pathway that is independent of HJ processing has come from work showing that non-crossover products can form before dHJs are created (Allers and Lichten, 2001). As a result, it has become difficult to establish whether the DSBR model is a good representation of DSB repair in both mitotic cells and meiotic cells where GC is not associated with a crossover. These data have provided support for an alternative model of GC, termed synthesis dependant strand annealing (SDSA).

The SDSA model (Figure 1.2) differs from DSBR in that newly synthesised DNA is displaced from the donor and returned to the broken molecule. Displacement is enacted by either topoisomerases or helicases (McGill et al., 1989), or by keeping the replication "bubble" as confined to the replication machinery as possible so that newly synthesised DNA is continuously displaced from the template (SDSA bubble migration model; Formosa and Alberts, 1986). The SDSA replication bubble could

support either leading or both leading and lagging strand synthesis (Figure 1.2), although recent evidence suggests that neither MCM nor lagging strand synthesis components are required for mitotic GC in *S.* cerevisiae (Wang et al., 2004). Following displacement, the two ends then reanneal to each other, after which ssDNA gaps are filled by leading strand synthesis and ligated. In this model DNA synthesis is conservative, avoids the formation of Holliday junctions and thus precludes crossing-over. Interestingly, conservative DNA synthesis has been experimentally observed during GC using the mating type switching system (Ira et al., 2006). Another interesting feature of the SDSA model is that DNA synthesis initiated by the invading strand can extend a long way before the second DSB end is captured. Such 'long-tract' GC events have been observed, where GC tracts of 400kb have been identified (Golin and Esposito, 1984). Indeed, these events are a potential cause of extensive LOH in mitotic cells. Although DSBR and SDSA mechanisms may explain the majority of DSB repair via GC, it is possible that different combinations or variations of these act during mitotic growth and meiosis depending on the lesion or situation encountered. Indeed, DSBR could still explain non-crossovers during mitotic growth if resolution was biased towards a non-crossover pathway using dHJ dissolution (Section 1.3.2.3). Conversely, it has been proposed that nicking of a DSBR 'type' structure without the formation of dHJs can produce crossovers (Osman et al., 2003).

Interestingly, mitotic cells tend to use a sister chromatid rather than a homologous chromosome or ectopic sequence for repair (Kadyk and Hartwell, 1992). Choosing a sister chromatid as a repair template seems intuitive since recombination using a homologous chromosome (interchromosomal/allelic) or ectopic sequence (heterologous) during mitotic growth could lead to LOH and promote genome instability. This has been observed in mouse ES cells, where DSB-induced allelic recombination has been shown to lead to localised LOH at the retinoblastoma (Rb)

locus (Moynahan and Jasin, 1997). However, it has also been suggested that the predominant LOH mechanism may differ between different types of diseases (Stark & Jasin, 2003): HR and nondisjunction segregation in retinoblastoma, and interstitial deletions in colorectal cancers. Interestingly, various factors also appear to affect crossover frequency in vegetative cells, including homology tract length, the activity of mismatch repair (MMR) proteins and RecQ family helicases (Section 1.3.2.3; (Inbar et al., 2000; Ira et al., 2003)). Indeed, crossovers between homologous chromosomes (allelic crossovers) can result in LOH if segregation during mitosis results in the separation of functional and non-functional alleles. Thus, both crossover control and regulation of template choice during HR are important pathways that act to promote genome stability and prevent (extensive) LOH during vegetative growth.

### 1.3.1.2. Single-strand annealing (SSA).

SSA occurs when 5'-3' resection of DSB ends uncovers complementary regions of DNA sequence flanking the break. These complementary regions anneal, producing extruding 3'-ssDNA tails which are removed prior to ligation to produce a reconstituted chromosome (Figure 1.3). Although SSA results in deletions, it is highly efficient when the sequences involved are 400bp or more (Sugawara et al., 2000). Furthermore, repair remains efficient even if repeats are separated by 15kb of interstitial sequence (Paques and Haber, 1999) A high degree of homology also appears essential as more than 3% divergence between 205bp repeats can reduce SSA five-fold (Sugawara et al., 1997). In addition to a number of HR genes, members of the MMR and NER pathways also play a role in the SSA pathway (Ivanov and Haber, 1995; Sugawara et al., 1997). Since SSA leads to deletions this mechanism is also a potential cause of LOH.

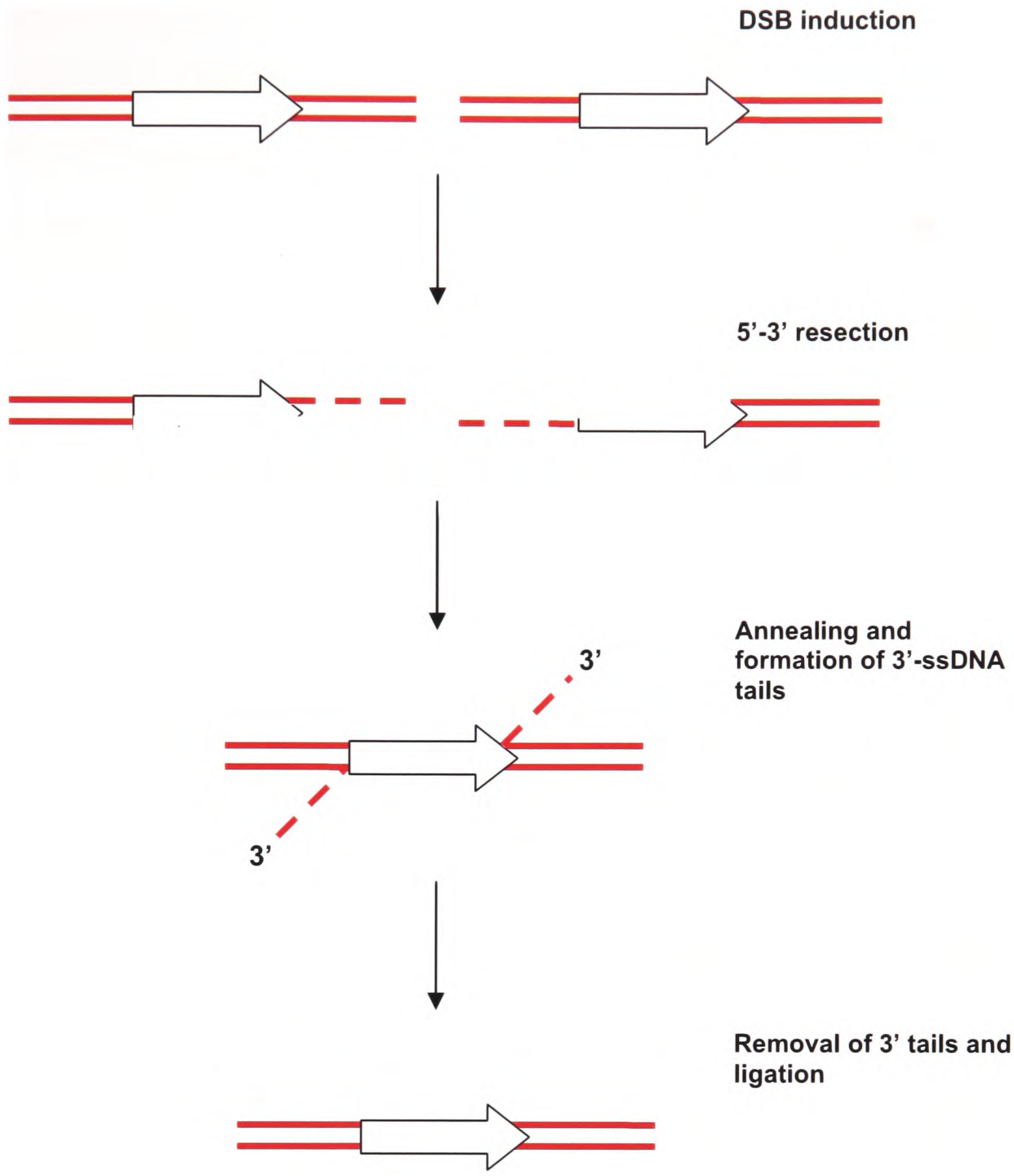



**Figure 1.3. Single-strand annealing (SSA).** SSA can occur when a DSB is formed between two direct repeats (white arrows). 5'-3' resection produces two complementary 3'-ssDNA tails that can anneal together. After the resulting overhangs have been removed (dotted lines), ligation occurs to restore the DNA molecule. Adapted from Paques and Haber, 1993.

### 1.3.1.3. Break-induced replication (BIR).

BIR, or recombination dependent DNA replication as it is also known, was a mechanism originally devised to explain the formation of crossovers during meiotic recombination. Here, a single 3'-ssDNA tail invades a homologous sequence, initiating DNA replication which progresses to the end of the chromosomal template i.e. a recombination dependent but origin independent replication event. This process is similar to the initiating stages of GC and has been shown to have similar genetic requirements (Section 1.3.2.2). Various experimental data from studies involving replication and repair in T4 and λ phage has supported the existence of BIR (McEachern and Haber, 2006). A similar mechanism has also been proposed to explain RecA and HR-dependent initiation of DNA replication from DNA damage-inducible origins in *E. coli* (Asai et al., 1993). Indeed, the formation of a replication fork by recombination has been shown by *in vitro* studies, supporting the replicative nature of BIR (Formosa and Alberts, 1986). *In vivo* support for this phenomenon was provided by experiments utilising a DNA fragment containing a centromere and two oppositely orientated DNA segments with homology to an endogenous chromosome (Morrow et al., 1997). Transformation of this fragment led to the recovery of a new chromosome in which both ends had recombined with the homologous chromosome and had copied to the end of the template. No change to the endogenous chromosomes was observed.

BIR is though to play a major role in the restarting of stalled replication forks (reviewed in McGlynn and Lloyd, 2002) and repair at telomeres (McEachern and Haber, 2006). The idea that BIR could also play a role in telomere capture at chromosome termini was provided by experiments using linearised plasmid, where one end lacking a telomere but carrying homology to a subtelomeric Y' region

acquired a telomere once transformed into yeast (Dunn et al., 1984). A one-ended recombination event may occur because only one end is available or successful at invasion, such as at a collapsed replication fork, or because there is no second end capture. Indeed, this later hypothesis has been recently tested in *S. cerevisiae*, where a modified diploid strain was constructed to contain a truncated chromosome and only 46bp of homology to a homologous chromosome, centromere distal to a *MAT*a cut site. Here, break-induction led to a large stimulation in repair via BIR and to the formation of non-reciprocal translocations with a huge reduction in GC (Malkova et al., 2005), suggesting that the presence of the second end is important in preventing BIR by promoting GC. Subsequent pedigree analysis showed that these translocations were a result of BIR and not allelic crossovers. Such translocations can affect gene dosage and result in extensive LOH. Indeed, a kinetic delay was also found to accompany the formation of BIR products, an impediment that was not observed for products acquired via GC (Malkova et al., 2005). Thus, whilst BIR and GC maybe mechanistically linked through the use of HR they appear to stem from kinetically distinct pathways.

Several models have been proposed to explain how BIR might occur and, as expected, these are similar to the proposed models of GC (Figures 1.4; McEachern and Haber, 2006). In the first, invasion of a single 3'-ssDNA tail creates a D-loop which initiates replication and migrates all the way to the end of the chromosome, similar to the conservative bubble migration model of SDSA (Figure 1.2). The single strand could then be filled using a process with differing requirements from lagging strand synthesis. Alternatively, invasion could be followed by the formation of a fully functional unidirectional replication fork. Here, DNA synthesis is semi-conservative with the formation of a single Holliday junction that requires resolution. Finally,

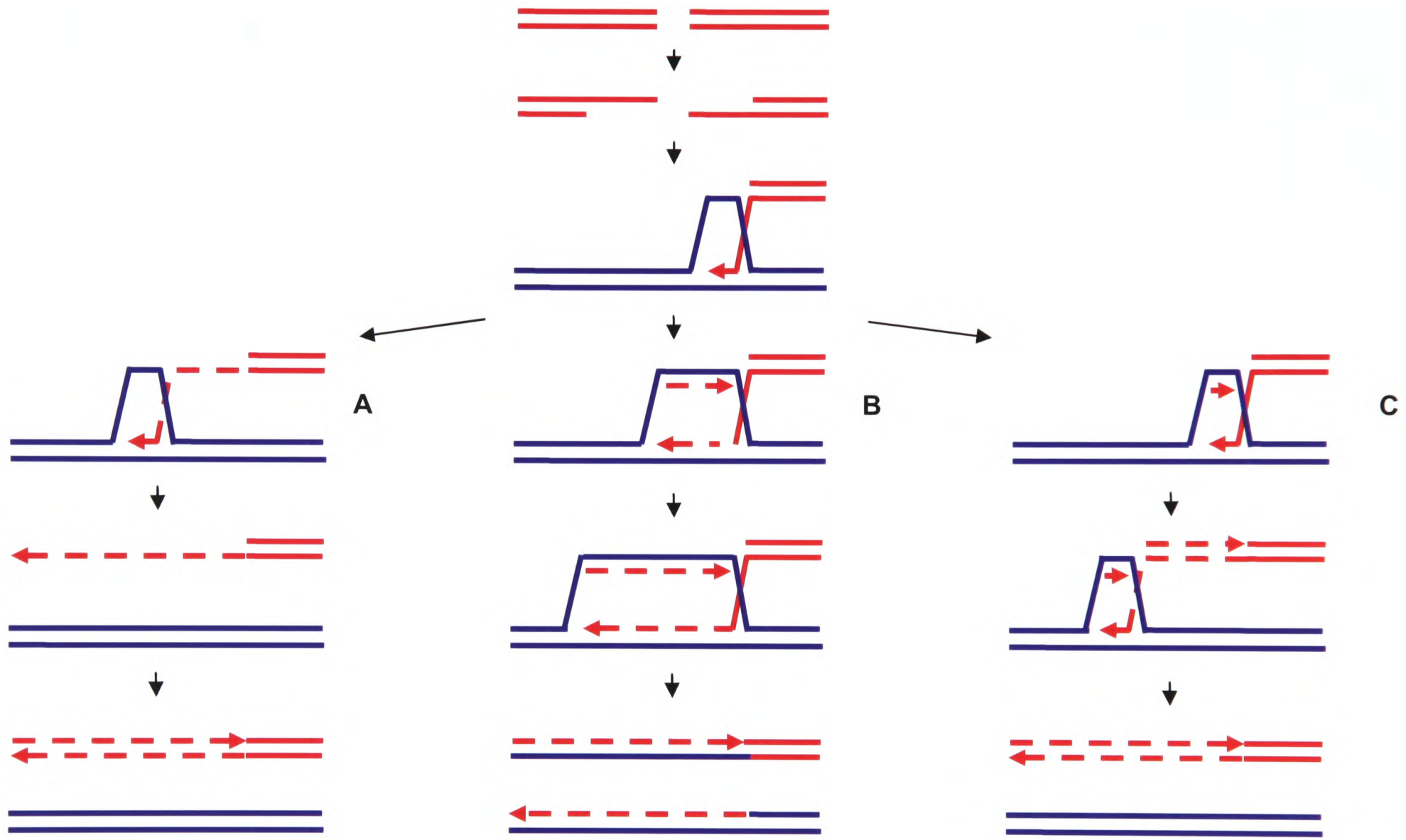



**Figure 1.4. Possible mechanisms of BIR.** **A.** Strand invasion leads tothe synthesis of a single new strand via a replication bubble migration type mechanism. This leads to the formation of a non-reciprocal translocation via a conservative process. **B.** A unidirectional replication fork assembles after strand invasion, which p roceeds towards the end of the template chromosome. HJ resolution results in the formation of semi-conservative replication products. **C.** Branch migration acts to promote conservative BIR. Adapted from McEachern and Haber, 2006.

branch migration might act with a migrating replication fork to remove newly synthesised DNA in a conservative manner.

### 1.3.2. GENES AND PROTEINS INVOLVED IN HR.

Genes and proteins involved in DSB repair were initially identified as IR sensitive mutants in budding yeast (Game and Mortimer, 1974). Subsequent identification of functional and structural homologues in other organisms (Table 1.2) has come about through a number of approaches including homology searches, complementation assays, genetic screens and degenerate PCR based techniques. In *S. cerevisiae*, HR requires proteins encoded by the *RAD52* epistasis group of genes. This group can be divided into two subfamilies; the *RAD51*, *RAD52*, *RAD54*, *RDH54*, *RAD55*, *RAD57*, and *RAD59* subfamily, which play a major role in strand invasion, break stabilization and branch migration; and the *MRE11*, *RAD50* and *XRS2* subfamily, which play roles in break recognition, resection, stabilization and checkpoint activation. Other important genes and proteins involved in HR e.g. Exo1, Srs2, RecQ helicases, and those with more general functions throughout cellular growth, e.g. RPA, will also be discussed.

#### 1.3.2.1. The MRX(N) complex and Exo1.

Insofar has been observed, null mutants of *MRE11*, *RAD50* or *XRS2* in *S. cerevisiae* have similar phenotypes i.e. sensitivity to DNA damaging agents, defects in both HR and NHEJ, aberrant checkpoint activation, telomere shortening and slow growth (Dudas and Chovanec, 2004). Deletion of homologues in higher eukaryotes leads to embryonic lethality, although various point mutations have been observed which are associated with genome instability syndromes such as ataxia-telangiectasia (A-T) like-disorder (A-TLD) and Nijmegen breakage syndrome (NBS) (Varon et al., 1998;

**Table 1.2. HR repair proteins identified in *S. cerevisiae*, *S. pombe* and humans.**

| *S. cerevisiae* | *S. pombe* | Humans | Biochemical function |
|---|---|---|---|
| Rad51 | Rhp51 | RAD51 | ATP-dependent DNA binding activity, DNA strand exchange activity. |
| Rad52 | Rad22 | RAD52 | DNA binding activity, ssDNA annealing activity, weak homologous pairing and strand exchange activities. |
| Rad54 | Rhp54 | RAD54 | DNA binding activity, dsDNA-dependent ATPase activity, dsDNA unwinding activity, branch migration. |
| Rdh54/Tid1 | Rdh54 | RAD54B | DNA binding activity, dsDNA-dependent ATPase activity. |
| Rad55 | Rhp55 | RAD51L2 | DNA binding activity, homologous pairing activity. |
| Rad57 | Rhp57 | XRCC3 | DNA binding activity, homologous pairing activity. |
| Rad59 | - | - | DNA binding activity, weak ssDNA annealing activity. |
| Mre11 | Rad32 | MRE11 | 3'-5' dsDNA exonuclease activity, ssDNA endonuclease. |
| Rad50 | Rad50 | RAD50 | ATP-dependent DNA binding. |
| Xrs2 | Nbs1 | NBS1 | Regulates DNA unwinding and nuclease activites of MRN. |

Stewart et al., 1999). Interestingly, proteins encoded by the *MRE11*, *RAD50*, and *XRS2* gene subfamily exist as a functional heterotrimeric molecule *in vivo* known as the MRX complex (MRN complex in *S. pombe* and mammals (see below); reviewed in D'Amours and Jackson, 2002). Several lines of evidence suggest that MRX(N) is the initial break sensor and accumulates at unresected DSB ends, suggesting it may be an important protein which can regulate pathway utilisation (Ira et al., 2004). Mre11 (*S. pombe* Rad32) has two DNA binding motifs and contains a nuclease domain which displays 3'-5' exonuclease activity towards ssDNA and dsDNA substrates *in vitro*, in addition to a structure specific ssDNA endonuclease activity (Trujillo and Sung, 2001; van den Bosch et al., 2003). Rad50 (*S. pombe* Rad50) is similar to the SMC family of proteins involved in sister chromatid cohesion and contains N-terminal Walker A and C-terminal Walker B motifs separated by a long coiled-coil domain. This structure can fold back on itself allowing both the Walker A and B motifs to interact, leading to the formation of a globular ABC ATPase domain (Hopfner et al., 2001) (Raji and Hartsuiker, 2006). A zinc hook is also formed at the apex of the coiled coil which is believed to mediate intermolecular interactions between other Rad50 molecules to promote break stabilisation (See below). The *XRS2* gene sequence has diverged rapidly over the course of evolution, although orthologues have been identified in both *S. pombe* and mammals (*nbs1*$^{+}$/*NBS1*, respectively; Matsuura et al., 1998; Chahwan et al., 2003; Ueno et al., 2003). NBS1 is a known substrate of the A-T mutated (ATM) protein proximal kinase (Section 1.4) and deletions result in defects in the intra-S phase checkpoint (Dudas and Chovanec, 2004). Indeed, Xrs2 has been shown to interact with the ATM homologue in *S. cerevisiae*, Tel1, and recruit it to the break site, a process which is required for efficient checkpoint activation in response to DNA damage (Falck et al., 2005).

The MRX(N) complex has several roles during HR repair (Figure 1.5a). Interestingly, a variety of evidence exists to suggest that this complex plays an important role in the 5'-3' resection of DSBs. Indeed, in addition to null mutations, various nuclease dead alleles of *MRE11* (*mre11-nd*) have defects in the processing of meiotic DSBs and a subset of IR induced damage (Moreau et al., 1999; Lee et al., 2002). This suggests that Mre11 and its nuclease activity are required for efficient break resection. It is interesting to note however, that *mre11-nd* alleles are not as sensitive to IR as *mre11Δ* (Llorente and Symington, 2004). Furthermore, *mre11-nd* alleles show no defects in the resection of a single HO-induced DSB, unlike *mre11Δ* strains (Moreau et al., 1999). The sensitivity of *mre11-nd* alleles to IR but not single HO-induced breaks was originally assumed to reflect an inability of mutant MRX(N) to process multiple break structures. However, it was recently shown that a nuclease dead allele, *mre11-D56N*, does not affect the kinetics or extent of ssDNA formation in response to multiple HO/phleomycin-induced breaks (Llorente and Symington, 2004). Together, these data suggest that whilst the MRX(N) complex is required for efficient resection at all DSBs, the nuclease activity of Mre11 is required for the processing of complex break structures produced via IR radiolysis or where break resection is inhibited by the presence of protein adducts e.g. Spo11 in meiosis (Llorente and Symington, 2004) . Indeed, MRX(N) may recruit an alternative exonuclease to the break or provide conditions wherein efficient resection can occur e.g. by unwinding duplex DNA and providing access to an as of yet unidentified ssDNA exonuclease. Interestingly, it has recently been suggested that Mre11 may be activated through a Cdk1 dependent phosphorylation event to promote resection (Ira et al., 2004). Surprisingly, however, 5' to 3' resection and repair at the mating-type locus of *S. cerevisiae*, although delayed, is not abolished in *rad50Δ*, and *xrs2Δ* backgrounds (Ivanov et al., 1994), suggesting that other factors exist to resect DSBs in the absence of MRX(N).

One such factor is encoded by the *EXO1* gene. Exo1 is a 5'-3' exonuclease that was originally identified through its ability to generate ssDNA from dsDNA substrates (Fiorentini et al., 1997). It is a member of a conserved family of nucleases which includes FEN-1 and XPG in humans, and is known to play roles in DNA replication, mismatch repair and HR (Tishkoff et al., 1997). *exo1Δ* is not affected by but acts synergistically with *mre11Δ* for IR sensitivity (Moreau et al., 2001), suggesting that Exo1 is not recruited by the MRX(N) complex to breaks. This correlates with studies in *S. pombe* where it was shown that, unlike *rad50Δ* or *exo1Δ* mutants, a *rad50Δexo1Δ* double mutant has impaired Rhp51 (Rad51 homologue *S. pombe*) foci formation following exposure to IR (Tomita et al., 2003). Furthermore, *EXO1* in high copy number can partially suppress the IR sensitivity and delayed mating type switching of *mre11Δ* mutants (Lewis et al., 2002). Together, these data suggest that Exo1 plays a redundant, although lesser role with MRX(N) in the 5'-3' resection of DSBs *in vivo* (Figure 1.5a).

Recent structural analysis and *in vitro* data has proposed that the MRX(N) complex may also function to tether both ends of a DSB together, thus facilitating second end capture during DSB repair (de Jager et al., 2001; Hopfner et al., 2002) (Figure 1.5a). Indeed, deletion of MRX components and mutations which affect the zinc hook of Rad50 leads to the mitotic mis-segregation of acentric chromosomal fragments produced by an unrepairable I-SceI-induced DSB (Lobachev et al., 2004). Furthermore, *rad50Δ* mutants in both budding and fission yeast display an increase in spontaneous HR between homologous chromosomes and reduced sister chromatid recombination (Bressan et al., 1999; Hartsuiker et al., 2001). These observations suggest that the MRN(X) complex can promote both intra and inter-chromatid interactions during HR repair and thus prevent second end loss or allelic recombination which can lead to LOH. This view was strengthened by recent data

suggesting that the MRX(N) complex is required for the recruitment of SMC5-6 to sites of DSB damage in mammalian cells (De Piccoli et al., 2006).

### 1.3.2.2. The *RAD51*, *RAD52*, *RAD54*, *RDH54*, *RAD55*, *RAD57*, *RAD59* subfamily and RPA.

*rad51* null mutants in yeasts (including *S. pombe*) are viable but display defects in mitotic recombination and are highly sensitive to IR and various other DNA damaging agents (reviewed in Dudas and Chovanec, 2004; Muris et al., 1993). Interestingly, *RAD51*$^{-/-}$ knockout mice arrest early in embryonic development (Tsuzuki et al., 1996). Furthermore, depletion of *RAD51* in DT40 chicken cells results in $G_2$/M cell cycle arrest and the accumulation of visible chromosome breaks (Sonoda et al., 1998). Together, these data suggest that *RAD51* is required for the repair of damage generated during DNA replication in vertebrate cells. Rad51 is a homologue of the bacterial RecA protein and plays a major role in the strand exchange reaction of HR (Figure 1.5a). It has been shown to bind to resected 3'-ssDNA tails with high affinity *in vitro* to produce a 'right handed' nucleoprotein filament capable of invading homologous dsDNA (Sung, 1994; Mazin et al., 2000b; Aylon and Kupiec, 2004). It is important to note that Rad51 can bind to ssDNA and dsDNA in an ATP-dependent manner with similar affinity *in vitro* (Shinohara et al., 1992), suggesting that processes must exist to prevent indiscriminate binding to the genome and that additional factors control appropriate nucleofilament formation onto ssDNA. The homology search itself is still poorly characterized but various data suggest that a relatively large region could be probed (Inbar and Kupiec, 1999). The efficiency of the *in vitro* strand exchange reaction can be increased by the addition of RPA (replication protein A), which is believed to remove secondary structures and facilitate the formation of a continuous Rad51 filament (Sugiyama et al., 1997). RPA

is a heterotrimeric protein complex (encoded by *RFA1*, *RFA2* and *RFA3* in *S. cerevisiae*) similar to the single strand binding (SSB) protein of *E. coli*. The complex itself is known to play an essential role in DNA replication and recombination through its ability to bind to ssDNA (Heyer et al., 1990; Firmenich et al., 1995). Interestingly, RPA appears to inhibit efficient strand invasion by Rad51 if it is added simultaneously to the strand exchange reaction (Sung, 1997b). Rad51 can successfully displace RPA, however, when mediator proteins i.e. Rad52 and Rad55/Rad57 are present, suggesting that the latter function to load Rad51 and initiate nucleation of the nucleofilament (Sung, 1997b; Sung, 1997a). A replication proficient but recombination deficient allele in the large subunit of RPA, *rfa1-t11*, has no defect in Rad51 nucleofilament formation but is unable to invade a homologous template, suggesting that RPA may also play an important role in strand invasion *in vivo* (Wang et al., 2004). Surprisingly, Rad51 is not required for all mitotic recombination and in some assays, such as those measuring direct repeat and spontaneous recombination, it is less important than Rad52 (Paques and Haber, 1999; See below). This has lead to the proposal of both *RAD51*-dependent and independent pathways of HR.

Several Rad51 paralogs have also been identified in both vertebrates and yeast. Both *RAD55* and *RAD57* (*S. pombe* $rhp55^{+}$ and $rhp57^{+}$) show weak homology to RecA/Rad51 and the proteins encoded by these genes interact to form a heterodimer *in vivo* (Kans and Mortimer, 1991; Lovett, 1994; Sung, 1997b). Rad55 also interacts with Rad51 (Johnson and Symington, 1995). In contrast, the *S. pombe* Rhp55/Rhp57 heterodimer has been shown to interact with Rhp51 via the Rhp57p subunit (Tsutsui et al., 2001). Mutations in either *RAD55* or *RAD57* result in sensitivity to IR which is exacerbated at lower temperatures (Dudas and Chovanec, 2004). Such cold sensitivity is usually associated with proteins that are members of multi-subunit complexes. *In vitro* data shows that the Rad55/Rad57 heterodimer can also stimulate Rad51-

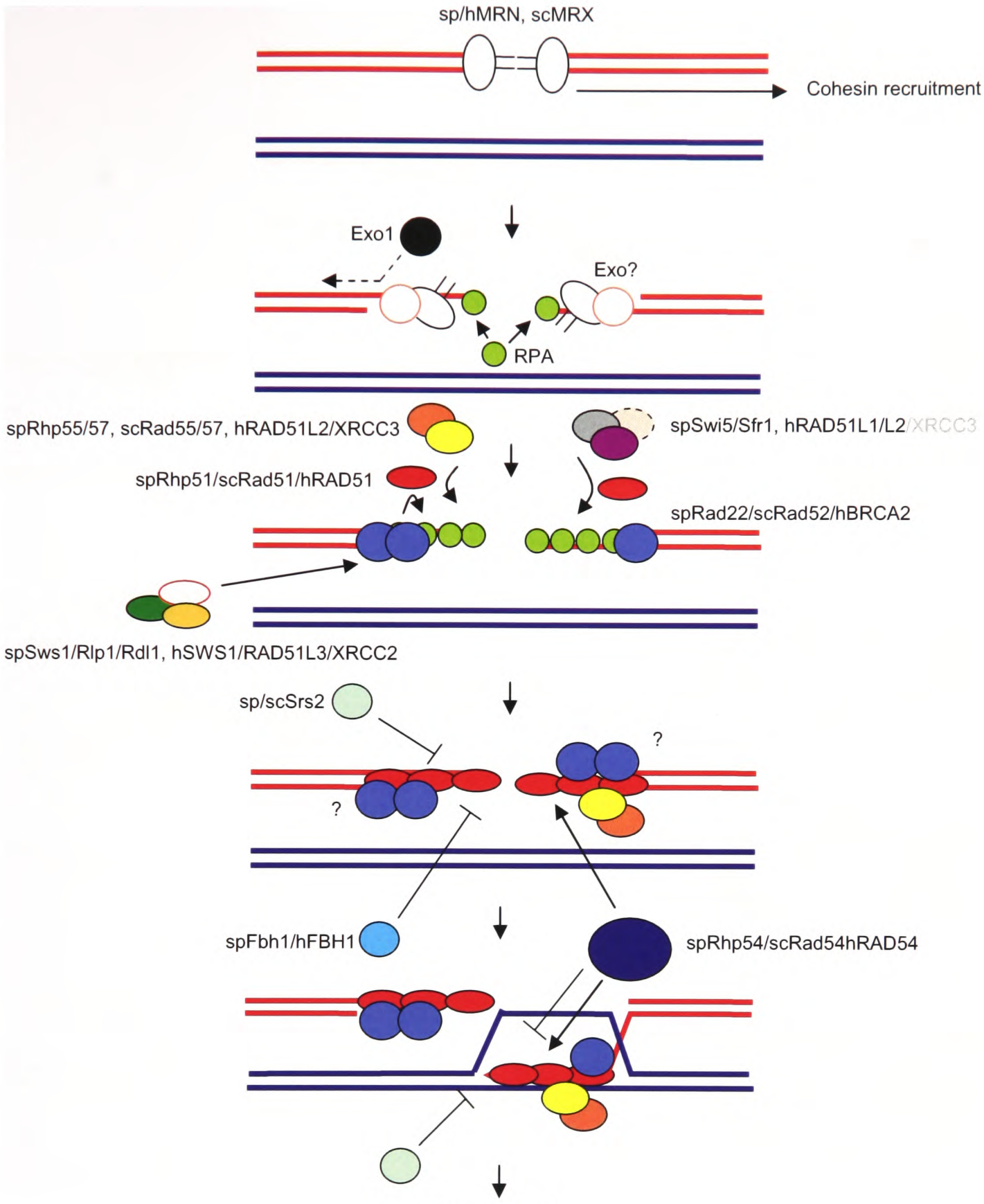



**Figure 1.5b**

**Figure 1.5a. Model of upstream events during DSB repair in eukaryotes.** The MRN/X complex arrives at the break and, with the help of other nucleases (including Exo1), facilitates 5'-3' resection of the DSB. The 3'-ssDNA ends produced from this process are rapidly bound by RPA, after which Rhp51/Rad51 is subsequently loaded by a process involving several mediator proteins and complexes e.g. Rad22/Rad52 and Rad55/57 (see text for details). XRCC3 has only been identified in mammalian cells. Rad22 binding is promoted by the Sws1/Rlp1/Rdl1 complex. The resultant Rhp51-Rad22-(Rhp55/57?)-ssDNA nucleofilament then promotes a homology search, which could be facilitated through the action of Srs2, Fbh1 and Rhp54. These proteins also play a role in attenuating nucleofilament formation as shown. The D-loop generated through invasion may also be stabilised through the action of Rhp54/Rad54. See Figure 1.5b for the remaining steps in the model. sp; *S. pombe*, sc; *S. cerevisiae*, h; human/mammalian.

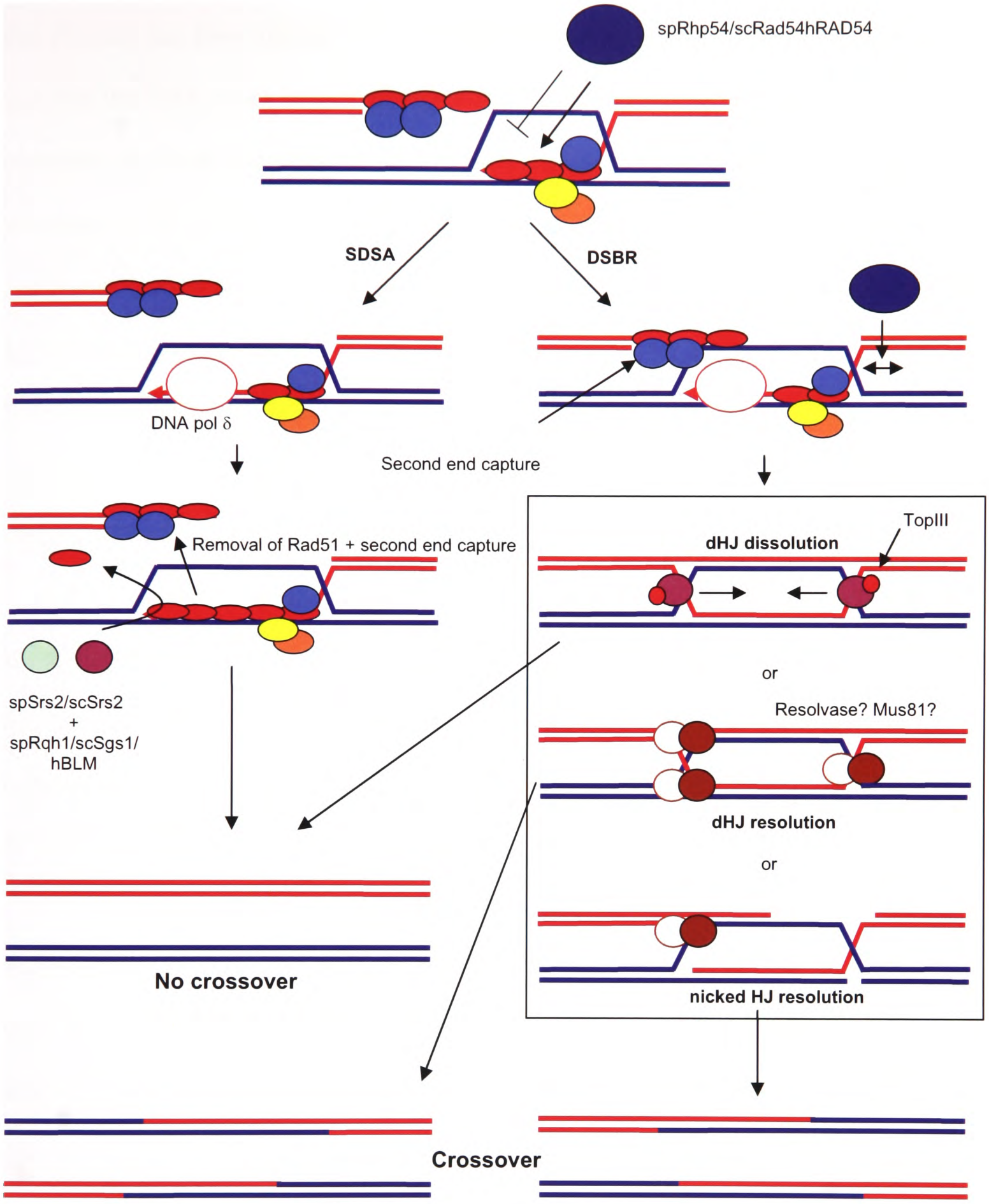



**Figure 1.5b. Model of downstream events during DSB repair in eukaryotes.** After strand invasion and heteroduplex formation, DNA pol extends the D-loop through DNA replication. Repair may subsequently occur via either SDSA or DSBR pathways. In SDSA, Srs2 and/or Rqh1/Sgs1 promote the dissociation of the D-loop, facilitating second end capture and the formation of non-crossover products. In DSBR, DNA replication by DNA pol facilitates second end capture to produce a dHJ which is processed by Sgs1/TopIII into a hemicatenated structure which results in non-crossover products. Alternatively, the dHJ formed may be cleaved by a HJ resolvase e.g. Mus81, to produce crossover products. It has also been proposed that Mus81-Eme1 cleaves nicked Holliday junctions to produce crossovers (Osman *et al.*, 2003) . sp; *S. pombe*, sc; *S. cerevisiae*, h; human/mammalian.

mediated strand exchange in the presence of inhibitory RPA (Sung, 1997b). Indeed, this function has been supported by the identification of *rad51* alleles that partially suppress the DNA repair defects of *rad55* and *rad57* mutants by allowing Rad51 to overcome the inhibitory effect of RPA (Fortin and Symington, 2002). This process still requires the presence of Rad52, however. Furthermore, both the cold sensitivity and recombination defects of *rad55Δ* and *rad57Δ* strains can be partially suppressed by the overexpression of Rad51 or completely suppressed by the overexpression of both Rad51 and Rad52 (Johnson and Symington, 1995; Hays et al., 1995). Thus, both Rad55/Rad57 and Rad52 play a crucial role in Rad51 nucleofilament formation (Figure 1.5a). Moreover, it appears that Rad55/Rad57 plays a greater role in HR at lower temperatures, perhaps through promoting the Rad52-Rad51 interaction. Rad55 is also phosphorylated in response to DNA damaging agents, although the significance of this is still unclear (Symington, 2002). Recent data from yeast and mammalian cell studies suggests that this complex may also play a post-synaptic role in DSB repair (Hope et al., 2005; Liu et al., 2004).

Recent studies in *S. pombe* have identified further RecA/Rad51 paralogs known as Rlp1 and Rdl1, which show homology to the mammalian Rad51-like proteins XRCC2 and RAD51L3, respectively (Khasanov et al., 2004; Martin et al., 2006). Both *rlp1Δ* and *rdl1Δ* mutants are mildly sensitive to IR and the proteins encoded by these genes physically interact (Khasanov et al., 2004; Martin et al., 2006). Indeed, Rlp1 and Rdl1 form a complex with a Srs2 interacting protein, Sws1, which plays a non-essential role in the loading of Rad22 (*S. cerevisiae* Rad52) onto RPA coated ssDNA (Figure 1.5a; (Martin et al., 2006). In vertebrates the RAD51 paralogs, RAD51L1, RAD51L2, RAD51L3, XRCC2 and XRCC3 (which shows homology to Rad57) were identified using sequence data base searches for homologues of RAD51, or through mutagenic screens in rodent cell lines (reviewed in Thacker and Zdzienicka, 2003). Knockout of

*RAD51*-like genes in mice also has lethal consequences (Shu et al., 1999; Deans et al., 2000). These paralogs have DNA-binding ability, but with different affinities (reviewed in Dudas and Chovanec, 2004). XRCC2 and RAD51L3 are known to form a complex with mammalian SWS1 that has been proposed to fulfil a function in promoting RAD51 nucleofilament formation similar to that of Rlp/Rdl1/Sws1 in *S. pombe* (Martin et al., 2006).

Another protein recently identified in *S. pombe*, Swi5, has suggested there may be further complexity in the pathways mediating Rad51 nucleofilament formation. Swi5 has been shown to interact with Swi2 in mating-type switching and Sfr1 in Rhp51 mediated DNA repair via HR (Akamatsu et al., 2003). It is conserved in higher eukaryotes but has been found to act independently of Rhp57 in yeast (Akamatsu et al., 2003). This has lead to the proposal that Swi5/Sfr1 and Rhp55/Rhp57 act in two parallel but redundant Rhp51 dependent sub pathways for the repair of DSBs (Figure 1.5a). Indeed, a *swi5Δrhp57Δ* double mutant is similar to a *rhp51Δ* mutant for the repair of IR induced DNA damage (Akamatsu et al., 2003).

*RAD52* null strains are more sensitive than any other *RAD* mutant to IR (Dudas and Chovanec, 2004). As expected, *rad52Δ* strains suffer severe defects in mitotic recombination (Sugawara and Haber, 1992), mating-type switching (White and Haber, 1990), *RAD51*-dependent GC (Rattray and Symington, 1994) and BIR (Bosco and Haber, 1998). Indeed, it appears Rad52 is absolutely required for all recombination events in *S. cerevisiae* and is the only member of the *RAD52* epistasis group to be required for SSA. Both yeast and human Rad52 are believed to form ring structures with preferential affinity for ssDNA (Shinohara et al., 1998; Ranatunga et al., 2001; Mortensen et al., 1996). As implied above, Rad52 is thought to bind and stimulate the removal of RPA from 3'-ssDNA tails during HR through promoting

Rad51 nucleofilament formation (Sung, 1997a). Surprisingly, *RAD52*$^{-/-}$ mice are viable and have only a slight sensitivity to IR, suggesting that other factors exist in mammals to promote RAD51-dependent strand invasion (Rijkers et al., 1998). Biochemical data shows that Rad52 can interact with both Rad51 and RPA (Song and Sung, 2000; Krejci et al., 2002). This process is thought to occur with the help of the Rad55/Rad57 complex. *In vitro* data suggests that RAD52 plays a more active role in strand invasion and can promote D-loop formation in the absence of RAD51 (Kagawa et al., 2001). A recent study has demonstrated, however, that Rad51 and Rad52 colocalise *in vivo* during strand exchange (Miyazaki et al., 2004). This suggests that, in addition to a presynaptic role in Rad51 loading, Rad52 plays a significant role during synapsis. The same study also implied a post-synaptic role for Rad52 in DSB repair, which correlates with more recent findings. Indeed, in addition to *in vitro* data which shows that Rad52 can promote annealing between complementary ssDNA substrates (Dudas and Chovanec, 2004), recent evidence has revealed that Rad52 is involved in second-end capture through its interaction with RPA during HR (Sugiyama et al., 2006). Thus, in addition to strand invasion, Rad52 also appears to play a role in break stabilization (Figure 1.5a). Again, this later role has been confirmed by data which has shown that acentric break fragments can mis-segregate during mitosis in the absence of Rad52 (Kaye et al., 2004). Two Rad52 homologues have been identified in *S. pombe*, Rad22 and Rti1. A *rad22Δ* mutant is highly sensitive to IR, whereas a *rti1Δ* strain is only mildly affected (Muris et al., 1997; van den Bosch et al., 2001). In addition, both Rad22 and Rti1 have been shown to interact with each other, Rhp51 and RPA (Raji and Hartsuiker, 2006). In vertebrates, BRCA2 is believed to play a role like yeast Rad52 in the formation of nucleofilaments by RAD51 (Esashi et al., 2005; Esashi et al., 2007) (Figure 1.5a).

In *S. pombe*, *rhp54* null mutants are highly sensitive to IR and other DNA-damaging agents (Muris et al., 1996). The budding yeast homolog, *rad54*Δ, is also sensitive to IR, shows defects in GC and exhibits genome-wide chromosome loss (Dudas and Chovanec, 2004). Deletion of *RAD54* in mammals results in similar phenotypes although *RAD54*$^{-/-}$ mice are viable (Essers et al., 1997). A homologue to *RAD54*, *RDH54* (*S. pombe rdh54*$^{+}$), has also been identified in yeasts which appears to play a role in meiotic DSB repair via HR (Klein, 1997; Catlett and Forsburg, 2003). Both Rad54 and Rdh54 show homology to members of the Swi2/Snf2 family of dsDNA-stimulated ATPases which are involved in chromatin remodelling (Eisen et al., 1995). They do not exhibit helicase activity but can translocate across DNA structures to promote conformational changes such as positive and negative supercoiling (Swagemakers et al., 1998; Sigurdsson et al., 2002; Van Komen et al., 2000). Evidence also exists which suggests that Rad54 can move nucleosomes along DNA (Dudas and Chovanec, 2004), a process that could expose the break to other repair factors. *In vitro* experiments show that both Rad54 and Rdh54 stimulate D-loop formation in the presence of Rad51 and RPA (Petukhova et al., 1998). This process requires the dsDNA stimulated ATPase activity of these proteins and mutations in this domain affect DSB repair via HR *in vivo* (Petukhova et al., 1999b). Indeed, human RAD54 has also been shown to promote D-loop formation in a similar manner (Sigurdsson et al., 2002; Mazina and Mazin, 2004). It has been suggested that Rad54 translocation via ATP hydrolysis can promote positive and negative supercoiling which may open the dsDNA substrate and render it accessible to strand invasion by the Rad51 nucleofilament (Figure 1.5a). Recent studies suggest that Rad54 may play additional roles during HR repair that are unrelated to chromatin remodeling. Intriguingly, Rad54 has been shown to enhance the assembly of Rad51 nucleofilaments through direct interaction (Mazin et al., 2000a; Mazin et al., 2003), promote Rad51 dissociation from D-loop complexes in an ATP dependent manner

(Solinger et al., 2002) and support branch migration of Holliday junctions (Bugreev et al., 2006) . It has been suggested from this and the data described above that Rad52, the *RAD51* paralogs, Srs2 (see below) and Rad54 come together to promote a dynamic balance between: the appropriate formation of Rad51 nucleofilaments and strand invasion; the initiation of downstream HR events by disrupting post-synaptic Rad51-sdDNA complexes; and the reversal of 'dead end' complexes that may form as a result of inappropriate nucleofilament formation or invasion during the homology search (Figure 1.5a) (Symington and Heyer, 2006).

The *RAD59* gene was identified in a screen for genes required for *RAD51*-independent spontaneous mitotic recombination (Bai and Symington, 1996). Indeed, *rad59* null mutants are sensitive to IR and show defects in mitotic recombination (Bai and Symington, 1996). Rad59 can also promote the annealing of complementary ssDNA *in vitro*, similar to the action of Rad52 (Petukhova et al., 1999a). Interestingly, *rad59* null mutants fail to undergo mitotic recombination in the absence of the *RAD52* gene (Davis and Symington, 2001), suggesting that Rad59 does not directly substitute for Rad52 function in HR. The homologues of *RAD59* in *S. pombe* and higher eukaryotes have not yet been identified.

BIR was first identified in *S. cerevisiae* as a *RAD52*-dependent but *RAD51*-independent recombination process that also occurred in the absence of *RAD54, RAD55* and *RAD57* (Malkova et al., 1996; Signon et al., 2001). Further analysis of the *RAD51*-independent BIR pathway revealed a requirement for other *RAD52* epistasis group genes including *MRE11*, *RAD50*, *XRS2*, *RAD59* and *RDH54*. Recent work suggests that there may be an additional pathway of BIR in *S. cerevisiae* which is *RAD51*-dependent and thus more efficient than the *RAD51*-independent pathway (Malkova et al., 2005). Indeed, it was later found that the *RAD51*-independent

pathway required a facilitating sequence proximal to the break on the broken chromosome (Malkova et al., 2001). Additional studies using a linear plasmid corroborated with the existence of *RAD51*-dependent and independent pathways and also found that the *RAD50* is not required for *RAD51*-dependent events (Davis and Symington, 2004).

### 1.3.2.3. Srs2/RecQ helicases.

*srs2* null mutants in yeast display a spontaneous hyper-recombinational phenotype (Gangloff et al., 2000; Wang et al., 2001; Doe and Whitby, 2004). *In vitro* data has shown that Srs2 can remove Rad51 from ssDNA (Krejci et al., 2003; Veaute et al., 2003). These data suggest that Srs2 dissociates Rad51-ssDNA complexes to prevent recombination at stalled replication forks and thus promotes post-replicative repair. Deletion of both *SRS2* and *SGS1* leads to a synthetic loss of viability which can be suppressed via deletion of *RAD51*, *RAD55* or *RAD57* (Gangloff et al., 2000). This suggests that both Srs2 and Sgs1 act to destabilise toxic recombination intermediates that form spontaneously in their absence. In addition to its anti-recombinogenic role Srs2 was also found to promote efficient DSB repair via SDSA (Ira et al., 2003) (Aylon et al., 2003). A downstream function is consistent with the fact that a *srs2Δrad54Δ* double mutant is synthetically lethal, which suggests that Srs2 is required to process aberrant nucleofilaments in the absence of Rad54 (Palladino and Klein, 1992). A similar observation has been made in fission yeast, although lethality can be rescued by deletion of $rhp51^{+}$ (Raji and Hartsuiker, 2006). As a result, it was also proposed that Srs2 can dissociate D-loops and thus promote second end capture (Figure 1.5a). However, it has recently been found that Srs2 is unable to dissociate Rad51-dsDNA structures resembling joint molecules intermediates *in vitro* (Veaute et al., 2003). Recent data has also demonstrated that Srs2 can suppress the formation of

crossovers during GC repair of a HO-induced DSB (Ira et al., 2003). This could occur by limiting the extent of nucleofilament formation and affecting the stability of D-loops, thus preventing the formation of dHJs (Lorenz and Whitby, 2006). Srs2 homologues have not been identified in humans as of yet but a related protein found in both *S. pombe* and higher eukaryotes, Fbh1/FBH1, has been shown to play a role in the removal of Rhp51 from ssDNA and has been proposed to perform a similar role to Srs2 in the removal of RAD51 from ssDNA in humans (Lorenz and Whitby, 2006; Symington and Heyer, 2006).

The loss of *RECQ* homologues in yeast and humans has been shown to result in spontaneous hyper-recombination like that observed with *srs2Δ* (reviewed in Karow et al., 2000; Gangloff et al., 2000). By comparison, such data suggest that RecQ helicases suppress aberrant recombination at stalled replication forks. It has been proposed that they perform this function through the reversal of 'chicken foot' structures which can be cleaved by HJ resolvases to give single-ended DSBs and thus promote recombination (Ralf et al., 2006). Consistent with this, partial suppression of the HU and UV sensitivities of an *rqh1Δ S. pombe* strain, which also shows increased levels of recombination after HU treatment (Stewart et al., 1997), can be brought about through the expression of a bacterial Holliday junction resolvase (Doe et al., 2000). Confusingly, loss of *RECQ* homologues leads to a hypo-recombination phenotype for induced recombination (Onoda et al., 2001). Mutations in the human RecQ helicase BLM also result in an increase in sister chromatid exchange (Wu and Hickson, 2003) suggesting that BLM suppresses crossovers during HR. A similar observation has been made in *S. cerevisiae*, where deletion of *SGS1* leads to an increase in DSB-induced GC with an associated crossover (Ira et al., 2003). The idea that RecQ helicases suppress crossovers is further supported by the observation that BLM can dissolve synthetic dHJs *in vitro* to produce hemicatenated structures that

require cleavage by TopIII for resolution (Wu and Hickson, 2003; Wu et al., 2006). This suggests that RecQ helicases prevent crossovers via the DSBR pathway (Figure 1.5b). However, BLM can also act independently of TopIII and has been shown to dissociate D-loops by itself (van Brabant et al., 2000). Genetic data from *S. cerevisiae* are consistent with the idea that Sgs1 functions alone and in conjunction with TopIII. Intriguingly, another RecQ helicase in humans, WRN, has also been shown to disassociate D-loops *in vitro* (Prince et al., 2001; Orren et al., 2002). The ability to reverse D-loop structures suggests that RecQ helicases may also play a role in preventing crossovers by SDSA (Figure 1.5b). Indeed, Srs2 and RecQ helicases may act to prevent homeologous interactions during strand invasion by dissolving dHJs or dissociating D-loop type structures to promote the homology search.

### 1.3.3. NON-HOMOLOGOUS END JOINING (NHEJ).

NHEJ plays a major role in DSB repair in higher eukaryotes. Mammalian cell lines with mutations in NHEJ genes show greater sensitivity to IR than that of HR mutants (Gu et al., 1997; Nussenzweig et al., 1997). Furthermore, a significant proportion of I-SceI endonuclease-induced DSBs (50%-70%) are repaired via NHEJ in mammalian cells (Liang et al., 1998a). This is an different situation to that observed in yeast, where HR is the predominant DSB repair pathway (Jeggo, 1998). Various forms of NHEJ are known to exist in all organisms, ranging from the simple re-joining of DSB ends to those which utilize the presence of nearby homologous sequences for repair, so called micro-homology mediated end joining (Pfeiffer et al., 1994).

Mechanistically, NHEJ can be divided into three steps (Figure 1.6; see Weterings and van Gent, 2004 for a review). First, the DSB is detected by the binding of NHEJ-

specific proteins to the ends of the break, forming a molecular bridge that acts to stabilize the DSB and bring ends into close proximity. This process also prevents degradation of DSB ends that may promote loss of genomic material or inappropriate repair via alternative pathways e.g. HR. Secondly, DSB ends are processed (if required) to generate ligatable termini, with the concomitant alignment of the DSB ends via micro-homologies. Finally gap-filling is performed, followed by the final ligation reaction.

### 1.3.4. GENES AND PROTEINS INVOLVED IN NHEJ.

In mammals, NHEJ requires KU, DNA-$PK_{cs}$, XRCC4, LIG4 and Artemis (Moshous et al., 2001; Kuhne et al., 2003). KU has been highly conserved throughout evolution, comprising of two subunits known as Ku70 and Ku80 in both yeast and mammals. These interact to produce a heterodimeric complex that is thought to bind to DSB ends with high affinity during the initial stages of NHEJ, along with the MRX(N) complex (Smith et al., 1999; see below). This is a process which may act to align and protect DSB ends from nucleolytic degradation (Figure 1.6; Bailey et al., 1999; Martin et al., 1999). X-ray crystallography shows that the KU heterodimer has a hollow ring like structure, which binds dsDNA by feeding it through the center of the ring (Weterings and van Gent, 2004). Indeed, KU has also been shown to translocate along DNA in an ATP-independent manner (Smith et al., 1999). KU is not required for all NHEJ pathways, however. For example, micro-homology mediated end joining has been found to occur in the absence of the KU heterodimer (Critchlow and Jackson, 1998). The binding of the MRN complex to DSB ends with KU has been proposed to aid strand alignment prior to ligation and *in vitro* evidence from yeast suggests that MRN promotes end joining (Chen et al., 2001; Huang and Dynan, 2002). The involvement of this complex in NHEJ *in vivo* has only been demonstrated

in *S. cerevisiae*, however (D'Amours and Jackson, 2002). In mammals, the KU complex retains the DNA protein kinase catalytic subunit (DNA-$PK_{cs}$) at DNA ends to form DNA protein kinase (DNA-PK) through an interaction with the KU80 subunit (West et al., 1998; Falck et al., 2005). *In vitro* data shows that this interaction activates the DNA-$PK_{cs}$ domain to phosphorylate downstream proteins including KU, Artemis, XRCC4, itself and various checkpoint proteins (Chan and Lees-Miller, 1996; Calsou et al., 1999; Weterings and van Gent, 2004). Phosphorylation of DNA-$PK_{CS}$ and KU is believed to increase accessibility to DNA ends and is required for repair *in vivo* (Chan et al., 2002). Phosphorylation is also thought to inhibit the binding of XRCC4 to the DSB which may allow processing enzymes, such as Artemis, access to the break. A poorly characterized process then allows XRCC4/LIG4 to bind the DNA-PK complex to repair the DSB (Figure 1.6). Indeed, this interaction is required to stimulate XRCC4/LIG4 ligase activity (Lee et al., 2000). In *S. cerevisiae*, the XRCC4 orthologue Lif1 is also believed to interact with Dnl4 (the LIG4 orthologue), an interaction that is required to promote Dnl4 stability (Herrmann et al., 1998; Chen et al., 2001). Homologues of DNA-$PK_{cs}$ have not been identified in yeasts, consistent with the predominance of HR in these organisms and the probable redundancy of checkpoint signaling (Hefferin and Tomkinson, 2005). Additional factors are required for NHEJ in *S. cerevisiae*, including the Nej1 protein which interacts with and regulates the nuclear distribution of Lif1 (Valencia et al., 2001). Others include members of the DNA integrity checkpoints, such as Rad9, Mec1, Mec3, Rad17, Rad24 and the Sir proteins, Sir2-4. The latter may facilitate NHEJ by altering chromatin structure (Martin et al., 1999; Mills et al., 1999), whilst the checkpoint proteins appear to aid relocation of Ku from telomeres to the sites of DSBs (Martin et al., 1999). In *S. pombe*, *in vitro* analysis suggests the MRN complex and the checkpoint proteins are not required for NHEJ (Manolis et al., 2001). Indeed, the only proteins identified and implicated so far in NHEJ in *S. pombe* are

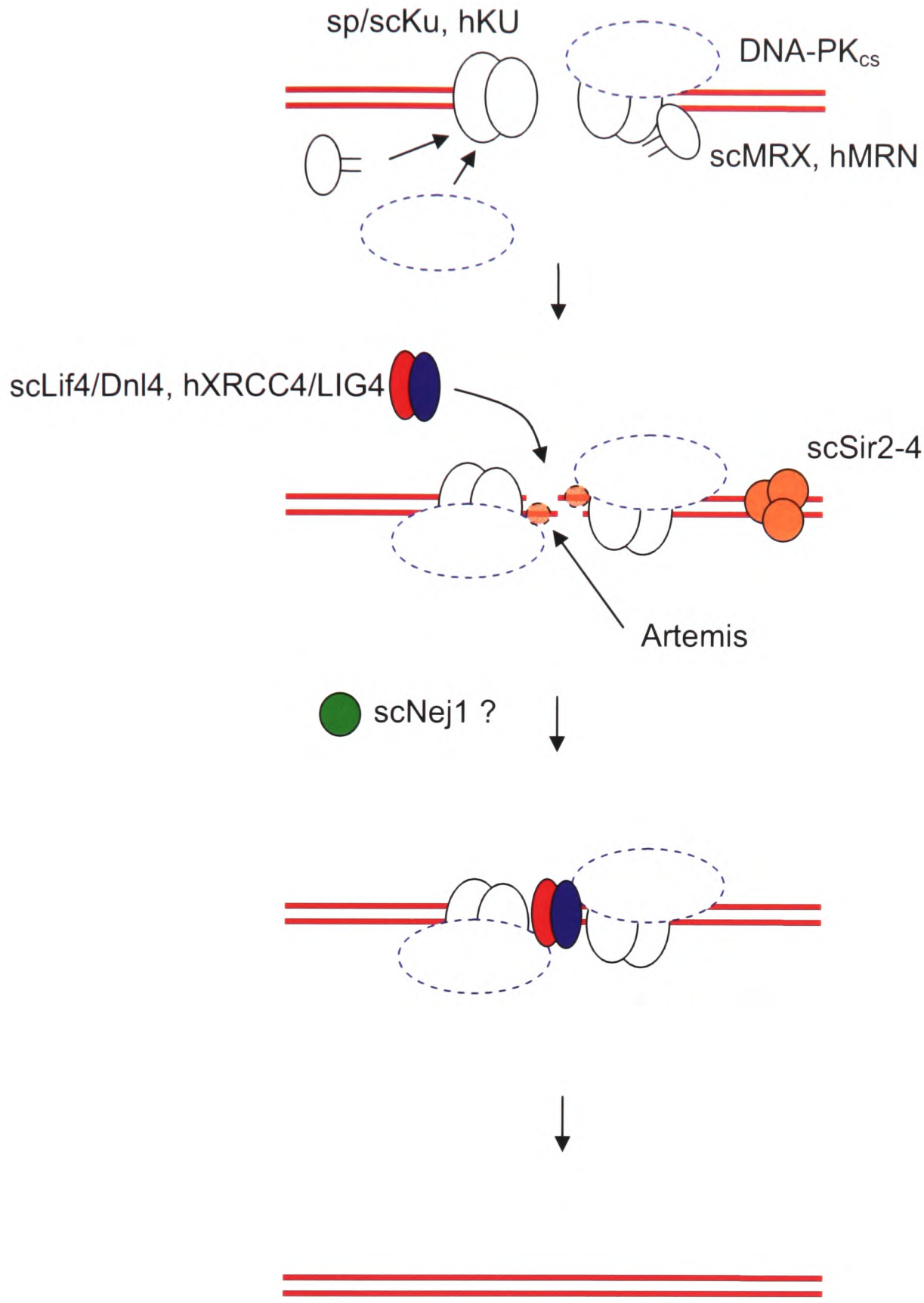



**Figure 1.6. Model of NHEJ in eukaryotes.** DSB ends are bound by Ku (and MRX/N), which aids in the co-ordination of break ends. DNA-$PK_{cs}$ is then recruited to the break by Ku to produce DNA-PK, which subsequently phosphorylates Ku, itself and various other proteins (see text). Break ends are then cleaved (if required) by nucleases ,including Artemis in mammalian cells, after which ends are ligated by the Lif4/Dnl4, XRCC4/LIG4 complex. Other proteins including Nej1 play a role in NHEJ. Human/mammalian proteins not identified in yeast e.g. DNA-$PK_{cs}$, are shown with dashed edges. sp; *S. pombe*, sc; *S. cerevisiae*, h; human/mammalian.

homologues of the mammalian LIG4, KU70 and KU80 proteins. The difference in the requirement for checkpoint proteins between these two yeast remains unclear, although this may reflect the fact that Ku proteins are not sequestered at the telomeres in fission yeast (Manolis et al., 2001).

## 1.4. THE DNA INTEGRITY CHECKPOINTS.

In addition to the DNA repair pathways described above, DNA damage induced via exogenous agents or endogenous processes can lead to the activation of pathways collectively known as the DNA integrity checkpoints. Indeed, cell cycle progression is delayed when cells are exposed to IR. Furthermore, mammalian cells that have defects in cell cycle arrest also exhibit an increase in sensitivity to genotoxic agents (Cliby et al., 1998; Lavin and Shiloh, 1997). Thus, checkpoint pathways appear to play a crucial role in maintaining genome stability through abrogating cell cycle progression, presumably to give cells time to repair damaged DNA. However, a variety of evidence suggests that, in addition to promoting cell cycle delay, the proteins involved in activating the DNA integrity checkpoints may also play a more direct role in DSB repair, as well as promoting transcriptional responses and sensitizing cells to apoptosis (at least in higher eukaryotes; Table 1.3). The cell cycle can be divided into phases comprising growth (phases G1 and G2), replication of genomic material (S-phase) and segregation of duplicate genomes into daughter cells (mitosis or M-phase). Progression through these phases requires the activity of cyclin dependent kinases (CDKs), which are regulated via a multitude of factors in yeast and mammals, including the DNA integrity checkpoints (reviewed in Mendenhall and Hodge, 1998; Obaya and Sedivy, 2002). Damage incurred during G1 activates a checkpoint response that prevents progression into S-phase. Unreplicated DNA leads

to the activation of the S-M phase checkpoint which prevents entry into mitosis, whilst DNA damage or a delay in DNA replication results in activation of the intra-S-phase checkpoint. In addition to halting cell cycle progression, the intra-S-phase checkpoint leads to the stabilization of replication forks and the inhibition of late firing replication origins (Boddy and Russell, 2001; Santocanale and Diffley, 1998). Finally, as expected, the G2/M checkpoint prevents entry into mitosis in response to damage incurred during G2 phase. The signalling cascades that enforce and amplify these responses ultimately result in the inactivation of CDKs through the inhibition of phosphatases and activation of kinases which regulate CDK activity (Mendenhall and Hodge, 1998; Obaya and Sedivy, 2002). The signalling cascades themselves in yeasts and humans can be described according to the functional roles of the key participating proteins (Figure 1.7): sensors, including proximal kinases; adaptors and; effector kinases (reviewed in Melo & Toczyski, 2002). Although an important area of research, cell cycle checkpoint activation is not the main focus of this Thesis, and as a result the reader is referred to a number of excellent reviews on the topic (Bartek and Lukas, 2007; Melo and Toczyski, 2002).

## 1.5. CELL CYCLE REGULATION OF REPAIR MECHANISM.

Although HR and NHEJ have been extensively studied, it is unclear how pathway utilization is regulated in response to DSBs. *KU70*$^{-/-}$ mammalian cells exhibit higher sensitivity to IR in G1/early S phase but are more resistant to IR in late S/G2 phase (Jeggo, 1990; Jeggo, 1997; Lee et al., 1997). Conversely, a *RAD54*$^{-/-}$ cell line is less resistant to IR in late S/G2 phase compared to G1 (Takata et al., 1998). This suggests that NHEJ has a predominant role in G1/early S phase where there is a lack of a repair template and that HR may be required to repair DSBs during G2 where a homologous

**Table 1.3. Evidence of direct roles for checkpoint factors in DSB repair and apoptosis.**

| Protein | Evidence | Reference |
|---|---|---|
| scRad24<br>spRad17 | Deletion of *RAD24* delays DSB end processing and repair in *S. cerevisiae*, resulting in cell death. Further evidence suggests this is not due to an inability to arrest cell cycle.<br>Repair via NHEJ is inefficient in *rad24* mutants.<br>Some *rad17* mutants display radiation sensitivity without abberant checkpoint activation. | Aylon and Kupiec, 2003.<br>De la Torre-Ruiz *et al.*, 1999.<br>Griffiths *et al.*, 1995. |
| scRad17 | Encodes a 3'-5' exonuclease that may be involved in DSB end processing. | Lydall and Weinert, 1995. |
| hATM | ATM-dependent phosphorylation of RAD51 promotes interaction with RAD52 *in vitro*. | Chen *et al.*, 1999. |
| spCrb2 | Role for Crb2 and Cdc2/Cyclin B in regulating HR repair. | Caspari *et al.*, 2002. |
| scRad53/Mec1 | Rad53 and Mec1 dependent phosphorylation of Rad55 promotes recovery after genotoxic stress. Checkpoint activation required? | Herberg *et al.*, 2006. |
| hCHK1 | CHK1 phosphorylates RAD51 in response to HU treatment, a modification required to promote HR dependent repair of stalled replication forks. | Sorensen *et al.*, 2006. |
| hCHK2 | CHK1 and CHK2 phosphorylate and activate the transcription factor p53, which plays a major role in apoptosis and the transcriptional responses to DNA damage. | Su., 2006. |

sequence is present. Indeed, further evidence is emerging to suggest that repair mechanism choice is regulated by cell cycle phase. Recent studies using a HO-inducible system in *S. cerevisiae* have shown that cells synchronized at G1 and released or blocked at G2 prior to DSB induction efficiently perform HR. Cells blocked at G1 prior to the formation of the break, however, fail to repair DSBs via HR and use NHEJ (Aylon et al., 2004). Further analysis of break ends in this system revealed that 5'-3' resection did not occur in G1 blocked cells, whereas processing was observed in cycling cells synchronised at G1 or blocked in G2 (Aylon et al., 2004). This data suggests that DSB ends do not undergo processing until S and/or G2 phase, and thus remain stable in G1. Intriguingly, biochemical studies have demonstrated that purified KU from humans binds preferentially to stable free ends, whilst RAD52 prefers ssDNA (Frank-Vaillant and Marcand, 2002). Furthermore, it has also been shown that Rad52 foci fail to form in G1 arrested cells in budding yeast (Lisby et al., 2004). The activity of NHEJ and HR thus correlates extremely well with the processing of ends during the cell cycle and the preferred substrate specificities of the major players in both of these DSB repair mechanisms. Since DSB processing was observed in cells synchronized and released from G1, this suggests that factors affecting cell cycle progression are directly involved in determining pathway utilization. Consistent with this, CDK activity appears to promote DSB processing via 5'-3' resection, which aids repair via HR and promotes checkpoint activation in *S. cerevisiae* (Aylon et al., 2004; Ira et al., 2004). It is unclear, however, how CDK promotes resection although it has been proposed that it might phosphorylate and direct the function of the MRN complex towards the initiation of resection. It has also been suggested that CDK activity has a downstream role in repair via HR (Ira et al., 2004).

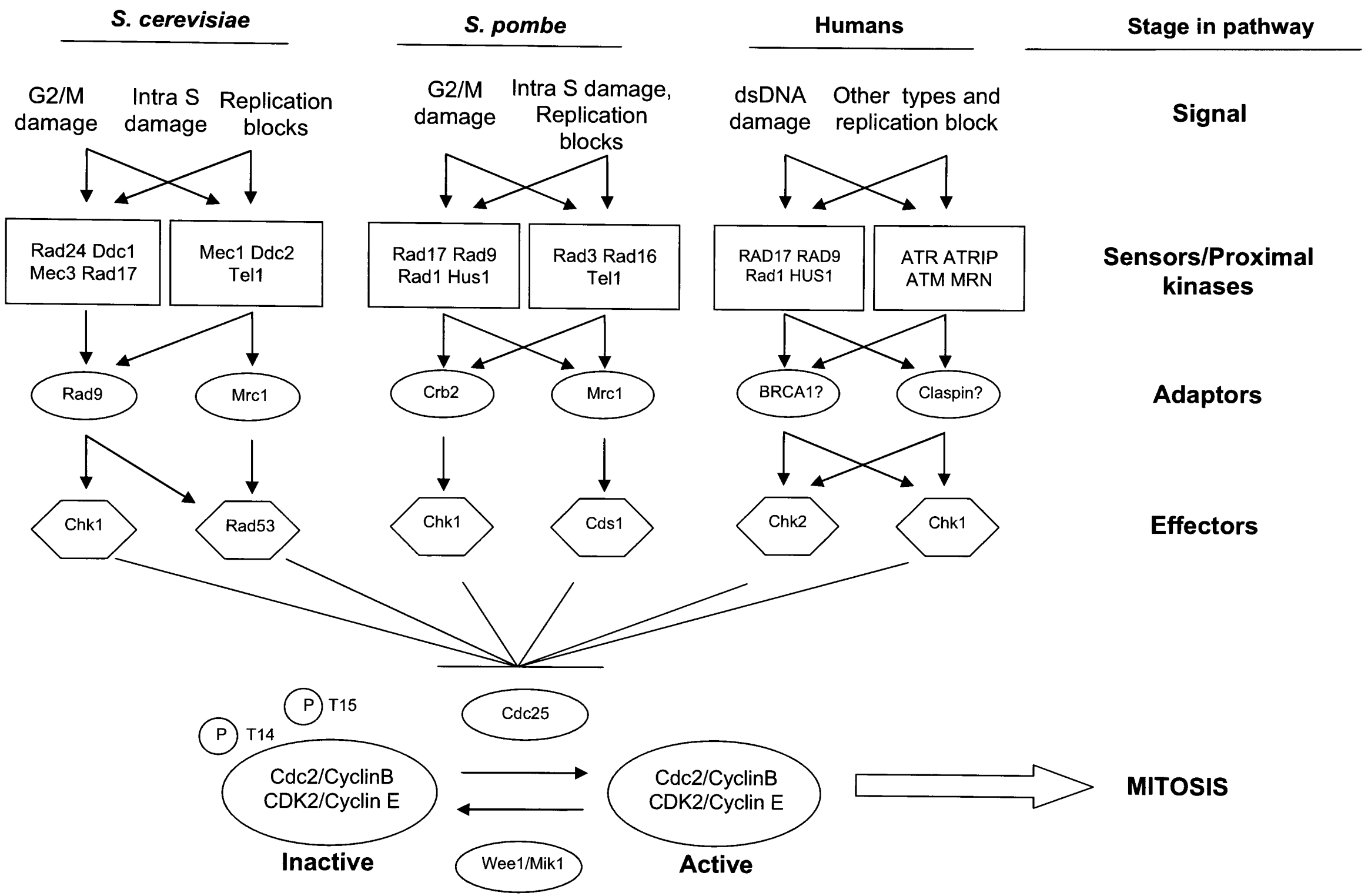



**Figure 1.7. Checkpoint response pathways in yeasts and humans.** Adapted from Meloand Toczyski , 2002.

In addition to cell cycle phase, other factors have been implicated in the regulation of HR repair and NHEJ. For example, cell ploidy also appears to have a bearing on DSB repair mechanism choice. In *S. cerevisiae*, it has been shown that in diploid cells, NHEJ is down-regulated (Valencia *et al.*, 2001), although the reason for this is not clearly understood.

## 1.6. TELOMERES, TELOMERASE AND DSBS.

### 1.6.1. Telomere structure and maintenance.

Telomeres are specialised DNA-protein structures present at the ends of linear eukaryotic chromosomes which are essential for the maintenance of genomic integrity (Viscardi et al., 2005). Although similar to the ends of a DSB, telomeres do not activate DNA integrity checkpoints and are usually protected from end to end fusions or other processing events that function to repair DSBs. In general, telomeric DNA is composed of GT-rich tandem repeats, about 5-8 bp in length, which terminate in a 3' ssDNA overhang known as the G-tail (Wellinger and Sen, 1997). The length and composition of these repeats varies from organism to organism. In humans, the most common repeat is usually 5' – TTAGGG – 3' (Harrington, 2004), whilst in *S. pombe* it is 5' – $G_{1-8}$TTACA – 3' (Sugawara, 1989). *S. cerevisiae* repeat sequences are more heterogeneous, however (5' – $C_{2-3}ACA_{1-6}/T_{1-6}GTG_{2-3}$ – 3'; (Louis, 1995)). A large variety of telomere specific proteins exist in eukaryotes which bind either dsDNA or the G-tail overhang to protect telomeres *in vivo* (Figure 1.8). These proteins 'cap' telomeres and regulate the function/accessibility of telomerase (see below), exonucleases, replication factors, etc at chromosome ends (Bertuch and Lundblad, 2006; de Lange, 2005; LeBel and Wellinger, 2005; Lydall, 2003). Although processes involved in detecting and repairing breaks are suppressed at telomeres, proteins

required for both checkpoint activation and DSB repair are also important for telomere function. ATM/Tel, ATR/Mec1, the 9-1-1 complex, Ku and the *RAD52* epistasis group have all been linked to telomere homeostasis in a number of eukaryotes (Naito et al., 1998; Chan and Blackburn, 2003; Jaco et al., 2003; Larrivee et al., 2004; Pandita et al., 2006). In higher eukaryotes, the G-tail overhang can invade upstream dsDNA telomere sequences, producing a structure known as a t-loop which is believed to hide chromosome ends from the DNA damage response machinery (Griffith et al., 1999). Indeed, it has recently been found that ATR and HR act consecutively to ensure telomeres are replicated appropriately and form t-loop structures (Verdun and Karlseder, 2006). Telomeres that fail to hide their ends initiate a DNA damage response which leads to cell cycle arrest and inappropriate processing by DSB repair mechanisms (Harrington, 2004; de Lange, 2005). Such processing may lead to end to end fusions or promote interchromosomal HR between telomeric repeats. In *S. cerevisiae*, mutants which fail to maintain telomere length overcome senescence by using a *RAD52*-dependent HR mechanism to maintain (dysfunctional) telomeres in a subpopulation of cells (Lundblad and Blackburn, 1993; Le et al., 1999). It has recently been demonstrated that mammalian KU represses sister telomere exchange at telomeres but promotes end to end fusions in the absence of TRF2 (Celli et al., 2006). Indeed, such a recombination based mechanism has been observed in human tumours which lack telomerase (Dunham et al., 2000). These data suggest that dysregulation of the activity of HR, NHEJ and checkpoint proteins at telomeres can have detrimental effects.

DNA replication fails to reach the ends of eukaryotic chromosomes due to the limitations of lagging strand synthesis, resulting in progressive loss of telomeric DNA over successive rounds of cell division. To prevent this loss, telomeres are maintained by a specialised RNA-protein complex known as telomerase (Figure 1.8). The core

telomerase protein consists of an RNA template molecule and a reverse transcriptase protein subunit (Greider and Blackburn, 1985), although other proteins are known to bind and regulate the function of this core complex *in vivo* (see below). Short telomeres are preferentially targeted for elongation by telomerase, although how this is achieved is still not fully understood (Loayza and de Lange, 2004). Furthermore, both telomerase action and lagging strand synthesis components are required to maintain native telomeres (Diede and Gottschling, 1999). Interestingly, only the reverse transcriptase subunit and RNA template are essential for telomerase activity *in vitro* (Lingner et al., 1997a). These components have been identified in *S. cerevisiae* (Est2 and TLC1, respectively) and humans (TERT and hTR, respectively) (Singer and Gottschling, 1994; Feng et al., 1995; Lingner et al., 1997b; Meyerson et al., 1997). In *S. pombe*, the transcriptase subunit has also been characterized ($trt1^+$), although the RNA template has eluded detection (Nakamura et al., 1997). As implied above, additional factors are required for telomerase activity *in vivo*. The *S. cerevisiae EST1* and *EST3* genes were characterized as mutants with extra short telomeres (Lendvay et al., 1996). The fact that these mutants display defects in telomere length suggests that they play an essential role in telomere maintenance. Indeed, Est1 has been shown to interact with another telomere binding protein, Cdc13, which is required for spontaneous GCRs arising as a result of *de novo* telomere addition (Qi and Zakian, 2000; Myung et al., 2001). In addition, it has been demonstrated that Est1 is dispensable for telomere maintenance in cells expressing a fusion between Cdc13 and Est2 (Evans and Lundblad, 1999). These data suggest that the Est1-Cdc13 interaction functions to recruit the Est2-TLC1 core complex to telomeres where it can extend the G-tail. Est3 has also been shown to play a similar role (Hughes et al., 2000). It has been found that Cdc13 preferentially binds to the 3'ssDNA G-tail overhang at native telomeres, where it functions to prevent excessive degradation of the overhang and prevents resection of the C-strand (Viscardi et al., 2005). Paradoxically, Cdc13 also

has an inhibitory role at long telomeres (Lydall, 2003; Viscardi et al., 2005). Interestingly, phosphorylation of Cdc13 by Mec1/Tel1 is also believed to aid recruitment and activation of telomerase via the Est1 pathway (Tseng et al., 2006). Homologues of Cdc13 in other eukaryotes have not yet been identified although it is believed POT1/Pot1 (protection of telomeres 1) represent the functional orthologues in humans and fission yeast, respectively (Baumann and Cech, 2001). There is a variety of evidence to suggest that Pot1 functions to prevent degradation at telomeres and has both stimulatory and inhibitory roles with respect to telomerase activity at chromosome ends, similar to that observed for Cdc13 (Baumann and Cech, 2001; Bunch et al., 2005). In addition to Cdc13, both RPA and Ku (Figure 1.8) have been shown to play a role in telomerase recruitment. Similar to Cdc13-Est1, an interaction between RPA and Est1 is important for normal telomerase activity at native telomeres (Schramke et al., 2004). It has also been demonstrated that Ku80 binds to the *S. cerevisiae* RNA template, *TLC1*, and such interaction is required to efficiently recruit telomerase to telomeres in G1 phase, a role which is conserved in humans (Stellwagen et al., 2003; Ting et al., 2005). Ku, in addition to Cdc13, also has a protective role at telomeres where it is believed to prevent telomere shortening, excessive resection of the C-strand and the creation of ssDNA (Gravel and Wellinger, 2002). Indeed, Ku80 mutants have critically short telomeres with a long G-tail and increased Cdc13 binding, a result which could be explained by the lack of telomerase recruitment and telomere protection in this background (Bertuch and Lundblad, 2003).

### 1.6.2. *De novo* telomere addition.

In addition to elongating shortened telomeres, telomerase can add telomeric DNA to other locations resulting in the formation of chromosomal truncations. Interestingly, *de novo* addition of telomeric sequence is a feature of normal development in ciliates

such as *Paramecium* and *Tetrahymena* (Baroin et al., 1987; Forney and Blackburn, 1988; Spangler et al., 1988). Indeed, chromosomal truncations produced through inappropriate telomere addition are also frequently observed in tumour cells (Pennaneach et al., 2006). In addition, *de-novo* telomere addition or 'chromosome healing' has been implicated in several genetic diseases, including α-thalassaemia and mental retardation (Wilkie et al., 1990; Wong et al., 1997). Various studies in both *S. cerevisiae* and human cells have shown that spontaneous damage and induced breaks can be repaired by the addition of telomeric sequence. For example, it was found that *de novo* telomere addition was responsible for the majority of spontaneously occurring GCR events in wild-type *S. cerevisiae* (Chen and Kolodner, 1999; Kolodner et al., 2002). Additional evidence has shown that HO-induced breaks can be 'healed' in both haploids and diploids by *de novo* telomere addition, although such repair occurs at low frequency (Kramer and Haber, 1993; Mangahas et al., 2001). Since telomere addition can lead to chromosomal truncations and loss of sequence, such a process is a cause of LOH. Indeed, the efficiency of *de novo* telomere addition in diploid cells was increased by the deletion of *RAD52* and the addition of a telomere like $(T_2G_4)_{13}$ sequence proximal to the DSB (Kramer and Haber, 1993). This suggests that HR suppresses *de novo* telomere addition and efficient repair by such a mechanism requires sequences which could possibly recruit various factors involved in telomere maintenance. The addition of an 81bp GT 'seeding' sequence proximal to the break can highly stimulate telomere addition after the break (Diede and Gottschling, 1999). The low frequency of chromosome healing that occurs spontaneously in wild-type budding yeast can also be increased 1000-fold by deletion of the *PIF1* gene, which has been shown to remove telomerase from telomeric DNA via its 5' to 3' DNA helicase activity (Myung et al., 2001). Indeed, a *pif1-m2* allele which has lost its nuclear function also results in an increase in spontaneous telomere

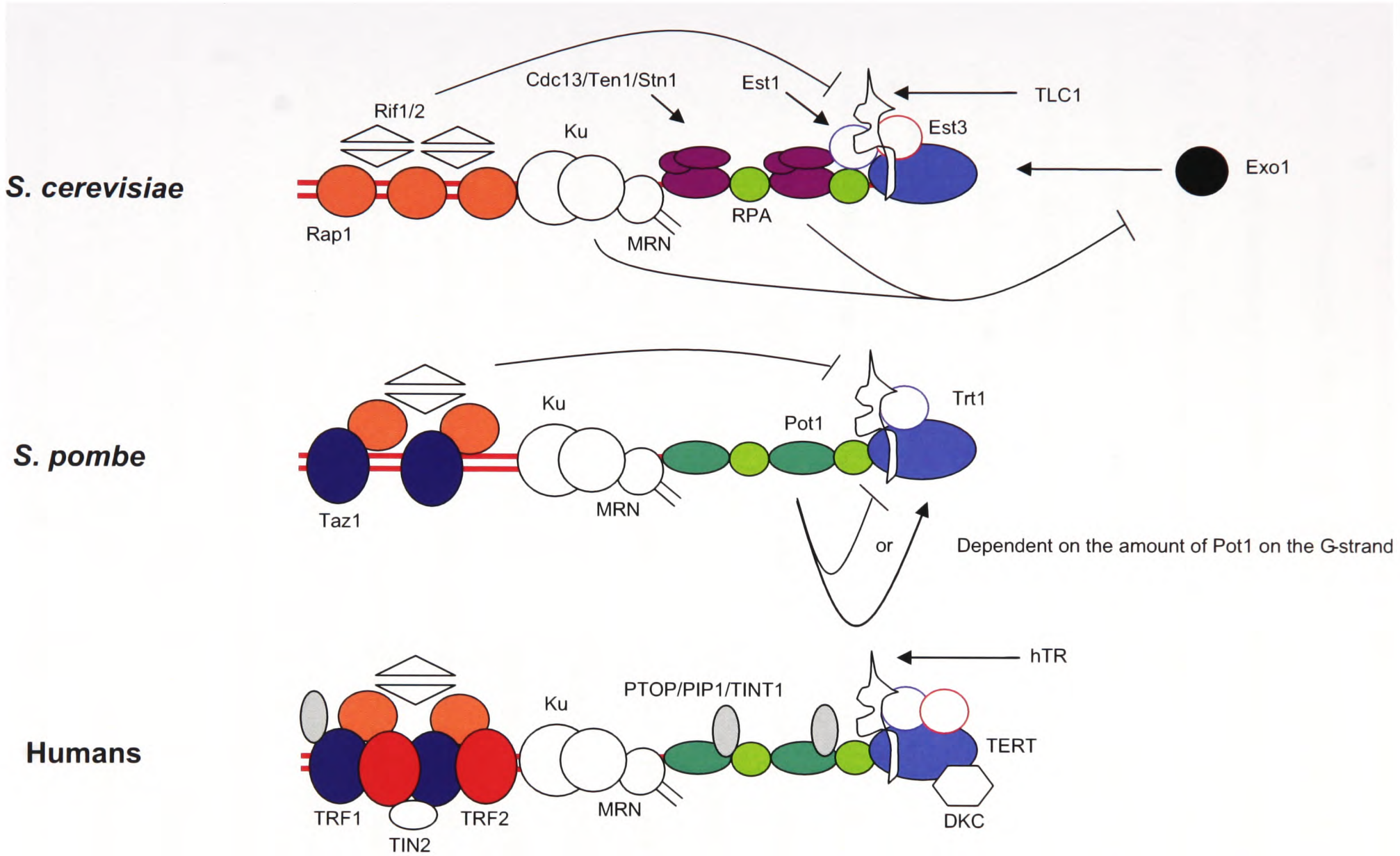



**Figure 1.8. Telomere binding proteins in eukaryotes.** The catalytic subunit of telomerase interacts with the G -strand overhang at chromosome ends, and with the help of the RNA template and various Est factors (including DKC in humans) promotes the extension of the G -strand. Lagging strand synthesis components are also involved (not shown). Various dsDNA binding proteins e.g. Taz1, TRF1, TRF2, together with several ssDNA binding factors e.g. Cdc13/Ten1/Stn1, Pot1 and RPA, 'cap' telomeres to prevent excessive degredation of the C-strand and modulate telomerase activity. A subset of inhibitory and stimulatory roles forthe pro teins in yeast is shown. The different telomere binding proteins identified thus far in yeasts and humans are depicted.

addition, although only by 250-fold over wild-type (Myung et al., 2001). Thus, in addition to Rad52-mediated HR it appears that more direct mechanisms are in place to prevent the inappropriate addition of telomeric sequence to DSB ends. Interestingly, in human α-thalassaemia, the 3-4 bp sequence preceding the point of telomere addition is complementary to the RNA template of the human telomerase (Flint et al., 1994). In addition, analysis of breakpoint junctions from 500 strains having undergone spontaneous or break induced telomere addition in *S. cerevisiae* demonstrated that telomeric sequence was preferentially added to 3-6bp of GT rich sequence (Pennaneach et al., 2006). Overall, these data seem to suggest that telomerase is recruited to the ends of DSBs and that addition occurs through annealing of break sequence to the RNA component of telomerase. No TG-like sequences (see above) were observed near the sites of addition, however, suggesting that such sequences are not required to recruit telomere maintenance factors which could promote addition (Putnam et al., 2004). Indeed, for DSB sites without such specific sequences, the mechanism by which telomerase is recruited is not well understood. It is possible, however, that telomere-maintenance proteins somehow recognize DSB ends as telomeres and thus promote healing. Of course, the low frequency of telomere addition observed in studies of spontaneous and break induced chromosomal rearrangements suggests that mechanisms and/or processes are in place to prevent or compete with this pathway for the repair of DSBs. Studies investigating the requirements of *de novo* telomere addition in the HO induced system with 'seeding' sequence suggest that proteins involved in the maintenance of normal telomeres may also play a role in chromosome healing. Indeed, the *EST1* and *CDC13* genes facilitate telomere extension in this context, presumably through their ability to recruit telomerase to the break (Bianchi et al., 2004). The role of these genes at breaks without 'seeding' sequence is less clear, however, although a *cdc13-2* allele with defects in telomere maintenance reduces the rate at which *de novo* telomere addition

occurs spontaneously in a *pif1-m2* mutant (Myung et al., 2001). Ku is also required for spontaneous telomere additions and a *yku80-135i* mutant that cannot bind with *TLC1* also has significantly reduced levels of MMS-induced rearrangements caused by telomere addition (Stellwagen et al., 2003). These data, along with the observation that Ku binds and transiently stabilizes break ends induced via HO endonuclease, suggests that Ku may play a role in telomerase recruitment at DSBs (Frank-Vaillant and Marcand, 2002).

So, the propensity for undergoing LOH in response to DSBs is present within all cells. Whether repair results in extensive LOH appears to depend largely on how appropriate DSB repair is co-ordinated within the cell. To investigate further, a system for examining the relationship between DSBs and extensive LOH in a non-essential context, and the mechanism/s responsible for such events, was developed in the model organism, *S. pombe*.

## 1.7. THE $CH^{16}$-MGH SYSTEM.

The studies described in this thesis have utilised a *S. pombe* strain containing a genetically stable non-essential minichromosomal derivative of chromosome III (ChIII), termed $Ch^{16}$ (Niwa et al., 1986). $Ch^{16}$ encodes an *ade -M216* heteroallele which complements *ade6-M210* on ChIII (Leupold and Gutz, 1964), resulting in an $ade^{+}$ phenotype. Prior to this study, a *MAT*a cut-site with an adjacent *kanMX6* gene (encoding a G418 resistance marker; G418$^{R}$) was integrated into the $rad21^{+}$ locus on $Ch^{16}$, 25kb distal to *ade6-M216*. A site-specific DSB was induced at the *MATa* cut site through expression of plasmid borne HO endonuclease, itself under the control of a no message in thiamine (nmt) promoter. This strain ($Ch^{16}$-MG) was used to examine

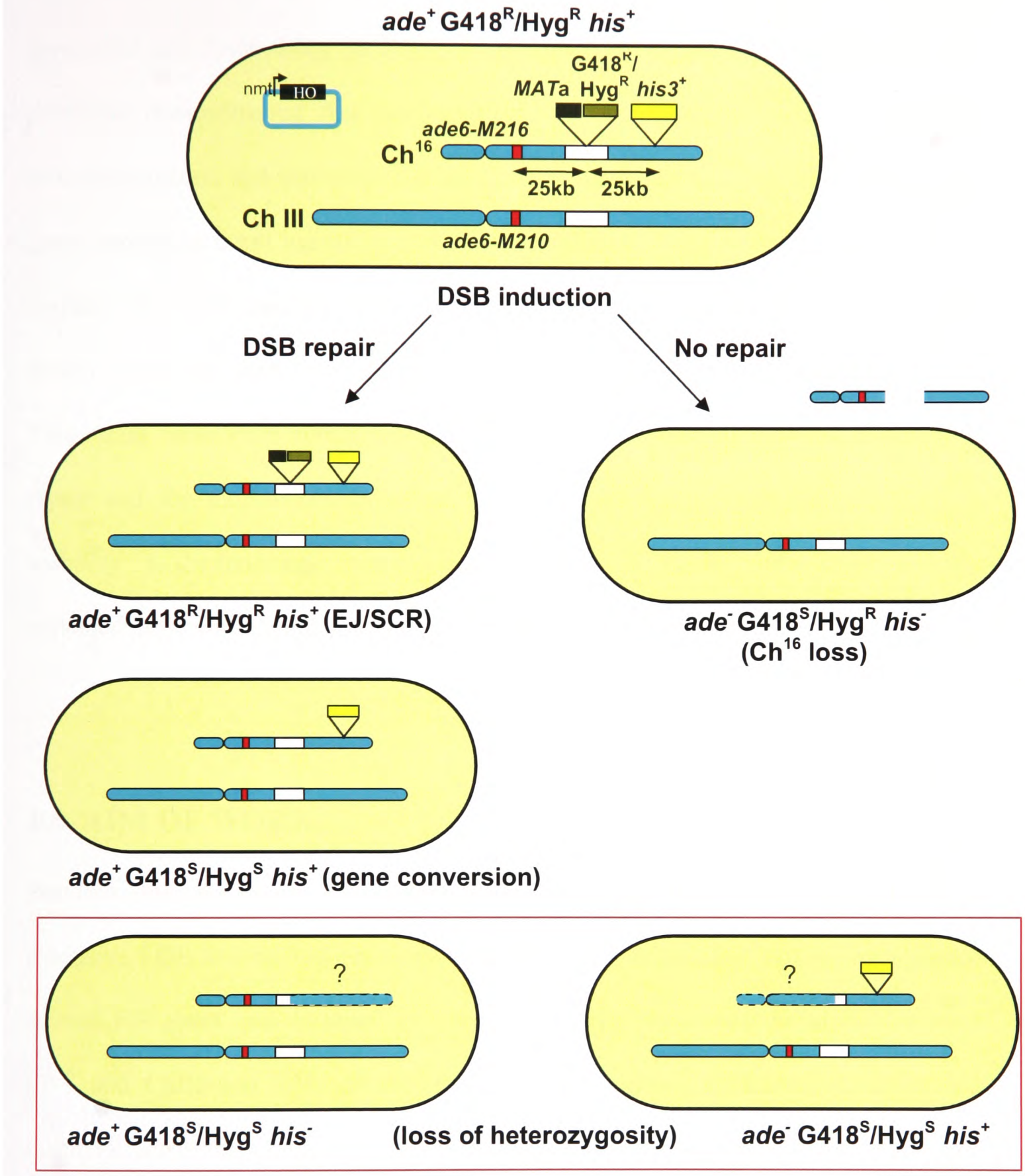



**Figure 1.9. Ch$^{16}$-MGH/MHH LOH assay (Phenotypic outcomes following DSB induction).** Ch$^{16}$-MGH, ChIII, complementary heteroalleles (*ade6-M216* and *ade6-M210*; red), *MATa* site (black) with an adjacent *kanMX6* resistance marker (green) are shown as previously described. The *his3*$^{+}$ marker (yellow) was inserted ~25kb downstream of the *MATa* site. Derepression of pREP81X-HO generates a DSB at the *MATa* target site. In Ch$^{16}$-MHH, *kanMX6* is replaced by *hph*. Repair can occur by end joining/sister chromatid exchange (EJ/SCR), gene conversion or result in extensive LOH (red box). Conversly, failure to repair results in minichromosome loss.

the genetic requirements of efficient DSB repair in a non-essential context and had also shown that a single HO-induced DSB was sufficient to activate a checkpoint dependent cell cycle delay in *S. pombe* (Prudden et al., 2003). Evidence was also presented demonstrating that *ade*$^{+}$ marker loss corresponded to loss of the Ch$^{16}$ minichromosome and that G418$^{R}$ marker loss was indicative of an interchromosomal gene conversion event using ChIII as a repair template (Prudden *et al.*, 2003). A *his3*$^{+}$ marker was subsequently integrated 25kb distal to the *MATa* site, giving a strain heterozygous for *ade6*, G418$^{R}$ and *his3* markers, termed Ch$^{16}$-MGH (Hussey, 2003). This strain could now be used in a genetic assay to investigate both DSB-induced repair and the mechanisms responsible for extensive LOH without affecting cell viability. A diagrammatic representation of the Ch$^{16}$-MGH/MHH strain and the expected outcomes of repair/mis-repair can be seen in Figure 1.9.

## 1.8. AIM OF WORK.

Previous studies using the Ch$^{16}$-MGH/MHH system had shown that DSB repair led to extensive LOH at low frequency in wild-type background cells. Such repair required several HR genes and occurred as a result of allelic crossovers during G2 between Ch$^{16}$ and ChIII and BIR. In the absence of HR genes, DSB-induced LOH still occurred, albeit via mechanism/s distinct from that promoted by HR. The main aims of this work were: To further investigate the requirements of HR in the formation of extensive DSB-induced LOH via translocations using the Ch$^{16}$-MGH/MHH system; To identify the mechanism/s behind break-induced LOH in HR and NHEJ mutants; and to determine how such mechanisms of LOH are co-ordinated.

# 2. MATERIALS AND METHODS.

# 2.1. GENERAL LABORATORY SUPPLIES.

## 2.1.1. Chemical reagents, kits and equipment.

General laboratory chemicals were of analytical grade and purchased from Sigma-Aldrich (Poole, U.K.), Fisher Scientific (Leicester, U.K.), BDH Laboratory Supplies (Poole, U.K.), Autogen Bioclear (Calne, U.K.) and Invitrogen (Paisley, U.K.). Bacto-agar and Bacto-tryptone were obtained from BD Biosciences (Oxford, U.K.) whilst EZmix™ yeast extract was purchased from Sigma-Aldrich. Gensieve LE agarose was obtained from Flowgen (Nottingham, U.K.) and malt extract agar was acquired from Oxiod (Basingstoke, U.K.). T4 Quick DNA ligase, DNA ladders and all DNA restriction endonucleases were purchased from New England Biolabs (Hitchin, U.K.). dNTPs and *Taq* DNA polymerase were obtained from Abgene (Epsom, U.K.) whilst all synthetic oligonucleotides were acquired from Sigma-Genosys (Cambridge, U.K.). *Pfu* DNA polymerase was purchased from Stratagene (Amsterdam, Netherlands.).

Several kits were used during the course of this research: Maxi-prep, Mini-prep, Agarose Gel and Nucleotide Extraction Kits were acquired from QIAGEN (Sussex, U.K.). A MasterPure™ Yeast DNA Purification Kit was purchased from Epicentre (Cambridge, U.K.). The Megaprime™ DNA Labelling System was obtained from Amersham Biosciences (Little Chalfont, U.K.) whilst the BigDye® Terminator V3.1 Cycle Sequencing Kit was purchased from Applied Biosystems (Warrington, U.K.).

## 2.1.2. Buffers and solutions.

Buffers required for use with commercially obtained restriction endonucleases, DNA ligases and DNA polymerases were purchased from New England Biolabs, Abgene,

**Table 2.1 Buffers and solutions used during this study.**

| Buffer/Solution | Constituents |
|---|---|
| **Tris-EDTA (TE) buffer** | 10mM tris-HCl (pH8.0), 1mM ethylenediaminetetraacetic acid (EDTA). |
| **Tris-acetate-EDTA (TAE) buffer** | 40mM tris-HCl (pH8.0), 1mM EDTA, 20mM acetic acid. |
| **10x DNA loading buffer** | 0.25% (w/v) bromophenol blue, 0.25% (w/v) xylene cyanole, 15% (w/v) ficoll. |
| **Phosphate buffered saline (PBS)** | 1 PBS tablet (Dulbecco A) per 100mL H2O. |
| **Magnesium solution** | 1M magnesium chloride, 1M magnesium sulphate. |
| **lithium acetate/TE buffer (LiA/TE)** | 100mM lithium acetate (pH8.0), 10mM tris-HCl (pH8.0), 1mM EDTA. |
| **Polyethylene glycol/lithium acetate/TE buffer (PEG/LiA/TE)** | 8g polyethylene glycol in 20mL, 100mM lithium acetate (pH8.0), 10mM tris-HCl (pH8.0), 1mM EDTA. |
| **Transfer buffer** | 0.5M sodium hydroxide, 1.5M sodium chloride. |
| **Post-transfer buffer** | 0.5M Sodium hydroxide, 1M Tris-HCl. |
| **20x Sodium salt citrate (SSC)** | 3M NaCl, 300mM Trisodium citrate. |
| **2x SSC, 0.1% SDS** | 300mM NaCl, 30mM Trisodium citrate, 0.1g SDS per 100mL. |
| **100x Denharts solution** | 2% (w/v) polyvinylpyrolidone, 2% (w/v) bovine serum albumin (BSA), 2% ficoll. |
| **Pre-hybridisation buffer** | 6x SSC, 5x Denharts solution, 0.2mg/mL herring sperm DNA, 1mM EDTA, 1% sodium dodecyl sulphate (SDS). |
| **Hybridisation buffer** | 6x SSC, 5x Denharts solution, 0.2mg/mL herring sperm DNA, 1mM EDTA, 10% dextran sulphate, 1% SDS. |

Strategene and Amersham Biosciences. Bovine serum albumin (BSA) for use in restriction digests was also acquired from New England Biolabs. All buffers acquired for use with commercially obtained kits are described where appropriate.

All non-commercially available buffers and solutions used during this research can be seen in Table 2.1 and were made using purified $H_2O$ (obtained through reverse osmosis in a Millipore filtration system) before being autoclaved at 120˚C at 15 pounds/inch$^2$ (psi) for 15 min. Filtration, using a vacuum-pump and a membrane filter purchased from Nalgene (Hertford, U.K.), was also conducted.

## 2.2. MEDIA.

All media, including amino-acid and nucleotide based solutions were prepared using purified $H_2O$. Subsequent sterilisation was performed via autoclaving or filtration as described above.

### 2.2.1. Escherichia coli (E. coli) media.

See Table 2.2 for a detailed list of media used for growth and selection of *E. coli* strains during this research.

### 2.2.2. Schizosaccharomyces pombe (*S. pombe*) media and solutions.

See Table 2.3 for a detailed list of *S. pombe* growth media and solutions used during the course of this research.

**Table 2.2 *E. coli* media.**

| Media/Solution | Constituents and Compilation |
|---|---|
| **Luria-Bertani (LB) broth and agar** | 10g Bacto-tryptone, 5g EZmix™ yeast extract, 10g Sodium chloride per litre $H_2O$. 2% Bacto-agar added for solid media. |
| **LB broth and agar with ampicillin (LB+Amp)** | LB broth, 50μg/ml filter sterilised ampicillin. 2% Bacto-agar added for solid media. |
| **SOB broth** | 20g Bacto-tryptone, 5g EZmix™ yeast extract, 0.58g Sodium chloride, 1.9g Potassium chloride, 10ml Magnesium solution (see Table 2.1) per litre $H_2O$. |
| **SOC broth** | 2mM filter sterilised glucose per litre of SOB broth. |

Supplements were used at 1x concentration (150mg/l) in EMM based media. Low adenine plates ($A_L$) were prepared using 500µl of a 50x stock in 400ml EMM broth (58.2µM). EMM based media described throughout this document is denoted by 'EMM' plus (+) the letter of the supplement added as detailed in Table 2.3.

## 2.3. PLASMIDS.

The plasmid maps of pREP81X (Osman et al., 1996), pREP82 (Maundrell, 1993), pREP81X-HO (Osman et al., 1996), pREP82X-HO (this study), pIRT3 (Smeets et al., 2003) and pIRT3-*rhp51* (Smeets et al., 2003), all used during this research, can be found in Appendix III. Section 2.5.8 describes how pREP82X-HO was constructed.

## 2.4. STRAINS.

### 2.4.1. *E. coli.*

DH5α$^{TM}$ (F- φ80*lac*ZΔM15 Δ(*lac*ZYA-*arg*F)U169 *rec*A1 *end*A1 *hsd*R17 (rk-, mk+) *pho*A *sup*E44 *thi*-1 *gyr*A96 *rel*A1 λ-) was purchased from Invitrogen.

### 2.4.2. *S. pombe.*

All *S. pombe* strains used during this research can be seen in Table 2.4.

**Table 2.3 *S.pombe* media.**

| Media/Solution | Constituents and Compilation |
|---|---|
| **Yeast extract and 5 supplement (YE5S) broth and agar** | 30g glucose, 5g EZmix™ yeast extract, 1.125g supplement mix (adenine, histidine, leucine, lysine, uracil – 1:1:1:1:2 ratio) per litre $H_2O$. 2% Bacto-agar added for solid media. |
| **YE5S agar with G418 (YE5S+G418); YE5S agar with hygromycin B (YE5S+HygB)** | YE5S agar, 500µg/ml G418; YE5S agar, 200µg/ml hygromycin B. |
| **Yeast freezing mix (YFM)** | 1:1 mix of YE5S and glycerol. |
| **Malt extract and 5 supplement (ME5S) agar** | 50g malt extract agar per litre $H_2O$. |
| **50x Salt stock** | 260mM magnesium chloride, 5mM calcium chloride, 670mM potassium chloride, 14.1mM di-sodium phosphate. |
| **1000x Vitamin stock** | 4.2mM pantothenic acid, 81.2mM nicotinic acid, 55.5mM inositol, 40.8µM biotin. |
| **10000x Mineral stock** | 80.9mM boric acid, 23.7mM manganese sulphate, 13.9mM zinc sulphate, 7.4mM iron chloride, 2.47mM molybdic acid, 6.02mM potassium iodide, 1.6mM copper sulphate, 47.6mM citric acid. |
| **Edinburgh minimal medium (EMM) broth and agar** | 14.7mM potassium hydrogen phthalate, 15.5mM di-sodium hydrogen orthophosphate, 93.5mM ammonium chloride, 111mM glucose, 1x Salt stock, 1x Vitamin stock, 1x Mineral stock per litre $H_2O$. |
| **Supplement stocks** | Adenine (**A**), leucine (**L**), histadine (**H**) and arginine (**R**) were prepared as 50x stocks (7.5g/l). Uracil (**U**) was prepared as a 25x stock (3.75g/l). |
| **Thiamine (T)** | 20mM thiamine (filter sterilised). Final concentration of 8µM used in all EMM media when required. |

# 2.5. EXPERIMENTAL PROCEDURES.

## 2.5.1. Growth, storage and manipulation of strains.

### 2.5.1.1. Growth of *E. coli* strains.

DH5α™ *E. coli*, transformed with plasmid DNA (encoding β-lactamase in all cases) and plated onto LB+Amp (Section 2.5.2.1, Table 2.3), were incubated O/N at 37°C.

For small scale plasmid DNA preparation (mini-prep; Section 2.5.3.1) single DH5α™ colonies containing plasmid were picked from an LB+Amp plate, inoculated into 5ml LB+Amp broth and cultured O/N at 37°C with agitation (200rpm). Large scale plasmid DNA preparations (maxi-prep; Section 2.5.3.2) were prepared from a 250ml LB+Amp broth culture, seeded using a 5ml starter culture of DH5α™ *E. coli* transformed with the relevant plasmid (cultured for 6-8hrs; see above) and grown O/N at 37°C with agitation (200rpm).

### 2.5.1.2. Storage of *E. coli* strains.

Permanent stocks of *E. coli* were prepared using 1ml of maxi-prep culture and 1ml of glycerol, mixed into a Nunc cryo-tube (Paisley, U.K.) and concomitantly frozen at -80°C until use.

### 2.5.1.3. Growth of *S. pombe* strains.

Conditions used for the growth and maintenance of *S. pombe* were based on previously developed protocols (Moreno et al., 1991). Yeast strains were revived,

## Table 2.4. *S. pombe* strains used during this study.

| Strains | Genotype | Source |
|---|---|---|
| TH2094 | *arg3-D4 leu1-32 ade6-D1 ura4-D18 his3-D1* $h^-$ | Lab stock |
| TH1436 | *leu1-32 ade6-M210 ura4-D18 his3-D1* Ch$^{16}$-MGH $h^-$ pREP81X-HO | Hussey, 2003 |
| TH2009 | *leu1-32 ade6-M210 ura4-D18 his3-D1* Ch$^{16}$-MHH $h^+$ pREP81X-HO | This study |
| TH3011 | *leu1-32 ade6-M210 ura4-D18 his3-D1* Ch16-MGH $h^+$ pREP81X | This study |
| TH2297, 2298, 2299 | *rad32:: kanMX6 leu1-32 ade6-M210 ura4-D18 his3-D1* Ch$^{16}$-MHH $h^+$ pREP81X-HO | This study |
| TH3012 | *rad32:: kanMX6 leu1-32 ade6-M210 ura4-D18 his3-D1* Ch$^{16}$-MHH $h^+$ pREP81X | This study |
| TH2013, 2014, 2015 | *rad50::kanMX6 leu1-32 ade6-M210 ura4-D18 his3-D1* Ch$^{16}$-MHH $h^+$ pREP81X-HO | This study |
| TH3013 | *rad50::kanMX6 leu1-32 ade6-M210 ura4-D18 his3-D1* Ch$^{16}$-MHH $h^+$ pREP81X | This study |
| TH1894, 1934, 1935 | *nbs1::ura4*$^+$ *leu1-32 ade6-M210 ura4-D18 his3-D1* Ch$^{16}$-MGH $h^+$ pREP81X-HO | This study |
| TH3015 | *nbs1::ura4*$^+$ *leu1-32 ade6-M210 ura4-D18 his3-D1* Ch$^{16}$-MGH $h^+$ pREP81X | This study |
| TH1607, 1608, 1609 | *exo1::ura4*$^+$ *leu1-32 ade6-M210 ura4-D18 his3-D1* Ch$^{16}$-MGH $h^+$ pREP81X-HO | Hussey, 2003 |
| TH1610 | *exo1::ura4*$^+$ *leu1-32 ade6-M210 ura4-D18 his3-D1* Ch$^{16}$-MGH $h^+$ pREP81X | This study |
| TH2199, 2200, 2201 | *rad11D223Y leu1-32 ade6-M210 ura4-D18 his3-D1* Ch$^{16}$-MGH $h^+$ pREP81X-HO | This study |
| TH2129 | *rad22::ura4*$^+$ *leu1-32 ura4-D18 his3-D1* $h^+$ | M. Whitby |
| TH2058 | *rad22::ura4*$^+$ *leu1-32 ade6-M210 ura4-D18 his3-D1* Ch$^{16}$-MHH $h^+$ | This study |
| TH2655, 2656, 2657 | *rad22::ura4*$^+$ *leu1-32 ade6-M210 ura4-D18 his3-D1* Ch$^{16}$-MHH $h^+$ | This study |
| TH2658, 2659, 2660 | *rad22::ura4*$^+$ *leu1-32 ade6-M210 ura4-D18 his3-D1* Ch$^{16}$-MHH $h^+$ pREP81X-HO | This study |
| TH2661 | *rad22::ura4*$^+$ *leu1-32 ade6-M210 ura4-D18 his3-D1* Ch$^{16}$-MHH $h^+$ pREP81X | This study |
| TH1760, 1761, 1762 | *rhp55::ura4*$^+$ *leu1-32 ade6-M210 ura4-D18 his3-D1* Ch$^{16}$-MGH $h^+$ pREP81X-HO | Hussey, 2003 |
| TH2988 | *rhp55::ura4*$^+$ *leu1-32 ade6-M210 ura4-D18 his3-D1* Ch$^{16}$-MGH $h^+$ pREP81X | This study |
| TH1579, 1580, 1581 | *rhp51::ura4*$^+$ *leu1-32 ade6-M210 ura4-D18 his3-D1* Ch$^{16}$-MGH $h^+$ pREP81X-HO | Hussey, 2003 |
| TH1582 | *rhp51::ura4*$^+$ *leu1-32 ade6-M210 ura4-D18 his3-D1* Ch$^{16}$-MGH $h^+$ pREP81X | This study |

## Table 2.4. continued.

| Strains | Genotype | Source |
|---|---|---|
| TH1998, 2050, 2051 | *rhp54::ura4*$^+$ *leu1-32 ade6-M210 ura4-D18 his3-D1* Ch$^{16}$-MGH $h^+$ pREP81X-HO | Yu-Wee, 2006 |
| TH3041 | *rhp54::ura4*$^+$ *leu1-32 ade6-M210 ura4-D18 his3-D1* Ch$^{16}$-MGH $h^+$ pREP81X | This study |
| TH2042, 2042, 2043 | *mus81::ura4*$^+$ *leu1-32 ade6-M210 ura4-D18 his3-D1* Ch$^{16}$-MGH $h^-$ pREP81X-HO | This study |
| TH3042 | *mus81::ura4*$^+$ *leu1-32 ade6-M210 ura4-D18 his3-D1* Ch$^{16}$-MGH $h^-$ pREP81X | This study |
| TH1443, 1444, 1445 | *ku70::ura4*$^+$ *leu1-32 ade6-M210 ura4-D18 his3-D1* Ch$^{16}$-MGH $h^+$ pREP81X-HO | Hussey, 2003 |
| TH1446 | *ku70::ura4*$^+$ *leu1-32 ade6-M210 ura4-D18 his3-D1* Ch$^{16}$-MGH $h^+$ pREP81X | This study |
| TH1671, 1672, 1673 | *lig4::ura4*$^+$ *leu1-32 ade6-M210 ura4-D18 his3-D1* Ch$^{16}$-MGH $h^+$ pREP81X-HO | Hussey, 2003 |
| TH1670 | *lig4::ura4*$^+$ *leu1-32 ade6-M210 ura4-D18 his3-D1* Ch$^{16}$-MGH $h^+$ pREP81X | This study |
| TH2813, 2814, 2815 | *ku70::ura4*$^+$ *rhp55::ura4*$^+$ *leu1-32 ade6-M210 ura4-D18 his3-D1* Ch$^{16}$-MHH $h^+$ pREP81X-HO | This study |
| TH2816 | *ku70::ura4*$^+$ *rhp55::ura4*$^+$ *leu1-32 ade6-M210 ura4-D18 his3-D1* Ch$^{16}$-MHH $h^+$ pREP81X | This study |
| TH2570, 2571, 2572 | *lig4::ura4*$^+$ *rhp55::ura4*$^+$ *leu1-32 ade6-M210 ura4-D18 his3-D1* Ch$^{16}$-MGH $h^+$ pREP81X-HO | This study |
| TH2573 | *lig4::ura4*$^+$ *rhp55::ura4*$^+$ *leu1-32 ade6-M210 ura4-D18 his3-D1* Ch$^{16}$-MGH $h^+$ pREP81X | This study |
| TH2810, 2811, 2812 | *rad32::kanMX6 rhp55::ura4*$^+$ *leu1-32 ade6-M210 ura4-D18 his3-D1* Ch$^{16}$-MHH $h^+$ pREP81X-HO | This study |
| TH3016 | *rad32::kanMX6 rhp55::ura4*$^+$ *leu1-32 ade6-M210 ura4-D18 his3-D1* Ch$^{16}$-MHH $h^+$ pREP81X | This study |
| TH2672, 2673, 2674 | *rad50::kanMX6 rhp55::ura4*$^+$ *leu1-32 ade6-M210 ura4-D18 his3-D1* Ch$^{16}$-MHH $h^+$ pREP81X-HO | This study |
| TH2675 | *rad50::kanMX6 rhp55::ura4*$^+$ *leu1-32 ade6-M210 ura4-D18 his3-D1* Ch$^{16}$-MHH $h^+$ pREP81X | This study |
| TH2906, 2907, 2908 | *nbs1::ura4*$^+$ *rhp55::arg3*$^+$ *leu1-32 ade6-M210 ura4-D18 his3-D1* Ch$^{16}$-MHH $h^+$ pREP81X-HO | This study |
| TH2909 | *nbs1::ura4*$^+$ *rhp55::arg3*$^+$ *leu1-32 ade6-M210 ura4-D18 his3-D1* Ch$^{16}$-MHH $h^+$ pREP81X | This study |
| TH2566, 2567, 2568 | *exo1::ura4*$^+$ *rhp55::ura4*$^+$ *leu1-32 ade6-M210 ura4-D18 his3-D1* Ch$^{16}$-MGH $h$+ pREP81X-HO | This study |

**Table 2.4. continued.**

| Strain | Genotype | Source |
|---|---|---|
| TH2569 | *exo1::ura4*$^+$ *rhp55::ura4*$^+$ *leu1-32 ade6-M210 ura4-D18 his3-D1* Ch$^{16}$-MGH *h+* pREP81X | This study |
| TH2766, 2790, 2792 | *rhp55::arg3*$^+$ *leu1-32 ade6-M210 ura4-D18 his3-D1 arg3-D4* Ch$^{16}$-MGH *h+* pREP82X-HO pIRT3 | This study |
| TH2767, 2768, 2791 | *rhp55::arg3*$^+$ *leu1-32 ade6-M210 ura4-D18 his3-D1 arg3-D4* Ch$^{16}$-MGH *h+* pREP82X-HO pIRT3-*rhp51* | This study |

Minichromosome 16 (Ch$^{16}$) was isolated as a non-essential genetic element, originally derived from ChIII (Niwa *et al.*, 1986). Ch$^{16}$-MGH (Ch$^{16}$ *ade6-M216 rad21::MATa-kanMX6 cid2::his3*$^+$). Ch$^{16}$-MHH (Ch$^{16}$ *ade6-M216 rad21::MATa-hphB cid2::his3*$^+$).

plated and sustained on non-selective YE5S or EMM agar plates containing the appropriate supplements (Table 2.3) to maintain selective growth conditions. All strains were incubated at either 32°C for three days or room temperature and restreaked once a week onto fresh media unless otherwise stated.

Liquid cultures were typically prepared by inoculating a single colony or loop of cells, taken from a fresh agar plate, into 50ml (unless otherwise stated) of either YE5S or EMM broth with the suitable supplements as described above. Cultures were grown with agitation (220rpm) at 30°C, again unless otherwise stated. In general, cultures were maintained in mid-exponential growth phase i.e. an $OD_{595nm}$ of 0.1 (~2 x $10^6$ cells/mL) to 0.5 (~1 x $10^7$ cells/mL), although dilutions were made such that $OD_{595nm}$ readings below 0.1 were acquired prior to O/N growth.

### 2.5.1.4. Storage of *S. pombe* strains.

*S. pombe* strains freshly restreaked and ready for permanent storage were inoculated into a Nunc cryo-tube containing 1ml of YE5S broth and 1ml of YFM media (Table 2.3). The ensuing sample was then rapidly frozen and stored at -80°C until use.

### 2.5.1.5. Genetic manipulation of *S. pombe* strains.

Procedures used for the genetic manipulation of *S. pombe* strains were based on previously developed protocols (Moreno et al., 1991). Genetic crosses were performed using freshly streaked strains of opposing mating types i.e. $h^+$ and $h^-$, which were mixed together on a ME5S agar plate (Table 2.3) using a small loop of purified $H_2O$. The plate, which provides conditions of nutrient starvation and thus promotes conjugation between strains, was then incubated at 25°C until asci and spores were observed by light microscopy (Section 2.5.1.6).

Tetrad analysis was performed by picking asci and placing them onto a YE5S agar plate using a Singer MSM micro-manipulator (Watchet, U.K.). Asci walls were allowed to break down at 37°C for ~3-5hrs, after which time the freed spores were separated, again using the micro-manipulator described above. The ensuing plate was then incubated at 32°C (unless otherwise stated) until colonies were observed. Desired progeny were identified by replica-plating colonies onto selective plates (YE5S agar, drug or EMM agar, supplements, T) to determine phenotype.

In free spore analysis, a loop of cells taken from the edges of the desired mating was inserted into a micro-centrifuge tube containing 1mL $H_2O$ and 5µl β-glucUronidase. Mixtures were incubated at 25°C for 1-2 days to allow for the digestion of asci walls and the killing of vegetative cells, after which time 1:100, 1:500 and 1:1000 dilutions were made in $H_2O$ and 150µl from each plated onto individual YE5S agar plates. Desired progeny were identified using replica-plating as for tetrad analysis.

### 2.5.1.6. Sensitivity of *S. pombe* strains to DNA damaging agents.

Testing strain sensitivity to DNA damaging agents was performed via spot dilution as follows. A loop of freshly streaked cells was first re-suspended into 1ml of PBS and cell concentration determined using an improved Neubauer haemocytometer. Cell concentration was subsequently adjusted to $1.25x10^7$ cells/ml i.e. $1x10^5$ cells per 8µl, and 10-fold serial dilutions made, again using PBS, into micro-centrifuge tubes. 8µl from each dilution was then plated onto YE5S or EMM (supplements, ±T) agar containing either 0.0008-0.001% MMS or 0.5-2.5µM CPT. Serially diluted strains were also plated onto non-selective YE5S or EMM (supplements, ±T) agar without drug as a control. The resultant plates were incubated at 32°C for 3 days and then photographed.

Rapid identification of non-suppressed *rad22Δ* strains was performed using a screen where candidates undergoing analysis were first diluted to a cell concentration of $1x10^6$ cells/ml and a single 8µl spot plated onto 0.0008% MMS, 0.5µM CPT and YE5S agar plates as described above. Appropriate wild-type and positive controls were also spotted onto each plate to aid identification of non-suppressed strains.

#### 2.5.1.7. Light microscopy.

*S. pombe* were visualised using a Nikon microscope-Eclipse E-E400 with 10x and 50x objective lenses. To visualise cells in culture, 5µl of cell suspension was placed onto a microscope slide. Cells growing on agar plates were visualised after streaking out using sterile toothpicks.

### 2.5.2. Transformation of Strains.

#### 2.5.2.1. Transformation of *E. coli* with DNA.

50µl of $CaCl_2$ competent DH5α™ *E. coli* were incubated on ice with 1µl of plasmid DNA or 2µl of a DNA ligation reaction (Section 2.5.4.4) for 30mins. The cell mixture was then heat shocked at 42°C for 30secs followed by a 1min incubation period on ice. 500µl of LB broth (Table 2.2) was subsequently added and the resultant cell suspension incubated at 37°C for 1hr with agitation (250rpm) to allow for recovery and expression of plasmid borne drug resistance genes. 250µl of this culture was then spread onto LB+Amp plates which were concomitantly incubated at 37°C until colonies were observed.

### 2.5.2.2. Transformation of *S.pombe* with DNA (Electroporation method).

The strain undergoing transformation was first cultured O/N as previously described (Section 2.5.1.3). The culture was then diluted to an $OD_{595}$ of 0.1 and incubated again at 30°C with agitation (220rpm) until an $OD_{595}$ of 0.3-0.5 was acquired. The resulting culture was chilled on ice for 30mins after which centrifugation at 2,000rpm for 2mins was performed to obtain a cell pellet. The ensuing pellet was washed once with 50mL $H_2O$, followed by centrifugation using the conditions above. Another wash and centrifugation cycle was performed using 50ml of 1M sorbitol after which the pellet was re-suspended in 1ml of 1M sorbitol and transferred to a 1.5ml micro-centrifuge tube. The cell preparation was again centrifuged (10secs at 10,000rpm) and the pellet resuspended in a 1:1 ratio of cells to 1M sorbitol. 45µl of this preparation was then inserted into a chilled electroporation cuvette (Bio-Rad) and 1µl of a 1µg/µl DNA plasmid preparation added. Electroporation was performed under the following conditions – Volts: 0.66kV, $\tau$: ~4.5secs. Immediately after the pulse, 600µl of 1M sorbitol was added to the cuvette. 150µl was subsequently removed and spread onto a selective plate (EMM agar, supplements, T) to select for the presence of transformed plasmid. A negative control without plasmid DNA was also performed to ensure that the appearance of colonies was dependent on the presence of plasmid DNA. Transformed strains were selected and re-tested using selective plates prior to freezing at -80°C as described (Section 2.5.1.4).

### 2.5.2.3. Transformation of *S.pombe* with DNA (Lithium acetate method).

The strain undergoing transformation was cultured O/N in 150mL of selective media (EMM broth, supplements, T) as previously described (Section 2.5.1.3). The culture was diluted to an $OD_{595}$ of 0.1 and incubated again at 30°C with agitation (220rpm) until an $OD_{595}$ of 0.4 was reached. The obtained culture was then centrifuged at

2,000rpm for 2mins to obtain a cell pellet. After removing the supernatant, the pellet was washed twice as above with 50ml of $H_2O$, after which it was re-suspended in 1ml of LiA/TE buffer (Table 2.1). The preparation was again centrifuged as above and the pelleted cells re-suspended in 150µL of the same solution. 100µl of this cell mix was inserted into a 2ml micro-centrifuge tube and subsequently incubated with 2µl of ssDNA (10µg/µl stock) and 45µl of transforming DNA (acquired via plasmid isolation or PCR with subsequent isolation; Section 2.5.3.2 and Sections 2.5.4.5/2.5.3.5, respectively). Following incubation at room temperature for 10mins, 200µl of PEG/LiA/TE buffer (Table 2.1) was added to the sample. This was mixed gently and the resulting solution incubated at 30°C for 45mins. 43µl of DMSO was then inserted into the micro-centrifuge tube and the sample heat shocked at 42°C for 5mins. After the heat shock, cells were pelleted at 5,000rpm for 3 mins, washed once with $H_2O$, re-pelleted using the same conditions and re-suspended in 500µl of YE5S broth. 250µl of this suspension was plated onto two individual YE5S plates which were subsequently incubated at 30°C for 20hrs. Replica plating was then performed using selective media (EMM or YE5S based) to select for clones containing transformed sequence. Transformed strains were re-tested and frozen at -80°C until use as described previously.

### 2.5.3. Isolation of DNA.

#### 2.5.3.1. Small scale plasmid DNA isolation from *E. coli.*

For small scale isolation of plasmid DNA, the required strain was cultured as described (Section 2.5.1.3). A bacterial pellet was then obtained through centrifugation (4,000rpm for 20mins) and plasmid DNA was isolated using a QIAGEN 'Mini-prep' kit as per the manufacturers' instructions (Appendix I).

Isolation was perfomed using agarose gel electrophoresis (Section 2.5.5.1) and purity determined using UV spectroscopy (Section 2.5.4.7).

### 2.5.3.2. Large scale plasmid DNA isolation from *E. coli.*

For large scale isolation of plasmid DNA the required strain was cultured as described and a pellet obtained through centrifugation at 6,000rpm for 10mins. DNA was then isolated as described above for the 'Mini-prep' isolation, this time using a QIAGEN 'Maxi-prep' kit (Appendix I). Isolation and purity was then perfomed as for the small scale method (Section 2.5.3.1) and DNA concentration adjusted to 1μg/mL.

### 2.5.3.3. Isolation of genomic DNA from *S. pombe.*

Genomic DNA was isolated and purified from *S.* pombe using a MasterPure$^{TM}$ Yeast DNA Purification Kit (Epicentre). The strain of interest was cultured O/N at 30°C in 5ml of selective media to an $OD_{595nm}$ of ~1. The cells were centrifuged (10,000rpm for 2-5mins), the supernatant decanted and the resulting pellet resuspended in 300μl of Yeast Cell Lysis Solution (provided). The suspension was then transferred to a 1.5ml micro-centrifuge tube and incubated at 65°C for 15mins after which it was placed on ice. Following a 5min incubation period, 150μl of MPC Protein Precipitation Reagent (provided) was added to the tube and the sample vortexed for 10secs. Cellular debris was pelleted by centrifugation for 10mins at 10,000rpm, after which the supernatant was transferred to a clean 1.5ml microcentrifuge tube and DNA precipitated through the addition of 500μl iso-propanol. DNA was pelleted, again by centrifugation (10,000rpm, 10mins), the supernatant removed by pipetting and the pellet washed with 0.5ml of 70% ethanol. The ethanol was then carefully removed, the sample centrifuged and any remaining ethanol removed. The DNA was re-

suspended in 35µl of TE buffer (provided), 1µl of 5µg/µl RNase A added and the resultant mixture incubated at 37°C for 30mins to degrade RNA. The resultant preparation was stored at -20°C until use.

### 2.5.3.4. Isolation of DNA from agarose gels.

DNA samples that had undergone enzymatic restriction to produce cleaved products (Section 2.5.4.1) were first separated via agarose gel electrophoresis as described. The band of interest was then excised from the gel using a sterile scalpel and linear DNA isolated using a QIAGEN gel extraction kit as per the manufacturers' instructions (Appendix I). Isolation and purity of linear DNA was subsequently confirmed again using agarose gel electrophoresis and UV spectroscopy.

### 2.5.3.5. Isolation of DNA from solution.

PCR amplification products (Section 2.5.4.5) obtained for sequencing analysis were isolated using a QIAGEN PCR purification kit as described by the manufacturer (Appendix I). Isolation was confirmed using agarose gel electrophoresis (Section 2.5.5.1) and purity determined using UV spectroscopy (Section 2.5.4.7).

## 2.5.4. Manipulation and analysis of DNA.

### 2.5.4.1. Enzymatic restriction of DNA.

For plasmid DNA, 25µL of $H_2O$ was inserted into a fresh 250µl micro-centrifuge tube. 1µl of appropriately diluted DNA was then added, followed by 3µl of enzyme specific buffer (10x stock, provided) and 0.3µl of BSA (100x stock, provided) if required. 1µl of restriction enzyme (5-10 U/µl, dependent on enzyme) was added and

the resulting mixture incubated at 37°C for 1hr 30mins (final volume ~30µl). Following this period the enzyme was inactivated through incubation at 65°C for 20mins or removed using the methodology described for isolating DNA from solution (Section 2.5.3.5). Digestion of plasmid DNA was confirmed using agarose gel electrophoresis (Section 2.5.5.1).

For digestion of genomic DNA prior to Southern analysis, a volume corresponding to 10µg of genomic DNA was inserted into a 1.5ml micro-centrifuge tube containing 5µl of enzyme specific buffer and 0.5µl BSA (if required). $H_2O$ was added to a volume of 45µl after which 5µl of restriction enzyme was inserted and the mixture incubated O/N at 37°C. Following this period, another 5µl of restriction enzyme was added and the reaction allowed to proceed for a further 4hrs prior to heat inactivation as previously described. The digest was subsequently analysed via agarose gel electrophoresis as previously detailed.

### 2.5.4.2. Phosphatase treatment of linearised DNA.

Self-ligation was prevented by dephosphorylating linearised vector DNA with calf-intestinal alkaline phosphatase (CIP) prior to ligations with 'insert' (Section 2.5.4.4). 1µl of a 1:10 CIP solution was added directly into the restriction mixture post digestion and incubated at 37°C for 30 min. CIP was subsequently removed and DNA purified using agarose gel electrophoresis.

### 2.5.4.3. Klenow and T4 DNA polymerase extension/resection of DNA.

Klenow fragment or T4 DNA polymerase was added to enzymatic digests to either fill in or recess 3' and 5'-SDNA overhangs, respectively (Section 2.5.4.1). This was performed post restriction. In a 30µl reaction, dNTPs were added to a concentration of

200μM (0.6μl of a 10mM dNTP solution) followed by 1μl of Klenow (units) or T4 (units) DNA polymerase. The resultant mixture was incubated at 25°C for 15mins (Klenow) or at 12°C for 15mins (T4) followed by a 20min inactivation period at 75°C. The modified product was subsequently isolated using agarose gel electrophoresis.

### 2.5.4.4. Ligation of DNA.

Ligation reactions were performed with an isolated 'insert'; derived from the digestion of a pre-existing plasmid (Section 2.5.4.1), and 'vector'; acquired from the digestion of a pre-existing plasmid as described above. For ligations using pre-digested DNA, an optimal 1:3 molar ratio of vector:insert was prepared in a reaction including 10μl of T4 Quick Ligase Buffer (10x stock, provided), 1μl of T4 Quick Ligase (2.5U/μl, provided), pre-determined volumes of insert and vector, and $H_2O$ up to a volume of 20μl. Controls were performed either without ligase or without insert. Reactions containing (CIP treated) vector and ligase only were also conducted to determine the frequency of vector re-ligation. All reaction mixtures were incubated at room temperature for 5mins and then placed on ice, after which transformation into the desired *E. coli* host was performed as described (Section 2.5.2.1).

### 2.5.4.5. The Polymerase Chain Reaction (PCR).

PCR is used to amplify or detect specific DNA targets either for analytical or preparative work. Amplification requires the development of suitable oligonucleotides or 'primers' flanking the region of interest i.e. 'forward' and 'reverse' primers. Primers were received as lypholysed powders and resuspended to 100μM using $H_2O$. *Pfu* polymerase, which contains a 3'-5' proofreading activity, was used for high

fidelity amplification. *Taq*, which is an error prone DNA polymerase lacking 3'-5' proof reading activity, was utilised for all other amplification reactions.

In a typical experiment with *Taq* polymerase, 36.5μL of $H_2O$ was inserted into a 500μL micro-centrifuge tube followed by the addition of 5μL Reaction Buffer IV (10x stock, provided), 1μL of a 10mM dNTP solution and 4μL of a 25mM $MgCl_2$ stock (provided). 0.5μL of each primer ('forward' and 'reverse') and 1μL of template DNA (10-100ng/μl plasmid DNA, 1ng/μl genomic DNA) was then added to the mixture followed by 0.5μL of thermostable *Taq* polymerase (5U/μl).

*Pfu* polymerase was used with its recommended buffers as follows. 40.5μL of $H_2O$ was inserted into a 500μL micro-centrifuge tube followed by the addition of 5μL *pfu* Reaction Buffer (10x stock, provided) and 1μL of a 10mM dNTP solution. Again, 0.5μL of each primer ('forward' and 'reverse') and 1μL of template DNA (10-100ng/μl plasmid DNA, 1ng/μl genomic DNA) was then added to the mixture followed by 1μL of thermostable *pfu* polymerase (2U/μl).

PCR was then performed using a programmable thermocycler under the following conditions:

35 Cycles

94°C, 3mins. (94°C, 45secs. x°C, 45secs. 72°C, y mins). 72°C, 10mins.

x = annealing temperature. This was usually set ~2°C below the melting temperature ($T_m$) of the primer with the lowest $T_m$. The annealing temperature required for successful amplification of target sequence was determined experimentally.

y = extension time. This was ascertained taking into consideration the size of the required product and the processivity of *Taq* (~2kb/min) or *Pfu* (~0.5kb/min) polymerases.

The presence of amplification product was examined via agarose gel electrophoresis. The DNA, if required, was subsequently purified and isolated as described above.

**2.5.4.6. Sequencing of DNA.**

PCR products or plasmid borne sequences were sequenced using suitable primers and the BigDye® Terminator V3.1 Cycle Sequencing Kit. 0.5µl from a PCR reaction or plasmid stock was first inserted into a 500µl micro-centrifuge tube containing 4µl of BigDye® reaction mix and 1.6µl of primer (10µM stock), designed to prime synthesis ~100bp upstream of the region requiring sequencing. Sterile $H_2O$ was then added to achieve a final volume 10 µl.

The PCR reaction was performed as follows:

26 Cycles

94°C, 3mins. (94°C, 40secs. 50°C, 45secs. 60°C, 2mins)

The amplification products were then purified by adding 90μL of 67% isopropanol to the micro-centrifuge tube and incubating it at room temperature for 15mins, followed by centrifugation at 13,000rpm for 20min. The supernatant was decanted and the DNA pellet washed with 250μL 75% isopropanol before being dried in a 37°C incubator for 30 min. The DNA sequence was subsequently read by a ABI Genetic Analyzer model AG3130xl.

#### 2.5.4.7. Quantification of DNA samples.

DNA concentration was determined spectrophotometrically using a Pharmacia Biotech Ultraspec 2000 spectrophotometer (Little Chalfont, U.K.). Suitable dilutions were first made in TE buffer prior to recording sample absorbance at 260nm and 280 nm using a disposable UV cuvette. An $OD_{260nm}$ of 1 corresponds to ~50mg/mL of dsDNA. An $A_{260}/A_{280}$ ratio of 1.8 signifies a pure, protein-less DNA solution.

### 2.5.5. Analysis of DNA by gel electrophoresis.

#### 2.5.5.1. Agarose gel electrophoresis.

For the separation of DNA using a 1% agarose gel, 1g of Gensieve LE agarose was first mixed with 100mL 1xTAE buffer (Table 2.1) and heated until dissolution. 5μL of a 10mg/mL ethidium bromide stock was added to 100mL of molten agarose which was then poured into a suitable gel mould. After the gel had set it was placed into an electrophoresis tank and submerged, again using 1xTAE buffer. DNA undergoing analysis was mixed with 10x DNA loading buffer (to a 1x DNA loading buffer concentration; Table 2.1) and loaded into the relevant well on the gel. DNA ladders with known fragment sizes were also loaded to act as size controls. After loading, the samples were separated using the following conditions - Volts: 100V, Amps: 400w,

time: 1hr. The resultant separation was observed using an ultraviolet (UV) transilluminator and photographed using a Sony monitor. Separation of lower sized DNA was achieved with 1.5 and 2% agarose gels and/or increased running times.

Genomic DNA examined by Southern analysis was first digested with the appropriate restriction enzyme (Section 2.5.4.1), mixed with 10x DNA loading buffer as described above and loaded into the relevant well on a 0.6% agarose gel. Electrophoresis was then performed using a two step methodology. First, the gel was subjected to conditions that ensured genomic DNA moved out of the wells - Volts: 100V, Amps: 400w, time: 1hr. DNA was then further separated using low voltage conditions prior to blotting as follows: Volts: 30V, Amps: 400w, time: 18hrs. A radioactive marker mix (Section 2.5.6.2) was also added to the appropriate lane prior to separation to aid sizing of blotted products and to also help determine the orientation of samples within the gel post blotting. The resultant gel was visualised and recorded as described above.

### 2.5.5.2. Preparation of chromosomal DNA for Pulsed-Field Gel Electrophoresis (PFGE).

The CHEF$^{TM}$ genomic plug kit from Bio-Rad was used to prepare chromosomal DNA from *S. pombe* strains in preparation for separation and visualisation via PFGE. Strains requiring analysis were first cultured O/N in 15mL of selective media (EMM broth, supplements, T). $OD_{595nm}$ readings were then made and cell concentration determined (Section 2.5.1.3). A volume corresponding to $5x10^8$ cells was taken from the culture, inserted into a 15mL Falcon tube and centrifuged at 2,000rpm for 2mins to obtain a cell pellet. The supernatant was decanted and the cells subjected to three washing and centrifugation cycles (as above) with 5mL of chilled 0.05M EDTA at

pH8.0, after which all traces of the supernatant were removed. To prepare three plugs, the pellet was resuspended in 122µl Cell Suspension Buffer (provided) followed by the addition of 6µl of Lyticase (provided). 80µl of pre-molten 2% Clean Cut™ agarose was then added to the suspension, after which the resultant mixture was transferred to plug moulds and allowed to set at 4°C for 15mins. The solidified plugs were removed from the moulds into 463µl of Lyticase Buffer (provided) and 16µl of Lyticase added. Following incubation O/N at 37°C, the lyticase solution was removed and the plugs washed three times with sterile $H_2O$. The plugs were then immersed in 470µl of Proteinase K Buffer with 19µl of Proteinase K (both provided). Following incubation at 50°C O/N the proteinase K solution was removed and the plugs were washed three times with 1 x Washing Buffer (provided) before being stored at 4°C in 2mL of the same buffer until use.

**2.5.5.3. Running and visualisation of pulsed-field gels.**

An agarose gel for use with the CHEF Mapper™ system (Hemel Hempstead, U.K.) was prepared by inserting 1.2 g ('low resolution'; 0.8%) or 1.8 g ('high resolution'; 1.2%) of agarose (pulsed-field certified) into 150mL of sterile 1xTAE buffer. After heating, the molten agarose was poured into a suitable gel mould and allowed to set. Pre-prepared agarose plugs containing chromosomal DNA (Section 2.5.5.2) were loaded into the wells and the resultant gel placed into a contour-clamp homogeneous electric field (CHEF Mapper™ system) electrophoresis tank filled with 2L of 1xTAE buffer. For 'low resolution' analysis, electrophoresis was performed using the following conditions: - 2 V/cm, 72 hr, 20 min/60 min switch time, 106° angle, and linear ramping. For 'high resolution' analysis i.e. the separation of chromosomal fragments ranging from 600-300kb, electrophoresis was performed using the following conditions: 4 V/cm, 48 hr, 1 min switch time, 112° angle, linear ramping.

After electrophoresis, gels were stained in 500mL of 1xTAE buffer containing 50 µl 10mg/mL ethidium bromide for 2-3hrs. Excess ethidium bromide was then washed off with 100mL $H_2O$ after which stained gels were visualised using a UV transilluminator and the image was captured using Quantity-One® software (Bio-Rad).

### 2.5.6. Southern blot analysis.

#### 2.5.6.1. Transfer of chromosomal/genomic DNA to nitrocellulose.

Chromosomal or genomic DNA separated via pulsed-field/agarose gel electrophoresis was transferred onto Genescreen™ nylon membrane (NEN® Life Science Products. Hounslow, U.K.) using slightly alkaline downward elution. The agarose gel used to separate DNA was first soaked in 0.1M HCl for 20mins at room temperature with agitation to depurinate DNA. DNA within the gel was then denatured and neutralized for blotting by soaking in transfer buffer (Table 2.1) for a further 20mins at room temperature, again with agitation. During this time, a nylon membrane cut just larger than the gel was equilibrated for 10mins in transfer buffer. Whilst the gel and membrane were soaking, an even stack of blue-paper towels was constructed to form a base for the transfer. Three pieces of Whatmann 3MM filter paper, again slightly larger than the gel, were dipped into transfer buffer and placed onto the centre of the towel base. The equilibrated membrane was then placed over this and air bubbles removed. The neutralised gel was placed over the nylon membrane, a further three pieces of pre-dipped 3MM paper (again in transfer buffer) placed on top and wicks constructed, again out of 3MM paper. These were soaked in transfer buffer, laid on top of the gel-paper towel stack and placed into reservoirs containing transfer buffer to enable downward transfer of DNA through capillary action. The stack was left O/N after which time it was dismantled, the membrane removed and crosslinking

performed using UV (120 J/cm$^2$). The resultant membrane was incubated in post transfer (Table 2.1) buffer for 20mins prior to storage at -20°C.

**2.5.6.2. Radioactive marker/probe compilation.**

An adapted Klenow protocol (Section 2.5.4.3) was used to incorporate $\alpha$-$^{32}$P dCTP into the 3' termini of a 1kb DNA ladder (New England Biolabs). 14µl of $H_2O$ was first inserted into a 1.5mL micro-centrifuge tube followed by 1µl of 1kb DNA ladder, 2µl NEbuffer 2 (New England Biolabs), 1µl of a 1mM dTTP, dGTP, dATP mix and 1µl of Klenow fragment (units). 1µl of a 10mCi/mL $\alpha$-$^{32}$P dCTP solution was then added and the mixture incubated at 25°C for 20-30mins to allow incorporation. Following this period, 2µl 0.5M EDTA was added to the reaction and unincorporated $\alpha$-$^{32}$P dCTP and other nucleotides removed by centrifugation at 5,000rpm for 3 min using a Quick Spin$^{TM}$ G-50 column (Boerhinger Mannheim, UK). Prior to agarose gel electrophoresis, 1.5µl of radiolabelled marker was mixed with 12µl of unlabelled marker, 46.5µl $H_2O$ and 12µl 10x DNA loading buffer. 20µl was then inserted into the relevant wells on the gel (Section 2.5.5.1), genomic DNA loaded and electrophoresis performed as described.

dsDNA probes, acquired through PCR or via the digestion of pre-existing plasmid, were radiolabelled with $\alpha$-$^{32}$P dCTP using the the Megaprime$^{TM}$ DNA Labelling kit as follows. A volume corresponding to 500ng of dsDNA probe was first inserted into a 500µl micro-centrifuge tube, followed by 5µl of Megaprime$^{TM}$ Random Primer Buffer (provided) and $H_2O$ to a final volume of 10µl. The micro-centrifuge tube was then placed into a beaker full of boiling water and left to cool slowly to room temperature (performed to denature the probe DNA and allow random primers to anneal). Once cooled, 10µl Megaprime$^{TM}$ Labelling Buffer (provided), 25µl $H_2O$, 2µl

Klenow (provided) and 3µl of α-$^{32}$P dCTP (10mCi/mL) were added to the probe-primer mixture and the resultant solution incubated at 37°C for 1 hour. Unincorperated α-$^{32}$P dCTP and protein were removed using a Quick Spin™ G-50 column as described above.

### 2.5.6.3. Southern probing.

Nylon membranes undergoing analysis were rolled up in a nylon mesh with the DNA facing inwards and placed within a hybridisation tube. 25ml of prehybridisation buffer (Table 2.1) was added and the tube incubated in a Thermo Electron Corporation Hybaid Maxi-14 hybridisation oven (Basingstoke, U.K.) at 65°C for 1hr. After this time, prehybridisation buffer was removed and 25ml of hybridisation buffer (Table 2.1) and radiolabelled probe inserted. Hybridisation was carried out O/N at 65°C. The membrane was then washed twice with 2x SSC for 5mins at room temperature followed by a further wash with 2x SSC, 0.1% SDS at 65°C for 10mins. Further washes were performed if required to reduce the amount of non-specific binding to the membrane. To visualise the blot, excess liquid was removed from the membrane and the blot exposed to a Bio-Rad Personal Molecular Imager FX phosphorimager screen for either 4hrs or O/N. The screen was then scanned using a Bio-Rad Phosphoimager Molecular-FX™ apparatus in conjunction with Quantity-One® software.

### 2.5.6.4. Stripping the blot.

Radioactive probe was removed from the nylon membrane using high levels of SDS. The blot was either incubated in 0.4M NaOH at 42°C for 30mins, followed by a further 30min incubation with 0.1xSSC, 0.1% SDS, 200mM Tris-HCl (pH7.5) at

42°C, or the blot was incubated with 1% SDS, 0.1xSSC at 100°C for 30mins. The stripped blot was exposed to Kodak film for four days to confirm that the probe had been removed. The blot was then either re-probed or stored as previously described.

### 2.5.7. Analysing cellular responses to a site-specific DNA double-strand break.

#### 2.5.7.1. A genetic assay for investigating DSB-induced loss of heterozygosity (LOH) – The LOH assay.

A typical experiment for HO endonuclease induced DSB production in a $Ch^{16}$-MGH or $Ch^{16}$-MHH strain is described. A schematic representation of the assay procedure can be found in Figure 2.1. Strains undergoing analysis were first revived on selective media (EMM agar, supplements, T), restreaked onto YE5S+G418 or YE5S+Hyg (for $Ch^{16}$-MGH and $Ch^{16}$-MHH, respectively) and incubated at 30°C O/N to remove cells that had lost their $G418^R$ or $Hyg^R$ marker due to leaky DSB induction and repair/misrepair. Strains were then cultured O/N at 30°C, again under selective conditions (EMM broth, supplements, T) to an $OD_{595}$ ~0.2, at which point a small sample was taken from the culture and an $OD_{595nm}$ measurement made. The appropriate volume of culture was then diluted in 10ml YE5S broth and 160µl plated onto YE5S agar in triplicate to achieve ~400 colonies per plate (t=0hrs). For example, with a wild-type $Ch^{16}$-MGH or $Ch^{16}$-MHH culture displaying an $OD_{595nm}$ of 0.2, 20µl was diluted in 10mL YE5S broth prior to plating to give ~400 colonies. The remaining culture was then split into two and centrifuged at 2,000 rpm for 2mins. Each sample was washed twice with PBS and resuspended in EMM+UAH with or without thiamine (Cultures termed 48hrs+T and 48hrs-T, respectively). Thiamine withdrawal de-represses HO endonuclease expression from pREP81X-HO and promotes subsequent DSB induction. The 48hrs+T culture was performed to investigate the level of spontaneous minichromosome loss. The two cultures were

subsequently incubated at 30°C for 48 hours with agitation and maintained in logarithmic phase throughout this time by diluting with EMM+UAH with or without thiamine. Following this period, further $OD_{595nm}$ measurements were made and samples taken from both the 48hrs+T and 48hrs-T cultures for plating as for t=0hrs. These plates were then incubated at the appropriate temperature until colonies were observed.

Colony number per YE5S plate was recorded at each timepoint i.e. t=0, 48hrs+T and 48hrs-T, after which the percentage of cells undergoing interchromosomal gene conversion (GC; *ade*$^+$ G418$^S$/HygB$^S$ *his*$^+$ colonies), end joining or sister chromatid recombination (EJ/SCR; *ade*$^+$ G418$^R$/HygB$^R$ *his*$^+$ colonies) and extensive LOH (centromere distal: *ade*$^+$ G418$^S$/HygB$^S$ *his*$^-$, centromere proximal: *ade*$^-$ G418$^S$/HygB$^S$ *his*$^+$ colonies) at all timepoints was identified using replica plating to EMM+ULHT (*ade*$^-$), EMM+ULAT (*his*$^-$) and YE5S+G418 or YE5S+Hyg plates. Levels of DSB-induced repair were calculated from 48hrs-T analyses. To determine levels of DSB-induced minichromosome loss, spontaneous Ch$^{16}$-MGH/Ch$^{16}$-MHH loss (*ade*$^-$ G418$^S$/HygB$^S$ *his*$^-$ colonies, calculated from LOH assays performed with vector only) was subtracted from the number of *ade*$^-$ G418$^S$/HygB$^S$ *his*$^-$ colonies 48h-T in strains containing HO vector. From strains where blank vector controls were not used, spontaneous Ch$^{16}$-MGH or Ch$^{16}$-MHH loss was calculated using *ade*$^-$ G418$^S$/Hyg$^S$ *his*$^-$ values from 48h+T cultures. More than 1000 colonies were scored for each time point (excluding vector only controls), and each experiment was performed three times using three independently derived isolates from each genetic background, except where noted. Colonies isolated for analysis either by PFGE and/or PCR were restreaked to singles, their markers confirmed and subsequently frozen as described.

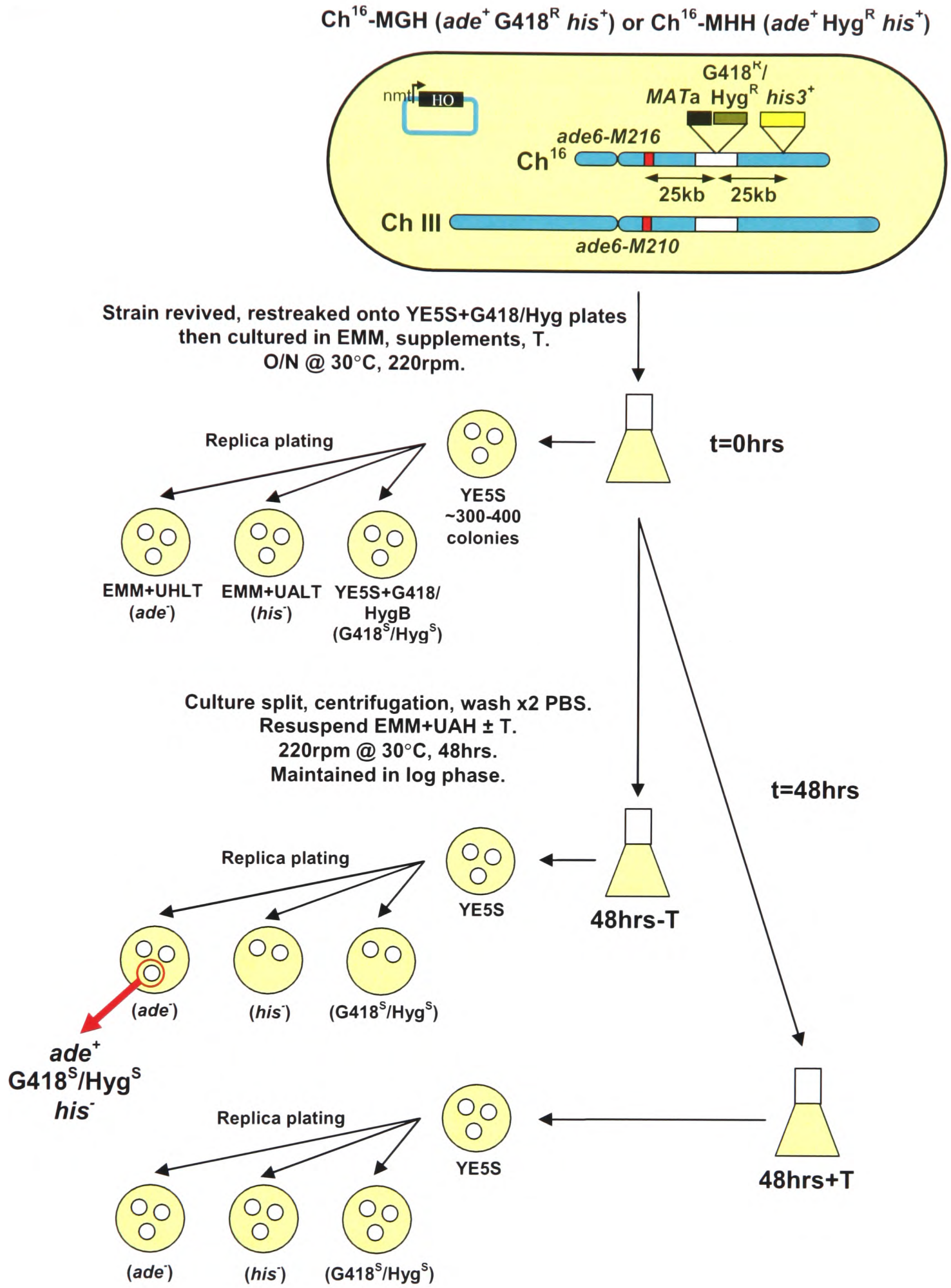



**Figure 2.1. LOH assay (Schematic of assay procedure).** See text for details.

The proportion of LOH attributed to translocations ($Ch^X$), *de novo* telomere addition (TEL+) or uncharacterised mechanisms ('Other') was subsequently calculated as a percentage of the overall level of DSB-induced LOH (see Tables 3.1 and 5.1) following PFGE and PCR analysis of ≥20 *ade*$^+$ $G418^S$/$HygB^S$ *his*$^-$ colonies, isolated from three individual strains from each genetic background (Table 2.4). Colonies which had undergone TEL+ or 'Other' were catergorised into either '$Ch^{16}$' or '$Ch^{XY}$' subgroups depending on whether they displayed ChI, ChII, ChIII and a minichromosome band similar in size to 'uncut' $Ch^{16}$-MGH/$Ch^{16}$-MHH ('$Ch^{16}$'), or ChI, ChII and either a singlet or doublet chromosomal band similar in size to $Ch^X$ ('$Ch^{XY}$') following PFGE analysis.

The proportion of EJ/SCR and GC colonies containing $Ch^{XY}$ was also calculated as a percentage of the overall level of DSB-induced repair via either of these mechanisms (see Table 5.1) following PFGE of ≥20 *ade*$^+$ $G418^R$/$HygB^R$ *his*$^+$ and *ade*$^+$ $G418^S$/$HygB^S$ *his*$^-$ and colonies, isolated from three individual strains from each genetic background (Table 2.4).

### 2.5.7.3. An assay to investigate strain viability in response to a DSB.

Strain viability in response to HO endonuclease dependent DSB induction was investigated using a single strain containing HO vector from each genetic background as follows. The strain of interest was initially treated as described for the LOH assay, however, 24hrs after initiation of the timecourse 1mL from both 48hrs+T and 48hrs-T cultures was removed and cell concentration determined using an improved Neubauer haemocytometer. The cell concentration from each sample was subsequently adjusted to $1.25x10^7$ cells/mL i.e. $1x10^5$ cells per 8μL, and 10-fold serial dilutions made, using either EMM+UHA (for 48hrs-T) or EMM+UHAT (48hrs+T), into micro-centrifuge

tubes. 8µl from each dilution was then plated onto EMM+UHA (for 48hrs-T) or EMM+UHAT (48hrs+T). The resultant plates were incubated at 32°C for 3 days and then photographed.

### 2.5.7.4. *De-novo* telomere addition assay.

This assay utilises a colony PCR based technique to detect and amplify telomeric sequence within 950bp of the *MAT*a break site on $Ch^{16}$-MGH or $Ch^{16}$-MHH. A toothpick full of target strain was first inserted into a 500µl micro-centrifuge tube. *Taq* mediated PCR was then performed with primers termed RAD21-5B and TELO-SENSE (see Appendix II) using the following conditions:

35 Cycles

94°C, 3 mins. (94°C, 45secs. 58°C, 45secs. 72°C, 4mins). 72°C, 10 mins.

The sample was then centrifuged at 10,000rpm for 10secs after which 30µl was removed and placed into another 500µl Eppendorf tube. Restriction was performed as previously described with *Mfe*I to ensure that amplification of telomeric sequence was specific. A 300bp fragment was expected from such a digest. The PCR products and digestions thereof were subsequently analysed via agarose gel electrophoresis as previously outlined.

### 2.5.7.5. Minichromosome loss assay.

The assay was performed as previously described to determine the rate of minichromosome loss per generation (Stewart *et al* 1997). The strains to be analysed were cultured overnight under selective conditions (EMM broth, supplements, T) and

diluted to an $OD_{595}$ ~0.1. A sample was taken, diluted in 10ml YE5S broth and a suitable volume plated onto YE5S agar in duplicate to give ~2000 colonies per plate (t=0). 10µl of this culture was also taken for cell counting (t=0) using an haemocytometer. The resulting culture was then centrifuged at 2,000rpm for 2mins, the pellet resuspended in YE5S broth and the resultant culture incubated at 30°C for 6hrs with agitation. Following this period, further samples were taken (t=6) for plating and counting as performed for t=0. All plates were incubated at 30°C for 48hrs after which colonies were replica plated to EMM agar, U, L, H, $A_L$, T. The proportion of pink colonies was determined for each time point and the rate of minichromosome loss per generation calculated using the following equation previously described (Murakami *et al* 1995):

$$\text{Rate of loss} = 1\text{-}e^{(1/n)\ln R_n/R_0}$$

### 2.5.8. Plasmid Construction.

#### 2.5.8.1. Construction of pREP82X-HO.

To construct pREP82X-HO, pREP81X-HO was first digested with *Sph*I and *Sac*I to excise the HO endonuclease ORF with flanking promoter and terminator regions (Appendix III). This was then ligated into pREP82, pre-digested with *Sph*I and *Sac*I and treated with CIP, transformed into DH5α™ cells and pREP82x-HO clones selected for using LB+Amp plates. Identification of pREP82x-HO clones was then performed using restriction with *Sph*I and *Sac*I.

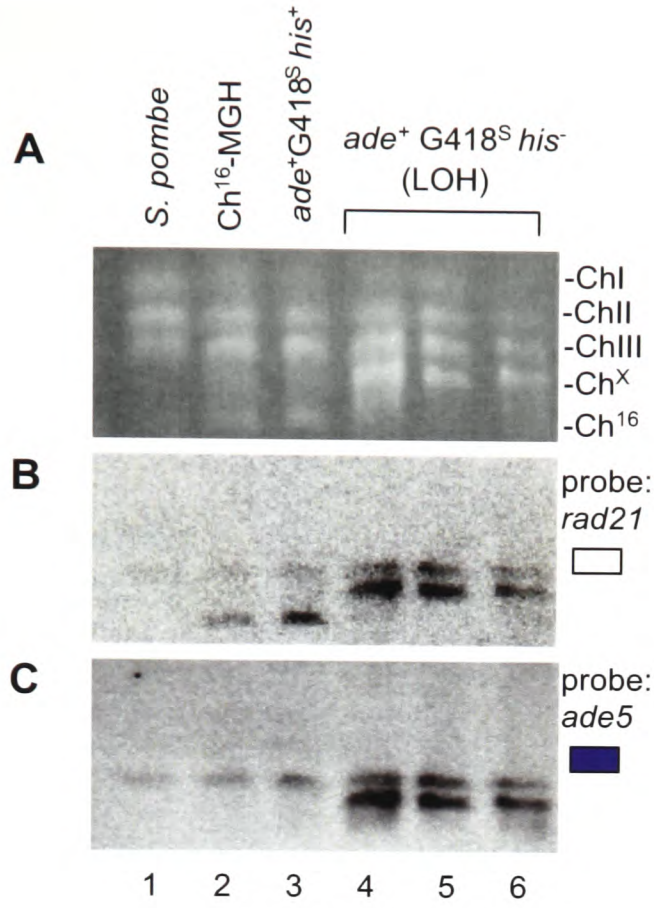
# 3. INVESTIGATING THE GENETIC REQUIREMENTS OF EXTENSIVE DSB-INDUCED LOH VIA TRANSLOCATIONS.

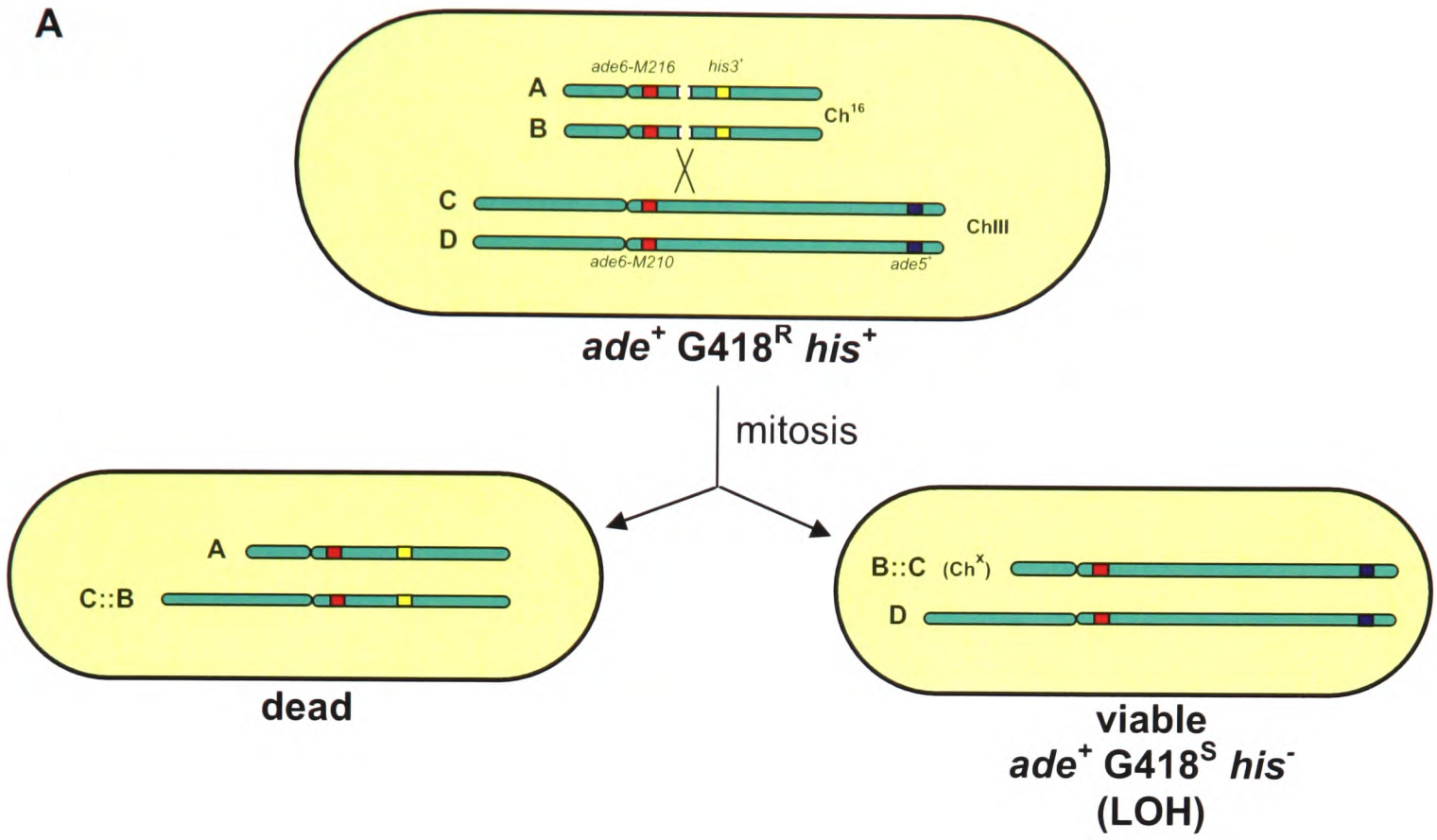
## 3.1. INTRODUCTION.

Initial studies using the $Ch^{16}$-MGH system had shown that extensive DSB-induced LOH in *S. pombe* was relatively inefficient, occurring with a frequency of 1.7% in wild-type background (Table 3.1; Hussey, 2003). Furthermore, whilst *ade*$^+$ G418$^S$ *his*$^-$ colonies were observed post DSB-induction, *ade*$^-$ G418$^S$ *his*$^+$ cells were not (Appendix IV). This indicated that extensive loss of allele specific information in wild-type $Ch^{16}$-MGH was directional. Subsequent analysis of 24 wild-type *ade*$^+$ G418$^S$ *his*$^-$ cells demonstrated that in 90% of cases extensive DSB-induced LOH was the result of a common translocation event between $Ch^{16}$ and ChIII. This resulted in the formation of a novel chromosomal element, $Ch^X$ (~2Mb), distinct from ChI, ChII and ChIII as observed via PFGE and Southern blotting (Table 3.2 and Figure 3.1A-E). Pedigree analysis subsequently revealed that such translocations most probably arose as a result of allelic crossovers (associated with either short or long tract GC) in G2-phase and BIR (Figure 3.2, 3.3B and data not shown).

Allelic crossovers and BIR are predicted to require HR. To test this, the genetic requirements of $Ch^X$ formation were subsequently investigated by analysing mutants of several genes responsible for HR in *S. pombe* i.e. *rhp55*$^+$, *rhp51*$^+$, *rhp54*$^+$ and *mus81*$^+$ (Hussey, 2003. Yu-Wee, 2006). Surprisingly, DSB-induced LOH was still observed in the absence of these genes, albeit to differing extents (Table 3.1). Indeed, the level of DSB-induced LOH, whilst comparable to wild-type in *rhp55Δ* cells, was significantly reduced in both *rhp54Δ* ($P$=0.004) and *mus81Δ* ($P$=0.001) cells (Table 3.1). In addition, no *ade*$^-$ G418$^S$/Hyg$^S$ *his*$^+$ colonies were detected in any of the tested mutants following a break (Appendix IV). Instead of losing the *his3*$^+$ marker via formation of $Ch^X$, the majority (≥90%) of *ade*$^+$ G418$^S$ *his*$^-$ or *ade*$^+$ Hyg$^S$ *his*$^-$ colonies from *rhp51Δ* (Figure 3.4A), *rhp54Δ* and *mus81Δ* cells exhibited a

**Figure 3.1. DSB-induced LOH results from large translocations in a wild-type background. A.** PFGE analysis of chromosomal DNA from a wild-type *S. pombe* strain (*S. pombe*; lane 1); an 'uncut' wild-type strain encoding $Ch^{16}$-MGH (TH1436; $Ch^{16}$-MGH; lane 2); a strain encoding $Ch^{16}$-MGH repaired by gene conversion following DSB induction (*ade*$^+$ G418$^S$ *his*$^+$; lane 3); three individually isolated *ade*$^+$ G418$^S$ *his*$^-$ colonies following DSB induction (lanes 4, 5 and 6). **B** and **C.** Southern blot analysis of the PFGE shown in (A) probed with *rad21* (C) and *ade5* (D). **D.** High resolution PFGE analysis of colonies described in (A). **E.** Schematic of the tranlsocation between $Ch^{16}$-MGH and ChIII to produce $Ch^X$. Red squares, *ade6* alleles; white square, *rad21::MAT*a/G418R; yellow square, *his3*$^+$; blue square, *ade5*$^+$. All gels and radioactive probing performed by S. Hussey, J. Prudden and C. Walker.


A
S. pombe
Ch16-MGH
ade+G418S his+
ade+ G418S his-
(LOH)
-ChI
-ChII
-ChIII
-ChX
-Ch16
B
probe:
rad21
C
probe:
ade5
1 2 3 4 5 6
D
S. pombe
Ch16-MGH
ade+G418S his+
ade+ G418S his-
(LOH)
I-
II-
III-
ChX-
Ch16-
-3.1Mb
-2.4Mb
-1.8Mb
-1.1Mb
-0.5Mb
1 2 3 4 5 6
E
ade6-M216
his3+
Ch16
ChIII
ade6-M210
ade5+
ChX (~2Mb)
ChIII



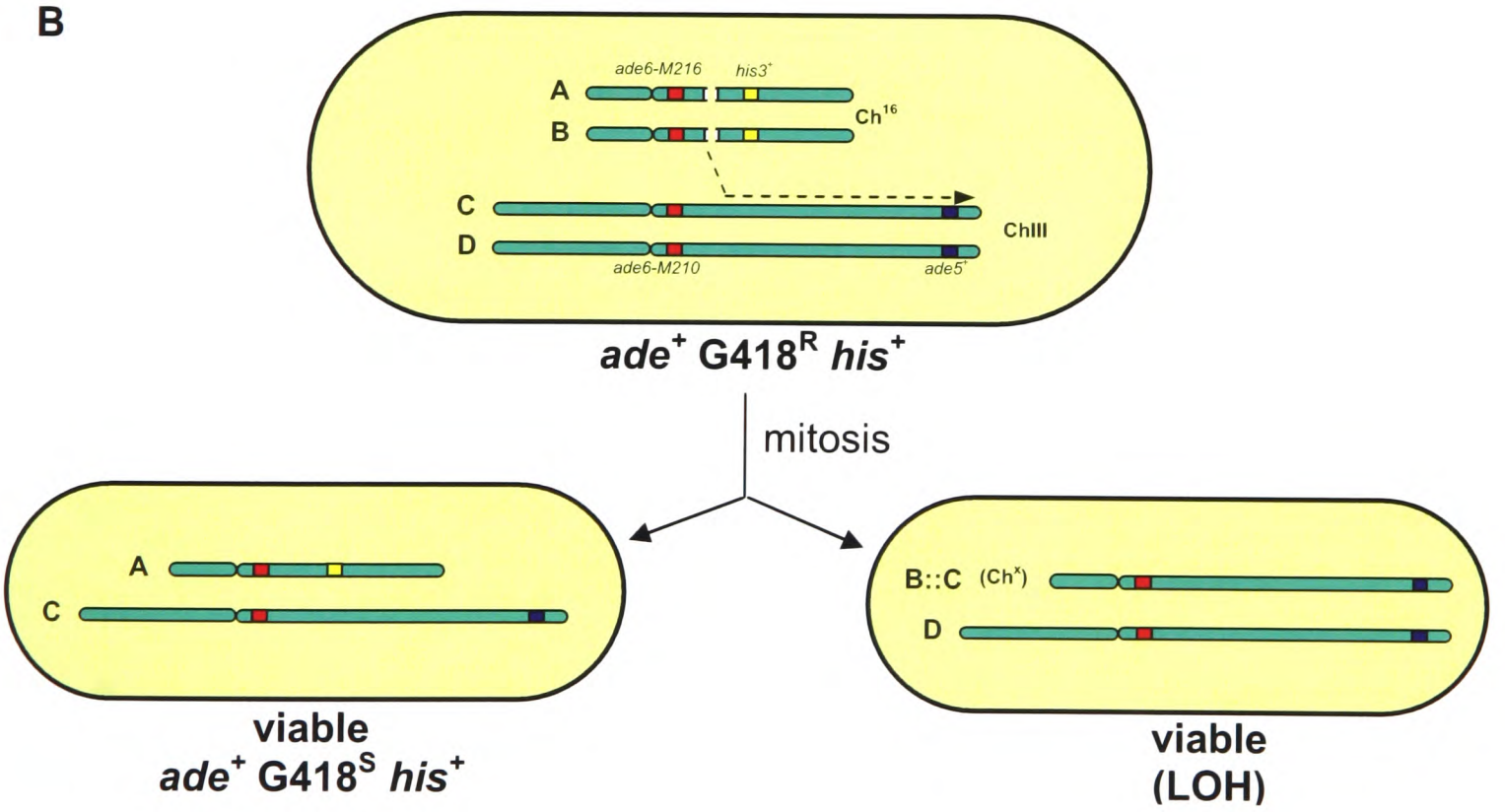




**Figure 3.2. Schematic of $Ch^X$ formation via allelic crossovers and BIR.** Diagram depicting the break-induced formation of $Ch^X$ from either: **A.** an allelic crossover between homologous chromatids during G2-phase, followed by the segregation of recombinant products (C::B and B::C) to separate daughter cells. The crossover may be associated with either a short tract (depicted) or long tract GC event (see Figure 3.3); and **B.** break-induced replication of the distal arm of ChIII in G2 cells. Replication could also be possible during G1 or S phase.

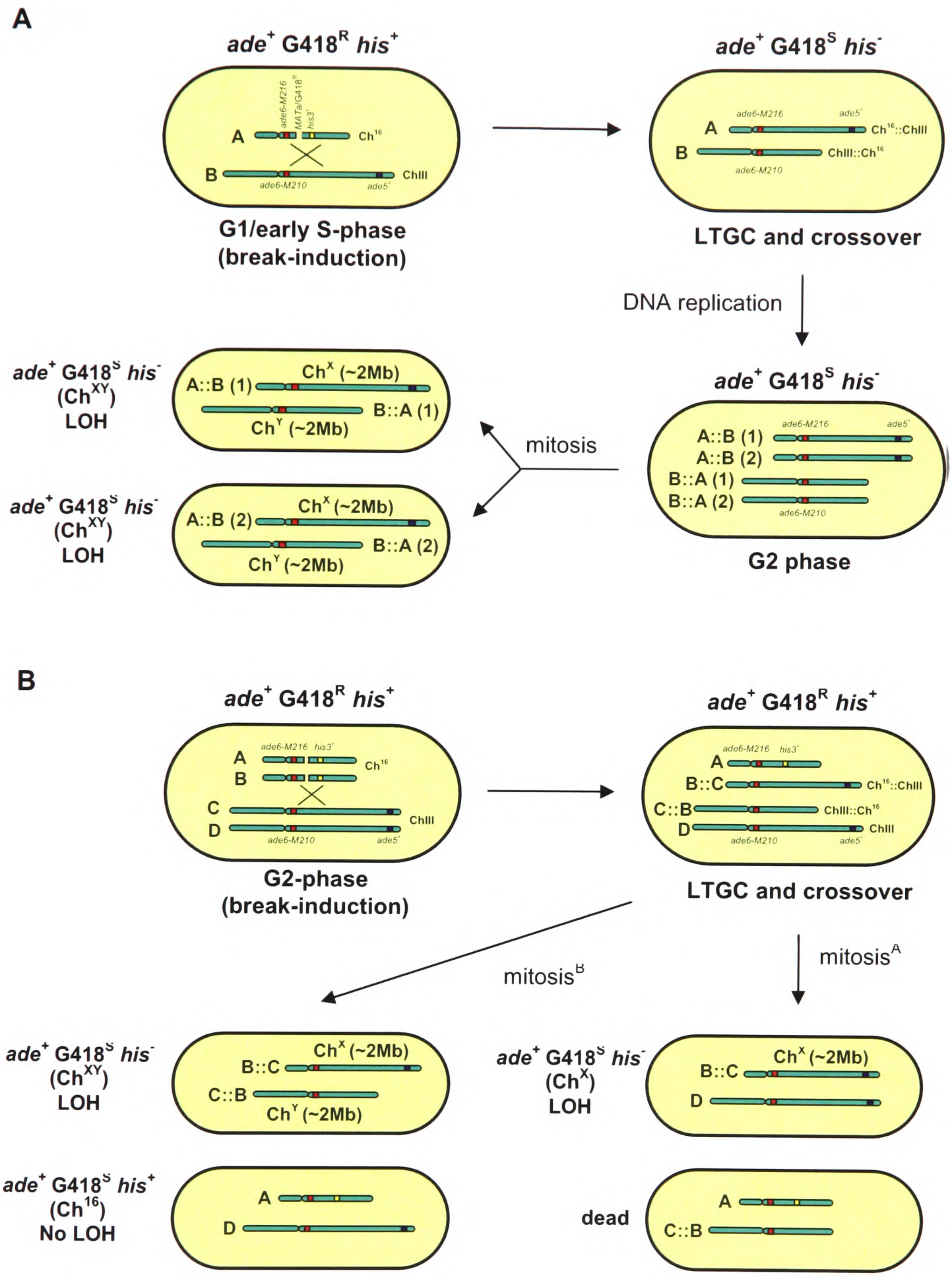



**Figure 3.3. Possible mechanisms of $Ch^{XY}$ formation in *ade*$^+$ $G418^S$/$Hyg^S$ *his*$^-$ cells from various HR mutants. A.** An allelic crossover occurs during G1/early S-phase after long tract gene conversion (LTGC), resulting in the formation of A::B and B::A recombinants and the occurrence of extensive LOH. After DNA replication, segregation results in two daughter cells containing $Ch^{XY}$. **B.** A LTGC event occurs with a single allelic crossover in G2 phase cells, resulting in the formation of B::C and C::B recombinants. Segregation leads to the formation of a cell which displays either $Ch^X$ (mitosis$^A$) or $Ch^{XY}$ (mitosis$^B$) following PFGE analysis. The sister cell in mitosis$^A$ is dead due to loss of essential sequence. The sister cell in mitosis$^B$ remains viable but has not undergone extensive LOH (Extensive LOH via an LTGC associated allelic crossover may also occur during the repair of this sister chromatid, however). ChI and II have been excluded for clarity.

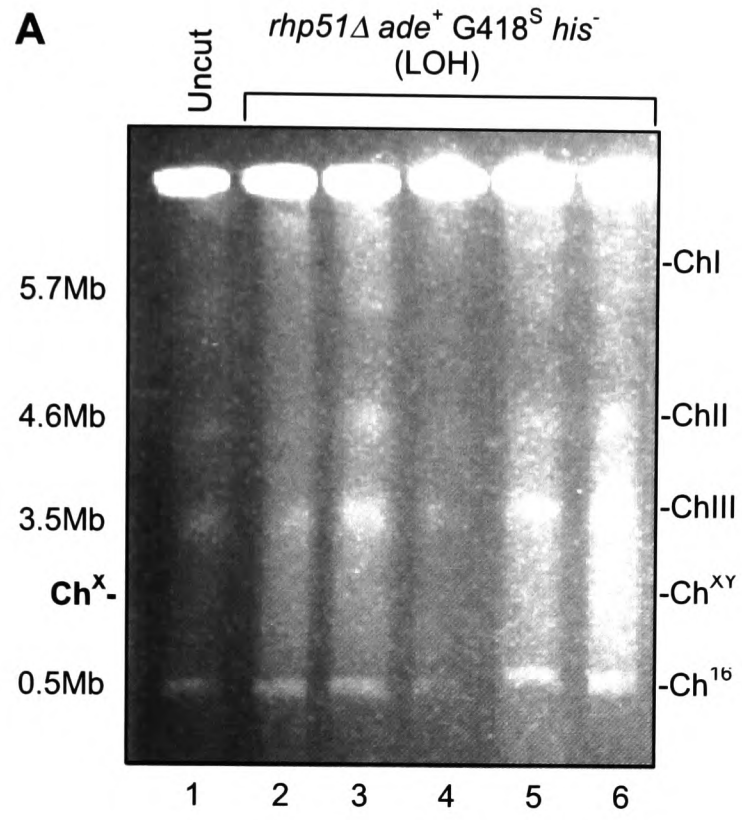



**Figure 3.4. $Ch^X$ is absent from *rhp51Δ* and *rhp55Δ* *ade*$^+$ G418$^S$ *his*$^-$ colonies.** Analysis of individually isolated *ade*$^+$ G418$^S$ *his*$^-$ colonies from *rhp51Δ* (**A**) and *rhp55Δ* (**B**) backgrounds via PFGE as described in Materials and Methods. 'Uncut' $Ch^{16}$-MGH ('Uncut') was run for comparison in **A** only. ChI, II, III, $Ch^{16}$, $Ch^X$ and $Ch^{XY}$ are depicted where appropriate. Those lanes displaying colonies excluded from further analysis (derived from a strain which had undergone an allelic crossover before analysis with the LOH assay; TH1761, data not shown) are shown. All gels performed by C. Walker and S. Hussey.

minichromosome band similar in size to uncut $Ch^{16}$ (J. Prudden, unpublished observations; Table 3.2). A small percentage of *ade*$^+$ G418$^S$/Hyg$^S$ *his*$^-$ colonies from *rhp51Δ* and *mus81Δ* backgrounds contained a single/doublet chromosomal band, approximately 2Mb in size, in addition to ChI and ChII (Table 3.2, see Figure 3.5 for a representative example). This PFGE profile is consistent with the formation of $Ch^{\underline{X}}$ and a recombinant chromosome similar in size to $Ch^X$, $Ch^{\underline{Y}}$ (Figure 3.3). No further characterisation of this chromosomal pattern, termed $Ch^{\underline{XY}}$, was performed for any mutant strain. Such a gel profile is consistent, however, with a long tract GC associated allelic crossover between $Ch^{16}$ and ChIII during G1/early S-phase or G2-phase (Figure 3.3). The situation was more complex in *rhp55Δ ade*$^+$ G418$^S$ *his*$^-$ colonies where 85% contained a band similar in size to $Ch^{16}$-MGH (Figure 3.4B) and 15% were missing a minichromosomal element altogether. Thus, extensive DSB-induced LOH arising as a result of allelic crossovers and BIR required *rhp55*$^+$, *rhp51*$^+$, *rhp54*$^+$ and *mus81*$^+$. To further investigate a requirement for HR in $Ch^X$ formation, DSB-induced repair and extensive LOH were investigated in *rad32Δ*, *rad50Δ*, *nbs1Δ*, *rad11D223Y* and *rad22Δ* backgrounds.

## 3.2. ALLELIC CROSSOVERS AND BIR REQUIRE THE MRN COMPLEX, *RAD11*$^+$ AND *RAD22*$^+$.

### 3.2.1. DSB repair and extensive LOH in MRN complex mutants.

To test whether the MRN complex was required for the formation of $Ch^X$, *rad32Δ* $Ch^{16}$-MHH, *rad50Δ* $Ch^{16}$-MHH and *nbs1Δ* $Ch^{16}$-MGH were first analysed using the LOH assay as described in Section 2.5.7.1. Three individually generated strains from each background containing pREP81X-HO were tested, in addition to a single strain

**Table 3.1. DSB-induced marker loss in wt and HR mutants.**

| Genetic background | G418$^R$ or Hyg$^R$ on Ch$^{16}$? | % *ade*$^+$ G418$^S$/Hyg$^S$ *his*$^+$ (GC) | % *ade*$^+$ G418$^R$/Hyg$^R$ *his*$^+$ (EJ/SCR) | % *ade*$^-$ G418$^S$/Hyg$^S$ *his*$^-$ (Ch$^{16}$ loss) | % *ade*$^+$ G418$^S$/Hyg$^S$ *his*$^-$ (LOH) | ***P* value** (relative to wild-type LOH) |
|---|---|---|---|---|---|---|
| *wild-type* | G418$^R$ | 49.7 ± 2.6 | 25.0 ± 1.4 | 23.7 ± 1.7 | 1.7 ± 0.3 | 1.000 |
| *rad32Δ* | Hyg$^R$ | 30.7 ± 2.0 | 25.6 ± 5.1 | 35.7 ± 5.8 | 0.6 ± 0.2 | 0.013 |
| *rad50Δ* | Hyg$^R$ | 18.3 ± 1.8 | 23.9 ± 0.6 | 49.7 ± 1.9 | 0.6 ± 0.2 | 0.011 |
| *nbs1Δ* | G418$^R$ | 15.6 ± 0.7 | 30.9 ± 2.6 | 43.6 ± 3.3 | 1.4 ± 0.2 | 0.441 |
| *exo1Δ* | G418$^R$ | 52.7 ± 1.0 | 33.1 ± 0.7 | 13.0 ± 0.8 | 1.1 ± 0.5 (0.09 ± 0.05) | 0.233 |
| *rad11D223Y*** | G418$^R$ | 20.5 ± 1.5 | 27.1 ± 1.3 | 43.2 ± 2.2 | 2.9 ± 0.9 | 0.339 |
| *rad22Δ** | Hyg$^R$ | 0.0 ± 0.0 | 22.3 ± 1.1 | 68.8 ± 1.7 | 2.3 ± 0.6 | 0.453 |
| *rhp55Δ* | G418$^R$ | 2.3 ± 0.5 | 54.7 ± 7.9 | 40.1 ± 7.2 | 0.8 ± 0.3 | 0.090 |
| *rhp51Δ* | G418$^R$ | 1.0 ± 0.5 | 35.9 ± 2.9 | 57.0 ± 2.9 | 0.8 ± 0.3 | 0.058 |
| *rhp54Δ* | G418$^R$ | 2.8 ± 1.9 | 36.8± 3.3 | 32.6 ± 4.5 | 0.4 ± 0.2 | 0.004 |
| *mus81Δ* | Hyg$^R$ | 29.0 ± 2.9 | 28.1 ± 3.4 | 38.1 ± 4.4 | 0.2 ± 0.1 | 0.001 |

The levels of interchromosomal gene conversion (GC), minichromosome loss (Ch$^{16}$ loss), loss of heterozygosity (LOH) and end-joining/sister chromatid recombination (EJ/SCR) are shown. Percentages were calculated as described in Materials and Methods. Values in parenthesis (where observed) represent the percentage of ade$^-$ G418$^S$/Hyg$^S$ his$^+$ colonies identified for the mutant analysed. *Gene conversion levels in *rad22Δ* strains described here are significantly lower than those previously described (Prudden et al., 2003) which were subsequently determined to carry a suppressor mutation (Doe et al 2004).**Levels of minichromosome loss were calculated using 48hrs+T *ade*$^+$ marker loss rather than blank plasmid values (See Materials and Methods).

**Table 3.2. PFGE analysis of *ade*$^+$ G418$^S$/Hyg$^S$ *his*$^-$ colonies from wt and HR mutants.**

| Genetic background | G418$^R$ or Hyg$^R$ on Ch$^{16}$? | % *ade*$^+$ G418$^R$/Hyg$^R$ *his*$^-$ (LOH) | # LOH endpoints analysed | Ch$^X$ (%) | Ch$^{16}$ (%) | Ch$^{XY}$ (%) | Missing (%) |
|---|---|---|---|---|---|---|---|
| *wild-type* | G418$^R$ | 1.7 ± 0.3 | 22 | 19/22 (86) | 2/22 (9) | 0/22 (0) | 1/22 (5) |
| *rad32*Δ | Hyg$^R$ | 0.6 ± 0.2 | 21 | 0/21 (0) | 19/21 (90) | 2/21 (10) | 0/21 (0) |
| *rad50*Δ | Hyg$^R$ | 0.6 ± 0.2 | 20 | 0/20 (0) | 13/20 (65) | 4/20 (20) | 3/20 (15) |
| *nbs1*Δ | G418$^R$ | 1.4 ± 0.2 | 21 | 0/21 (0) | 19/21 (90) | 2/21 (10) | 0/21 (0) |
| *exo1*Δ | G418$^R$ | 1.1 ± 0.5 | 22 | 3/22 (14) | 19/22 (86) | 0/22 (0) | 0/22 (0) |
| *rad11D223Y* | G418$^R$ | 2.9 ± 0.9 | 20 | 0/20 (0) | 19/20 (95) | 1/20 (5) | 0/20 (0) |
| *rad22*Δ | Hyg$^R$ | 2.3 ± 0.6 | 24 | 0/24 (0) | 23/24 (96) | 1/24 (4) | 0/24 (0) |
| *rhp55*Δ | G418$^R$ | 0.8 ± 0.3 | 13 | 0/13 (0) | 11/13 (85) | 0/13 (0) | 2/13 (15) |
| *rhp51*Δ | G418$^R$ | 0.8 ± 0.3 | 25 | 0/25 (0) | 24/25 (86) | 1/25 (4) | 0/25 (0) |
| *rhp54*Δ | G418$^R$ | 0.4 ± 0.2 | 20 | 0/20 (0) | 20/20 (100) | 0/20 (0) | 0/20 (0) |
| *mus81*Δ | Hyg$^R$ | 0.2 ± 0.1 | 22 | 0/22 (0) | 20/22 (91) | 2/22 (9) | 0/22 (0) |

LOH colonies (*ade*$^+$ G418$^S$/Hyg$^S$ *his*$^-$) from each strain were analysed using PFGE analysis as described in Materials and Methods. The number of *ade*$^+$ G418$^S$/Hyg$^S$ *his*$^-$ cells displaying each profile is indicated. The percentage each profile contributes to LOH is shown in parentheses. **Ch$^X$**, ChI, ChII, ChIII and Ch$^X$ observed via PFGE. Profile is indicative of a translocation between Ch$^{16}$ and ChIII i.e. allelic crossover (associated with short or long tract GC) during G2 or BIR; **Ch$^{16}$**, ChI, ChII, ChIII and a minichromosome band similar in size to 'uncut' Ch$^{16}$-MGH/MHH observed via PFGE; **Ch$^{XY}$**, ChI, ChII and Ch$^{XY}$ observed via PFGE. Such a profile is consistent with a single long tract GC associated allelic crossover between Ch$^{16}$ and ChIII during G1/early S-phase or G2 (if recombinant products co-segregate to the same daughter cell); **Missing**, ChI, ChII and ChIII but no minichromosome observed via PFGE analysis.

transformed with blank vector (Table 2.4). In order to ensure that changes in marker loss were not due to reductions in cell viability following DSB induction, spot dilutions on selective plates with or without HO induction were performed as described (Section 2.5.7.3).

Interestingly, interchromosomal gene conversion was reduced and minichromosome loss increased in *rad32Δ, rad50Δ* and *nbs1*Δ backgrounds compared to that of wild-type cells, consistent with a role for the MRN complex in efficient interchromosomal HR (Table 3.1; Bressan et al., 1999). Closer analysis revealed that the level of interchromosomal gene conversion in a *nbs1Δ* background (15.6%) was significantly lower than that observed in *rad32Δ* cells (30.7%; $P$=0.011), but comparable to that observed in *rad50Δ* cells (18.3%; $P$=0.258). Surprisingly, DSB-induced LOH still occurred in these backgrounds, although break induction lead to significantly different levels of LOH in each of the mutants. Break-induced LOH was significantly reduced in *rad32Δ* (0.6%; $P$=0.013) and *rad50Δ* (0.6%; $P$=0.011) cells compared to wild-type $Ch^{16}$-MGH (Table 3.1). LOH was also significantly decreased in both *rad32Δ* ($P$=0.034) and *rad50Δ* ($P$=0.032) compared to *nbs1Δ* cells (Table 3.1). In *nbs1Δ* $Ch^{16}$-MGH, however, extensive DSB-induced LOH (1.4%) occurred with comparable frequency ($P$=0.441) to that observed in wild-type background. Such extensive loss of allele specific information was break-dependent in all backgrounds as $G418^R/Hyg^R$ and *his3*$^+$ marker loss was not observed following incubation for 48 hours in the presence of thiamine, or in strains transformed with blank vector (Appendix IV). In addition, no *ade*$^-$ $G418^S/Hyg^S$ *his*$^+$ colonies were observed after break-induction in *rad32Δ, rad50Δ* or *nbs1Δ* cells. Since all strains showed no loss of viability in response to a DSB (Appendix V) the difference in phenotype between *rad32Δ,*

*rad50Δ* and *nbs1Δ* null mutants may reflect a number of additional roles for the MR complex in promoting extensive DSB-induced LOH.

### 3.2.2. $Ch^X$ formation requires *rad32*$^+$, *rad50*$^+$ and *nbs1*$^+$.

To test whether components of the MRN complex were required for the formation of $Ch^X$, greater than or equal to 20 *ade*$^+$ $G418^S/Hyg^S$ *his*$^-$ colonies isolated from the three independently tested strains from each background were analysed by 'low resolution' PFGE as described in Section 2.5.5.2 and 2.5.5.3.

PFGE analysis failed to identify the presence of $Ch^X$ in any of the *ade*$^+$ $G418^S/Hyg^S$ *his*$^-$ cells isolated from *rad32Δ*, *rad50Δ* or *nbs1Δ* backgrounds (Figure 3.5, Table 3.2). Instead, in addition to ChI, ChII and ChIII, the majority of *ade*$^+$ $G418^S/Hyg^S$ *his*$^-$ colonies (≥80%) from these strains contained a minichromosomal band similar in size to 'uncut' $Ch^{16}$-MGH (Table 3.2). Interestingly, a minichromosomal band was missing in 15% of *rad50Δ ade*$^+$ $Hyg^S$ *his*$^-$ cells. Similar to *rhp51Δ* and *mus81Δ*, approximately 10% of *rad32Δ ade*$^+$ $Hyg^S$ *his*$^-$ colonies exhibited $Ch^{XY}$, as did 20% of *rad50Δ ade*$^+$ $Hyg^S$ *his*$^-$ and 10% of *nbs1Δ ade*$^+$ $G418^S$ *his*$^-$ cells (Figure 3.5, Table 3.2). Since $Ch^X$ was not observed in any of the *ade*$^+$ $G418^S/Hyg^S$ *his*$^-$ colonies tested and $Ch^{XY}$ was observed at very low frequency, these data are consistent with a requirement for the MRN complex in DSB-induced LOH via allelic crossovers and BIR in *S. pombe*.

### 3.2.3. DSB repair and extensive LOH in *rad11D223Y*.

*rad11*$^+$ encodes the orthologue of the large subunit of RPA in *S. pombe*, which is known to play essential roles in both DNA replication and HR (Section 1.3.2.2). An

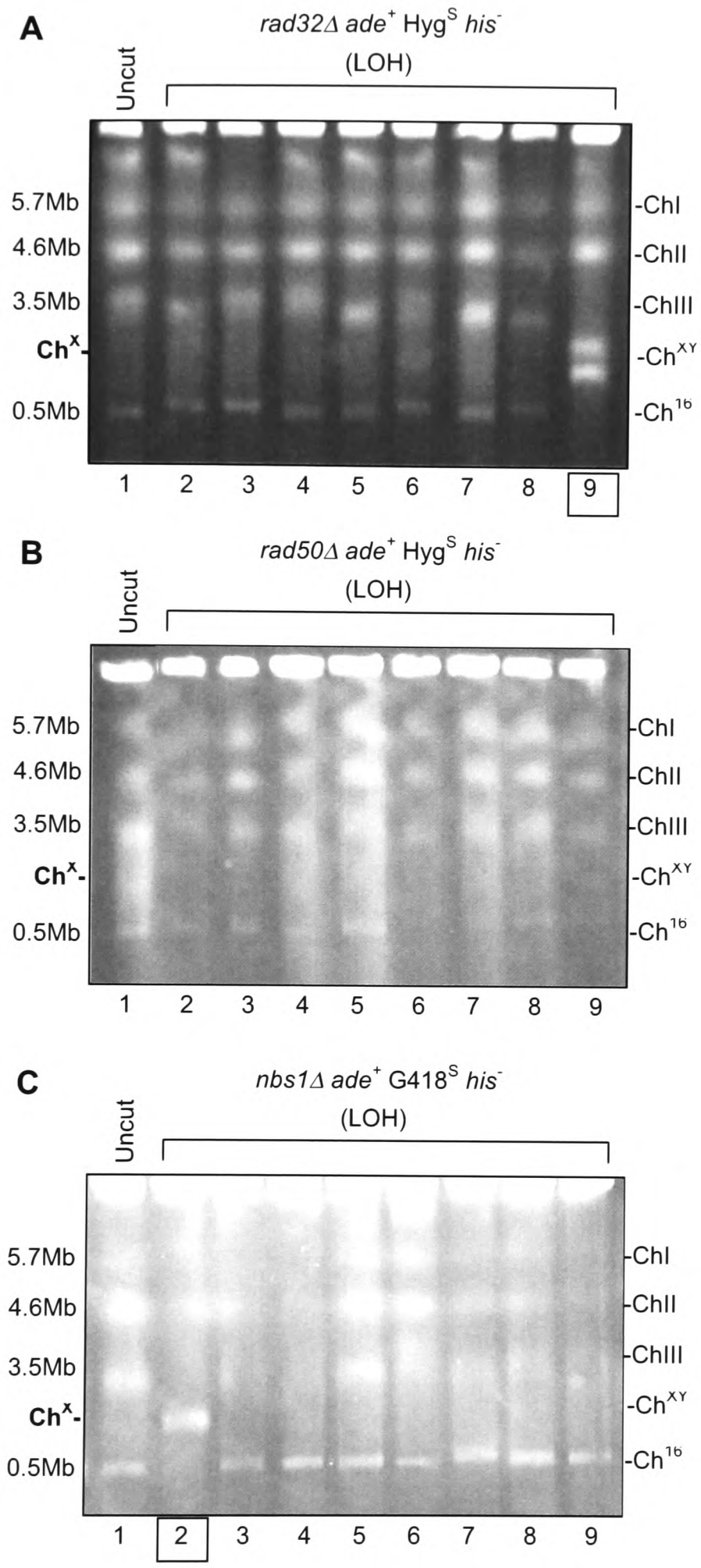



**Figure 3.5. $Ch^X$ is absent from *rad32Δ*, *rad50Δ* and *nbs1Δ* *ade*$^+$ $G418^S/Hyg^S$ *his*$^-$ colonies.** Analysis of individually isolated *ade*$^+$ $G418^S$ *his*$^-$ colonies from *rad32Δ* (**A**), *rad50Δ* (**B**) and *nbs1Δ* (**C**) backgrounds via PFGE as described in Materials and Methods. 'Uncut' $Ch^{16}$-MGH/MHH from each background ('Uncut') was run for comparison. ChI, II, III, $Ch^{16}$ and $Ch^{XY}$ are depicted where appropriate. Lanes in which $Ch^{XY}$ was observed are marked by boxes. *rad50Δ* and *nbs1Δ* gels performed by C. Walker.

allele of *rad11*$^{+}$, *rad11D223Y*, has previously been found to have defects in HR repair and telomere maintenance (Ono et al., 2003). To test whether this mutation affected the formation of Ch$^{X}$, *rad11D223Y* Ch$^{16}$-MGH was first analysed using the LOH assay (Section 2.5.7.1). Three individual strains were tested as previously described (Table 2.4).

Break-induction in *rad11D223Y* Ch$^{16}$-MGH also lead to a decrease in interchromosomal GC (20.5%) and an increase in minichromosome loss (43.2%) compared to wild-type, suggesting that *rad11*$^{+}$ is required for efficient repair via HR in *S. pombe* (Table 3.1). Interestingly, the level of extensive DSB-induced LOH was substantially higher than that observed in wild-type background, occurring with a frequency of 2.9%. Again, break-induced LOH was directional such that no *ade*$^{-}$ G418$^{S}$ *his*$^{+}$ colonies were observed (Table 3.1 and Appendix IV). This data suggested that mutations in RPA can lead to increases in genome instability by promoting extensive DSB-induced LOH.

### 3.2.4. Ch$^{X}$ is not observed in *rad11D223Y*.

To test whether the *D223Y* mutation affected the ability of Rad11 and thus RPA to promote the formation of Ch$^{X}$, 20 *rad11D223Y ade*$^{+}$ G418$^{S}$ *his*$^{-}$ colonies isolated from three independently tested strains were analysed using 'low resolution' PFGE (Section 2.5.5.2 and 2.5.5.3).

As with MRN null mutants, Ch$^{X}$ was not detected in any of the 20 *rad11D223Y ade*$^{+}$ G418$^{S}$ *his*$^{-}$ colonies tested via PFGE (Figure 3.6A, Table 3.2). Interestingly, all but one of the *ade*$^{+}$ G418$^{S}$ *his*$^{-}$ cells from this background exhibited a minichromosomal band similar to 'uncut' Ch$^{16}$-MGH. The remaining colony displayed Ch$^{XY}$. Thus, the

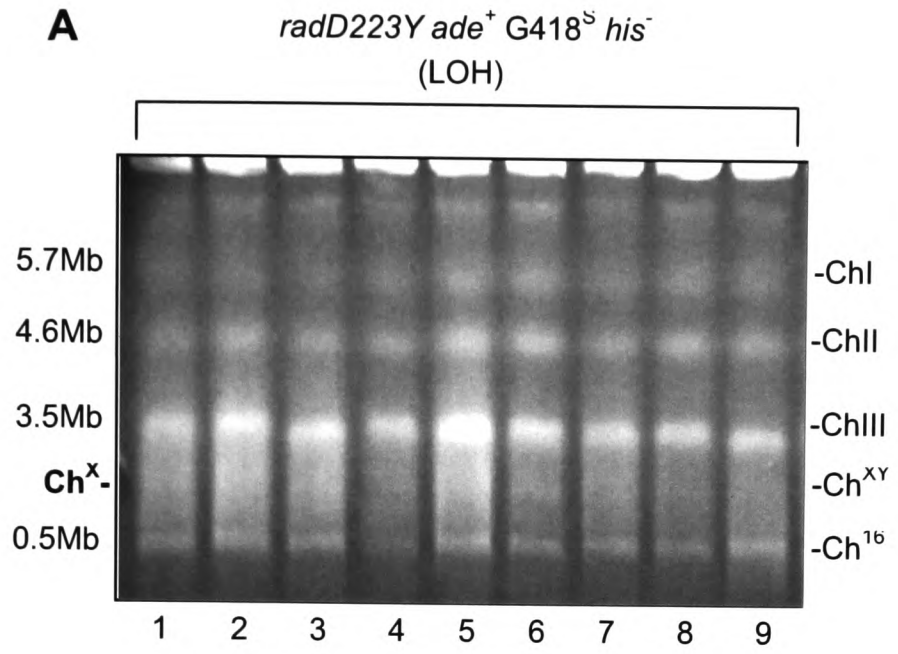



**Figure 3.6. $Ch^X$ is absent from *rad11D223Y* and *rad22Δ* *ade*$^+$ G418$^S$/Hyg$^S$ *his*$^-$ colonies.** Analysis of individually isolated *ade*$^+$ G418$^S$ *his*$^-$ colonies from *rad11D223Y* (**A**) and *rad22Δ* (**B**) backgrounds via PFGE as described in Materials and Methods. ChI, II, III, $Ch^{16}$ and $Ch^{XY}$ are depicted where appropriate. Lanes in which $Ch^{XY}$ was observed are marked by boxes. Gels performed by C. Walker.

*D223Y* mutation in *rad11*$^{+}$ abrogates the formation of allelic crossovers and BIR, promoting a slight increase in extensive DSB-induced LOH via an alternative mechanism/s.

### 3.2.5. DSB repair and extensive LOH in *rad22Δ*.

Previous reports have detailed the ease with which both the slow growth phenotype of *rad22Δ* and its sensitivity to DNA damaging agents can be suppressed. Indeed, it was recently discovered that mutations in a gene involved in regulating Rhp51 nucleoprotein filament formation, *fbh1*$^{+}$, can partially suppress these defects (Osman et al., 2005). To ensure suppressor mutations were absent in *rad22Δ* Ch$^{16}$-MHH prior to analysis using the LOH assay, a *rad22Δ* strain with suppressed sensitivity to DNA damaging agents (TH2058; Figure 3.7A) was first backcrossed to a wild-type *S. pombe* strain (TH2094; Table 2.4) and candidates with the desired markers selected and screened for sensitivity to 0.0008% (v/v) MMS and 0.5μM CPT (Sections 2.5.1.5 and 2.5.1.6). A wild-type and non-suppressed *rad22Δ* strain (TH2129; Osman et al., 2005) were used for comparison. Candidates containing the correct markers were quickly frozen as described in Materials and Methods to prevent the accumulation of suppressing mutations.

### 3.2.6. Isolation and analysis of non-suppressed *rad22Δ* Ch$^{16}$-MHH.

Several unsuppressed *rad22Δ* Ch$^{16}$-MHH candidates were identified using the screen method, each displaying MMS and CPT sensitivity similar to that of TH2129 (data not shown). Three of these candidates were selected and their sensitivity subsequently confirmed via spot dilution. Indeed, all three strains were as sensitive as TH2129 to both 0.0008% (v/v) MMS and 0.5μM CPT, suggesting that they did not harbour

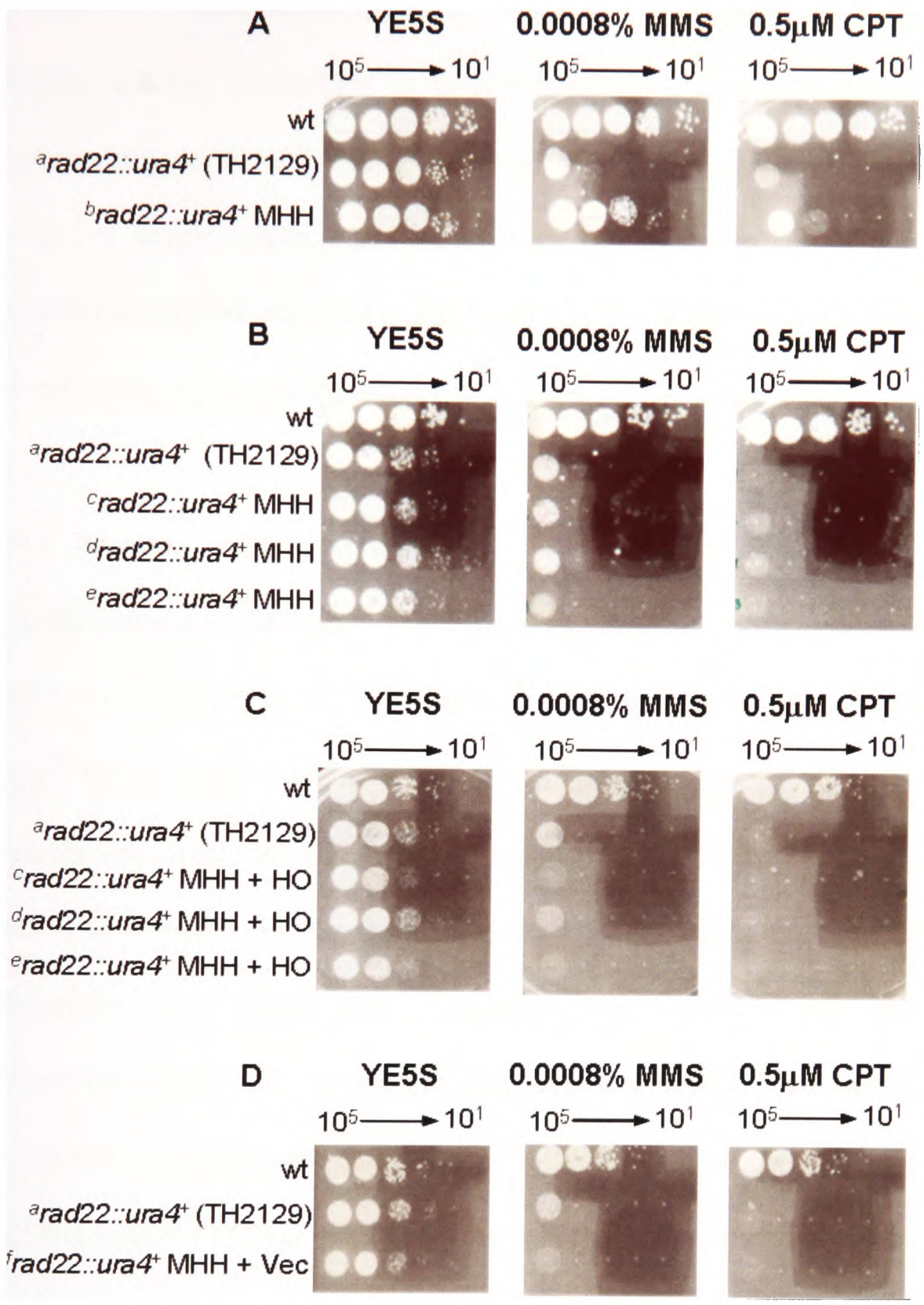



**Figure 3.7. Isolation of non-suppressed *rad22Δ* Ch[16]-MHH. A.** Spot dilutions of wild-type Ch[16]-MGH (TH1436; wt), non-suppressed *rad22Δ* (TH2129; [a]*rad22::ura4*$^+$) and suppressed *rad22Δ* Ch[16]-MHH (TH2058; [b]*rad22::ura4*$^+$ Ch[16]-MHH) strains on YE5S, 0.0008% (v/v) MMS and 0.5μM CPT. **B, C.** Spot dilutions of three individually isolated non-suppressed *rad22Δ* Ch[16]-MHH strains ([c,d,e]*rad22::ura4*$^+$ Ch[16]-MHH, TH2655, TH2656, TH2657, respectively) onto media described in A before (**B**) and after (**C**) transformation with pREP81X-HO (+HO, TH2658, TH2659, TH2660). Wild-type and non-suppressed controls are also shown. **D.** Spot dilutions of a *rad22Δ* Ch[16]-MHH strain ([f]*rad22::ura4*$^+$ Ch[16]-MHH, TH2661) onto media described in (**A**) after transformation with blank vector (+ Vec).

suppressing mutations (Figure 3.7B). The individually isolated, non-suppressed *rad22Δ* $Ch^{16}$-MHH strains were first transformed with pREP81X-HO as described in Section 2.5.2.2. Sensitivity to both 0.0008% (v/v) MMS and 0.5μM CPT was subsequently confirmed (Figure 3.7C) for all isolates prior to analysis using the LOH assay. A single strain transformed with blank vector was also tested for drug sensitivity and DSB-induced LOH (Figure 3.7D). Viability during DSB-induction was investigated as previously described (Section 2.5.7.3, Appendix V).

DSB induction in non-suppressed *rad22Δ* $Ch^{16}$-MHH lead to a complete ablation of interchromosomal GC and a significant increase in $Ch^{16}$ loss (68.8%) compared to that seen in wild-type (23.7%; Table 3.1). These levels were substantially different from those observed in *rad22Δ* $Ch^{16}$-MGH carrying a suppressor, where interchromosomal GC and minichromosome loss occurred with a frequency of 10% and 51%, respectively (Hussey, 2003). As DSB-induction did not affect cell viability (Appendix V), these data suggested that *rad22*$^{+}$ was required for all interchromosomal GC events and that suppression of a null mutation in this gene promoted GC, subsequently preventing minichromosome loss. Surprisingly, the level of DSB-induced LOH in a non-suppressed *rad22Δ* background (2.3%), whilst slightly elevated compared to that observed in wild-type background (Table 3.1), was lower than that seen in suppressed strains (3.7%; Hussey, 2003). As seen in other mutant backgrounds, extensive LOH was break dependent and directional (Appendix IV). Indeed, *ade*$^{-}$ $Hyg^{S}$ *his*$^{+}$ colonies were not observed over the 48 hour assay period and viability was also unaffected by break-induction (Appendix V).

### 3.2.7. $Ch^X$ formation requires *rad22*$^+$.

To examine the role of *rad22*$^+$ in $Ch^X$ formation, 24 *ade*$^+$ $Hyg^S$ *his*$^-$ and a single 'uncut' strain from *rad22Δ* $Ch^{16}$-MHH were analysed using 'low resolution' PFGE as previously described (Section 2.5.5.2 and 2.5.5.3).

As expected, $Ch^X$ was absent from all *ade*$^+$ $Hyg^S$ *his*$^-$ cells tested, with the majority of colonies displaying a minichromosome band similar in size to 'uncut' $Ch^{16}$-MGH (Figure 3.6B and Table 3.2). 4.2% displayed $Ch^{XY}$. These results suggested that *rad22*$^+$ is required for break-induced LOH arising as a result of allelic crossovers and BIR in *S. pombe*, and that extensive loss of allele specific information occurred predominantly via an alternative mechanism.

## 3.3. DISCUSSION.

Previous studies have suggested that the majority of extensive DSB-induced LOH events in wild-type $Ch^{16}$-MGH/MHH, whilst relatively infrequent, were due to allelic crossovers during G2 and BIR. The data presented in this chapter, together with previous results, has identified a key role for the MRN complex, encoded by *rad32*$^+$, *rad50*$^+$ and *nbs1*$^+$, together with the large subunit of RPA, *rad11*$^+$ and the HR genes, *rad22*$^+$, *rhp55*$^+$, *rhp51*$^+$, *rhp54*$^+$ and *mus81*$^+$ in such extensive homozygosis across a whole chromosomal arm in *S. pombe*. Indeed, deletion of the HR genes *rad22*$^+$, *rhp55*$^+$, *rhp51*$^+$ and *rhp54*$^+$ was found to abrogate both interchromosomal gene conversion and DSB-induced formation of $Ch^X$. Since orthologues of these genes in *S. cerevisiae* have been shown to play a role in the strand invasion step of HR (Krogh and Symington, 2004), these data imply that such a step is common to gene conversion, allelic crossovers and BIR in fission yeast (Figure 3.8). In the absence of such genes, DSB-induced LOH occurred via an alternative mechanism (Figure 3.9). Interestingly, a small percentage of *ade*$^+$ $G418^S/Hyg^S$ *his*$^-$ colonies from *rad22Δ*, *rhp51Δ* and *mus81Δ* backgrounds displayed a PFGE profile consistent with a long tract gene conversion associated allelic crossover i.e. $Ch^{XY}$. As previously detailed, $Ch^{XY}$ could form during either G1/early S or G2 phase, although the latter would require recombinant products to co-segregate to the same daughter cell (Figure 3.3). This data suggests that allelic crossovers may still occur at low frequency, albeit by a different mechanism, in some HR mutant backgrounds. In contrast, deletion of *rad32*$^+$, *rad50*$^+$ and *nbs1*$^+$ led to a complete ablation of $Ch^X$ formation whilst allowing interchromosomal gene conversion to occur (Figure 3.9), albeit at significantly reduced levels. Since deletion of the budding yeast orthologs of the MRN complex has been shown to significantly delay 5'-3' resection at DSB ends (Ivanov et al., 1994; Tsubouchi and Ogawa, 1998) and affect break stabilisation (de

Jager et al., 2001; Lobachev et al., 2004), these findings suggest that proficient end processing and/or break stabilisation is not only required for efficient interchromosomal gene conversion but that is also required for the efficient formation of allelic crossovers in G2 and BIR (Figure 3.8). DSB-induced LOH can still occur via an alternative mechanism in the absence of MRN complex function, however (Figure 3.9). As described for several HR mutants a small percentage of *ade*$^{+}$ G418$^{S}$/Hyg$^{S}$ *his*$^{-}$ colonies from *rad32Δ*, *rad50Δ* and *nbs1Δ* backgrounds displayed Ch$^{XY}$. Thus, allelic crossovers may still be possible in MRN mutants at low frequency. In addition to attenuating DSB end processing and destabilizing break-structures, deletion of individual MRN components is also known to affect intra-S phase but not G2 checkpoint activation in *S. pombe* (Chahwan et al., 2003). Whilst loss of intra-S phase checkpoint function might affect BIR, such a defect would not be expected to perturb allelic crossovers that occur during G2. Indeed, since the formation of Ch$^{X}$ was ablated in the absence of MRN complex components, this suggests that attenuation of 5'-3' resection/break stabilisation and not loss of checkpoint signalling is responsible for the inhibition of allelic crossovers and BIR in *rad32Δ*, *rad50Δ* and *nbs1Δ* backgrounds. Consistent with a role for resection in such mechanisms of LOH, deletion of *exo1*$^{+}$ was previously found to reduce the efficiency of Ch$^{X}$ formation (Hussey, 2003). Interestingly, however, the levels of interchromosomal gene conversion in this strain were comparable to wild-type background. This implies that Exo1-mediated resection, whilst dispensable for interchromosomal gene conversion, plays a substantial role in the formation of allelic crossovers and/or BIR (Figure 3.9A). Such a finding is also consistent with a greater role for MRN in DSB end processing (Section 1.3.2.1). Indeed, this may explain why gene conversion, allelic crossovers and BIR are more severely affected in the absence of MRN compared to *exo1Δ*.

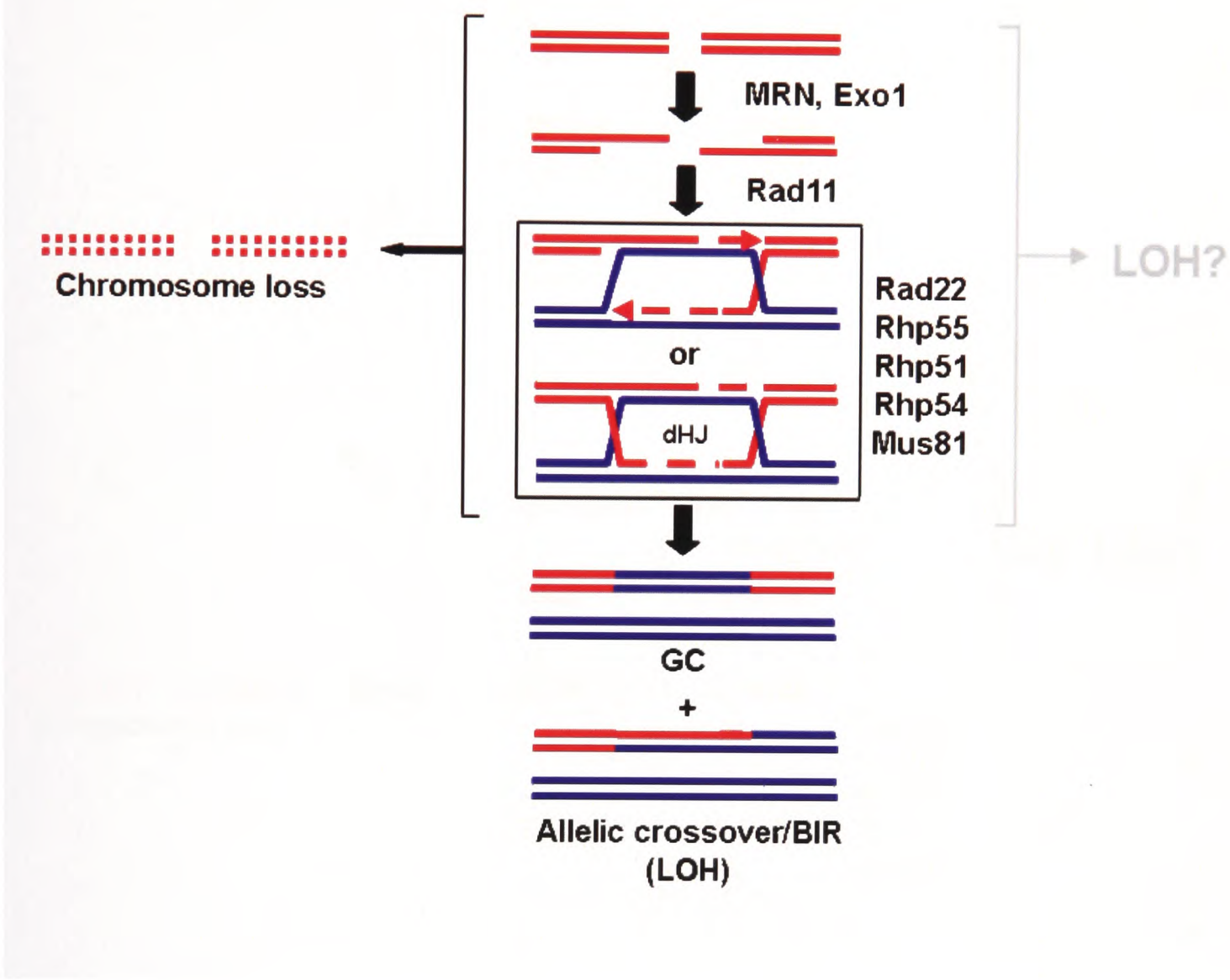



**Figure 3.8. Working model of DSB-induced repair and extensive LOH in wild-type background (1).** HR promotes GC, allelic crossovers and BIR while additionally preventing LOH via an alternative mechanism/s. Chromosome loss occurs at relatively low frequency. See text for details.

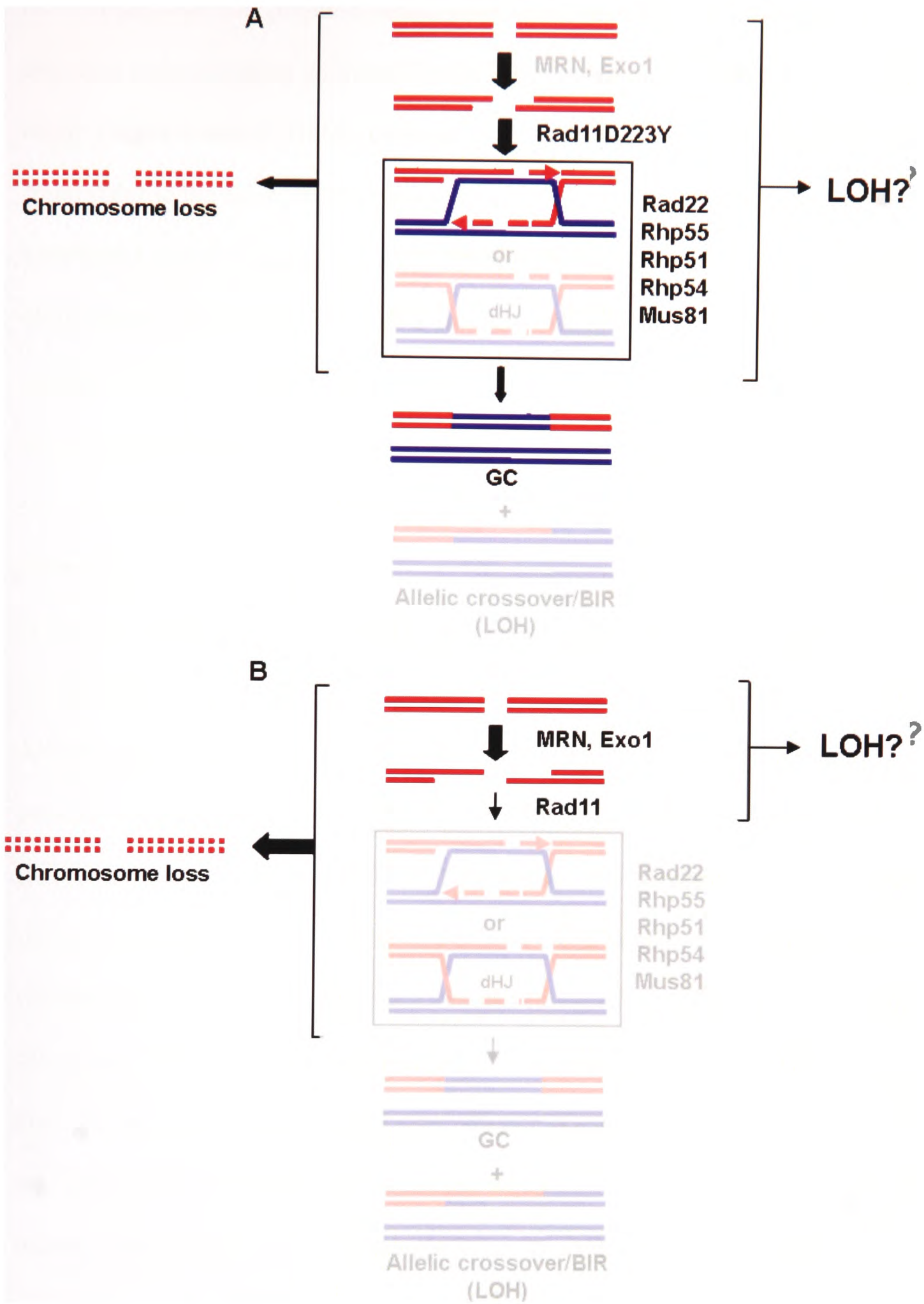



**Figure 3.9. Working model of DSB-induced repair and LOH in HR mutant backgrounds (1).** Repair via GC, allelic crossovers and BIR is abrogated in **A.** MRN deletes and *rad11D223Y* cells, and **B.** HR mutants. DSB-induced LOH in these cells occurs via an alternative mechanism. Minichromosome loss is significantly elevated in all HR mutants except *rhp55Δ*. See text for details.

How might resection promote allelic crossovers and BIR? One explanation is that extensive end processing promoted by the MRN complex and Exo1 might encourage repair via the classical DSBR pathway (Paques and Haber, 1999). Such a process could stabilise the heteroduplex intermediate formed between homologous chromatids after strand invasion, increasing the probability that repair leads to 1) the formation of dHJs which can be resolved to give an allelic crossover or 2) the stabilisation of a structure which can then act as a substrate for BIR. In the absence of such activity, dHJs or stable single-ended invasion intermediates may not form efficiently and thus the occurrence of allelic crossovers and BIR is reduced or even precluded (as observed in several HR mutants; Figure 3.9). Intriguingly, a role for DSB resection in crossover formation has previously been postulated (Prado and Aguilera, 2003). Previous experiments using a plasmid gap repair assay have suggested that deletion of *MRE11* leads to shorter heteroduplex tract lengths and reduced crossover formation in budding yeast (Symington et al., 2000). Recent data has demonstrated, however, that defects in resection do not affect hDNA formation or crossover frequency during interchromosomal gene conversion in a chromosomal context in diploid *S. cerevisiae* (Krishna et al., 2007). The difference between this result and our data may be due to differences in the regulation of repair between the two yeasts or reflect differences in the DSB context or assays used. In the absence of the MRN complex or Exo1 gene conversion may still proceed via SDSA, which can prevent crossovers and BIR through promoting the displacement of the invading strand during HR. Efficient resection, break stabilisation and/or checkpoint activation must still be important for SDSA, however, as deletion of MRN significantly perturbs interchromosomal gene conversion in the $Ch^{16}$-MGH/MHH system. Perhaps end processing mediated by the MRN complex is required to resect past the non-homologous *MAT*a site and $G418^R$ marker adjacent to the HO cut site on $Ch^{16}$-MGH/MHH. Indeed, such a process would

promote efficient strand invasion and thus facilitate gene conversion. Together, these observations strongly suggest that efficient resection is a common event in interchromosomal gene conversion, allelic crossovers and BIR in fission yeast. Interestingly, however, a slight perturbation of this process appears to have a dramatic effect on the generation of translocations associated with LOH in *S. pombe*. Previous studies have shown that *EXO1* in high copy number can partially suppress the IR sensitivity and delayed mating type switching of null mutations in *MRE11*, the homolog of *rad32*$^{+}$ in *S. cerevisiae* (Lewis et al., 2002). Indeed, it would be interesting to see if the overexpression of Exo1 in either *rad32Δ*, *rad50Δ* or *nbs1Δ* cells could promote both gene conversion and the formation of $Ch^{X}$ in the $Ch^{16}$-MGH/MHH system.

A requirement for *rad22*$^{+}$, *rhp55*$^{+}$, *rhp51*$^{+}$ and *rhp54*$^{+}$ in $Ch^{X}$ formation is consistent with the genetic requirements of *RAD51*-dependent BIR in *S. cerevisiae* (Davis and Symington, 2004; Malkova et al., 2005). The data presented here also indicates that the MRN complex is required for such *rhp51*$^{+}$-dependent events in *S. pombe*. This contrasts with results from budding yeast, where analysis of BIR utilizing a chromosome fragmentation assay has indicated that mutation of *RAD50* results in no significant defect in BIR in either *RAD51* or *rad51* strains (Davis and Symington, 2004). A similar result concerning *RAD51*-dependent BIR has also been observed in a chromosomal context on deletion of *RAD50* (Malkova et al., 2005). Intriguingly, $Ch^{X}$ formation was not observed after break-induction in *rhp51Δ* cells, suggesting that a pathway analogous to *RAD51*-independent BIR in budding yeast (Signon et al., 2001; Davis and Symington, 2004; Malkova et al., 1996) may be absent in *S. pombe*. Again, the difference between these two yeasts may be species specific or reflect the DSB context and type of assay used. The finding that *mus81*$^{+}$ is required for allelic

crossovers is consistent with a role for Mus81-Eme1 endonuclease in the resolution of recombination intermediates and the generation of crossovers during meiosis (Osman et al., 2003). Furthermore, a role for Mus81 in BIR conforms with a proposed role in resolving D-loops at stalled or collapsed replication forks thus facilitating replication restart following strand invasion of a homologous template (Doe et al., 2004).

Similar to the situation observed in MRN deletes, break induction in a *rad11D223Y* mutant led to a complete abrogation of DSB-induced LOH via the formation of $Ch^X$, whilst permitting gene conversion at reduced levels. Again, DSB-induced LOH was found to occur via an alternative mechanism. It is has been suggested that the *rad11D223Y* mutation might affect the ability of RPA to promote the formation and/or strand exchange activity of Rad22-Rhp51-ssDNA nucleofilaments *in vivo* (Ono et al., 2003). Perhaps the inability to promote efficient nucleofilament formation or stable strand invasion in *rad11D223Y* favours repair via SDSA rather than DSBR, and as such prevents the formation of structures required for both allelic crossovers and/or BIR, similar to the situation observed in MRN and Exo1 mutants (Figure 3.9). Indeed, a role for RPA in strand invasion during HR is well documented in *S. cerevisiae* (Wang and Haber, 2004). The reduction in interchromosomal gene conversion observed in this strain corroborates with previous data which show that *rad11D223Y* is sensitive to IR (Ono et al., 2003) and is consistent with the fact that efficient strand invasion must also be important for SDSA. These results, together with the HR null mutant data, support a common role for strand invasion in gene conversion, allelic crossovers and BIR in fission yeast.

As described above, the data presented here suggests that DSB-induced LOH may be associated with an allelic crossover (long tract GC) during either G1/early S-phase or

G2 in a minority of *ade*$^{+}$ G418$^{S}$/Hyg$^{S}$ *his*$^{-}$ colonies from *rad32Δ*, *rad50Δ*, *nbs1Δ*, *rad11D223Y*, *rhp51Δ* and *mus81Δ* cells. If allelic crossovers are possible during G2 in these mutants, why is Ch$^{X}$ not observed? Assuming that random segregation of recombinant products can occur in these mutant backgrounds after a single crossover event, *ade*$^{+}$ G418$^{S}$/Hyg$^{S}$ *his*$^{-}$ colonies contaning Ch$^{X}$ or Ch$^{XY}$ should be found in equal proportions (Figure 3.3B). The absence of Ch$^{X}$ from these analyses might therefore suggest that Ch$^{XY}$ is the result of a crossover between Ch$^{16}$ and ChIII during G1/early S-phase rather than G2 (Figure 3.3A). Ch$^{XY}$ could also arise through two independent crossover events between both Ch$^{16}$ and ChIII chromatids during G2 phase. However, since a single crossover in G2 is not possible in these strains, the occurance of two crossover events seems unlikely. So, how might crossovers occur in G1/early S but not G2 phase in HR mutants? One explaination is that the mechanism of crossover may be distinct between G1/early S and G2-phase cells. Interestingly, Ch$^{XY}$ was not observed in any wild-type *ade*$^{+}$ G418$^{S}$ *his*$^{-}$ cells. Assuming that break-induction in the Ch$^{16}$-MGH system is asynchronous, this result suggests that crossovers are inhibited during repair in G1/early S and provides further evidence that the control of reciprocal exchanges may be distinct between G1/early S and G2-phase cells. Indeed, further work will be required to investigate these possibilities.

# 4. HR PREVENTS EXTENSIVE DSB-INDUCED LOH VIA *DE NOVO* TELOMERE ADDITION.

## 4.1. INTRODUCTION.

Although DSB-induced LOH was still observed in HR mutants, $Ch^X$ was not (Table 3.1). This suggested that alternative mechanisms to BIR and allelic crossovers were responsible for the majority of extensive LOH in the absence of HR. To investigate the mechanism of DSB-induced LOH in HR mutants, chromosomal DNA from five *rhp51Δ ade*$^+$ G418$^S$ *his*$^-$ colonies, isolated from three independently tested strains, was previously probed for several sequences both proximal and distal to the *MAT*a break site on $Ch^{16}$-MGH (Figure 4.1B). The experiments had shown that loci directly proximal (*rad22*), 3kb distal (SPCC338.14, here termed *deletion mutant 1* - '*dm1*') and 25kb distal (*his3*) to the *MAT*a site were absent from the minichromosome in all five *rhp51Δ ade*$^+$ G418$^S$ *his*$^-$ colonies tested (Figure 4.1C; Hussey, 2003). As expected, these loci were found on both ChIII (data not shown) and $Ch^{16}$-MGH from an 'uncut' *rhp51*Δ $Ch^{16}$-MGH control. Thus, DSB-induced LOH in *rhp51Δ ade*$^+$ G418$^S$ *his*$^-$ cells appeared to occur through a deletion based mechanism rather than long tract gene conversion. In order to characterise the extent of the deletion in these *rhp51Δ ade*$^+$ G418$^S$ *his*$^-$ colonies, Southern analysis was initially conducted with a dsDNA probe designed to anneal to a locus present at the distal end of $Ch^{16}$-MGH (SPCC61.05, here termed *deletion mutant 11* - '*dm11*').

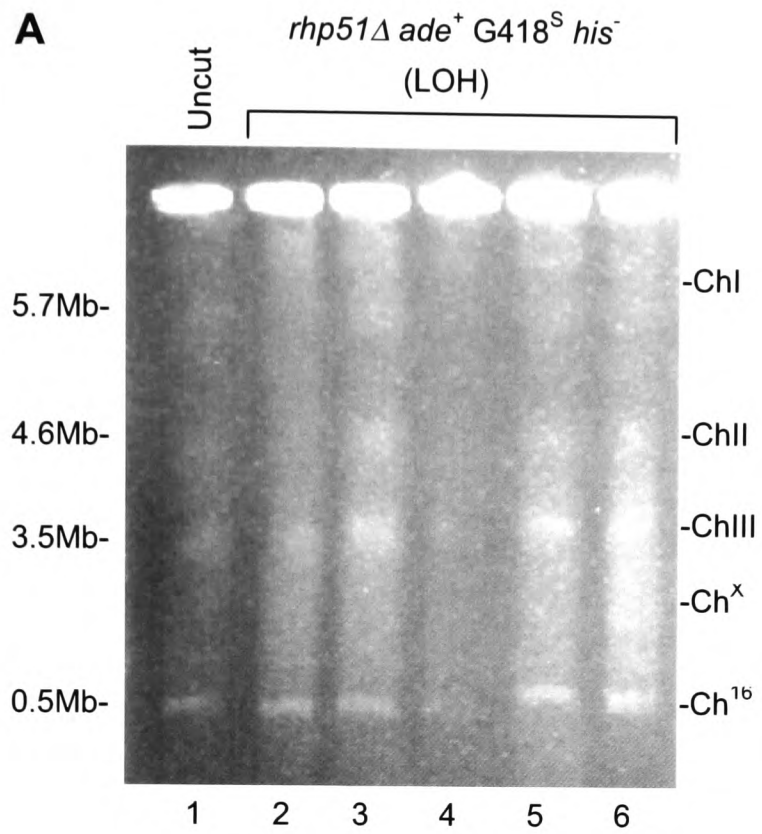
## 4.2. DSB-INDUCED LOH OCCURS VIA *DE NOVO* TELOMERE ADDITION IN HR MUTANTS.

### 4.2.1. DSB-induced LOH in *rhp51Δ* occurs predominantly from truncation of $Ch^{16}$.

The *'dm11'* probe was first constructed via PCR (Section 2.5.4.5) using suitable primers (DM11F/DM11R, Appendix II) and genomic DNA. The acquired PCR product was isolated, radioactively labelled (Section 2.5.6.2) and used in subsequent probing experiments as described in Materials and Methods with the same membrane probed for *rad21,* '*dm1*' and *his3* sequences (Section 2.5.6.3).

Surprisingly, probing for '*dm11*' showed that in all but one of the five *rhp51Δ* $ade^+$ $G418^S$ $his^-$ colonies this locus, although present on ChIII (data not shown), was absent from the minichromosome (Figure 4.1C). As expected, '*dm11*' was found on 'uncut' *rhp51*Δ $Ch^{16}$-MGH (Figure 4.1C, lane 1). In the one case where '*dm11*' was present (Figure 4.1C lane 5) it was concluded that an interstitial deletion of undefined size had occurred. Together, these data are consistent with extensive break-induced LOH arising through truncation of $Ch^{16}$ at or near the break site in the majority of *rhp51Δ* $ade^+$ $G418^S$ $his^-$ colonies tested. Such a break-induced truncation was anticipated to result in shortening of the minichromosome from ~530kb (the size of 'uncut' $Ch^{16}$-MGH) to ~400kb. Indeed, this was confirmed using 'high resolution' PFGE conditions (Section 2.5.5.2/2.5.5.3 and Figure 4.1D). The novel chromosomal element identified through this analysis was subsequently termed $Ch^{16}$-T (truncated).

**Figure 4.1. DSB-induced LOH in *rhp51Δ* cells result from $Ch^{16}$ truncations. A.** PFGE analysis of chromosomal DNA from a parental *rhp51Δ* $Ch^{16}$-MGH strain (lane 1); and individual *rhp51Δ* $ade^{+}$ $G418^{S}$ $his^{-}$ strains isolated following DSB induction (lanes 2-6). Performed by C. Walker. **B.** Schematic of the distal arm of $Ch^{16}$-MGH indicating distances of markers from the break-site. **C.** Southern blot analysis of above gel probed with distal marker '*dm1*' (SPCC338.14; Dr. A. George), *his3* (Dr. J. Prudden), '*dm11*' (SPCC61.05) and *rad21* (as indicated; Dr. J. Prudden). **D.** High resolution PFGE analysis of strains described above. λ Size markers are shown (M). Performed by C. Walker.


A
rhp51Δ ade+ G418S his-
(LOH)
Uncut
5.7Mb-
4.6Mb-
3.5Mb-
0.5Mb-
-ChI
-ChII
-ChIII
-ChX
-Ch16
1 2 3 4 5 6
B
Ch16-MGH
(0.5Mb)
rad21
dm1
his3
dm11
0
+3kb
+25kb
+110kb
C
rhp51Δ ade+ G418S his-
(LOH)
Uncut
0.5Mb-
'dm1'
0.5Mb-
his3
0.5Mb-
'dm11'
0.5Mb-
rad21
1 2 3 4 5 6
D
rhp51Δ ade+ G418S his-
(LOH)
M
Uncut
530kb-
480kb-
430kb-
-Ch16
-Ch16-T
1 2 3 4 5 6

### 4.2.2. Truncated $Ch^{16}$ is genetically stable with telomeric sequence at the HO break site.

In order to test if $Ch^{16}$-T was genetically stable, the rate of minichromosome loss per generation in three individual *rhp51Δ* $Ch^{16}$-MGH strains (TH1579, 1580, 1581; Table 2.4) and *rhp51Δ ade*$^+$ G418$^S$ *his*$^-$ colonies containing $Ch^{16}$-T was investigated using the assay described in Section 2.5.7.5. Wild-type $Ch^{16}$-MGH (TH1230; Table 2.4) and *ade*$^+$ G418$^S$ *his*$^-$ colonies containing $Ch^X$ were also examined for comparison.

As expected, $Ch^{16}$ was relatively stable in wild-type background, lost with a frequency of $4.03\times10^{-5}$ minichromosomes per generation. Indeed, $Ch^X$ from wild-type *ade*$^+$ G418$^S$ *his*$^-$ colonies was as stable as $Ch^{16}$-MGH (Figure 4.2A). The minichromosome from *rhp51Δ* $Ch^{16}$-MGH was, in contrast, lost with greater frequency ($8.1\times10^{-3}$ minichromosomes per generation). This suggested that *rhp51*$^+$ was required to efficiently maintain $Ch^{16}$ as had previously been observed (Prudden et al., 2003). Interestingly, $Ch^{16}$-T was lost at a rate comparable to that of $Ch^{16}$-MGH in an *rhp51Δ* background, implying that $Ch^{16}$-T was as stable as 'uncut' $Ch^{16}$-MGH. These results indicated that $Ch^{16}$-T could have been stabilised by telomere addition at or near the break site. To examine this hypothesis, Southern blot analysis of *EcoR*I digested genomic DNA from the three individually tested *rhp51Δ ade*$^+$ G418$^S$ *his*$^-$ colonies containing $Ch^{16}$-T described above, and an 'uncut' *rhp51Δ* $Ch^{16}$-MGH control was performed (Section 2.5.6.3).

Probing for *rad21* sequence revealed the existence of a 6kb band in the 'uncut' *rhp51Δ* $Ch^{16}$-MGH control lane (Figure 4.2C). This was the expected fragment size between *EcoR*I sites on $Ch^{16}$-MGH (Figure 4.2B). However, no 6kb band was

observed when probing for telomeric sequence (TEL), suggesting that such a structure was not at this site (data not shown). This was in contrast to what was observed in the *rhp51Δ ade*$^{+}$ G418$^{S}$ *his*$^{-}$ colonies containing Ch$^{16}$-T. Here, a truncated 2.8kb band was observed when probing for both *rad21* and telomeric repeats (Figure 4.2C). This showed that telomeric sequence was indeed present at or near the break site. Furthermore, since the distance between the proximal *EcoR*I site and the *MAT*a cut site is 2.5kb, this suggested that the size of telomeric repeat sequence adjacent to the break in these colonies was ~300bp. Indeed, this was consistent with previous observations of telomere length in *S. pombe* (Matsumoto et al., 1987).

### 4.2.3. Extensive DSB-induced LOH in *rhp51Δ* occurs predominantly via telomere addition.

To directly demonstrate the addition of a telomere at the *MAT*a break-site in *rhp51Δ ade*$^{+}$ G418$^{S}$ *his*$^{-}$ cells, PCR using a primer specific to *rad21* and another predicted to anneal specifically to *S. pombe* telomere repeat sequence was performed as described (R1/T1, Appendix II; Section 2.5.7.4 and Figure 4.2B). 25 individually isolated *rhp51Δ ade*$^{+}$ G418$^{S}$ *his*$^{-}$ colonies were tested and an 'uncut' *rhp51Δ* Ch$^{16}$-MGH strain was used as a negative control.

As expected, no telomere specific PCR products were observed with 'uncut' *rhp51Δ* Ch$^{16}$-MGH (Figure 4.2D, lanes 1 and 2). In contrast, 20 of the 25 *rhp51Δ ade*$^{+}$ G418$^{S}$ *his*$^{-}$ colonies tested gave rise to telomere specific PCR products, a representative example of which can be seen in Figure 4.2D, lanes 3-6. This suggested that 80% of the *rhp51Δ ade*$^{+}$ G418$^{S}$ *his*$^{-}$ cells analysed had undergone DSB-induced LOH as a result of *de-novo* telomere addition (Table 4.1). The remaining 20% therefore

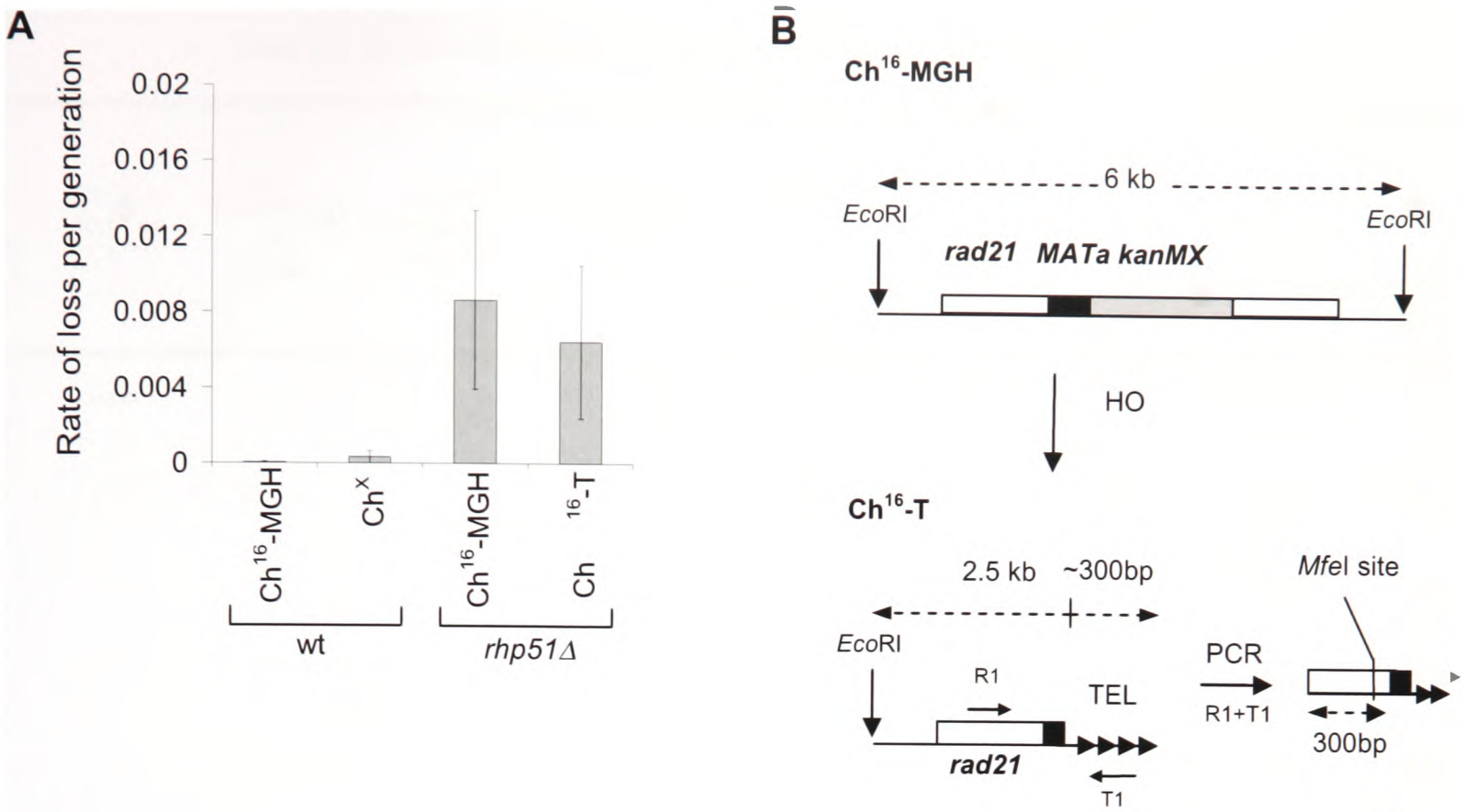



**Figure 4.2. Break-induced LOH results from *de novo* telomere addition in *rhp51Δ* cells. A.** Analysis of loss per generation of $Ch^{16}$-MGH, $Ch^{X}$ and $Ch^{16}$-T minichromosomes in wild-type or *rhp51Δ* backgrounds, as shown. Errors bars (±S. E. M.). **B.** Schematic of *Eco*RI fragments derived from an 'uncut' $Ch^{16}$-MGH strain and $Ch^{16}$-T. *rad21*$^{+}$ (white), *MATa* (black), *kanMX6* (grey) and telomere (TEL) sequences with R1 and T1 PCR primer binding sites are shown. Digestion of R1 and T1 derived PCR products with *Mfe*I leads to the formation of a 300bp fragment, ensuring that the PCR products obtained were not from the non-specific amplification of other regions of chromosomal DNA. **C.** Southern blot analysis of *Eco*RI digested chromosomal DNA from an 'uncut' *rhp51Δ* $Ch^{16}$-MGH strain (Uncut; lane 1) and three individual *rhp51Δ ade*$^{+}$ G418$^{S}$ *his*$^{-}$ colonies containing $Ch^{16}$-T (*rhp51Δ* $Ch^{16}$-T; lanes 2-4) probed with *rad21* (upper panel; performed by Dr. J. Prudden) and telomeric sequence (TEL; lower panel). λ Size markers are shown (M). **D.** PCR products from 'uncut' *rhp51Δ* $Ch^{16}$-MGH (lanes 1,2) and *rhp51Δ* colonies containing $Ch^{16}$-T, obtained using R1 and T1 primers (see B) with the *de novo* telomere addition assay, were analysed before (-) or after (+) digestion with *Mfe*I. M1 and M2 are 1kb and 100bp DNA ladders, respectively (NEB).

**Table 4.1. Mechanisms of break-induced LOH in wt and HR mutants.**

| Genetic background | G418$^R$ or Hyg$^R$ on Ch$^{16}$? | % *ade*$^+$ G418$^R$/Hyg$^R$ *his*$^-$ (LOH) | # LOH endpoints analysed | Translocation i.e. Ch$^X$ (%) | Telomere addition (%) | | Other (%) | | |
|---|---|---|---|---|---|---|---|---|---|
| | | | | | Ch$^{16}$ | Ch$^{XY}$ | Ch$^{16}$ | Ch$^{XY}$ | Missing |
| *wild-type* | G418$^R$ | 1.7 ± 0.3 | 22 (100) | 19/22 (86) | 0/22 (0) (1/100 (1)) | 0/22 (0) | 2/22 (9) | 0.0 (0/22) | 1/22 (5) |
| *rad32Δ* | Hyg$^R$ | 0.6 ± 0.2 | 21 | 0/21 (0) | 9/21 (43) | 2/21 (9) | 10/21 (48) | 0/21 (0) | 0/21 (0) |
| *rad50Δ* | Hyg$^R$ | 0.6 ± 0.2 | 20 | 0/20 (0) | 5/20 (25) | 1/20 (5) | 8/20 (40) | 3/20 (15) | 3/20 (15) |
| *nbs1Δ* | G418$^R$ | 1.4 ± 0.2 | 21 | 0/21 (0) | 17/21 (80) | 0/21 (0) | 2/21 (10) | 2/21 (10) | 0/21 (0) |
| *exo1Δ* | G418$^R$ | 1.1 ± 0.5 | 22 | 3/22 (14) | 10/22 (46) | 0/22 (0) | 9/22 (40) | 0/22 (0) | 0/22 (0) |
| *rad11D223Y* | G418$^R$ | 2.9 ± 0.5 | 20 | 0/20 (0) | 9/20 (45) | 0/20 (0) | 10/20 (50) | 1/20 (5) | 0/20 (0) |
| *rad22Δ* | Hyg$^R$ | 2.3 ± 0.6 | 24 | 0/24 (0) | 18/24 (75) | 0/24 (0) | 6/24 (21) | 1/24 (4) | 0/24 (0) |
| *rhp55Δ* | G418$^R$ | 0.8 ± 0.3 | 13 | 0.0 (0/13) | 9/13 (70) | 0/13 (0) | 2/13 (15) | 0/20 (0) | 2/13 (15) |
| *rhp51Δ* | G418$^R$ | 0.8 ± 0.3 | 25 | 0/25 (0) | 20/25 (80) | 0/25 (0) | 4/25 (16) | 1/25 (4) | 0/25 (0) |
| *rhp54Δ* | G418$^R$ | 0.4 ± 0.2 | 20 | 0/20 (0) | 18/20 (90) | 0/20 (0) | 2/20 (10) | 0/20 (0) | 0/20 (0) |
| *mus81Δ* | Hyg$^R$ | 0.2 ± 0.1 | 22 | 0/22 (0) | 6/22 (28) | 0/22 (0) | 14/22 (63) | 2/22 (9) | 0/22 (0) |

LOH colonies (ade$^+$ G418$^S$/Hyg$^S$ his$^-$) from each strain were analysed for the presence of Ch$^X$, Ch$^{16}$, Ch$^{XY}$ and *de novo* telomere. The number of ade$^+$ G418$^S$/Hyg$^S$ his$^-$ cells undergoing these and 'other' uncharacterized mechanisms of LOH is presented. The percentage of colonies undergoing distinct mechanisms of LOH from each mutant is shown in parenthesis. Values in red depict the number and percentage of colonies (from 100 individually isolated samples) which gave rise to telomere specific PCR products when tested with the *de novo* telomere addition assay. **Ch$^X$**, ChI, ChII, ChIII and Ch$^X$ observed via PFGE. Profile is indicative of a translocation between Ch$^{16}$ and ChIII i.e. allelic crossover during G2 or BIR; **Ch$^{16}$**, ChI, ChII, ChIII and a minichromosome band similar in size to 'uncut' Ch$^{16}$-MGH/MHH observed via PFGE. Such a profile is indicative of telomere addition when telomere-specific PCR products are observed (see 'Telomere addition') or suggestive of long-tract gene conversion/interstitial deletion/telomere addition proximal to the R1 primer used in the *de novo* telomere addition assay (Figure 4.2) when telomere-specific PCR products are absent (see 'Other'); **Ch$^{XY}$**, ChI, ChII and Ch$^{XY}$ observed via PFGE. Such a profile is consistent with a single long tract GC associated allelic crossover between Ch$^{16}$ and ChIII during G1/early S-phase, or G2 (if recombinant products co-segregate to the same daughter cell). Exchange may be associated with telomere addition (see 'Telomere addition'), otherwise such a profile is suggestive of a long tract gene conversion event with an associated crossover as described above; **Missing**, ChI, ChII and ChIII but no minichromosome observed via PFGE analysis. *ade6-M216* may have integrated into either ChI, ChII or ChIII.

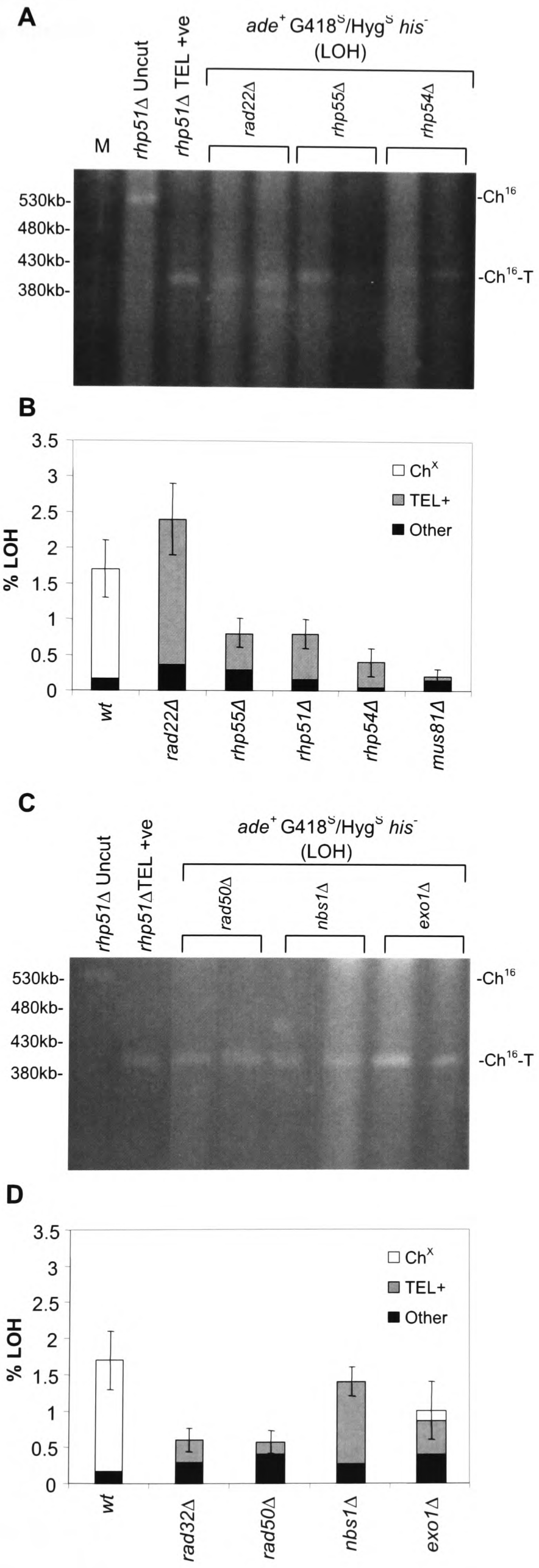
underwent DSB-induced LOH by mechanisms distinct from that which gave rise to $Ch^X$ or telomere addition within 950bp of the HO cut site ('Other'; Table 4.1). Indeed, such mechanisms may include long tract gene conversion (with or without an associated crossover during G1/early S or G2-phase), an interstitial deletion or telomere addition proximal to the forward primer used in the *de-novo* telomere addition assay (Figure 4.2B). Break-point sequencing of five randomly selected colonies that had given specific PCR products (RAD21-5, Appendix II; Section 2.5.4.6) revealed that telomere repeat sequence, $G_{(2-4)}TTACA_{(0-1)}$ (Sugawara, 1989), was added directly to or near the *MAT*a break-site in each case (Table 4.2). These results indicated that *de novo* telomere addition was responsible for the majority of extensive DSB-induced LOH events in *rhp51Δ* (Figure 4.3B). As expected, break-induced telomere addition corresponded with minichromosome truncation in all cases (Figure 4.3A, representative example).

### 4.2.3. *rad22*$^+$, *rhp55*$^+$, *rhp54*$^+$ and *mus81*$^+$ also prevent break-induced telomere addition.

It was next asked whether *de-novo* telomere addition was also responsible for the majority of extensive break-induced LOH in *rad22Δ*, *rhp54Δ*, *rhp55Δ* and *mus81Δ* cells. To answer this, no less than 20 *ade*$^+$ $G418^S/Hyg^S$ *his*$^-$ colonies previously isolated from three individually tested strains from each background were analysed using both PCR and break-point sequencing as described above. An *rhp51Δ ade*$^+$ $G418^S$ *his*$^-$ colony that had undergone break-induced telomere addition was used as a positive control.

PCR confirmed the presence of telomere repeat sequence at or near the *MAT*a cut site in ≥ 70% of the *ade*$^+$ G418$^S$/Hyg$^S$ *his*$^-$ colonies tested from *rad22Δ*, *rhp55Δ* and *rhp54Δ* backgrounds (Table 4.1 and 4.2). *De novo* telomere addition was observed in only 28% of *mus81Δ ade*$^+$ Hyg$^S$ *his*$^-$ colonies, however (Table 4.1). As observed in *rhp51Δ*, break-induced *de novo* telomere addition in *rad22Δ*, *rhp55Δ* and *rhp54Δ* *ade*$^+$ G418$^S$/Hyg$^S$ *his*$^-$ cells corresponded with minichromosome truncation in all cases, a representative example of which can be seen in Figure 4.3A. Break-point telomere sequencing of five randomly selected colonies from each background revealed that telomere repeat sequence was added directly to or near the *MAT*a break-site in each case (Table 4.2). The remaining population from each background underwent break-induced loss of the heterozygous G418$^R$/Hyg$^R$ and *his3*$^+$ markers by mechanisms distinct from that which gave rise to either Ch$^X$ or telomere addition within 990bp of the break-site ('Other', Table 4.1). Indeed, the PFGE profile of these colonies suggested that such mechanisms may include long tract gene conversion (with or without an associated crossover during G1/early S or G2-phase), interstitial deletion or integration of *ade6-M216* into either ChI, ChII or ChIII. Break-point sequencing of five randomly selected colonies from each background which had given specific PCR products (RAD21-5, Appendix II; Section 2.5.4.6) revealed that telomere repeat sequence was again added directly to or near the *MAT*a break-site in each case (Table 4.2). These results therefore indicated that *de-novo* telomere addition, whilst representing only a small proportion of LOH events in *mus81Δ*, was the major mechanism of extensive DSB-induced LOH in *rad22Δ*, *rhp55Δ* and *rhp54Δ* cells (Figure 4.3B).

**Figure 4.3. HR prevents LOH from *de novo* telomere addition at break-sites. A.** PFGE analysis of chromosomal DNA from 'uncut' *rhp51Δ* $Ch^{16}$-MGH (*rhp51Δ* uncut), *rhp51Δ ade*$^+$ $G418^S$ *his*$^-$ (*rhp51Δ* TEL+ve) encoding $Ch^{16}$-T, and two individual DSB-induced *ade*$^+$ $G418^S$/$Hyg^S$ *his*$^-$ strains from *rad22Δ*, *rhp55Δ* and *rhp54Δ* backgrounds (C. Walker). **B.** Analysis of the frequency of break-induced LOH mechanisms in HR mutants. **C.** PFGE analysis of chromosomal DNA from 'uncut' *rhp51Δ* $Ch^{16}$-MGH (*rhp51Δ* uncut), *rhp51Δ ade*$^+$ $G418^S$ *his*$^-$ (*rhp51Δ* TEL+ve) encoding $Ch^{16}$-T, and two individual DSB-induced *ade*$^+$ $G418^S$/$Hyg^S$ *his-* strains from *rad50Δ*, *nbs1Δ* and *exo1Δ* backgrounds (C. Walker). **D.** Analysis of the frequency of break-induced LOH mechanisms in MRN and *exo1Δ* mutants. The percentage of *ade*$^+$ $G418^S$/$Hyg^S$ *his*$^-$ strains exhibiting $Ch^X$ (white), telomere addition (grey), or 'other' (black), in which neither $Ch^X$ or *de novo* telomere addition at the break site were observed, are shown for each background (see Materials and Methods). 'Others' also include *ade*$^-$ $G418^S$/$Hyg^S$ *his*$^+$ colonies were applicable. Error bars (±S.E.M) for LOH values are depicted.


A
ade+ G418S/HygS his-
(LOH)
rad22Δ
rhp55Δ
rhp54Δ
rhp51Δ Uncut
rhp51Δ TEL +ve
M
530kb-
480kb-
430kb-
380kb-
-Ch16
-Ch16-T
B
% LOH
ChX
TEL+
Other
wt
rad22Δ
rhp55Δ
rhp51Δ
rhp54Δ
mus81Δ
C
ade+ G418S/HygS his-
(LOH)
rad50Δ
nbs1Δ
exo1Δ
rhp51Δ Uncut
rhp51ΔTEL +ve
530kb-
480kb-
430kb-
380kb-
-Ch16
-Ch16-T
D
% LOH
ChX
TEL+
Other
wt
rad32Δ
rad50Δ
nbs1Δ
exo1Δ

### 4.2.4. Telomere addition is observed in *rad11D223Y*.

To examine whether *de-novo* telomere addition was also responsible for extensive DSB-induced in *rad11D223Y*, 20 *ade*$^{+}$ G418$^{S}$ *his*$^{-}$ colonies from this background were again analysed using PCR as previously detailed (Sections 2.5.7.4). An *rhp51Δ* *ade*$^{+}$ G418$^{S}$ *his*$^{-}$ colony that had undergone break-induced telomere addition was used as a positive control as before.

PCR analysis indicated that *de novo* telomere addition occurred in 45% of the *rad11D223Y* colonies tested (Table 4.1). Alternative mechanisms of extensive DSB-induced LOH were responsible for G418$^{R}$ and *his3*$^{+}$ marker loss in the remaining 55% of *rad11D223Y ade*$^{+}$ G418$^{S}$ *his*$^{-}$ colonies (Table 3.3). Interestingly, however, 'high resolution' PFGE demonstrated that the majority of this population also had a truncated minichromosome (around the 400kb range indicative of telomere addition; Figure 4.4A, representative example). The absence of telomere specific PCR products in this population could be explained by the addition of telomeric sequence upstream of the R1 primer (Figure 4.2B). Alternatively, an interstitial deletion type mechanism may have been responsible. These results suggested that extensive DSB-induced LOH occurred via *de-novo* telomere addition at or near the break site in 45% of *rad11D223Y ade*$^{+}$ G418$^{S}$ *his*$^{-}$ colonies. The fact that the minichromosome in the remaining 55% of *ade*$^{+}$ G418$^{S}$ *his*$^{-}$ cells could have been truncated through addition of telomeric repeats suggested that *de-novo* telomere addition may actually be responsible for the majority of DSB-induced LOH in *rad11D223Y* cells (Figure 4.4).

Together, these analyses revealed an increase in DSB-induced LOH via *de novo* telomere addition in HR mutants, a phenomenon that was most strikingly observed in a *rad22Δ* background when compared to wild-type (Figure 4.3B). Indeed, PCR

analysis of 100 individual wild-type *ade*$^{+}$ G418$^{S}$ *his*$^{-}$ cells identified only one colony in which DSB-induced LOH had arisen from *de novo* telomere addition (Section 2.5.7.4, Table 4.1), suggesting that such a process is suppressed in wild-type *S. pombe*. Together, these results identify a role for HR in preventing extensive DSB-induced LOH through *de novo* telomere addition.

### 4.2.5. A role for the MRN complex and *exo1*$^{+}$ in break-induced telomere addition.

The fact that break-induced telomere addition was highest in a *rad22Δ* background that affects HR after resection, suggested that such processing may promote telomere addition at break-sites (Figure 3.9). To investigate whether inhibiting resection reduced break-induced telomere addition, PCR and break-point sequencing was performed with *ade*$^{+}$ G418$^{S}$/Hyg$^{S}$ *his*$^{-}$ colonies from MRN deletes in which resection is believed to be compromised (Ivanov et al., 1994; Tsubouchi and Ogawa, 1998).

Analysis of no less than 20 *ade*$^{+}$ G418$^{S}$/Hyg$^{S}$ *his*$^{-}$ colonies from *rad32Δ* and *rad50Δ* backgrounds indicated that the level of break-induced telomere addition, whilst higher than that seen in wild-type background, was significantly reduced compared to that observed in *rad22Δ* cells (Figure 4.3D, Table 4.1). Intriguingly, a very small subpopulation of *rad32Δ* and *rad50Δ ade*$^{+}$ Hyg$^{S}$ *his*$^{-}$ colonies that exhibited telomere-specific PCR products also contained ChI, ChII and Ch$^{XY}$ (Table 4.1). *rad50Δ ade*$^{+}$ Hyg$^{S}$ *his*$^{-}$ cells which did not display Ch$^{XY}$, contained a truncated minichromosome band (Figure 4.3C, representative example). The remaining population of *ade*$^{+}$ Hyg$^{S}$ *his*$^{-}$ cells from these backgrounds underwent mechanisms distinct to that of Ch$^{X}$ formation and telomere addition at or near the break as described above (Table 4.1).

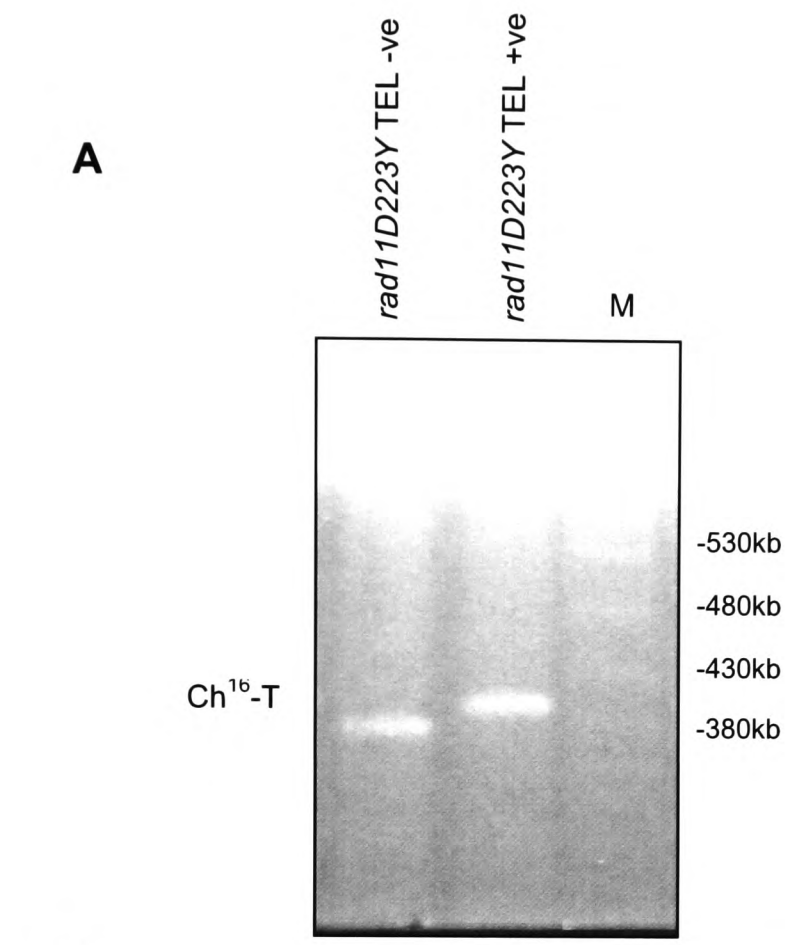



**Figure 4.4. Telomere addition is responsible for DSB-induced LOH in *rad11D223Y*. A.** High resolution PFGE analysis of *rad11D223Y ade*$^{+}$ G418$^{S}$ *his*$^{-}$ colonies which gave either a telomere-specific PCR product (TEL +ve) or failed to give rise to bands (TEL-ve) with the *de novo* telomere addition assay (See Materials and Methods; C. Walker). **B.** Analysis of the frequency of break-induced LOH mechanisms in wild-type, *rad11D223Y* and *rad22Δ*. The percentage of *ade*$^{+}$ G418$^{S}$ *his*$^{-}$ strains exhibiting Ch$^{X}$ (white), telomere addition (grey), or 'Other' (black), in which neither Ch$^{X}$ or *de novo* telomere addition at the break site were observed, are shown for each background (see Materials and Methods). Error bars (± S.E.M) for LOH values are depicted. λ marker is shown (M).

In contrast, the level of DSB-induced LOH via *de novo* telomere addition in *nbs1Δ* Ch$^{16}$-MGH was significantly higher than that observed in wild-type, *rad32Δ* or *rad50Δ* cells (Figure 4.3D, Table 4.1, Section 3.2.1). Indeed, telomere addition corresponded with minichromosome truncation in all cases (Figure 4.3C, representative example and Table 4.1). Alternative mechanisms of extensive DSB-induced LOH were observed but only in 19% of the *nbs1Δ ade*$^{+}$ G418$^{S}$ *his*$^{-}$ colonies analysed (Table 4.1). The fact that telomere addition at the break-site was associated with an allelic crossover in a minor population of *rad32Δ* and *rad50Δ* cells suggested that the MR complex may also play a role in preventing such exchanges. Break-point telomere sequencing of five randomly selected colonies from *rad32Δ*, *rad50Δ* and *nbs1Δ* backgrounds also revealed that telomere-repeat sequence was added directly to or near the *MAT*a break-site in each case (Table 4.2). This data, together with the sequencing of break-telomere junctions from the other HR mutants, indicated that telomeres were added preferentially after CA, AC or CC dinucleotides, with over half occurring within 1bp of the cleaved *MAT*a 5'-AACA-3' overhang (Table 4.2). Telomeres from all mutants initiated with the *S. pombe* telomeric consensus sequence G$_{(1-4)}$TTACA$_{(0-1)}$ (Sugawara, 1989) although subtle variations from this were observed in subsequent repeats (Table 4.2). Thus, these data indicated that telomere addition, whilst observed in *rad32Δ* and *rad50Δ* cells was more frequent in *nbs1Δ* cells, suggesting that the MR complex may play a greater role in telomere addition and/or resection than Nbs1.

It has previously been proposed that Exo1 plays a redundant role with the MRN complex and/or alternative exonucleases in the resection of DSBs, thus promoting HR in fission yeast (Tomita et al., 2003). Indeed, previous studies with *exo1Δ* Ch$^{16}$-MGH had shown that DSB-induced minichromosome loss and interchromosomal GC were

largely unaffected in the absence of *exo1*$^{+}$ compared to wild-type (Table 3.1). Furthermore, although DSB induction largely favoured extensive LOH distal to the break site, a small proportion of *ade*$^{-}$ G418$^{S}$ *his*$^{+}$ colonies were also observed (Table 3.1; Hussey, 2003). To test how deletion of *exo1*$^{+}$ affected the mechanism of DSB-induced LOH, 22 *exo1Δ ade*$^{+}$ G418$^{S}$ *his*$^{-}$ colonies previously acquired were analysed using the *de-novo* telomere addition assay and break-point sequencing as detailed above. A *rhp51Δ* LOH endpoint that was known to have a *de-novo* telomere at the HO cut site was again used as a positive control. Cells that had undergone centromere proximal DSB-induced LOH i.e. *ade*$^{-}$ G418$^{S}$ *his*$^{+}$ colonies, were not analysed.

Interestingly, only 45% of the 22 *exo1Δ ade*$^{+}$ G418$^{S}$ *his*$^{-}$ colonies tested gave rise to telomere specific PCR products (Table 4.1). Associated truncation of the minichromosome was again confirmed via a 'high resolution' separation of Ch$^{16}$ using PFGE (Figure 4.3C). Break-point sequencing of five independent isolates revealed a minimally resected *MAT*a site to which telomeric sequence had been added (Table 4.2). Of the remaining 55% that did not give a positive result with the assay, 14% had previously been shown to have undergone DSB-induced LOH via an allelic crossover during G2 and/or BIR (Table 4.1; Hussey, 2003). The remaining 41% underwent other mechanisms as previously described (Table 4.1). Thus, it appeared that deletion of *exo1*$^{+}$ reduced the efficiency of DSB-induced LOH via allelic crossovers during G2 and BIR compared to wild-type cells, resulting in an increase in *de novo* telomere addition at the break. This increase in telomere addition was lower than that observed in *rad22 Δ* cells, however, suggesting that rapid resection may be required for efficient telomere addition and that such processing also promotes translocations (Figure 4.3D).

**Table 4.2. Break-point telomere junctions in HR mutants.**

| | |
|---|---|
| ***MATa*** | AGTCGGGTTTTTCTTTTAGTTTCAGCTTTCCGCAACAAAAATTTTATAAACCCTGGTTTTG |
| *rad32Δ* | AGTCGGGTTTTTCTTTTAGTTTCAGGTTACGGTTACGGTTACGGTTACAGGGTTACAGGGG |
| | AGTCGGGTTTTTCTTTTAGTTTCAGCTTACGGTTACAGGGGTTACGGTTACAGGGTTACGG |
| | AGTCGGGTTTTTCTTTTAGTTTCAGCTTTCCGCAACACGTTACAGGTTACAGGGGTTACGG |
| | AGTCGGGTTTTTCTTTTAGTTTCAGCTTTCCGGTTACAGGGGTTACGGTTACAGGGTTACA |
| | AGTCGGGTTTTTCTTTTAGTTTCAGCTTTCCGCAACGGTTACAGGTTACGGTTACAGGTTA |
| *rad50Δ* | AGTCGGGTTTTTCTTTTAGTTTCAGCTTTCCGCGGTTACAGGGTTACAGGTTACAGGTTAC |
| | AGTCGGGTTTTTCTTTTAGTTTCAGCTTTCCGGGTTACAGGGTTACGGTTACAGTTACGGT |
| | AGTCGGGTTTTTCTTTTAGTTTCAGCTTTCCGGTTACAGGTTACAGGTTACGGTTACAGGG |
| | AGTCGGGTTTTTCTTTTAGTTTCAGGTTACAGGTTACGGTTACGGTTACACGGTTACAGAG |
| | AGTCGGGTTTTTCTTTTAGTTTCGGTTACACGGTTACGGTTACGGTTACAGGTTACAGGGT |
| *nbs1Δ* | AGTCGGGTTTTTCTTTTAGTTTCAGCTTTCCGCAACAGTTACAGGTTACAGGTTACAGGTT |
| | AGTCGGGTTTTTCTTTTAGTTTCAGCTTTCCGCAACACGGTTACACGGTTACACGGTTACA |
| | AGTCGGGTTTTTCTTTTAGTTTCAGCTTTCCGCAACAGTTACACGGTTACAGGTTACAGGT |
| | AGTCGGGTTTTTCTTTTAGTTTCAGCTTTCCGCAACACGGTTACAGGTTACAGGTTACAGG |
| | AGTCGGGTTTTTCTTTTAGTTTCAGCTTTCCGCGGTTACAGGTTACACGGTTACAGGGTTA |
| *exo1Δ* | AGTCGGGTTTTTCTTTTAGTTTCAGGGGTTACAGGTTACAGGTTACGGTTACGGTTAGGTT |
| | AGTCGGGTTTTTCTTTTAGTTTCAGCTTTCCGCAACAGGGGTTACGGTTACAGGGGTTACG |
| | AGTCGGGTTTTTCTTTTAGTTTCAGCTTTCCGCAACGGTTACAGGTTACGGTTACAGGGGTT |
| | AGTCGGGTTTTTCTTTTAGTTTCAGCTTTCCGCAACAGGGGTTACGGTTACAGGGTTACGG |
| *rad22Δ* | AGTCGGGTTTTTCTTTTAGTTTGGTTACAGGTTACCGGGTTTACGGTTACAGGGGTTACGG |
| | AGTCGGGTTTTTCTTTTAGTTCGGTTACAGGTTACAGGGGTTACGGTTACAGGGTACAGGG |
| | AGTCGGGTTTTTCTTTTAGTTTCAGCTTTCCGCAACGGTTACAGGGGTTACGGTTACAGGT |
| | AGTCGGGTTTTTCTTTTAGTTTCAGCTTTCCGCAACGGTTACAGTTACAGGGTTACAGGTTA |
| | AGTCGGGTTTTTCTTTTAGTTTCAGCTTTCCGGTTACAGTTACAGGGTTACGGTTACAGGTT |
| *rhp55Δ* | AGTCGGGTTTTTCTTTTAGTTTCAGCTTTCCGCAACAGTTACGGTTACAGGGTTACACGGT |
| | AGTCGGGTTTTTCTTTTAGTTTCAGCTTTCCGCAACAGTTACGGTTACAGGGGTTACGGTT |
| | AGTCGGGTTTTTCTTTTAGTTTCAGCTTTCCGCAACACGGTTACAGGTTACAGGTTACGGT |
| | AGTCGGGTTTTTCTTTTAGTTTCAGCTTTCCGGTTACACGGTTACAGGTTACAGGGGGTAC |
| | AGTCGGGTTTTTCTTTTAGTTTCACGGTTACACGGTTACAGGTTACGGTTACAGGTTACGG |
| *rhp51Δ* | AGTCGGGTTTTTCTTTTAGTTTCAGCTTTCCGCAACAGGTTACAGGTTACAGGTTACAGGT |
| | AGTCGGGTTTTTCTTTTAGTTTCAGCTTTCCGCAACGGTTACAGGGTACGGTTACAGGGTT |
| | AGTCGGGTTTTTCTTTTAGTTTCAGCTTTCCGCAACGGTTACAGGTTACAGGTTACAGGGT |
| | AGTCGGGTTTTTCTTTTAGTTTCAGCTTTCCGGTTACAGGGTTACAGGGGGTTACGGTTAC |
| | AGTCGGGTTTTTCTTTTAGTTTCAGCTTTCCGGTTACAGGTTACAGGTTACGGTTACAGGG |
| *rhp54Δ* | AGTCGGGTTTTTCTTTTAGTTTCAGCTTTCCGCAACAGGGTTACGGTTACACGGTACAGGG |
| | AGTCGGGTTTTTCTTTTAGTTTCAGCTTTCCGCAACAGGGTTACGGTTACAGGTTACAGGG |
| | AGTCGGGTTTTTCTTTTAGTTTCAGCTTTCCGCAACGGTTACGGTTACGGTTACGGTTACG |
| | AGTCGGGTTTTTCTTTTAGTTTCAGCTTTCCGCAACGGTTACAGGGTTACGGTTACAGGGT |
| | AGTCGGGTTTTTCTTTTACGGTTACAGGGTACGGTTACGGTTACAGTTACGGTTACAGGGG |
| *mus81Δ* | AGTCGGGTTTTTCTTTTAGTTTCAGCTTTCCGCAACAGGGTTACAGGTTACAGTTACAGGG |
| | AGTCGGGTTTTTCTTTTAGTTTCAGCTTTCCGCAACACGGTTACAGGTTACAGGTTACGGT |

Examples of break-point telomere junctions in HR mutants. Sequences of PCR products acquired from individual TEL+ve strains from each background are shown. 61bp of *MATa* are depicted, together with the HO endonuclease cleavage site (arrow). The 4bp overhang is underlined. Telomeric repeat sequence ($G_{2\text{-}5}TTACA_{0\text{-}1}$) is shown (black shading).

## 4.4. DISCUSSION.

### 4.4.1. HR prevents *de novo* telomere addition at DSB sites.

Previous studies had shown that HR was required for the major mechanisms of extensive DSB-induced LOH in wild-type background cells. Surprisingly, extensive DSB-induced LOH was still observed in the absence of HR, albeit to differing extents. Break induction in this context, however, led to a distinct hemizygous LOH profile due to *de-novo* telomere addition at or near the break site in the majority of cases examined (Figure 4.6), suggesting that HR prevents chromosomal truncations by *de-novo* telomere addition (Figure 4.5).

Interestingly, telomere addition was most frequently observed in a *rad22Δ* mutant that disrupts HR after resection. This suggests that resected ssDNA ends may be the preferred substrate for break-induced *de novo* telomere addition. DSB induction also led to a large increase in *de novo* telomere addition in *rad11D223Y* cells, in which strand invasion may be perturbed due to the inefficient formation of Rhp51-Rad22-ssDNA nucleofilaments or a stable heteroduplex intermediate (Ono et al., 2003). Break-induced telomere addition was also reduced compared to *rad22Δ* cells in *rhp54Δ* and *mus81Δ* backgrounds, which disrupt HR at later stages. Presumably, during the later stages of HR ssDNA ends have been sequestered in downstream intermediates that arise as a result of strand invasion and are thus incapable of interacting with the telomere addition machinery. Here, the minichromosome is lost, resulting in a reduction in telomere addition and a slight increase in minichromosome loss. Together, these data suggest that resection may facilitate chromosome healing at break ends and that strand invasion during HR may also prevent *de novo* telomere addition (Figure 4.6). This data agrees with previous findings in *S. cerevisiae*, where

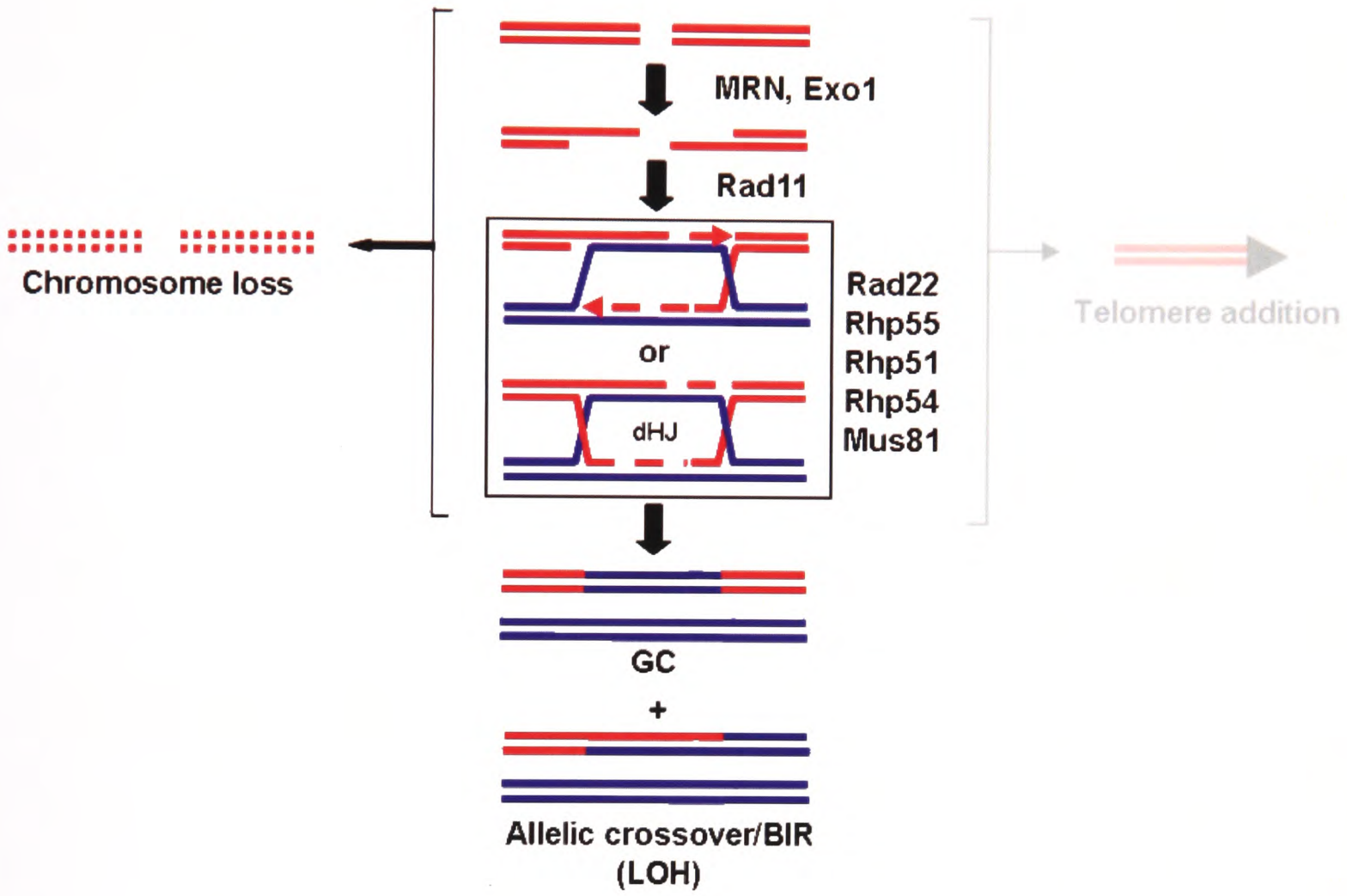



**Figure 4.5. Working model of DSB-induced repair and LOH in wild-type background (2).** HR promotes GC, allelic crossovers and BIR while additionally preventing LOH via *de novo* telomere addition. Chromosome loss occurs at relatively low frequency. See Figures 3.7 and 4.7 for comparison.

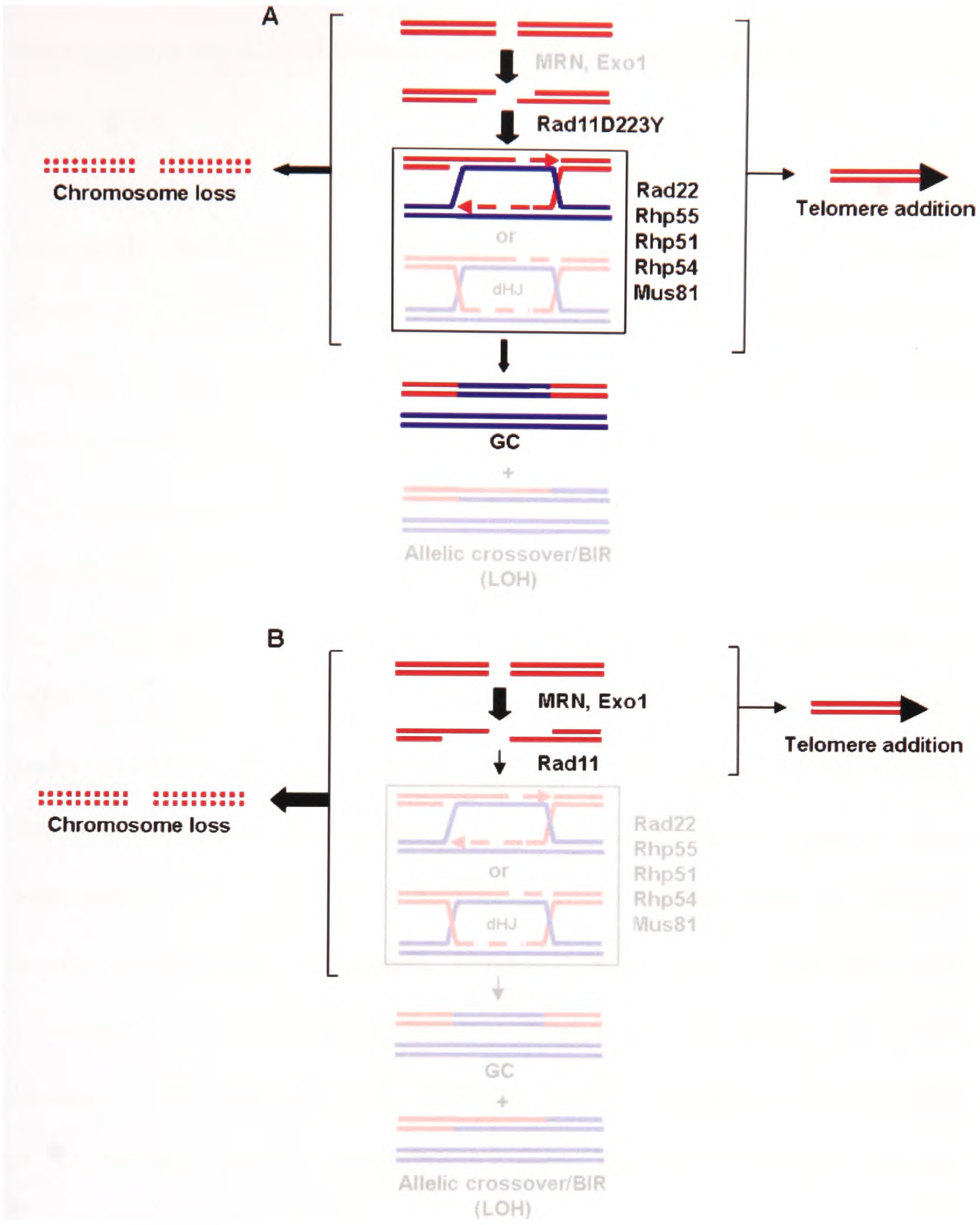



**Figure 4.6. Working model of DSB-induced repair and LOH in HR mutant backgrounds (2).** DSB-induced LOH in **A.** MRN deletes and *rad11D223Y* cells, and **B.** HR mutants occurs via *de novo* telomere addition. These model suggest that HR prevents telomere addition through promoting GC and allelic crossovers/BIR and that resection may be required for both efficient interchromosomal HR and telomere addition in *S. pombe*. See Figures 3.8 and 4.6 for comparison.

loss of *RAD52* was also found to promote an increase in break-induced chromosomal rearrangements via *de novo* telomere addition (Bosco and Haber, 1998; Kramer and Haber, 1993).

Interestingly, the deletion of early acting HR genes, *rad32*$^{+}$, *rad50*$^{+}$ and *exo1*$^{+}$ resulted in a significant reduction in the levels of both DSB-induced LOH and chromosome healing compared to that observed in *rad22Δ* cells. This data is consistent with a role for resection in facilitating telomere addition at break ends and with recent findings indicating that the MRN complex is not absolutely required for *de novo* telomere addition in *S. cerevisiae* (Smith et al., 2005). If resection is required for telomere addition, however, why is the level of telomere addition higher in *rad32Δ* and *rad50Δ* cells compared to wild-type Ch$^{16}$-MGH? As previously detailed, interchromosomal gene conversion can still occur in MR complex mutants, albeit at reduced levels. Such repair is abrogated in *rad22Δ* Ch$^{16}$-MHH, however, where break-induced *de novo* telomere addition occurs to a higher degree than that observed in *rad32Δ* and *rad50Δ* backgrounds. Perhaps gene conversion (and other repair processes e.g. SCR) compete with factors involved in *de novo* telomere addition for the repair of DSB ends. This could explain why telomere addition is lower in *rad32Δ* and *rad50Δ* cells compared to *rad22Δ*, but higher than that observed in wild-type background (where the majority of breaks are repaired via gene conversion). Indeed, further experiments are required to clarify the role of resection in *de novo* telomere addition and how competition between various DSB repair processes can affect DSB-induced LOH via this mechanism (see Chapter V). In *nbs1Δ*, DSB-induced LOH and *de novo* telomere addition occurred to a level significantly higher than that observed in *rad32Δ* and *rad50Δ* cells. This suggests that unlike Rad32 and Rad50, Nbs1 does not play a large role in chromosome healing. This conflicts with previous findings in

*S. pombe* which suggest that *rad32*$^{+}$, *rad50*$^{+}$ and *nbs1*$^{+}$ are all required for efficient telomere maintenance (Ueno et al., 2003). It is possible, however, that telomere maintenance and telomere addition have differing genetic requirements. Since MRN is believed to exist as a trimeric protein complex at DSBs (van den Bosch et al., 2003) and *rad32Δ*, *rad50Δ* and *nbs1Δ* cells have comparable defects in intra-S-phase checkpoint activation (Chahwan et al., 2003), the phenotypic difference between these mutants in terms of the level of DSB-induced LOH via telomere addition was surprising. It is possible that these differences reflect a greater role for Rad32 and Rad50 in resection and/or telomere addition than Nbs1 in fission yeast. Consistent with this hypothesis, a recent *in vitro* study using nuclear extracts from primary human fibroblasts and telomeric DNA has suggested that NBS1 plays a greater role than MRE11 in promoting strand invasion (Verdun and Karlseder, 2006). This finding is also consistent with the significant difference in interchromosomal gene conversion between *rad32Δ* and *nbs1Δ* in the Ch$^{16}$-MGH/MHH system (Section 3.2.1). Reports in human cells also suggest that NBS1 is required for the recruitment/retention of the MR complex at break sites (Iijima et al., 2004; Kobayashi et al., 2004). Perhaps lack of MR retention in *nbs1Δ* cells leads to reduced strand invasion after 5'-3' resection has occurred. This may lead to an increase in the amount of ssDNA substrate available for *de novo* telomere addition and thus explain why the level of telomere addition is higher than *rad32Δ* in *nbs1Δ* cells. Indeed, it would be interesting to see whether a *nbs1Δku70Δ* mutant has increased levels of resection compared to *nbs1Δ* and thus increased levels of break induced telomere addition in the Ch$^{16}$-MGH/MHH system. How might strand invasion and interchromosomal gene conversion occur in the absence of Rad32? Perhaps Nbs1 and/or Rad50 retain some residual *in vivo* function which promotes strand invasion, albeit at reduced levels compared to wild-type background. Since *rad50Δ* and *nbs1Δ* strains have similar defects in

interchromosomal gene conversion, the reduction in telomere addition in *rad50Δ* cells may be due to a distinct mechanism to that proposed for *nbs1Δ* cells.

Deletion of *exo1*$^{+}$ does not result in a large stimulation of *de-novo* telomere addition like that observed in the homologous recombination mutants. As previously detailed, *exo1Δ* has levels of gene conversion and minichromosome loss similar to wild-type background cells (Hussey, 2003), suggesting that DSB repair is not significantly affected in the absence of this exonuclease. Perhaps resection at the break is delayed in *exo1Δ* (although not to the same extent as MRN mutants), retarding the formation of dHJs but leading to a population of breaks in a configuration which allows *de-novo* telomere addition to occur. Over time these breaks are resected to a stage that allows normal DSB repair via gene conversion (and to some extent, allelic crossovers during G2 and/or BIR) but prevents chromosome healing. This corroborates with reports which show that the kinetics of resection are delayed in *S. cerevisiae* cells deficient for *EXO1* in a HO-inducible DSB system (Llorente and Symington, 2004). Thus, Exo1 might help prevent *de novo* telomere addition in wild type cells through promoting rapid and efficient resection at the DSB, together with MRN. Interestingly, however, such a process appears not only to promote repair via gene conversion, but to promote the extensive loss of allele specific information via allelic crossovers during G2 and/or BIR.

Sequence analysis of break-telomere junctions from all mutants tested suggested that telomeres were added preferentially after CA, AC or CC dinucleotides and were initiated with the *S. pombe* telomere consensus sequence, $G_{(1-4)}TTACA_{(0-1)}$ (Sugawara, 1989). Although such addition occurred predominantly at or near the *MAT*a cleavage site, this might be expected given that the preferred sites of addition

occur within the cleaved 5'-AACA-3' overhang. In contrast, sequence analysis of over 500 break-telomere junctions obtained from spontaneous events in budding yeast revealed that the majority of telomeres were added preferentially after GT, TG and GG dinucleotides and started with a distinct initiating sequence (GTGTGGGTGTG; (Putnam et al., 2004)). A similar result has also been observed at low frequency following DSB-induction using HO endonuclease in *rad52Δ* cells, although such addition required the presence of telomere-like $(T_2G_4)_{13}$ sequences (Kramer and Haber, 1993). These data are consistent with telomeres being added to short sequences of chromosomal DNA with homology to the 3' end of the telomerase guide RNA (TLC1) although this domain is not used as a template during the synthesis of subsequent repeats (Putnam et al., 2004). The data presented here exhibits similar patterns, with telomeres almost always beginning with the same permutation of $G_{2\text{-}5}TTACA_{0\text{-}1}$, although the initiating sequence and subsequent repeats show less heterogeneity than that observed in *S. cerevisiae*. This suggests that *de novo* telomere addition may occur by a similar mechanism in *S. pombe*, although synthesis utilizing the as-yet unidentified RNA template in fission yeast may be more processive and stringent.

Surprisingly, break-induced telomere addition only occurs at relatively low levels in the HR mutants. Indeed, the levels of minichromosome loss in *rhp51Δ*, *rad22Δ*, and *rhp54Δ* cells are significantly higher than that observed in wild-type background. If HR prevents chromosome healing, why are telomeres not added to all break ends in the absence of these genes? It is possible that the lack of healing under these conditions is due to the absence of structures required for efficient addition at the break e.g. a short tract of telomeric sequence proximal to the DSB to act as a seeding structure for telomere addition proteins or the RNA component of telomerase (Diede

and Gottschling, 1999). An alternative explanation could be that mechanisms in addition to HR are responsible for preventing *de novo* telomere addition at internal break-sites. One candidate mechanism could involve an orthologue of a DNA helicase identified in *S. cerevisiae*, Pif1. Previous studies have shown that Pif1 suppresses *de-novo* telomere addition at subtelomeric seed sequences and at HO break sites (Schulz and Zakian, 1994). It is thought to perform this function by preventing an interaction between TLC1 and the G-strand overhang of a shortened telomere tract *in vivo* (Boule et al., 2005). It would be interesting to see if chromosome healing is augmented and minichromosome loss attenuated in *pfh1Δ* (the *S. pombe PIF1* orthologue) cells compared to wild-type background using the $Ch^{16}$-MGH based system. The relationship between homologous recombination and Pfh1 in terms of preventing *de-novo* telomere addition could also be investigated in a *rad22Δpif1Δ* mutant. Interestingly, it has been found that *rqh1*$^{+}$ suppresses *de novo* telomere addition in $Ch^{16}$-MGH in the absence of *rhp55*$^{+}$, suggesting that other mechanisms are in place to suppress break-induced telomere addition in *S. pombe* (A. Dave, unpublished observations).

### 4.3.3. Telomere addition is associated with an allelic crossover in *rad32Δ* and *rad50Δ* cells.

Curiously, telomere addition was associated, albeit at extremely low levels, with an allelic crossover in both *rad32Δ* and *rad50Δ ade*$^{+}$ $Hyg^{S}$ *his*$^{-}$ cells. A possible explanation to describe this observation is that telomere addition occurred after

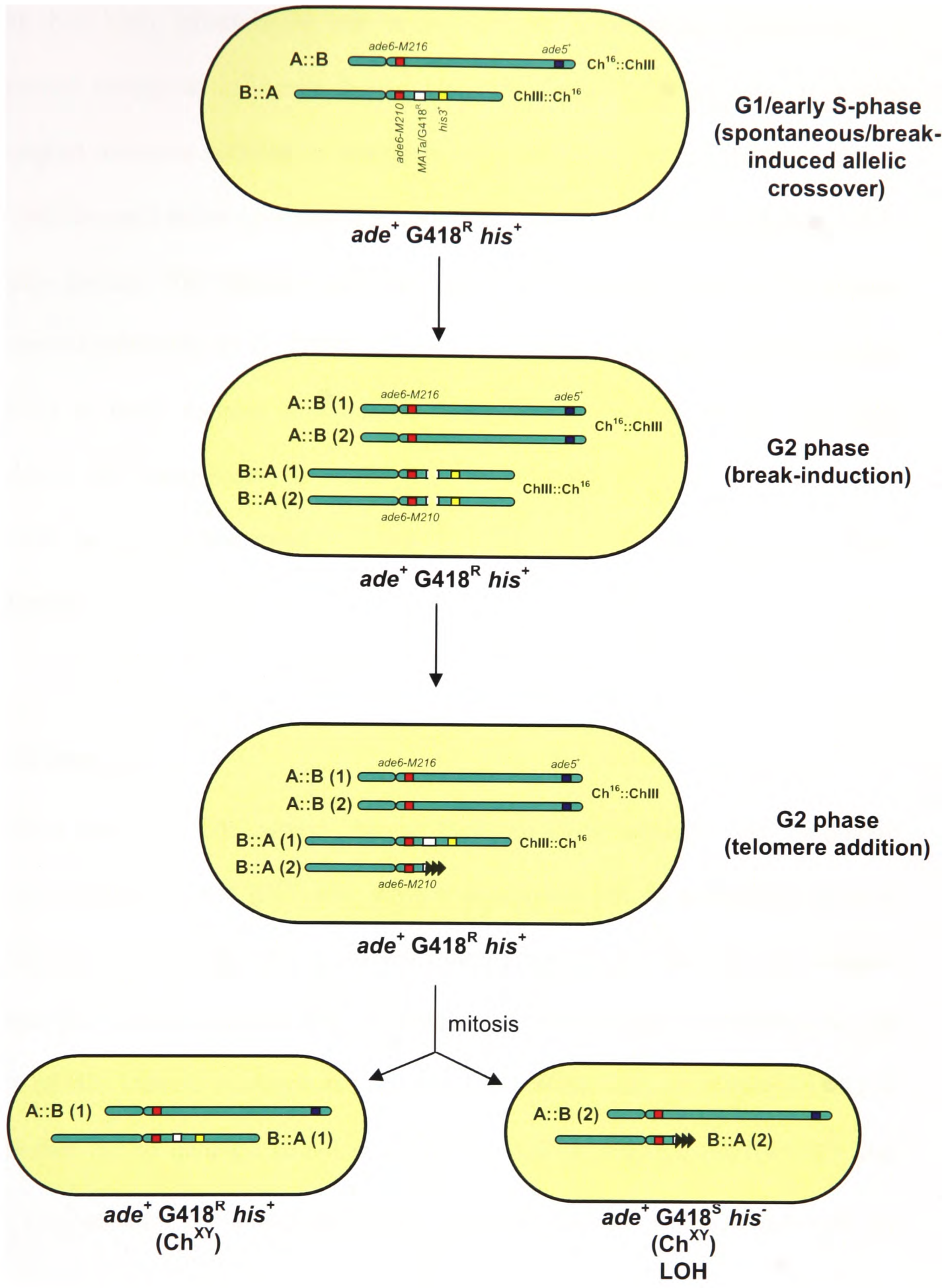



**Figure 4.7. Possible mechanism to describe telomere addition with an allelic crossover in HR mutants.** An allelic crossover occurs spontaneously in G1/early S-phase, resulting in the formation of A::B and B::A recombinants. After DNA replication a break is induced at the *MAT*a site in B::A (1 and 2) resulting in repair via *de novo* telomere addition. Segregation results in one *ade*$^{+}$ G418$^{R}$ *his*$^{+}$ cell displaying a PFGE profile consistent with Ch$^{XY}$. The other daughter is *ade*$^{+}$ G418$^{S}$ *his*$^{-}$ as a result of extensive LOH via *de novo* telomere addition at the *MAT*a site. PFGE analysis also leads to the observation of Ch$^{XY}$ in this colony.

a break had been reintroduced into a recombinant chromosome formed from a spontaneous reciprocal exchange during G1/early S-phase (Figure 4.7). It is also possible that telomere addition is mechanistically linked to the reciprocal exchange event (which could occur in either G1/early S or G2-phase). Previous findings in *S. cerevisiae* indicate that telomere addition occurs predominantly during late S/early G2-phase (Goudsouzian et al., 2006). If telomere addition is mechanistically linked to crossovers in these mutants it would be interesting to investigate the cell cycle dependency of this process. It would also be of interest to see whether allelic crossovers occur spontaneously during S-phase to a higher extent in these backgrounds.

### 4.3.4. Summary.

Thus, it appears that HR, whilst able to facilitate DSB-induced LOH via allelic crossovers during G2 and BIR, also plays a significant role in preventing *de-novo* telomere addition at break-sites in fission yeast. Interestingly, the data also suggest that resection might facilitate the generation of chromosomal truncations in the absence of HR. Indeed, this appears to be most prominent form of extensive LOH in mutants that fail to undergo strand invasion i.e. *rad22Δ*, *rhp55Δ*, *rad11D223Y* and *nbs1Δ*. Furthermore, our data suggest that telomere addition is associated with an allelic crossover in a small proportion of *ade*$^{+}$ Hyg$^{S}$ *his*$^{-}$ cells from *rad32Δ* and *rad50Δ* backgrounds, although the mechanism behind this remains unclear.

# 5. HR COMPETES WITH TELOMERE ADDITION FOR THE REPAIR OF RESECTED DSB ENDS.

## 5.1. INTRODUCTION.

The data presented in Chapter IV suggested that 3'-ssDNA overhangs may be the preferred substrate for *de novo* telomere addition in HR gene deletes. If true, this would imply that 5'-3' resection at DSB ends is required for efficient telomere addition in mutants where ssDNA is expected to accumulate. It was decided to forgo analysis using *rad22Δ*, a background susceptible to suppression, and instead perform all further experiments in *rhp55Δ* $Ch^{16}$-MGH, which is less susceptible to suppressing mutations. In order to investigate a requirement for DSB end processing in *de-novo* telomere addition in the absence of competing HR, DSB-induced repair and extensive LOH were first investigated in *exo1Δ rhp55Δ*, *ku70Δ rhp55Δ* and *lig4Δ rhp55Δ* backgrounds.

## 5.2. INVESTIGATING A ROLE FOR DSB END PROCESSING IN *DE-NOVO* TELOMERE ADDITION.

### 5.2.1. DSB repair and extensive LOH in *exo1Δ rhp55Δ* .

Exo1 has previously been shown to play a redundant role with the MRN complex in break processing (Moreau et al., 2001; Tomita et al., 2003). Thus, to examine the role of resection on DSB repair and extensive LOH in the absence of $rhp55^{+}$, three individually generated *exo1Δ rhp55Δ* $Ch^{16}$-MGH strains transformed with pREP81X-HO were analysed using the LOH assay as described in Section 2.5.7.1. Viability and DSB-induced marker loss in the presence of blank plasmid were assessed as previously detailed (Section 2.5.7.3).

**Table 5.1. DSB-induced marker loss in wt, NHEJ and *rhp55Δ* mutants.**

| Genetic background | G418$^R$ or Hyg$^R$ on Ch$^{16}$? | % *ade*$^+$ G418$^S$/Hyg$^S$ *his*$^+$ (GC) | % *ade*$^+$ G418$^R$/Hyg$^R$ *his*$^+$ (EJ/SCR) | % *ade*$^-$ G418$^S$/Hyg$^S$ *his*$^-$ (Ch$^{16}$ loss) | % *ade*$^+$ G418$^R$/Hyg$^R$ *his*$^-$ (LOH) | P *value* (relative to wild-type LOH) |
|---|---|---|---|---|---|---|
| *wild-type* | G418$^R$ | 49.7 ± 2.6 | 25.0 ± 1.4 | 23.7 ± 1.7 | 1.7 ± 0.3 | 1.000 |
| *rhp55Δ* | G418$^R$ | 2.3 ± 0.5 | 54.7 ± 7.9 | 40.1 ± 7.2 | 0.8 ± 0.3 | 0.090 |
| *rad32Δ rhp55Δ* | Hyg$^R$ | 0.6 ± 0.4 | 20.1 ± 0.2 | 61.7 ± 0.1 | 6.6 ± 0.2 | <<0.05 |
| *rad50Δ rhp55Δ* | Hyg$^R$ | 1.0 ± 0.3 | 29.2 ± 6.3 | 53.9 ± 5.4 | 4.9 ± 0.7 | 0.088 |
| *nbs1Δ rhp55Δ* | G418$^R$ | 0.1 ± 0.1 | 23.4 ± 1.9 | 61.9 ± 1.6 | 2.6 ± 0.5 | 0.163 |
| *exo1Δ rhp55Δ* | G418$^R$ | 5.8 ± 2.4 | 54.4 ± 7.3 | 37.2 ± 5.8 | 1.0 ± 0.4 | 0.197 |
| *ku70Δ* | G418$^R$ | 53.4 ± 2.8 | 38.5 ± 2.1 | 6.0 ± 1.0 | 1.5 ± 0.1 (0.39 ± 0.14) | 0.613 |
| *lig4Δ* | G418$^R$ | 47.2 ± 3.6 | 39.1 ± 3.1 | 12.8 ± 0.5 | 0.7 ± 0.1 (0.19 ± 0.09) | 0.042 |
| *ku70Δ rhp55Δ* | Hyg$^R$ | 15.4 ± 0.9 | 46.7 ± 2.4 | 27.2 ± 2.1 | 7.6 ± 0.7 | 0.006 |
| *lig4Δ rhp55Δ* | G418$^R$ | 3.6 ± 1.3 | 58.8 ± 6.2 | 32.5 ± 5.7 | 2.3 ± 0.2 | 0.145 |

The levels of interchromosomal gene conversion (GC), minichromosome loss (Ch16 loss), loss of heterozygosity (LOH) and end-joining/sister chromatid recombination (EJ/SCR) are shown. Percentages were calculated as described in Materials and Methods. Values in parenthesis (where observed) represent the percentage of *ade*$^-$ G418$^S$/Hyg$^S$ *his*$^+$ colonies identified for the mutant analysed.

**Table 5.2. Mechanisms of break-induced LOH in wt, NHEJ and *rhp55Δ* mutants.**

| Genetic background | G418$^R$ or Hyg$^R$ on Ch$^{16}$? | % *ade*$^+$ G418$^R$/Hyg$^R$ *his*$^-$ (LOH) | # LOH endpoints analysed | % Translocations (Ch$^X$) | % Telomere addition | | % Other | | |
|---|---|---|---|---|---|---|---|---|---|
| | | | | | Ch$^{16}$ | Ch$^{XY}$ | Ch$^{16}$ | Ch$^{XY}$ | Missing |
| *wild-type* | G418$^R$ | 1.7 ± 0.3 | 22 (100) | 19/22 (86) | 0/22 (0) (1/100 (1)) | 0/22 (0) | 2/22 (9) | 0/22 (0) | 1/22 (5) |
| *rhp55Δ* | G418$^R$ | 0.8 ± 0.3 | 13 | 0/13 (0) | 9/13 (70) | 0/13 (0) | 2/13 (15) | 0/20 (0) | 2/13 (15) |
| *rad32Δ rhp55Δ* | Hyg$^R$ | 6.6 ± 0.2 | 22 | 0/22 (0) | 16/22 (73) | 0/22 (0) | 6/22 (27) | 0/22 (0) | 0/22 (0) |
| *rad50Δ rhp55Δ* | Hyg$^R$ | 4.9 ± 0.7 | 23 | 0/23 (0) | 21/23 (91) | 0/23 (0) | 2/23 (9) | 0/23 (0) | 0/23 (0) |
| *nbs1Δ rhp55Δ* | Hyg$^R$ | 2.6 ± 0.5 | 22 | 0/22 (0) | 20/22 (90) | 0/22 (0) | 1/22 (5) | 1/22 (5) | 0/22 (0) |
| *exo1Δ rhp55Δ* | G418$^R$ | 1.0 ± 0.4 | 20 | 0/20 (0) | 17/20 (85) | 0/20 (0) | 3/20 (15) | 0/20 (0) | 0/20 (0) |
| *ku70Δ* | G418$^R$ | 1.5 ± 0.1 | 24 (100) | 7/24 (29) | 2/24 (8) (18/100 (18)) | 0/24 (0) | 6/24 (25) | 6/24 (25) | 3/24 (13) |
| *lig4Δ* | G418$^R$ | 0.7 ± 1.1 | 20 (100) | 9/20 (45) | 2/20 (10) (5/100 (5)) | 0/20 (0) | 9/20 (45) | 0/20 (0) | 0/20 (0) |
| *ku70Δ rhp55Δ* | Hyg$^R$ | 7.6 ± 0.7 | 22 | 0/22 (0) | 15/22 (68) | 3/22 (14) | 4/22 (18) | 0/22 (0) | 0/22 (0) |
| *lig4Δ rhp55Δ* | G418$^R$ | 2.3 ± 0.2 | 24 | 0/24 (0) | 19/24 (79) | 0/24 (0) | 5/24 (21) | 0/24 (0) | 0/24 (0) |
| *rhp55Δ* + pIRT3 | G418$^R$ | 1.1 ± 0.3 | 20 | 0/20 (0) | 17/20 (85) | 0/20 (0) | 3/20 (15) | 0/20 (0) | 0/20 (0) |
| *rhp55Δ* + pIRT3-*rhp51* | G418$^R$ | 0.5 ± 0.1 | 20 | 0/20 (0) | 12/20 (60) | 2/20 (10) | 2/20 (10) | 4/20 (20) | 0/20 (0) |

LOH colonies (*ade*$^+$ G418$^S$/Hyg$^S$ *his*$^-$) from each strain were analysed for the presence of Ch$^X$, Ch$^{16}$, Ch$^{XY}$ and *de novo* telomere. The number of *ade*$^+$ G418$^S$/Hyg$^S$ *his*$^-$ cells undergoing these and 'other' uncharacterized mechanisms of LOH is presented. The percentage of colonies undergoing distinct mechanisms of LOH from each mutant is shown in parenthesis. Values in red depict the number and percentage of colonies (from 100 individually isolated samples) which gave rise to telomere specific PCR products when tested with the *de novo* telomere addition assay. **Ch$^X$**, ChI, ChII, ChIII and Ch$^X$ observed via PFGE. Profile is indicative of a translocation between Ch$^{16}$ and ChIII i.e. allelic crossover during G2 or BIR; **Ch$^{16}$**, ChI, ChII, ChIII and a minichromosome band similar in size to 'uncut' Ch$^{16}$-MGH/MHH observed via PFGE. Such a profile is indicative of telomere addition when telomere specific PCR products are observed (see 'Telomere addition') or suggestive of long-tract gene conversion/interstitial deletion/telomere addition proximal to the R1 primer used in the *de novo* telomere addition assay (Figure 4.2) in the absence of such products (see 'Other'); **Ch$^{XY}$**, ChI, ChII and Ch$^{XY}$ observed via PFGE. Such a profile is consistent with a single long tract GC associated allelic crossover between Ch$^{16}$ and ChIII during G1/early S-phase, or G2 (if recombinant products co-segregate to the same daughter cell). Exchange may be associated with telomere addition (see 'Telomere addition'), otherwise such a profile is suggestive of a long tract gene conversion event with an associated crossover as described above; **Missing**, ChI, ChII and ChIII but no minichromosome observed via PFGE analysis. *ade6-M216* may have integrated into either ChI, ChII or ChIII.

In *exo1Δ rhp55Δ* cells, the levels of interchromosomal GC (5.8%) and minichromosome loss (37.2%) were comparable to that observed in *rhp55Δ* (Table 5.1). Together with a comparable frequency of EJ/SCR (54.4%), these data suggested that deletion of *exo1*$^{+}$ had a minimal effect on the levels of repair in a *rhp55Δ* background. Indeed, this correlates with a minor role for Exo1 in resection at DSB ends (Moreau et al., 2001; Tomita et al., 2003). The level of extensive DSB-induced LOH in this background (1.0%) was comparable to that observed in both *rhp55Δ* (0.8%, $P$=0.597) and *exo1Δ* cells (1.0%; Table 3.1). As had been seen in other backgrounds, extensive LOH in *exo1Δ rhp55Δ* was break-dependent (Appendix VI). In addition, no *ade*$^{-}$ G418$^{S}$ *his*$^{+}$ colonies were observed post-induction. Since *exo1Δrhp55Δ* Ch$^{16}$-MGH showed no loss of viability in response to a DSB (Appendix VII) these data suggested that *exo1*$^{+}$ plays a minor role in promoting extensive DSB-induced LOH in the absence of *rhp55Δ*.

### 5.2.2. Deletion of *exo1*$^{+}$ does not affect telomere addition in *rhp55Δ*.

To test whether deletion of *exo1*$^{+}$ in *rhp55Δ* Ch$^{16}$-MGH led to a decrease in *de novo* telomere addition, 20 *exo1Δ rhp55Δ ade*$^{+}$ G418$^{S}$ *his*$^{-}$ colonies isolated from the three independently tested strains were analysed using 'low resolution' PFGE and the *de novo* telomere addition assay (Sections 2.5.7.4, 2.5.5.2 and 2.5.5.3).

As expected, PFGE analysis failed to identify the presence of Ch$^{X}$ in any of the 20 *exo1Δ rhp55Δ ade*$^{+}$ G418$^{S}$ *his*$^{-}$ colonies tested (Figure 5.1A and Table 5.2). PCR subsequently indicated that *de-novo* telomere addition had occurred in 85% of the *exo1Δ rhp55Δ ade*$^{+}$ G418$^{S}$ *his*$^{-}$ cells analysed (Table 5.2). Of those cells which gave telomere-specific PCR products all displayed a minichromosome band similar in size

to 'uncut' $Ch^{16}$-MGH. $Ch^{XY}$ was not observed in any of the *exo1Δ rhp55Δ* $ade^+$ $G418^S$ *his*$^-$ cells analysed via PFGE (Figure 5.1A and Table 5.2). The remaining 15% of *exo1Δ rhp55Δ* $ade^+$ $G418^S$ *his*$^-$ cells appeared to undergo other mechanism/s of extensive LOH. Indeed, these colonies also displayed a minichromosome band similar in size to 'uncut' $Ch^{16}$-MGH, suggesting that they had undergone an interstitial deletion, long tract gene conversion or telomere addition proximal to the forward primer used in the *de-novo* telomere addition assay (Figure 4.2B and Table 5.2). Since break-induced telomere addition was similar in *exo1Δrhp55Δ* compared to *rhp55Δ* $Ch^{16}$-MGH (Figure 5.2A), these data suggested that Exo1-mediated resection plays a minor role in *de-novo* telomere addition at break ends.

### 5.2.3. DSB repair and extensive LOH in *ku70Δ rhp55Δ* and *lig4Δ rhp55Δ*.

Several studies have suggested that Ku can attenuate extensive processing at DSB ends (Lee et al., 1998; Tomita et al., 2003). If Ku limits resection at DSBs, and telomere addition requires resection, then removal of Ku should promote an increase in *de-novo* telomere addition after break induction. To test this hypothesis, DSB-induced repair and extensive LOH were subsequently investigated in *ku70Δ rhp55Δ* and *lig4Δ rhp55Δ* backgrounds. Three independently derived strains from each background transformed with pREP81X-HO were analysed. A single strain containing blank plasmid was also tested for comparison and viability was assessed as previously described.

The frequency of interchromosomal GC (3.6%) and minichromosome loss (32.5%) in *lig4Δ rhp55Δ* $Ch^{16}$-MGH was comparable to that seen in *rhp55Δ*, as was the

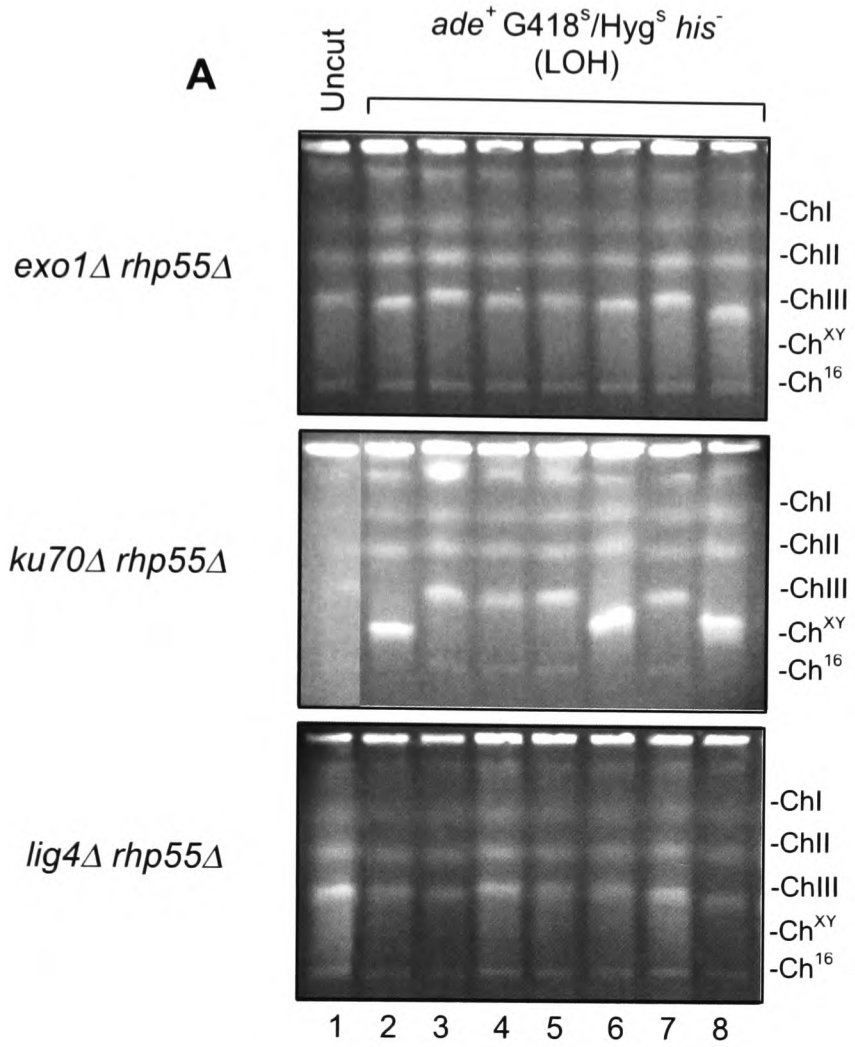



**Figure 5.1. PFGE analysis of LOH colonies from various *rhp55Δ* mutants.** Analysis of individually isolated *ade*$^+$ G418$^S$/Hyg$^S$ *his*$^-$ colonies from **A.** *exo1Δ rhp55Δ*, *ku70Δ rhp55Δ*, *lig4Δ rhp55Δ* and **B.** *rhp55Δ* + pIRT3/pIRT3-*rhp51* backgrounds via PFGE as described in Materials and Methods. 'Uncut' Ch$^{16}$-MGH ('Uncut') was run for comparison. ChI, II, III, Ch$^{16}$ and Ch$^{XY}$ are depicted where appropriate. *exo1Δ rhp55Δ* and *lig4Δ rhp55Δ* gels performed by C. Walker.

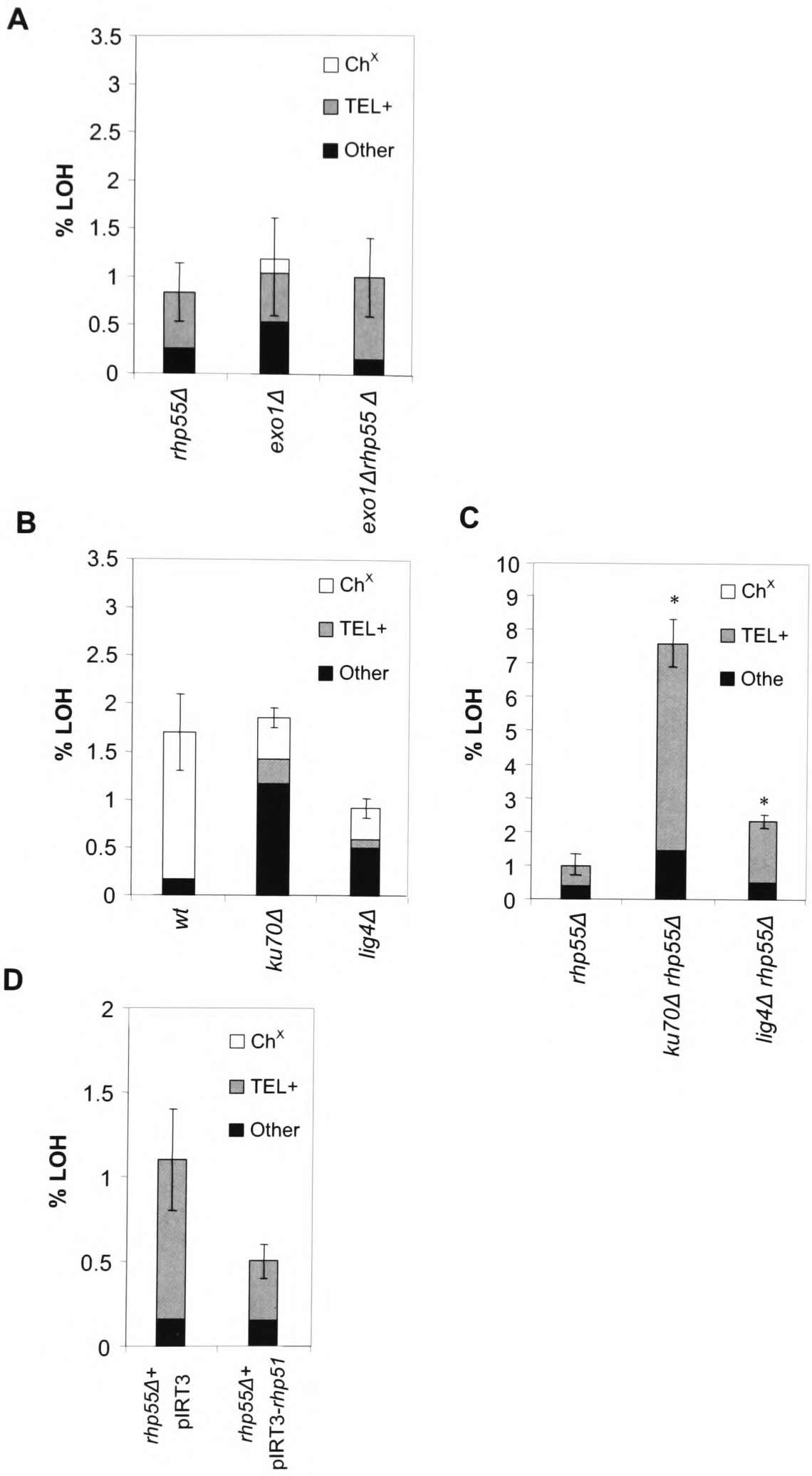



**Figure 5.2. HR competes with telomere addition for the repair of ssDNA ends.** Analysis of the frequency of break-induced LOH mechanisms in **A.** *exo1Δ*, *exo1Δ rhp55Δ*, **B.** *ku70Δ*, *lig4Δ*, **C.** *ku70Δ rhp55Δ*, *lig4Δ rhp55Δ* and **D.** *rhp55Δ* ± pIRT3-*rhp51* backgrounds. The percentage of *ade*$^+$ G418$^S$/Hyg$^S$ *his*$^-$ strains exhibiting Ch$^X$ (white), telomere addition (grey), or 'other' (black), in which neither Ch$^X$ or *de-novo* telomere addition at the break site were observed, are shown for each background (see Materials and Methods). 'Others' also include *ade*$^-$ G418$^S$/Hyg$^S$ *his*$^+$ colonies were applicable. Error bars (± S.E.M) for LOH values are depicted. *indicates a significant change in DSB-induced LOH compared to *rhp55Δ*.

frequency of EJ/SCR (58.8%) observed following break induction (Table 5.1). In contrast, DSB induction in *ku70Δ rhp55Δ* Ch$^{16}$-MHH led to an increase in interchromosomal GC (15.4%) and a reduction in minichromosome loss (27.2%) compared to that seen in *rhp55Δ* Ch$^{16}$-MGH (Table 5.1). Sequence analysis of *ku70Δ rhp55Δ ade*$^{+}$ G418$^{R}$ *his*$^{+}$ colonies failed to identify any mutations, insertions of deletions across the *MAT*a site, as did sequence analysis of *rhp55Δ ade*$^{+}$ G418$^{R}$ *his*$^{+}$ cells (A. Savory, unpublished observations). Intriguingly, the level of EJ/SCR (46.7%) was also similar to *rhp55Δ* in *ku70Δ rhp55Δ* Ch$^{16}$-MHH. This suggested that Ku70, but not Lig4, prevents repair via interchromosomal GC in the absence of Rhp55. This data also suggested that the uncharacteristically large population of *ade*$^{+}$ G418$^{R}$ *his*$^{+}$ cells observed in the absence of *rhp55*$^{+}$ was not due to an increase in 'end joining' via NHEJ. Interestingly, the level of extensive DSB-induced LOH in *ku70Δ rhp55Δ* Ch$^{16}$-MHH (7.6%) was significantly elevated compared to that seen in *rhp55Δ* ($P$=0.014). Although the level of extensive break-induced LOH in *lig4Δ rhp55Δ* Ch$^{16}$-MGH was elevated compared to that of *rhp55Δ* cells ($P$=0.046; Table 5.1), it was significantly smaller than that observed in *ku70Δ rhp55Δ* cells ($P$=0.011). Furthermore, *ade*$^{-}$ G418$^{S}$/Hyg$^{S}$ *his*$^{+}$ colonies were not observed in either mutant. Since LOH was break dependent and there was no change in cell viability following break induction in either background (Appendix VI and VII), these results indicated that *ku70*$^{+}$ plays a greater role than *lig4*$^{+}$ in limiting the level of DSB-induced LOH in the absence of *rhp55*$^{+}$.

### 5.2.4. *ku70*$^{+}$ represses break-induced de-novo telomere addition in *rhp55Δ* cells.

PCR and PFGE were again used to determine if *de-novo* telomere addition was responsible for the increase in extensive DSB-induced LOH in *ku70Δ rhp55Δ* cells.

As a result, 20 *ku70Δ rhp55Δ ade*$^{+}$ Hyg$^{S}$ *his*$^{-}$ colonies were analysed as previously described (Sections 2.5.7.4, 2.5.5.2 and 2.5.5.3). 20 *ade*$^{+}$ G418$^{S}$ *his*$^{-}$ cells from *lig4Δ rhp55Δ*, *ku70Δ* and *lig4Δ* backgrounds were also tested for comparison. An 'uncut' strain from each background was run as a control during PFGE.

As expected, Ch$^{X}$ was absent from all *ku70Δ rhp55Δ* and *lig4Δ rhp55Δ ade*$^{+}$ Hyg$^{S}$ *his*$^{-}$ colonies analysed (Figure 5.1A and Table 5.2). PCR subsequently identified the presence of telomere-specific PCR products in 81.8% of *ku70Δ rhp55Δ ade*$^{+}$ Hyg$^{S}$ *his*$^{-}$ cells. A subpopulation of cells which had undergone *de-novo* telomere addition also contained Ch$^{XY}$ (Figure 5.1A and Table 5.2; Section 3.2.3). Such exchanges were associated exclusively with colonies that had undergone telomere addition (Table 5.2). This was observed at relatively low frequency, however. Indeed, the majority of *ku70Δ rhp55Δ ade*$^{+}$ Hyg$^{S}$ *his*$^{-}$ colonies which gave rise to telomere-specific PCR products contained a minichromosome band similar in size to 'uncut' Ch$^{16}$-MGH (Table 5.2). The remaining 18.2% of *ku70Δ rhp55Δ ade*$^{+}$ Hyg$^{S}$ *his*$^{-}$ colonies underwent distinct mechanism/s of DSB-induced LOH as previously described. Thus, *de-novo* telomere addition was significantly increased in *ku70Δ rhp55Δ* cells compared to *rhp55Δ* Ch$^{16}$-MGH (Figure 5.2C). PCR analysis also revealed elevated levels of telomere addition in *lig4Δ rhp55Δ* Ch$^{16}$-MGH to that observed in the absence of *rhp55*$^{+}$, although this was significantly less than that observed in *ku70Δ rhp55Δ* cells (Figure 5.2C and Table 5.2). Unlike *ku70Δ rhp55Δ*, however, all colonies which gave rise to telomere specific PCR products displayed a minichromosome band similar in size to 'uncut' Ch$^{16}$-MGH (Figure 5.1A and Table 5.2). Indeed, Ch$^{XY}$ was not observed in any of the *lig4Δ rhp55Δ ade*$^{+}$ G418$^{S}$ *his*$^{-}$ colonies tested. The remaining 20.8% of *ade*$^{+}$ G418$^{S}$ *his*$^{-}$ colonies from *lig4Δ rhp55Δ*

underwent distinct mechanism/s of DSB-induced LOH as previously detailed (Table 5.2).

Intriguingly, previous analysis via PFGE revealed a marked decrease in $Ch^X$ formation in both *ku70Δ* and *lig4Δ* strains, suggesting that such genes are required for efficient crossover formation during G2 and/or BIR in *S. pombe* (Hussey, 2003. A. Davé, unpublished observations; Table 5.2). This is consistent with previous observations in *S. cerevisiae* (Myung et al., 2001). Interestingly, a similar profile of *de novo* telomere addition to that observed in *ku70Δ rhp55Δ* and *lig4Δ rhp55Δ* was seen in *ku70Δ* and *lig4Δ* strains. Indeed, analysis of 100 *ku70Δ ade*$^+$ $G418^S$ *his*$^-$ colonies by PCR revealed a small increase in the level of telomere addition compared to wild-type (18%; Figure 5.2B and Table 5.2). In contrast, the level of *de-novo* telomere addition in *lig4Δ* (4%) was similar to that observed in wild-type cells (1%; Table 5.2). Together, these data are consistent with a role for Ku70 and Lig4 in suppressing *de-novo* telomere addition in *rhp55Δ*. Furthermore, they suggest that Ku also plays an NHEJ independent role in limiting break-induced telomere addition, possibly through preventing extensive 5'-3' resection at DSB ends.

## 5.3. HOMOLOGOUS RECOMBINATION COMPETES WITH TELOMERE ADDITION FOR RESECTED DNA ENDS.

The evidence described above and in Chapter III was not only consistent with a role for DSB end processing in *de-novo* telomere addition but had also demonstrated that HR prevents chromosome healing. This raised the possibility that HR might prevent

telomere addition at DSB ends by competing for the repair of 3'-ssDNA overhangs generated by resection. Interestingly, it has previously been shown that overexpression of Rhp51 can suppress the sensitivity of a *rhp55Δ* strain to DNA damaging agents, presumably through promoting efficient nucleofilament formation and subsequent GC (Hays et al., 1995; Hope et al., 2005). Thus, to test whether HR competes with telomere addition, DSB repair and extensive LOH were investigated in an *rhp55Δ* $Ch^{16}$-MGH strain overexpressing *rhp51*.

### 5.3.1. DSB repair and extensive LOH in *rhp55Δ* $Ch^{16}$-MGH + pIRT3/pIRT3-*rhp51*.

*rhp55Δ* $Ch^{16}$-MGH strains used prior to this analysis were originally generated through deletion of a large proportion of the *rhp55*$^+$ ORF with *ura4*$^+$ (Prudden et al., 2003). In order to accommodate additional markers from pIRT3/pIRT3-*rhp51*$^+$, a different *rhp55Δ* strain in which the complete *rhp55*$^+$ ORF had been deleted with *arg3*$^+$ (Khasanov et al., 1999) was used to generate distinct *rhp55Δ* $Ch^{16}$-MGH cells. Three strains individually generated by this process were subsequently co-transformed with a combination of either pREP81X-HO/pIRT3 (*rhp55Δ* $Ch^{16}$-MGH + pIRT3) or pREP81X-HO/pIRT3-*rhp51*$^+$ (*rhp55Δ* $Ch^{16}$-MGH + pIRT3-*rhp51*$^+$) prior to analysis using the LOH assay (Section 2.5.7.1). Viability in response to a DSB was determined as previously described (Appendix VII).

Break-induction in *rhp55Δ* $Ch^{16}$-MGH + pIRT3 led to a large decrease in interchromosomal GC (3.1%) with a concomitant increase in minichromosome loss (45.3%) compared to wild-type $Ch^{16}$-MGH (Table 5.3). The frequency of EJ/SCR

**Table 5.3. Effect of *rhp51* overexpression on DSB-induced marker loss in *rhp55Δ*.**

| Genetic background | % *ade*$^+$ G418$^S$ *his*$^+$ (GC) | % *ade*$^+$ G418$^R$ *his*$^+$ (EJ/SCR) | % *ade*$^-$ G418$^S$ *his*$^-$ (Ch$^{16}$ loss) | % *ade*$^+$ G418$^R$ *his*$^-$ (LOH) | P *value* (relative to *rhp55Δ* LOH) |
|---|---|---|---|---|---|
| *rhp55Δ* + pIRT3 | 3.1 ± 1.1 | 46.2 ± 3.5 | 45.3 ± 4.6 | 1.1 ± 0.3 | 1.000 |
| *rhp55Δ* + pIRT3-*rhp51* | 12.2 ± 0.2 | 71.5 ± 0.4 | 15.4 ± 0.3 | 0.5 ± 0.1 | 0.166 |

The levels of interchromosomal gene conversion (GC), minichromosome loss (Ch$^{16}$ loss), loss of heterozygosity (LOH) and end-joining/sister chromatid recombination (EJ/SCR) are shown. Percentages were calculated as described in Materials and Methods. Levels of minichromosome loss were calculated using 48hrs+T *ade*$^+$ loss rather than blank plasmid values (See Materials and Methods).

observed post DSB-induction (46.2%) was also significantly increased compared to wild-type (Table 5.3). Interestingly, break-induction in *rhp55Δ* $Ch^{16}$-MGH + pIRT3-*rhp51*$^{+}$ resulted in a large decrease in minichromosome loss (15.4%) and increase in interchromosomal GC (12.2%) compared to that observed in *rhp55Δ* $Ch^{16}$-MGH + pIRT3 cells (Table 5.3). The frequency of EJ/SCR (71.5%) was also significantly increased in this background compared to *rhp55Δ* $Ch^{16}$-MGH + pIRT3 cells. This result suggested that Rhp51 overexpression promotes repair in the absence of *rhp55*$^{+}$ and was consistent with the reduced drug sensitivity of *rhp55Δ* strains in which *rhp51*$^{+}$ had previously been overexpressed (Hope et al., 2005). As predicted, overexpression of *rhp51*$^{+}$ in *rhp55Δ* $Ch^{16}$-MGH led to a substantial decrease in extensive DSB-induced LOH (0.5%) compared to that seen in *rhp55Δ* cells with blank plasmid (1.1%, Table 5.3). Since viability was unaffected in response to DSB induction (Appendix VII), these data suggested that overexpression of *rhp51*$^{+}$ promotes DSB repair via interchromosomal GC and EJ/SCR in the absence of *rhp55*$^{+}$, and that such induction reduces extensive DSB-induced LOH in *rhp55Δ* cells.

### 5.3.2. Overexpression of *rhp51* reduces break-induced *de novo* telomere addition in *rhp55Δ* cells.

To determine whether the reduction in extensive DSB-induced LOH observed after overexpression of *rhp51*$^{+}$ in *rhp55Δ* $Ch^{16}$-MGH was due to a reduction in telomere addition, 20 *ade*$^{+}$ $G418^{S}$ *his*$^{-}$ colonies isolated from *rhp55Δ* $Ch^{16}$-MGH + pIRT3 and *rhp55Δ* $Ch^{16}$-MGH + pIRT3-*rhp51*$^{+}$ backgrounds were analysed via PFGE and PCR as previously described (Sections 2.5.5.2, 2.5.5.3 and 2.5.7.4).

Interestingly, PFGE analysis failed to identify the presence of $Ch^X$ in any *rhp55Δ* *ade*$^+$ G418$^S$ *his*$^-$ cells in which *rhp51* had or had not been overexpressed (Figure 5.1B and Table 5.2). As predicted, PCR analysis subsequently revealed a substantial decrease in *de-novo* telomere addition in *rhp55Δ* $Ch^{16}$-MGH + pIRT3-*rhp51* cells compared to that observed in *rhp55Δ* $Ch^{16}$-MGH strains with blank plasmid (Table 5.2 and Figure 5.2D). All *rhp55Δ* + pIRT3 *ade*$^+$ G418$^S$ *his*$^-$ colonies which gave rise to telomere specific PCR products contained a minichromosome band similar in size to 'uncut' $Ch^{16}$-MGH (Figure 5.1B and Table 5.2). Although this was observed in the majority of *rhp55Δ* + pIRT3-*rhp51* *ade*$^+$ G418$^S$ *his*$^-$ cells, $Ch^{XY}$ was detected in a small subpopulation of colonies which gave telomere specific products (Figure 5.1B and Table 5.2). Not all crossovers were associated with telomere addition in *ade*$^+$ G418$^S$ *his*$^-$ colonies isolated from *rhp55Δ* $Ch^{16}$-MGH + pIRT3-*rhp51*$^+$ cells, however (Table 5.2). The remaining *ade*$^+$ G418$^S$ *his*$^-$ cells taken from each background underwent distinct mechanisms of DSB-induced LOH as previously detailed (Table 5.2). Together, these data suggested that overexpression of *rhp51*$^+$ in *rhp55Δ* cells promoted break-induced GC and EJ/SCR, which subsequently prevented telomere addition at *MAT*a. Overexpression also promoted the formation of reciprocal exchanges in a small proportion of cells which underwent telomere addition. These findings strongly suggested a role for HR in preventing *de novo* telomere addition by competing for resected ends.

## 5.4. INVESTIGATING THE ROLE OF THE MRN COMPLEX IN *DE-NOVO* TELOMERE ADDITION.

Data from Chapter IV had suggested that Rad32 and Rad50 were required for efficient break-induced chromosome healing. To further investigate a role for the MRN complex in *de-novo* telomere addition and EJ/SCR in the absence of *rhp55*$^{+}$, DSB repair and extensive LOH were subsequently investigated in *rad32Δ rhp55Δ* Ch$^{16}$-MHH, *rad50Δ rhp55Δ* Ch$^{16}$-MHH and *nbs1Δ rhp55Δ* Ch$^{16}$-MGH.

### 5.4.1. DSB repair and extensive LOH in *rad32Δ rhp55Δ*, *rad50Δ rhp55Δ* and *nbs1Δ rhp55Δ*.

Three individually generated Ch$^{16}$-MGH/MHH strains from *rad32Δ rhp55Δ*, *rad50Δ rhp55Δ*, and *nbs1Δ rhp55Δ* backgrounds were first transformed with pREP81X-HO and subsequently analysed using the LOH assay as described in Section 2.5.7.1. Viability and DSB-induced marker loss in the presence of blank plasmid were also assessed as previously detailed (Section 2.5.7.3).

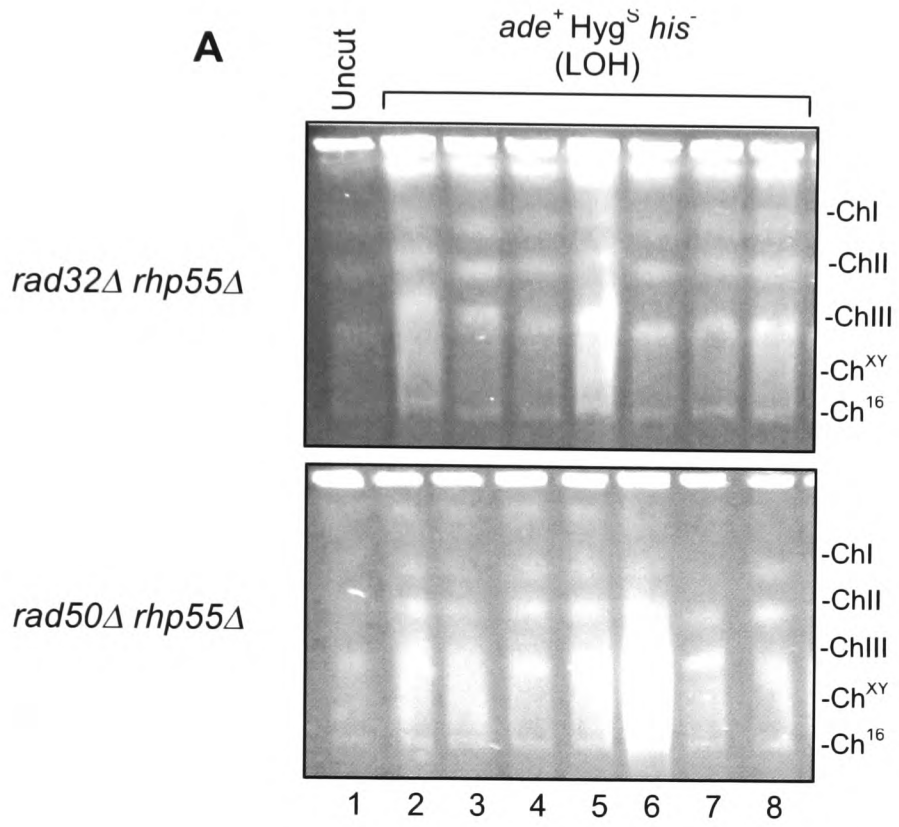
The frequency of break-induced interchromosomal GC in *rad32Δ rhp55Δ* (0.6%) and *rad50Δ rhp55Δ* (1.0%) was slightly lower than that observed in *rhp55Δ*, whilst minichromosome loss was increased (61.7% and 53.9%, respectively; Table 5.1). Interestingly, the frequency of EJ/SCR observed post DSB-induction in *rad32Δ rhp55Δ* (20.1%) and *rad50Δ rhp55Δ* (29.2%) cells was significantly decreased compared to that seen in *rhp55Δ* Ch$^{16}$-MGH (54.7%; Table 5.1). This suggested that the MR complex was required for efficient EJ/SCR in *rhp55Δ* Ch$^{16}$-MGH. Interchromosomal GC (0.1%) and EJ/SCR (23.4%) were also significantly reduced in

*nbs1Δ rhp55Δ* compared to *rhp55Δ* $Ch^{16}$-MGH (Table 5.1). Minichromosome loss (61.9%) was elevated compared to that seen in *rhp55Δ* $Ch^{16}$-MGH (Table 5.1). Thus, Nbs1 was also required for efficient EJ/SCR in *rhp55Δ* $Ch^{16}$-MGH cells. Surprisingly, extensive DSB-induced LOH was significantly increased in *rad32Δ rhp55Δ* (6.6%, $P$=0.005) and *rad50Δ rhp55Δ* cells (4.9%, $P$=0.046) compared to that observed in *rhp55Δ* $Ch^{16}$-MGH. Break-induction in *nbs1Δ rhp55Δ* $Ch^{16}$-MGH also led to a significant increase in extensive LOH (2.6%, $P$=0.039) compared to that seen in *rhp55Δ* $Ch^{16}$-MGH (0.8%). The increase observed was not as dramatic as that observed on deletion of $rad32^+$ and $rad50^+$ in *rhp55Δ* $Ch^{16}$-MGH, however. No $ade^-$ $G418^S/Hyg^S$ $his^+$ colonies were observed in either background. Since viability was not affected by DSB-induction (Appendix VII), these results suggested that the MRN complex plays a role in preventing DSB-induced LOH in *rhp55Δ* cells, presumably through promoting efficient EJ/SCR. These data also suggest that the MR complex plays a greater role than Nbs1 in preventing extensive LOH in the absence of $rhp55^+$.

### 5.4.2. $rad32^+$, $rad50^+$ and $nbs1^+$ repress *de-novo* telomere addition in *rhp55Δ*.

To examine the role of MRN in *de-novo* telomere addition in the absence of $rhp55^+$, ≥20 $ade^+$ $G418^S/Hyg^S$ $his^-$ colonies from *rad32Δ rhp55Δ*, *rad50Δ rhp55Δ* and *nbs1Δ rhp55Δ* cells were analysed using 'low resolution' PFGE and the *de-novo* telomere addition assay as previously described (Section 2.5.5.2, 2.5.5.3 and 2.5.7.4).

As expected $Ch^X$ was absent from all $ade^+$ $G418^S/Hyg^S$ $his^-$ cells tested from each background (Figure 5.3 and Table 5.2). Subsequent, PCR analysis revealed the presence of telomere specific products in 73% of *rad32Δ rhp55Δ* and 91% of *rad50Δ*



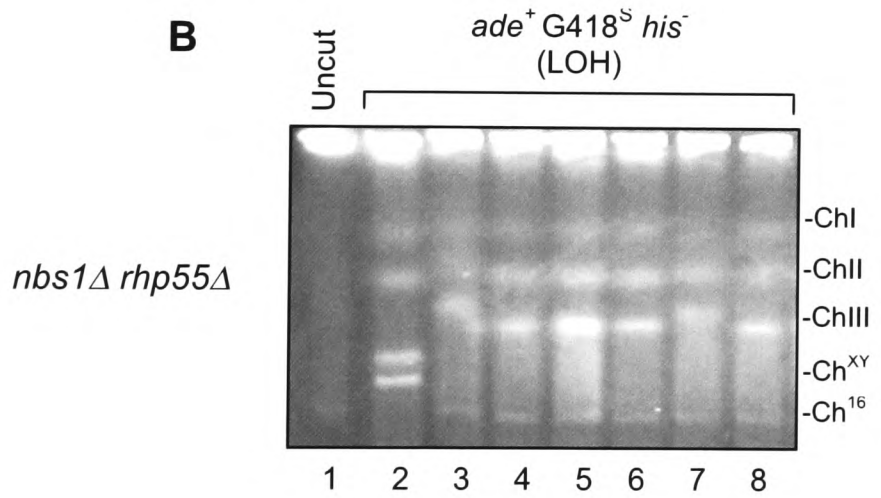




**Figure 5.3. PFGE analysis of LOH colonies from various *rhp55Δ* and MRN double mutants.** Analysis of individually isolated *ade*$^+$ G418$^S$/Hyg$^S$ *his*$^-$ colonies from **A.** *rad32Δ rhp55Δ*, *rad50Δ rhp55Δ* and **B.** *nbs1Δ rhp55Δ* backgrounds via PFGE as described in Materials and Methods. 'Uncut' Ch$^{16}$-MGH ('Uncut') was run for comparison. ChI, II, III, Ch$^{16}$ and Ch$^{XY}$ are depicted where appropriate. *nbs1Δ rhp55Δ* gel performed by C. Walker.

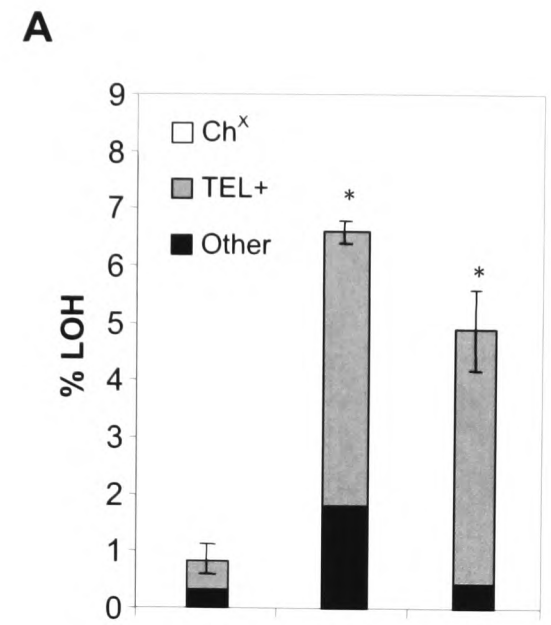



**Figure 5.4. The MRN complex prevents telomere addition in the absence of *rhp55*$^+$.** Analysis of the frequency of break-induced LOH in **A.** *rad32Δ rhp55Δ*, *rad50Δ rhp55Δ* and **B.** *nbs1Δ rhp55Δ* backgrounds. The percentage of *ade*$^+$ G418$^S$/Hyg$^S$ *his*$^-$ colonies exhibiting Ch$^X$ (white), telomere addition (grey), or 'Other' (black), in which neither Ch$^X$ or *de novo* telomere addition at the break site were observed, are shown for each background (see Materials and Methods). Error bars (± S.E.M) for LOH values are depicted. *indicates a significant change in DSB-induced LOH compared to *rhp55Δ*.

*rhp55Δ ade*$^{+}$ Hyg$^{S}$ *his*$^{-}$ cells (Table 5.2). Interestingly, *ade*$^{+}$ Hyg$^{S}$ *his*$^{-}$ colonies from *rad32Δ rhp55Δ* and *rad50Δ rhp55Δ* which had undergone *de novo* telomere addition all displayed a minichromosome band similar in size to 'uncut' Ch$^{16}$-MGH (Figure 5.3A and Table 5.2). PFGE failed to identify the presence of Ch$^{XY}$ in any of the *rad32Δ rhp55Δ* or *rad50Δ rhp55Δ ade*$^{+}$ Hyg$^{S}$ *his*$^{-}$ colonies tested. The remaining proportion of *ade*$^{+}$ Hyg$^{S}$ *his*$^{-}$ cells from *rad32Δ rhp55Δ* or *rad50Δ rhp55Δ* backgrounds also contained a minichromosome similar in size to 'uncut' Ch$^{16}$-MHH, suggesting that extensive DSB-induced LOH occurred via either long tract gene conversion, an interstitial deletion or telomere addition proximal to the forward primer used in the *de novo* telomere addition assay in these colonies (Table 5.2). Thus, *de-novo* telomere addition was significantly increased in *rad32Δ rhp55Δ* and *rad50Δ rhp55Δ* backgrounds when compared to *rhp55Δ* cells (Figure 5.4A). Telomere specific PCR products were also observed in approximately 91% of *nbs1Δ rhp55Δ ade*$^{+}$ G418$^{S}$ *his*$^{-}$ colonies (Table 5.2). Like *rad32Δ rhp55Δ* and *rad50Δ rhp55Δ*, all *nbs1Δ rhp55Δ ade*$^{+}$ Hyg$^{S}$ *his*$^{-}$ colonies which had undergone *de novo* telomere addition displayed a minichromosome band similar in size to 'uncut' Ch$^{16}$-MGH (Figure 5.3B and Table 5.2). The remaining population of *nbs1Δ rhp55Δ ade*$^{+}$ Hyg$^{S}$ *his*$^{-}$ colonies underwent distinct mechanism/s of DSB-induced LOH as previously described. Thus, loss of Nbs1 in *rhp55Δ* also led to a significant increase in telomere addition compared to *rhp55Δ* Ch$^{16}$-MGH, although such increase was not as dramatic as observed on deletion of *rad32*$^{+}$ and *rad50*$^{+}$ in *rhp55Δ* (Figure 5.4B). Together, these data suggest that the MRN complex prevents break-induced *de-novo* telomere addition in the absence of *rhp55*$^{+}$, presumably through promoting EJ/SCR. These results also suggest that the MR complex plays a greater role than Nbs1 in preventing telomere addition in the absence of *rhp55*$^{+}$

## 5.5. OVEREXPRESSION OF *RHP51* MAY PROMOTE CROSSOVERS DURING REPAIR IN *RHP55Δ* CELLS.

Telomere addition in *rhp55Δ ade*$^{+}$ G418$^{S}$ *his*$^{-}$ cells transformed with pIRT3 was not associated with an allelic crossover (Table 5.2 and Figure 5.1B). Overexpression of *rhp51* lead to an increase in the level of crossovers associated with telomere addition in *rhp55Δ* cells, however (Table 5.2 and Figure 5.1B). To investigate whether overexpression of *rhp51* promoted allelic crossovers in all repair populations from *rhp55Δ* Ch$^{16}$-MGH, ≥20 *ade*$^{+}$ G418$^{R}$ *his*$^{+}$ colonies isolated from wild-type Ch$^{16}$-MGH, *rhp55Δ* Ch$^{16}$-MGH + pIRT3 and *rhp55Δ* Ch$^{16}$-MGH + pIRT3-*rhp51* were analysed using 'low resolution' PFGE as described (Sections 2.5.7.4 and 2.5.5.2). 20 *ade*$^{+}$ G418$^{S}$ *his*$^{+}$ colonies from *wild type* Ch$^{16}$-MGH and *rhp51Δ* Ch$^{16}$-MGH + pIRT3-*rhp51* were also analysed.

PFGE analysis of *ade*$^{+}$ G418$^{R}$ *his*$^{+}$ cells from *wild-type* and *rhp55Δ* Ch$^{16}$-MGH + pIRT3 failed to identify the presence of Ch$^{XY}$ (Figure 5.5 and Table 5.4). Allelic crossovers were observed in 5% of *ade*$^{+}$ G418$^{R}$ *his*$^{+}$ colonies isolated from *rhp55Δ* Ch$^{16}$-MGH + pIRT3-*rhp51* cells, however, an observation which extended to 10% of *ade*$^{+}$ G418$^{S}$ *his*$^{+}$ colonies from the same background (Figure 5.5 and Table 5.4). 2.5% of *wild-type ade*$^{+}$ G418$^{S}$ *his*$^{+}$ colonies also displayed Ch$^{XY}$. Thus, crossovers were a feature of repair in *ade*$^{+}$ G418$^{R}$ *his*$^{+}$ colonies from *rhp55Δ* Ch$^{16}$-MGH + pIRT3-*rhp51* but not *rhp55Δ* Ch$^{16}$-MGH + pIRT3 cells. Together with results suggesting that *rhp51* overexpression promotes repair via both interchromosomal GC and end joining in *rhp55Δ* cells, and crossover formation in *rhp55Δ ade*$^{+}$ G418$^{S}$ *his*$^{-}$ cells, these data

**Table 5.4. PFGE analysis of EJ/SCR and GC populations from wt and *rhp55Δ* mutant cells.**

| Genetic background | % *ade*$^+$ G418$^R$ *his*$^+$ (EJ/SCR) | # endpoints analysed | Ch$^{16}$ (%) | Ch$^{XY}$ (%) | % *ade*$^+$ G418$^S$ *his*$^+$ (GC) | # endpoints analysed | Ch$^{16}$ (%) | Ch$^{XY}$ (%) |
|---|---|---|---|---|---|---|---|---|
| *wild-type* | 25.0 ± 1.4 | 20 | 20/20 (100) | 0/20 (0) | 49.7 ± 2.6 | 40 | 39/40 (98) | 1/40 (2) |
| *rhp55Δ* + pIRT3 | 46.2 ± 3.5 | 20 | 20/20 (100) | 0/20 (0) | 3.1 ± 1.1 | N.D. | N.D. | N.D. |
| *rhp55Δ* + pIRT3-*rhp51*$^+$ | 71.5 ± 0.4 | 20 | 19/20 (95) | 1/20 (5) | 12.2 ± 0.2 | 20 | 18/20 (90) | 2/20 (10) |

EJ/SCR (*ade*$^+$ G418$^R$ *his*$^+$) and GC (*ade*$^+$ G418$^S$ *his*$^+$) colonies from each strain were analysed for the presence of Ch$^{XY}$. The number of cells displaying Ch$^{XY}$ in these distinct populations is presented. The percentage of colonies displaying this profile from each mutant is shown in parenthesis. **Ch$^{16}$**, ChI, ChII, ChIII and a minichromosome band similar in size to 'uncut' Ch$^{16}$-MGH/MHH are observed via PFGE. This suggests repair is not associated with an allelic crossover; **Ch$^{XY}$**, ChI, ChII and Ch$^{XY}$ observed via PFGE. Such a profile is consistent with an allelic crossover between Ch$^{16}$ and ChIII during G1/early S-phase, or G2 (if recombinant products co-segregate to the same daughter cell).

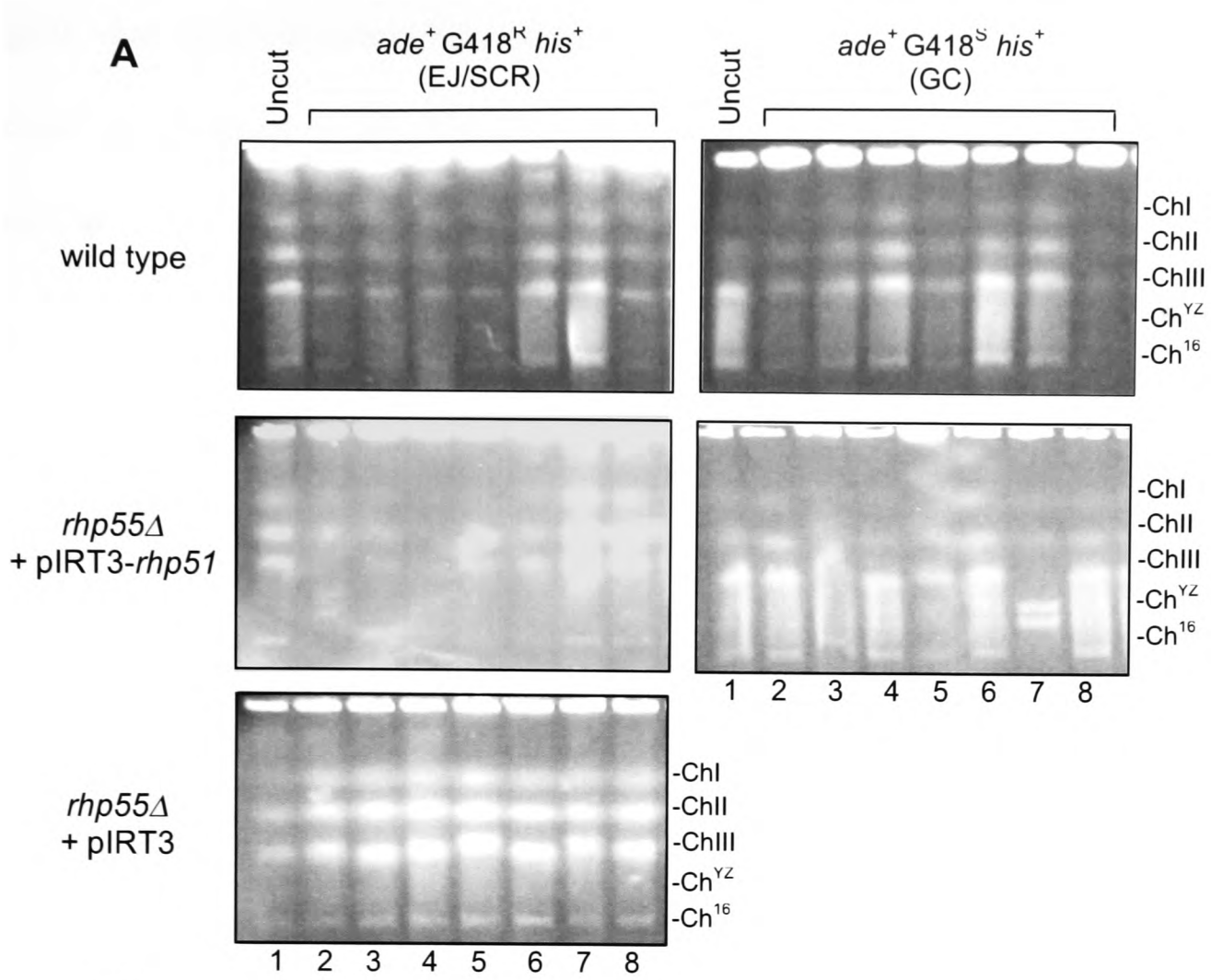



**Figure 5.5. Overexpression of *rhp51* promotes EJ/SCR, interchromosomal GC and possibly crossover formation in *rhp55Δ*. A.** Analysis of individually isolated *ade*$^+$ G418$^R$ *his*$^+$ (EJ/SCR) and *ade*$^+$ G418$^S$ *his*$^-$ (GC) colonies from wild-type Ch$^{16}$-MGH and *rhp55Δ* Ch$^{16}$-MGH + pIRT3/pIRT3-*rhp51* via PFGE as described in Materials and Methods. 'Uncut' Ch$^{16}$-MGH ('Uncut') was run for comparison. ChI, II, III, Ch$^{16}$ and Ch$^{XY}$ are depicted where appropriate. *ade*$^+$ G418$^R$ *his*$^+$ *rhp55Δ* + pIRT3-*rhp51* gels performed by C. Walker. **B.** Analysis of the frequency of crossover formation in EJ/SCR (*ade*$^+$ G418$^R$ *his*$^+$) and GC populations from wild-type (wt) and *rhp55Δ* Ch$^{16}$-MGH + pIRT3/pIRT-*rhp51* backgrounds. The percentage of colonies exhibiting Ch$^{XY}$ (+ Crossovers) are shown for each background (see Materials and Methods). Error bars (± S.E.M) for repair values are depicted.

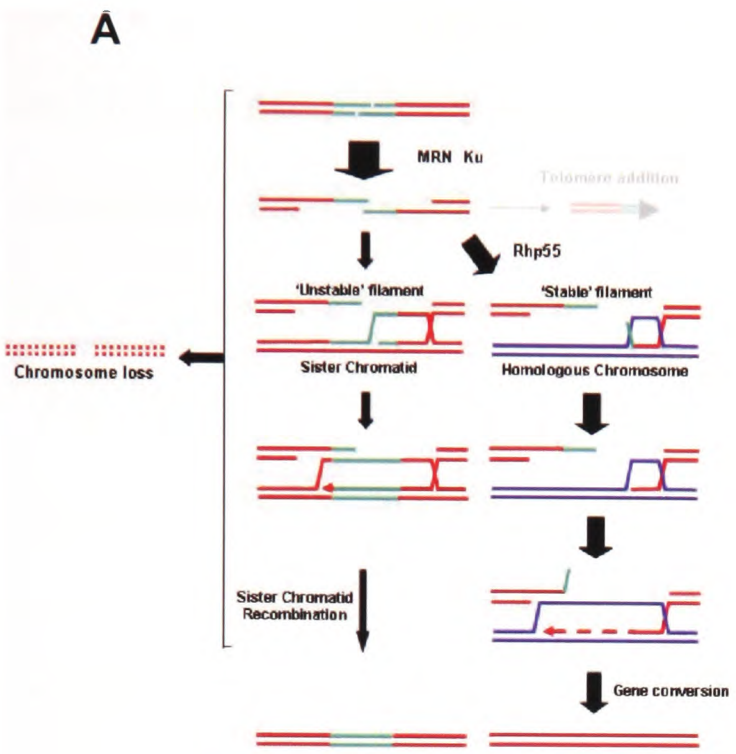
suggest that nucleofilament/heteroduplex formation may not only regulate the mechanism of repair in *rhp55Δ* cells but also the outcome i.e. whether repair is associated with a crossover or not.

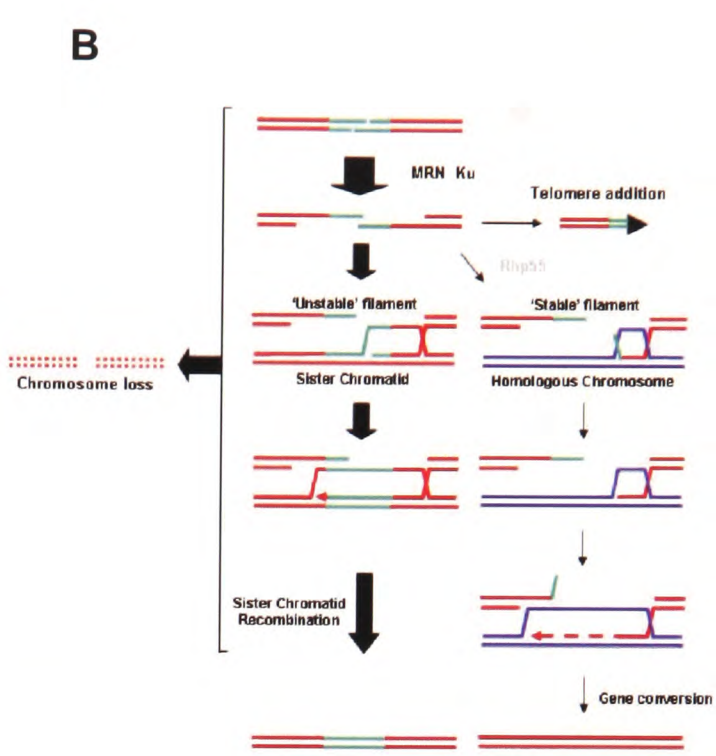
## 5.6. DISCUSSION.

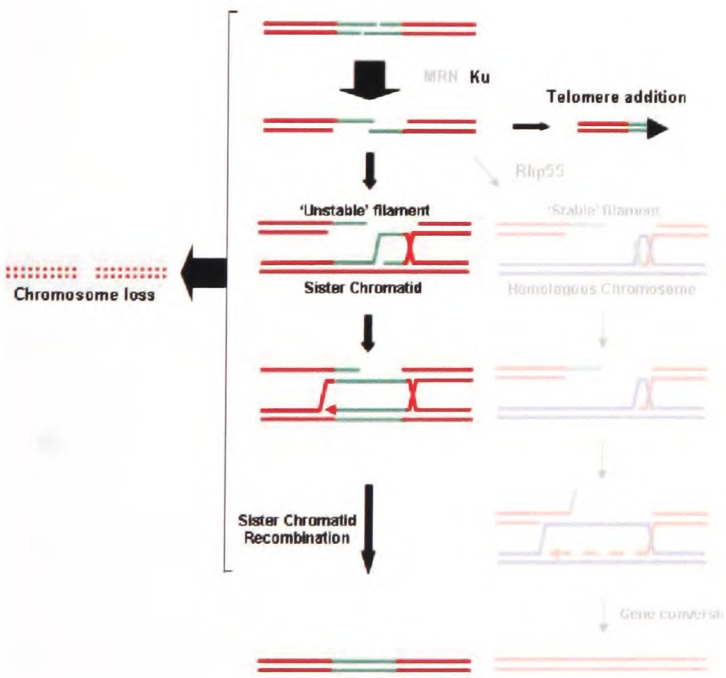
### 5.6.1. Investigating repair in *rhp55Δ* Ch$^{16}$-MGH.

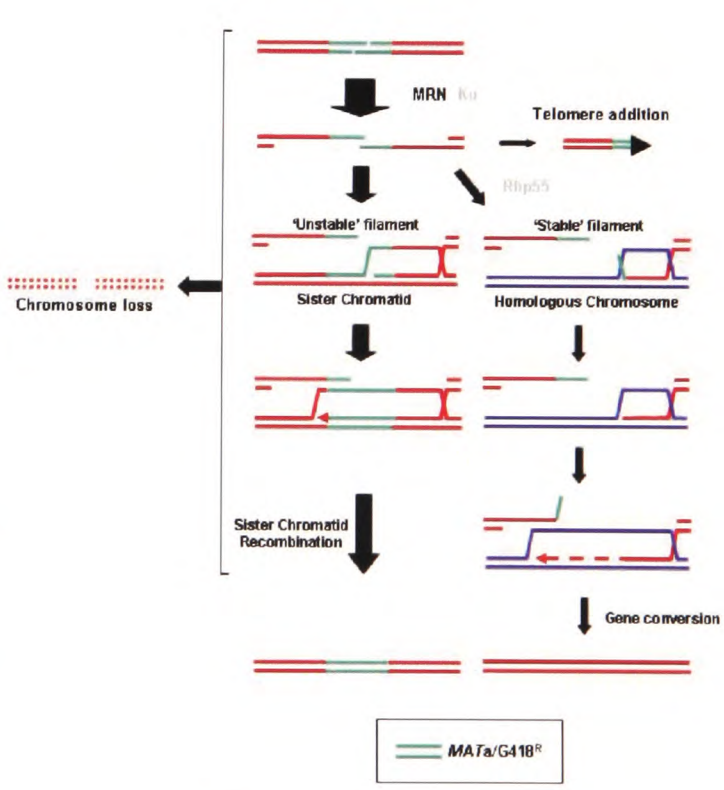
Intruigingly, DSB-induction in *rhp55Δ* Ch$^{16}$-MGH led to an increase in the level of *ade*$^{+}$ G418$^{R}$ *his*$^{+}$ cells compared to that observed in wild-type background. Previous experiments had demonstrated that there was no difference in break-induction between wild-type and *rhp55Δ* Ch$^{16}$-MGH, and that the increase in *rhp55Δ ade*$^{+}$ G418$^{R}$ *his*$^{+}$ cells was dependent on *rhp51*$^{+}$ (Table 5.1; Prudden et al., 2003). Sequence analysis of 20 *rhp55Δ ade*$^{+}$ G418$^{R}$ *his*$^{+}$ colonies also failed to identify any insertions, deletions or point mutations across the *MAT*a cut site, indicating that repair in these colonies was error free. Together, these results suggest that repair occurs predominantly via sister chromatid recombination (SCR) or a HR-dependent end joining event (EJ) in the absence of *rhp55*$^{+}$. It has previously been shown that repair occurs preferentially by SCR in mitotic cells (Kadyk and Hartwell, 1992). So, why is gene conversion the predominant mechanism of repair in wild-type background using the Ch$^{16}$-MGH system? Given the requirement for long induction times it is possible that, although SCR may predominante during DSB repair in wild-type Ch$^{16}$-MGH, multiple rounds of breakage and repair at *MAT*a increase the probability that HR will utilise the homologous chromosome as a repair template. This hypothesis assumes that the probability of both sister chromatids being cut at any one time is relatively low, an important issue which will require further investigation in the Ch$^{16}$-MGH system. So why is gene conversion inhibited in the absence of *rhp55*$^{+}$? Given that the Rhp55/Rhp57 complex is believed to promote nucleofilament formation in the presence of inhibitory factors e.g. RPA (Sung, 1997b) and Fbh1 (Osman et al., 2005), perhaps loss of Rhp55 function leads to the formation of an unstable nucleofilament

**Figure 5.6. Model of DSB-induced repair in wt, *rhp55Δ*, *rad32Δ/rad50Δ/nbs1Δ rhp55Δ* and *ku70Δ rhp55Δ*. A.** Repair in wild-type cells occurs predominantly via sister chromatid recombination (SCR) or a HR-dependent end joining process ((EJ), not depicted) but results in interchromosomal GC as a result of multiple rounds of break-induction at *MAT*a. GC is facilitated by the formation of a 'stable' nucleofilament that can promote interactions between homologous chromosomes. **B.** The absence of Rhp55 leads to the formation of an 'unstable' nucleofilament/heteroduplex intermediate that, whilst unable to promote GC, is capable of repair by SCR or EJ. The absence of Rhp55 also affects proper nucleofilament formation, leading to an increase in ssDNA which can be utilised by telomere addition factors. **C.** The absence of MRN complex components in *rhp55Δ* perturbs nucleofilament/heteroduplex formation, presumably through affecting resection, break stabilisation and/or intra S-phase checkpoint activation, which subsequently leads to a reduction in repair via SCR and/or EJ. The absence of end joining leads to a significant increase in ssDNA substrate for *de novo* telomere addition. The majority of ends do not undergo addition due to the presence of inhibitory mechanisms e.g. *Pfh1*. **D.** Removal of Ku mediated end protection in *rhp55Δ* promotes extensive resection, which promotes interactions between homologous chromosomes and facilitates the formation of an interchromosomal heteroduplex intermediate capable of undergoing GC. SCR and/or EJ occurs at the same frequency as *rhp55Δ* cells. Extensive resection at the break site also leads to a better ssDNA substrate for *de novo* telomere addition. See text for details


A
MRN Ku
Telomere addition
Rhp55
'Unstable' filament
'Stable' filament
Chromosome loss
Sister Chromatid
Homologous Chromosome
Sister Chromatid Recombination
Gene conversion


B
MRN Ku
Telomere addition
Rhp55
'Unstable' filament
'Stable' filament
Chromosome loss
Sister Chromatid
Homologous Chromosome
Sister Chromatid Recombination
Gene conversion


C
MRN Ku
Telomere addition
Rhp55
'Unstable' filament
Chromosome loss
Sister Chromatid
Sister Chromatid Recombination


D
MRN Ku
Telomere addition
Rhp55
'Unstable' filament
'Stable' filament
Chromosome loss
Sister Chromatid
Homologous Chromosome
Sister Chromatid Recombination
Gene conversion
MATa/G418R

that, whilst able to facilitate SCR and/or EJ to an extent (note that break-induction leads to an increase in $Ch^{16}$ loss in *rhp55Δ* $Ch^{16}$-MGH compared to wild-type), cannot support a productive interaction with a homologous chromosome and thus promote interchromosomal gene conversion (Figure 5.6A, B). Rhp55 is also known to play a post-synaptic role during HR (Hope et al., 2005), suggesting that it might also promote GC by facillitating heteroduplex stability between homologous chromosomes during repair. The fact that interchromosomal gene conversion was extremely infrequent in *rhp55Δ* also suggests that 1) Rhp57 cannot facilitate conversion in the absence of its binding partner and 2) that Swi5/Sfr1, a heterodimeric complex which has been shown to act independently of Rhp55/Rhp57 in *rhp51*$^{+}$-dependent repair (Akamatsu et al., 2003) cannot substitute for loss of Rhp55 function during gene conversion.

Data presented in this chapter has subsequently shown that efficient repair in *rhp55Δ* deletes requires the MRN complex. Given that MRN mutants display defects in resection, break-stabilisation and intra S-phase checkpoint activation (Chahwan et al., 2003; de Jager et al., 2001; Ivanov et al., 1994; Lobachev et al., 2004; Tsubouchi and Ogawa, 1998), this suggests that either one or all of these activities are required for efficient SCR and/or EJ in *rhp55Δ* $Ch^{16}$-MGH. Attenuating these processes may perturb the formation of a stable heteroduplex intermediate between sister chromatids in the absence of a fully functional Rhp51-Rad22-ssDNA nucleofilament, or affect the formation of the nucleofilament itself (Figure 5.6C). This is consistent with previous studies which suggest that the MRN complex promotes repair via SCR (Bressan et al., 1999; Hartsuiker et al., 2001) and with the observed increase in minichromosome loss in *rad32Δ rhp55Δ*, *rad50Δ rhp55Δ* and *nbs1Δ rhp55Δ* $Ch^{16}$-MGH following break-induction in the $Ch^{16}$-MGH system. Recent data from mammalian cells has shown

that CHK1 phosphorylates RAD51 in response to HU treatment, a modification required for efficient repair at stalled replication forks (Sorensen et al., 2005). It would be interesting to see whether Rhp51 is modified by a similar process to promote efficient repair at DSBs through MRN-Tel1-Chk1 signaling in *S. pombe*. Interestingly, deletion of Exo1 did not affect the overall levels of repair in *rhp55Δ*. This suggests that resection may not play a significant role in promoting SCR and/or EJ in the absence of *rhp55*$^{+}$. However, this may also reflect a greater role for MRN in break processing (Moreau et al., 2001; Tomita et al., 2003). If efficient resection is required for *rhp51*$^{+}$-dependent EJ and/or SCR then encouraging such processing might promote an increase in *ade*$^{+}$ G418$^{R}$ *his*$^{+}$ colonies in *rhp55Δ* Ch$^{16}$-MGH. Interestingly, however, deletion of *ku70*$^{+}$ in *rhp55Δ* cells, which has previously been shown to inhibit resection at DSBs (Lee et al., 1998; Tomita et al., 2003), did not affect repair via SCR and/or EJ, but led to an increase in interchromosomal gene conversion. How might increased DSB end processing promote such conversion in *rhp55Δ* cells? Deletion of *ku70*$^{+}$ in this context may increase the length of the 'unstable' nucleofilament generated through the absence of Rhp55/Rhp57, leading to a longer invasion tract during repair. It is possible that such an event facilitates the formation of an interchromosomal heteroduplex intermediate or the generation of a nucleofilament structure that can promote interchromosomal gene conversion to a greater extent (Figure 5.6D) It has recently been reported, however, that gene conversion tract lengths are not affected by deletion of *KU70* in *S. cerevisiae* (Krishna et al., 2007). It is possible that Ku plays a more direct role in preventing gene conversion in the absence of a fully functional nucleofilament, although such a role must be separate from the NHEJ functions of Ku as deletion of *lig4*$^{+}$ does not affect the level of gene conversion, SCR and/or EJ in *rhp55Δ*. Indeed, this result provides

further evidence that repair occurs by SCR and/or EJ in the absence of *rhp55*$^{+}$, and not via NHEJ.

The data presented here also suggests that the nature of the nucleofilament/heteroduplex formed during HR may not only regulate the mechanism of repair in *rhp55Δ* cells but also the outcome i.e. whether repair is associated with a crossover or not. Intriguingly, not only did overexpression of *rhp51* lead to a significant increase in EJ/SCR and interchromosomal gene conversion in *rhp55Δ* Ch$^{16}$-MGH, but it led to the formation of allelic crossovers i.e. Ch$^{XY}$, in a proportion of *ade*$^{+}$ G418$^{R}$ *his*$^{+}$ and *ade*$^{+}$ G418$^{S}$ *his*$^{-}$ colonies from this background. Such exchanges were not observed in *ade*$^{+}$ G418$^{R}$ *his*$^{+}$ colonies from either wild-type or *rhp55Δ* cells containing pIRT3, although crossovers were observed in *wild-type* cells that had undergone interchromosomal GC. Unfortunately, *rhp55Δ ade*$^{+}$ G418$^{S}$ *his*$^{+}$ colonies were not tested during this study. Recent data has suggested, however, that Rhp57 is required for crossover formation during interchromosomal gene conversion in the Ch$^{16}$-MG system (Akamatsu et al., 2007). Assuming that gene conversion populations from *rhp57Δ* and *rhp55Δ* display similar characteristics with regard to crossover formation, these data suggest that overexpression of Rhp51 promotes repair in addition to crossover formation in *rhp55Δ*. An interesting question therefore is, how might excess Rhp51 promote such changes? Perhaps overexpression of *rhp51* leads to an increase in the 'stability' of either the nucleofilament or heteroduplex formed during repair in the absence of the Rhp55/Rhp57 complex. Here, increased stability promotes the interaction between homologous chromosomes and thus facilitates interchromosomal gene conversion with or without a crossover. Overexpression may not augment Rhp51-ssDNA and/or heteroduplex stability to the same degree in all cells, however. This could explain the increase in *rhp51*$^{+}$-

dependent repair with or without a reciprocal crossover in a proportion of cells from this background. The fact that crossovers were observed in *ade*$^{+}$ G418$^{R}$ *his*$^{+}$ cells from this background suggests that repair may not be due to an increase in SCR but a HR-dependent end joining event in which the homologous chromosome is used as a repair template. It also possible, however, that *rhp51* overexpression increases the frequency of spontaneously occurring crossovers during S-phase in *rhp55Δ*. Indeed, this could also account for the presence of Ch$^{XY}$ in a proportion of *ade*$^{+}$ G418$^{R}$ *his*$^{+}$ cells obtained after break-induction in *rhp55Δ* Ch$^{16}$-MGH + pIRT3-*rhp51*. Given that overexpression of *rhp51* promotes gene conversion, excess Rhp51 should also promote Ch$^{X}$ formation in *rhp55Δ* Ch$^{16}$-MGH. This was not observed however, suggesting that gene conversion during G2 phase cannot occur with an associated crossover in the absence of *rhp55*$^{+}$, regardless of the status of the Rhp51-Rad22-ssDNA nucleofilament. Together, these findings are consistent with a role for Rhp55 in promoting Rhp51-Rad22-ssDNA nucleofilament stability and/or heteroduplex formation, activities which might encourage gene conversion and promote the formation of reciprocal crossovers between homologous chromosomes. Recent data from budding yeast suggests that excess Rad51 actually reduces HR efficiency and has little effect on HR outcome in wild-type cells (Paffett et al., 2005). Indeed, further investigations are required to determine the nature of the nucleofilament produced in wild-type and mutant cells and how such structures differentially regulate repair and outcome.

### 5.6.2. HR competes with telomere addition for the repair of ssDNA overhangs.

Results discussed in the previous chapter had suggested that *de-novo* telomere addition may be facilitated by DSB end resection. The data presented in this chapter has strengthened this hypothesis by identifying an additional role for *ku70*$^{+}$ in both

the prevention of break-induced LOH via *de-novo* telomere addition in fission yeast, respectively. Together with evidence demonstrating that 1) overexpression of *rhp51* in *rhp55Δ* cells reduces *de-novo* telomere addition and 2) deletion of MRN components in *rhp55Δ* (which promote repair via SCR and/or EJ) leads to an increase in telomere addition, these data demonstrate that HR may prevent telomere addition at DSB ends by competing for the repair of ssDNA overhangs (Figure 5.8).

Indeed, deletion of $ku70^{+}$ in *rhp55Δ* cells was found to significantly increase DSB-induced LOH via telomere addition. The majority of such events were not associated with a reciprocal crossover event, although a subpopulation was found to have undergone exchange. This observation appears to contrast with findings in *S. cerevisiae* in which an interaction between Ku80 and *TLC1* was found to promote *de novo* telomere addition (Stellwagen et al., 2003). This difference may reflect distinct mechanisms of chromosome healing between these two evolutionarily divergent yeasts, although it is possible that redundant mechanisms of telomerase recruitment can facilitate *de novo* telomere addition when such repair occurs at low levels. The large increase in telomere addition in *ku70Δ rhp55Δ* cells must be specific to the NHEJ-independent function/s of Ku, however, since the level of telomere addition in *lig4Δ rhp55Δ* cells, although higher than *rhp55Δ*, was significantly lower than that observed in *ku70Δ rhp55Δ*. Since loss of $ku70^{+}$ has previously been shown to increase 5'-3' resection at DSBs (Lee et al., 1998; Tomita et al., 2003), this suggests that such processing may facilitate *de-novo* telomere addition at ssDNA ends. Minichromosome loss was reduced in *ku70Δ rhp55Δ*, most probably due to the increase in telomere addition and gene conversion. This suggests that not only does extensive resection generate a better substrate for telomere addition, it also promotes interchromosomal gene conversion in the absence of Rhp55/Rhp57 complex function (Figure 5.6C).

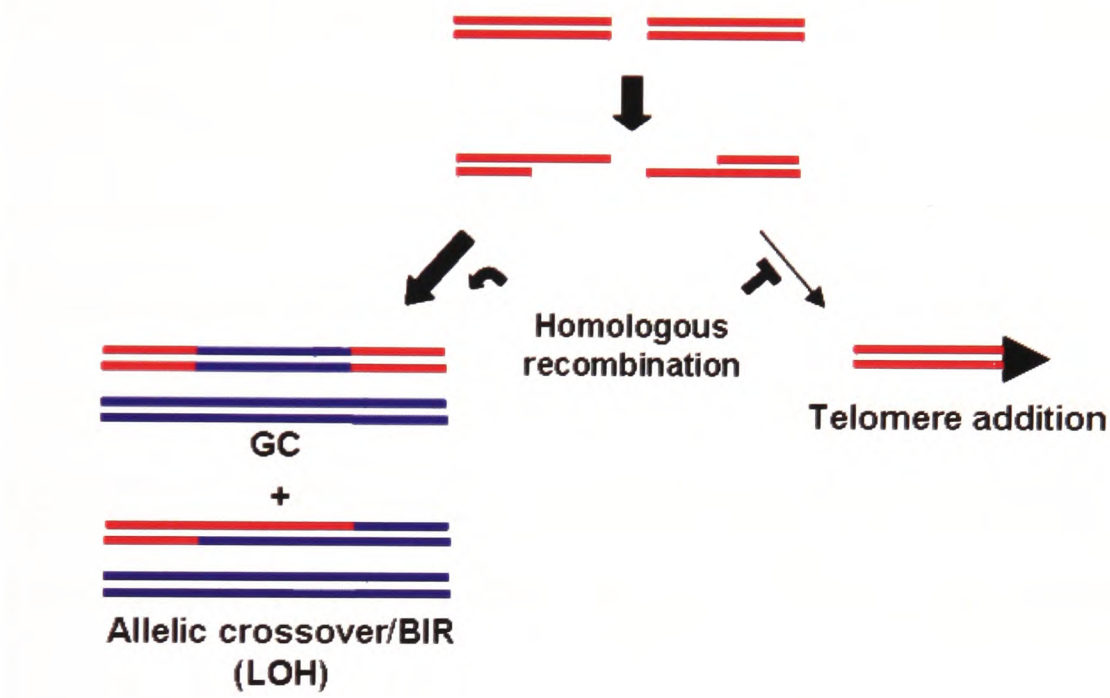



**Figure 5.7. Model depicting dual roles for HR in extensive DSB-induced LOH.** HR promotes allelic crossovers and BIR, while additionally preventing *de-novo* telomere addition through competition for resected ends. See text for details.

Interestingly, however, deletion of *exo1*$^{+}$ in *rhp55Δ* did not lead to a significant change in *de novo* telomere addition. Indeed, this is consistent with a greater role for MRN in break resection (see above). Together with the data from *rad32Δ* and *rad50Δ* strains (Section 4.2.4), these findings strongly suggest that resected single-stranded 3' overhangs are the preferred substrates for *de novo* telomere addition at DSBs, as has been observed at telomeres (Lee et al., 1993). I speculate that ssDNA produced via extensive resection may facilitate telomere addition by 1) exposing sequences which can promote efficient recruitment of the RNA template and/or 2) provide a platform for ssDNA binding proteins which are involved in *de-novo* telomere addition. It has recently been suggested that broken chromosomes might undergo telomere addition after recruitment to subnuclear compartments that maintain telomeres through telomerase but exclude DNA repair activities (Pennaneach et al., 2006). It would be of interest to determine whether resected ends are recruited to such compartments in the absence of HR.

Surprisingly, deletion of *rad32Δ*, *rad50Δ* and *nbs1Δ* in *rhp55Δ* Ch$^{16}$-MGH resulted in a significant increase in DSB-induced LOH via *de-novo* telomere addition compared to that observed in *rhp55Δ* cells. If resection is required for telomere addition, why does deletion of MRN components promote an increase in such repair in the absence of *rhp55*$^{+}$? The data presented here suggests that MRN is also required for *rhp51*$^{+}$-dependent repair in *rhp55Δ* cells (see above). Perhaps loss of SCR and/or EJ in this context leads to an increase in ssDNA availability as competing repair pathways are unable to repair the break (Figure 5.6B). In this model, ssDNA ends may be processed over time by Exo1 and/or alternative nucleases into a configuration which permits *de-novo* telomere addition to a greater extent than is observed in *rhp55Δ* cells. The large

majority of breaks, however, fail to undergo healing due to either Rhp51 nucleofilament formation and/or the activity of pathways inhibiting chromosome healing e.g. an orthologous pathway to *PIF1* in *S. cereviaie* (Schulz and Zakian, 1994). Indeed, this is consistent with a significant increase in minichromosome loss in *rad32Δ rhp55Δ*, *rad50Δ rhp55Δ* and *nbs1Δ rhp55Δ* cells compared to *rhp55Δ*. A role for resection in telomere addition could be investigated further by deleting $ku70^+$ and $exo1^+$ in the absence of Rad32/Rad50 and Rhp55. Indeed, recent studies have suggested that deletion of $ku70^+$ can suppress the IR and MMS sensitivity of *rad32Δ* and *rad50Δ* strains (Tomita et al., 2003). The suppression of MMS sensitivity in *ku70Δ rad50Δ* mutants was dependent on $exo1^+$, suggesting that $ku70^+$ prevents Exo1 mediated resection in the absence of MRN function. Loss of Ku in *rad32Δ rhp55Δ* cells might therefore promote an increase in Exo1 dependent resection, leading to an increase in telomere addition and possibly $rhp51^+$-dependent repair/gene conversion (Section 5.6.1). Indeed, deletion of $exo1^+$ would have the opposite effect in this context. If intra-S phase checkpoint activation is responsible for promoting repair in the absence of $rhp55^+$, then loss of Ku might not affect $rhp51^+$-dependent repair/gene conversion in *rad32Δ rhp55Δ* cells. Such an experiment might therefore be used to distinguish between a requirement for resection, checkpoint activation and/or break-stabilisation in $rhp51^+$-dependent repair/gene conversion in *rhp55Δ*.

Curiously, whilst perturbing SCR and/or EJ in *rhp55Δ* cells, loss of $nbs1^+$ did not lead to a large increase in *de-novo* telomere addition (2.4-fold) like that observed on deletion of $rad32^+$ or $rad50^+$ in *rhp55Δ* cells. If loss of individual MRN components has comparable effects on 5'-3' resection, break stabilisation and checkpoint activation (see above), why does loss of $nbs1^+$ lead to a relatively small increase in *de-novo* telomere addition in the absence of Rhp55? This may again be due to

differences in resection or strand invasion between *rad32Δ* and *nbs1Δ* deletes as described in Section 4.4.1. Given that telomere addition is approximately 4 fold greater in *rad32Δ rhp55Δ* compared to *rhp55Δ*, this would suggest that residual strand invasion events (using either the sister chromatid and/or the homologous chromosome) in *rad32Δ rhp55Δ* promote *de novo* telomere addition. Such invasion would not be productive for repair, however, as *rhp51*$^{+}$-dependent SCR and/or EJ is significantly reduced in *rad32Δ rhp55Δ* compared to *rhp55Δ* cells. Interestingly, a requirement for strand invasion in telomere addition is consistent with data demonstrating that deletion of *rhp51*$^{+}$ leads to a reduction in chromosome healing in *rhp55Δ rqh1Δ* cells (A. Davé, unpublished observations). It is also consistent with the increase in telomere addition observed in *ku70Δ rhp55Δ* Ch$^{16}$-MGH. In *nbs1Δ rhp55Δ* cells, residual invasion may be not possible and thus telomere addition is only slightly increased due to the increased availability of ssDNA ends. How might residual strand invasion promote telomere addition in *rhp55Δ*? Perhaps invasion using short ssDNA overhangs results in a kinetic delay or a structure which aids the recruitment of telomere-addition factors. Alternatively, the difference in phenotype between these strains may be due to differences in genetic background.

Finally, overexpression of *rhp51*$^{+}$ in *rhp55Δ* cells led to a reduction in DSB-induced LOH via telomere addition. Overexpression also led to 1) an increase in interchromosomal gene conversion and *rhp51*$^{+}$-dependent SCR and/or EJ, and 2) a decrease in minichromosome loss. As previously described, this is consistent with experiments in both *S. pombe* and *S. cerevisiae*, which have shown that overexpression of Rhp51/Rad51 can suppress the sensitivity of *rhp55Δ* strains to DNA damaging agents (Hays et al., 1995; Hope et al., 2005; Johnson and Symington, 1995). Together with the data described above, these observations provide further

evidence that telomere addition competes with HR for the repair of break ends. Interestingly, a similar reduction in *de novo* telomere addition has also been observed in *ku70Δ rhp55Δ* cells overexpressing *rhp51*$^{+}$ (W. Bridge, unpublished observations). Here, overexpression induced a further increase in interchromosomal gene conversion and a substantial reduction in both minichromosome loss and *de-novo* telomere addition compared to *ku70Δ rhp55Δ* cells. The level of *rhp51*$^{+}$-dependent EJ/SCR remained comparable to that observed in *ku70Δ rhp55Δ* Ch$^{16}$-MGH, however, suggesting that excess Rhp51 promotes a further increase in repair via gene conversion in this background. This may be due to an increase in Rhp51-Rad22-ssDNA nucleofilament stability or interchromosomal heteroduplex formation as described in Section 5.4.1. Together, these data suggest that efficient telomere addition requires ssDNA overhangs and that HR competes with telomere addition factors for the repair of such substrates.

### 5.6.3. Summary.

The data presented here suggests that the nature of the Rhp51-Rad22-ssDNA nucleofilament or heteroduplex formed can determine whether repair occurs between sister chromatids or homologous chromosomes, and whether such events are associated with crossover formation. In addition, these results have identified 1) a requirement for the MRN complex in efficient *rhp51*$^{+}$-dependent repair via SCR and/or EJ and 2) a role for Ku in preventing gene conversion in *rhp55Δ* cells. Finally, these data suggest that DSB end processing plays a significant role in *de-novo* telomere addition. Indeed, deletion of *ku70*$^{+}$ promoted telomere addition in *rhp55Δ* cells to a greater extent than deletion of *lig4*$^{+}$. Although loss of MRN complex components which facilitate resection promoted telomere addition, this result is

consistent with data which strongly suggests that chromosome healing competes with HR for the repair of ssDNA overhangs generated through DSB processing.

# 6. GENERAL DISCUSSION.

Previous studies using the $Ch^{16}$-MGH/MHH system had found that extensive break-induced LOH in wild-type *S. pombe* was associated predominantly with large translocations resulting from both allelic crossovers in G2 and BIR (Hussey, 2003). Such extensive homozygosis across a whole chromosomal arm was also found to require several genes involved in HR i.e. $rhp55^+$, $rhp51^+$, $rhp54^+$ and $mus81^+$. Analysis of the genetic requirements for such extensive LOH described in this study has identified a further role for the MRN complex, RPA and Rad22 in facilitating such translocations (Chapter III), suggesting that resection and strand invasion are common steps which not only aid gene conversion but promote allelic crossovers and BIR. A role for resection in allelic crossovers during G2 and/or BIR is strengthened by the observation that deletion of $exo1^+$ leads to a reduction in translocation formation in $Ch^{16}$-MGH cells (Chapter IV). Surprisingly, break-induced extensive LOH was still observed in HR mutants, but was found to arise through *de novo* telomere addition at, or near, the *MAT*a break-site (Chapter IV). Thus, in contrast to that of wild-type cells, DSB induction in HR mutants led to a distinct hemizygous LOH profile in which a whole chromosomal arm was lost. Together these data identify dual roles for HR in break-induced LOH in both facilitating translocations that occur as a result of allelic crossovers in G2 and BIR, and preventing *de novo* telomere addition in fission yeast.

Interestingly, break-induced LOH was directionally biased towards $ade^+$ $G418^S$ $his^-$ colonies in all strains tested. Such directional bias may result from several causes. In wild-type cells, $ade^+$ $G418^S$ $his^-$ colonies arising from allelic crossovers between $Ch^{16}$ and ChIII would be inviable, as such cells would lack the distal 1.6 Mb arm of ChIII. Secondly, BIR initiated through strand invasion by the distal arm of $Ch^{16}$, encoding

the *his3*$^{+}$ marker, may be compromised by the presence of ~2kb of non-homologous *kanMX6* sequence directly adjacent to the *MATa* break-site on this arm. Thirdly, the observation of *ade*$^{+}$ G418$^{S}$ *his*$^{-}$ colonies would necessitate break-induced replication through the centromere, which in *S. cerevisiae* can block unscheduled DNA replication (Morrow et al., 1997). A small proportion of *ade*$^{+}$ G418$^{S}$ *his*$^{+}$ colonies were previously observed in *exo1*Δ, *ku70*Δ and *lig4*Δ backgrounds, which may have arisen through long-tract gene conversion. In HR mutants, *ade*$^{-}$ G418$^{S}$/HygB$^{S}$ *his*$^{+}$ colonies would also be inviable due to loss of the Ch$^{16}$ centromere, which is required for the correct propagation and segregation of chromosomes.

An interesting question which arises from these studies is how does the cell differentiate between interchromosomal gene conversion, a process responsible for the majority of DSB repair events in the Ch$^{16}$-MGH system (See Table 3.1), and crossover formation/BIR in response to break-induction. The fact that common steps i.e. resection and strand invasion, are required for each of these mechanisms suggests that they each initiate in a similar manner. All must deviate from this point however. More work is needed to determine whether the utilisation of crossovers and/or BIR instead of GC is an active process promoted by the cell or the result of defects in normal gene conversion processes. DNA helicases, such as Srs2 and Sgs1 are known to play active roles in crossover avoidance in mitotic cells (Ira et al., 2003). Perhaps the relatively low level of translocations formed in the Ch$^{16}$-MGH/MHH system is due to the action of such proteins (Srs2 and Rqh1), whose activity is promoted during vegetative growth. Other factors, including Mus81, an endonuclease capable of producing reciprocal exchanges from dHJ type structures (Gaillard et al., 2003; Osman et al., 2003), may also be attenuated to prevent crossover formation during mitosis. Indeed, it has previously been shown in *S. pombe* that phosphorylation of

Mus81 by Cds1, a checkpoint kinase responsible for mediating the downstream effects of intra and S-M phase checkpoint activation in *S. pombe* (Lindsay et al., 1998), results in the removal of Mus81-Eme1 from stalled replication forks (Kai et al., 2005). Perhaps a similar process involving either Cds1 or Chk1 occurs at DSBs to prevent crossovers after strand invasion. These data therefore suggest that crossover formation may be a by-product of residual endonuclease and/or a lack of helicase activity at DSBs. What is the relationship between GC and BIR? One hypothesis to explain how BIR may result from GC is that the former is promoted by inhibition of second end capture during DSB repair. Indeed, it has recently been shown that BIR most likely occurs as a result of several strand invasion events, followed by replication and dissociation, which occur in an attempt to complete repair via GC (Smith et al., 2007). Such reinvasion eventually results in the formation of a unidirectional replication fork, most probably due to the absence of second end capture (Smith et al., 2007). In this scenario it may be better to duplicate a stretch of DNA than lose it altogether and risk death. Thus, perhaps LOH via BIR could be studied in greater detail in *S. pombe* if second end capture was compromised. This approach seems to have worked in *S. cerevisiae*, where it was recently shown that removing homology distal to the break site can abrogate gene conversion whilst significantly stimulating BIR (Malkova et al., 2005). Indeed, this data provides further evidence that second end capture during normal gene conversion is an important mechanism which suppresses the occurrence of BIR.

The data presented here also suggest that gene conversion itself might be regulated to some extent by the nature of the nucleofilament/heteroduplex intermediate formed during repair. As previously described, repair in *rhp55Δ* cells appears to result from a *rhp51*$^{+}$-dependent process, which promotes error free repair at the *MAT*a site. Such

repair requires the MRN complex (Chapter V) and may be dependent on the presence of a homologous chromosome or occur as a result of SCR. In any case, it appears that efficient GC requires the presence of Rhp55, which suggests that the Swi5/Sfr1 complex (Akamatsu et al., 2003) cannot compensate for loss of *rhp55*$^{+}$ in the Ch$^{16}$-MGH system. The fact that interchromosomal GC, EJ/SCR and crossover formation in *rhp55Δ* can be promoted through the overexpression of *rhp51* (Chapter V) provides further evidence that the nature of the Rhp51-Rad22-ssDNA nucleofilament plays an important role in determining the mechanism and outcome of repair. The fact that crossovers were observed in *rhp55Δ* cells that had undergone EJ/SCR after overexpression of *rhp51* suggests that end joining might require a homologous chromosome, and may not therefore result from SCR. It also possible, however, that *rhp51* overexpression increases the frequency of spontaneously occurring crossovers during S-phase in *rhp55Δ*. Indeed, this could also account for the presence of Ch$^{XY}$ in a proportion of *ade*$^{+}$ G418$^{R}$ *his*$^{+}$ cells obtained after break-induction in *rhp55Δ* Ch$^{16}$-MGH + pIRT3-*rhp51*. This could be investigated further by inducing a break in a chromosome without a homologous partner. If SCR is responsible for the increase in end joining in *rhp55Δ*, then break-induction would not be expected to significantly affect the level of EJ/SCR in these cells.

*De novo* telomere addition was most frequently observed in *rad22*Δ, *rhp55*Δ or *rhp51Δ* backgrounds that disrupt HR following end resection (Chapter IV). In addition, it was found that the levels of telomere addition, while increased in *ku70*Δ *rhp55*Δ, were reduced in an *rhp55*Δ strain overexpressing *rhp51* (Chapter V). Together, these findings support a model in which HR prevents *de novo* telomere addition at DSBs by competing for resected ssDNA ends. lt will be interesting to determine what proteins are recruited to resected break ends and what genes are

required in the absence of HR to promote such break-induced truncations. Such a study could be performed using a *rhp55Δ* $Ch^{16}$-MGH strain in which the Pfh1 helicase, whose orthologue in *S. cerevisiae* (Pif1) has been shown to inhibit telomere addition at enzymatically induced DSBs (Schulz and Zakian, 1994), has been deleted. A high level of telomere addition may facilitate genetic or chromatin immunoprecipitation studies to identify additional factors which are required for telomere addition and bind to the DSB in the absence of HR. It was also found that telomeric repeats were most frequently added at or near the HO endonuclease cut site. Closer analysis of break-telomere junctions revealed a pattern similar to that observed in *S. cerevisiae*, where addition occurs at sequences with homology to the telomerase guide RNA (Putnam et al., 2004). The fact that telomere addition occurred at or near the break site also suggests that telomere-associated sequences are dispensable for chromosomal stability during mitosis in *S. pombe*, consistent with previous observations (Matsumoto et al., 1987; Sugawara, 1989). This result also suggests that *de novo* telomere addition has the potential to occur widely throughout the *S. pombe* genome. Indeed, a role for HR in maintaining telomeres in the absence of telomerase is now well documented (McEachern and Haber, 2006). The finding that *de novo* telomere addition can maintain broken chromosomes in the absence of HR strongly suggests a more general functional interplay between these two processes, not only at telomeres but at *bona fide* two-ended DSBs.

Together, these data identify a role for DSBs in promoting extensive LOH in *S. pombe* through allelic recombination and BIR in wild-type cells, or through chromosome healing in HR mutants. As extensive LOH caused by chromosomal rearrangements is less likely to result in cell death than that resulting from chromosome loss, these mechanisms of LOH are likely to be more pernicious, thus

contributing to genetic disease, including tumourigenesis in higher eukaryotes. Although evidence for allelic crossovers and BIR in genetic disease awaits formal demonstration, allelic recombination has previously been identified as a mechanism leading to localised LOH at tumour suppressor loci in human cancer (Jasin, 2000) and is significantly stimulated by DSB induction (Moynahan and Jasin, 1997). Extensive LOH in response to a single DSB appears to be suppressed by allelic recombination in mammalian cells, however (Stark and Jasin, 2003). Interestingly, *de novo* telomere addition has been associated with genetic diseases including α thalassaemia and mental retardation (Wilkie et al., 1990; Wong et al., 1997). This data therefore suggests that determining the functional status of the HR machinery may be predictive of the types of extensive break-induced LOH that may arise, and thus may contribute towards understanding the etiology of genetic disease.

# 7. REFERENCES.

Akamatsu, Y., Dziadkowiec, D., Ikeguchi, M., Shinagawa, H., and Iwasaki, H. (2003). Two different Swi5-containing protein complexes are involved in mating-type switching and recombination repair in fission yeast. Proc Natl Acad Sci U.S.A *100*, 15770-15775.

Akamatsu, Y., Tsutsui, Y., Morishita, T., Siddique, M. S., Kurokawa, Y., Ikeguchi, M., Yamao, F., Arcangioli, B., and Iwasaki, H. (2007). Fission yeast Swi5/Sfr1 and Rhp55/Rhp57 differentially regulate Rhp51-dependent recombination outcomes. EMBO J *26*, 1352-1362.

Allers, T., and Lichten, M. (2001). Differential timing and control of noncrossover and crossover recombination during meiosis. Cell *106*, 47-57.

Asai, T., Sommer, S., Bailone, A., and Kogoma, T. (1993). Homologous recombination-dependent initiation of DNA replication from DNA damage-inducible origins in *Escherichia coli*. EMBOJ *12*, 3287-3295.

Aylon, Y., and Kupiec, M. (2004). New insights into the mechanism of homologous recombination in yeast. Mutat Res *566*, 231-248.

Aylon, Y., Liefshitz, B., Bitan-Banin, G., and Kupiec, M. (2003). Molecular dissection of mitotic recombination in the yeast *Saccharomyces cerevisiae*. Mol Cell Biol *23*, 1403-1417.

Aylon, Y., Liefshitz, B., and Kupiec, M. (2004). The CDK regulates repair of double-strand breaks by homologous recombination during the cell cycle. EMBO J *23*, 4868-4875.

Bai, Y., and Symington, L. S. (1996). A Rad52 homolog is required for RAD51-independent mitotic recombination in *Saccharomyces cerevisiae*. Genes Dev *10*, 2025-2037.

Bailey, S. M., Meyne, J., Chen, D. J., Kurimasa, A., Li, G. C., Lehnert, B. E., and Goodwin, E. H. (1999). DNA double-strand break repair proteins are required to cap the ends of mammalian chromosomes. Proc Natl Acad Sci U.S.A *96*, 14899-14904.

Baroin, A., Prat, A., and Caron, F. (1987). Telomeric site position heterogeneity in macronuclear DNA of Paramecium primaurelia. Nucleic Acids Res *15*, 1717-1728.

Bartek, J., and Lukas, J. (2007). DNA damage checkpoints: from initiation to recovery or adaptation. Curr Opin Cell Biol *19*, 238-245.

Baumann, P., and Cech, T. R. (2001). Pot1, the putative telomere end-binding protein in fission yeast and humans. Science *292*, 1171-1175.

Baylin, S. B., and Chen, W. Y. (2005). Aberrant gene silencing in tumor progression: implications for control of cancer. Cold Spring Harb Symp Quant Biol *70*, 427-433.

Bell, D. W., Varley, J. M., Szydlo, T. E., Kang, D. H., Wahrer, D. C., Shannon, K. E., Lubratovich, M., Verselis, S. J., Isselbacher, K. J., Fraumeni, J. F., Birch, J. M., Li, F. P., Garber, J. E., Haber, D.A. (1998). Heterozygous germ line hCHK2 mutations in Li-Fraumeni syndrome. Science *286*, 2528-31.

Beranek, D. T. (1990). Distribution of methyl and ethyl adducts following alkylation with monofunctional alkylating agents. Mutat Res *231*, 11-30.

Bertuch, A. A., and Lundblad, V. (2003). The Ku heterodimer performs separable activities at double-strand breaks and chromosome termini. Mol Cell Biol *23*, 8202-8215.

Bertuch, A. A., and Lundblad, V. (2006). The maintenance and masking of chromosome termini. Curr Opin Cell Biol *18*, 247-253.

Bianchi, A., Negrini, S., and Shore, D. (2004). Delivery of yeast telomerase to a DNA break depends on the recruitment functions of Cdc13 and Est1. Mol Cell *16*, 139-146.

Boddy, M. N., and Russell, P. (2001). DNA replication checkpoint. Curr Biol *11*, R953-956.

Borgdorff, V., van Hees-Stuivenberg, S., Meijers, C. M., and de Wind, N. (2005). Spontaneous and mutagen-induced loss of DNA mismatch repair in Msh2-heterozygous mammalian cells. Mutat Res *574*, 50-57.

Bosco, G., and Haber, J. E. (1998). Chromosome Break-Induced DNA Replication Leads to Nonreciprocal Translocations and Telomere Capture. Genetics *150*, 1037-1047.

Boule, J. B., Vega, L. R., and Zakian, V. A. (2005). The yeast Pif1p helicase removes telomerase from telomeric DNA. Nature *438*, 57-61.

Bressan, D. A., Baxter, B. K., and Petrini, J. H. (1999). The Mre11-Rad50-Xrs2 protein complex facilitates homologous recombination-based double-strand break repair in *Saccharomyces cerevisiae*. Mol Cell Biol *19*, 7681-7687.

Bugreev, D. V., Mazina, O. M., and Mazin, A. V. (2006). Rad54 protein promotes branch migration of Holliday junctions. Nature *442*, 590-593.

Bunch, J. T., Bae, N. S., Leonardi, J., and Baumann, P. (2005). Distinct requirements for Pot1 in limiting telomere length and maintaining chromosome stability. Mol Cell Biol *25*, 5567-5578.

Calsou, P., Frit, P., Humbert, O., Muller, C., Chen, D. J., and Salles, B. (1999). The DNA-dependent protein kinase catalytic activity regulates DNA end processing by means of Ku entry into DNA. J Biol Chem *274*, 7848-7856.

Carney, J. P., Maser, R. S., Olivares, H., Davis, E. M., Le Beau, M., Yates, J. R. 3rd., Hays, L., Morgan, W. F., Petrini, J. H. (1998). The hMre11/hRad50 protein complex and Nijmegen breakage syndrome: linkage of double-strand break repair to the cellular DNA damage response. Cell *93*, 477-86.

Caspari, T., Murray, J. M., Carr, A. M. (2002). Cdc2-cyclin B kinase activity links Crb2 and Rqh1-topoisomerase III. Genes Dev. *16*, 1195-208.

Catlett, M. G., and Forsburg, S. L. (2003). *Schizosaccharomyces pombe* Rdh54 (TID1) acts with Rhp54 (RAD54) to repair meiotic double-strand breaks. Mol Biol Cell *14*, 4707-4720.

Celli, G. B., Denchi, E. L., and de Lange, T. (2006). Ku70 stimulates fusion of dysfunctional telomeres yet protects chromosome ends from homologous recombination. Nat Cell Biol *8*, 885-890.

Chahwan, C., Nakamura, T. M., Sivakumar, S., Russell, P., and Rhind, N. (2003). The Fission Yeast Rad32 (Mre11)-Rad50-Nbs1 Complex Is Required for the S-Phase DNA Damage Checkpoint. Mol Cell Biol *23*, 6564-6573.

Chan, D. W., Chen, B. P., Prithivirajsingh, S., Kurimasa, A., Story, M. D., Qin, J., and Chen, D. J. (2002). Autophosphorylation of the DNA-dependent protein kinase catalytic subunit is required for rejoining of DNA double-strand breaks. Genes Dev *16*, 2333-2338.

Chan, D. W., and Lees-Miller, S. P. (1996). The DNA-dependent protein kinase is inactivated by autophosphorylation of the catalytic subunit. J Biol Chem *271*, 8936-8941.

Chan, S. W., and Blackburn, E. H. (2003). Telomerase and ATM/Tel1p protect telomeres from nonhomologous end joining. Mol Cell *11*, 1379-1387.

Chen, C., and Kolodner, R. D. (1999). Gross chromosomal rearrangements in Saccharomyces cerevisiae replication and recombination defective mutants. Nat Genet *23*, 81-85.

Chen, L., Trujillo, K., Ramos, W., Sung, P., and Tomkinson, A. E. (2001). Promotion of Dnl4-catalyzed DNA end-joining by the Rad50/Mre11/Xrs2 and Hdf1/Hdf2 complexes. Mol Cell *8*, 1105-1115.

Chen, G., Yuan, S. S., Liu, W., Xu, Y., Trujillo, K., Song, B., Cong, F., Goff, S. P., Wu, Y., Arlinghaus, R., Baltimore, D., Gasser, P. J., Park, M. S., Sung, P., Lee, E. Y. (1999). Radiation-induced assembly of Rad51 and Rad52 recombination complex requires ATM and c-Abl. J Biol Chem *274*, 12748-52.

Chlebowicz, E., and Jachymczyk, W. J. (1979). Repair of MMS-induced DNA double-strand breaks in haploid cells of Saccharomyces cerevisiae, which requires the presence of a duplicate genome. Mol Gen Genet *167*, 279-286.

Choy, J. S., and Kron, S. J. (2002). NuA4 Subunit Yng2 Function in Intra-S-Phase DNA Damage Response. Mol Cell Biol *22*, 8215-8225.

Cliby, W. A., Roberts, C. J., Cimprich, K. A., Stringer, C. M., Lamb, J. R., Schreiber, S. L., and Friend, S. H. (1998). Overexpression of a kinase-inactive ATR protein causes sensitivity to DNA-damaging agents and defects in cell cycle checkpoints. EMBO J *17*, 159-169.

Colleaux, L., D'Auriol, L., Galibert, F., and Dujon, B. (1988). Recognition and Cleavage Site of the Intron-Encoded omega Transposase. Proc Natl Acad Sci U.S.A *85*, 6022-6026.

Critchlow, S. E., and Jackson, S. P. (1998). DNA end-joining: from yeast to man. Trends Biochem Sci *23*, 394-398.

Cromie, G. A., Hyppa, R. W., Taylor, A. F., Zakharyevich, K., Hunter, N., and Smith, G. R. (2006). Single Holliday junctions are intermediates of meiotic recombination. Cell *127*, 1167-1178.

D'Amours, D., and Jackson, S. P. (2002). The Mre11 complex: at the crossroads of dna repair and checkpoint signalling. Nat Rev Mol Cell Biol *3*, 317-327.

Davis, A. P., and Symington, L. S. (2001). The yeast recombinational repair protein Rad59 interacts with Rad52 and stimulates single-strand annealing. Genetics *159*, 515-525.

Davis, A. P., and Symington, L. S. (2004). *RAD51*-dependent break-induced replication in yeast. Mol Cell Biol *24*, 2344-2351.

de Jager, M., van Noort, J., van Gent, D. C., Dekker, C., Kanaar, R., and Wyman, C. (2001). Human Rad50/Mre11 is a flexible complex that can tether DNA ends. Mol Cell *8*, 1129-1135.

de Lange, T. (2005). Shelterin: the protein complex that shapes and safeguards human telomeres 10.1101/gad.1346005. Genes Dev *19*, 2100-2110.

de la Torre-Ruiz, M., Lowndes N. F. (2000). The Saccharomyces cerevisiae DNA damage checkpoint is required for efficient repair of double strand breaks by non-homologous end joining. FEBS Lett. *467,* 311-5.

De Piccoli, G., Cortes-Ledesma, F., Ira, G., Torres-Rosell, J., Uhle, S., Farmer, S., Hwang, J.-Y., Machin, F., Ceschia, A., McAleenan, A., *et al.* (2006). Smc5-Smc6 mediate DNA double-strand-break repair by promoting sister-chromatid recombination. Nat Cell Biol *8*, 1032-1034.

Deans, B., Griffin, C. S., Maconochie, M., and Thacker, J. (2000). Xrcc2 is required for genetic stability, embryonic neurogenesis and viability in mice. EMBOJ *19*, 6675-6685.

Deininger, P. L., and Batzer, M. A. (1999). Alu repeats and human disease. Mol Genet Metab *67*, 183-193.

Diede, S. J., and Gottschling, D. E. (1999). Telomerase-mediated telomere addition in vivo requires DNA primase and DNA polymerases alpha and delta. Cell *99*, 723-733.

Doe, C. L., Dixon, J., Osman, F., and Whitby, M. C. (2000). Partial suppression of the fission yeast rqh1(-) phenotype by expression of a bacterial Holliday junction resolvase. EMBO J *19*, 2751-2762.

Doe, C. L., Osman, F., Dixon, J., and Whitby, M. C. (2004). DNA repair by a Rad22-Mus81-dependent pathway that is independent of Rhp51. Nucleic Acids Res *32*, 5570-5581.

Doe, C. L., and Whitby, M. C. (2004). The involvement of Srs2 in post-replication repair and homologous recombination in fission yeast. Nucl Acids Res *32*, 1480-1491.

Dudas, A., and Chovanec, M. (2004). DNA double-strand break repair by homologous recombination. Mutat Res *566*, 131-167.

Dunham, M. A., Neumann, A. A., Fasching, C. L., and Reddel, R. R. (2000). Telomere maintenance by recombination in human cells. Nat Genet *26*, 447-450.

Dunn, B., Szauter, P., Pardue, M. L., and Szostak, J. W. (1984). Transfer of yeast telomeres to linear plasmids by recombination. Cell *39*, 191-201.

Eisen, J. A., Sweder, K. S., and Hanawalt, P. C. (1995). Evolution of the SNF2 family of proteins: subfamilies with distinct sequences and functions. Nucleic Acids Res *23*, 2715-2723.

Ellis, N. A., Groden, J., Ye, T. Z., Straughen, J., Lennon, D. J., Ciocci, S., Proytcheva, M., German, J. (1995). The Bloom's syndrome gene product is homologous to RecQ helicases. Cell *83*,655-66.

Esashi, F., Christ, N., Gannon, J., Liu, Y., Hunt, T., Jasin, M., and West, S. C. (2005). CDK-dependent phosphorylation of BRCA2 as a regulatory mechanism for recombinational repair. *434*, 598-604.

Esashi, F., Galkin, V. E., Yu, X., Egelman, E. H., and West, S. C. (2007). Stabilization of RAD51 nucleoprotein filaments by the C-terminal region of BRCA2. Nature *14*, 468-474.

Essers, J., Hendriks, R. W., Swagemakers, S. M., Troelstra, C., de Wit, J., Bootsma, D., Hoeijmakers, J. H., and Kanaar, R. (1997). Disruption of mouse *RAD54* reduces ionizing radiation resistance and homologous recombination. Cell *89*, 195-204.

Evans, S. K., and Lundblad, V. (1999). Est1 and Cdc13 as comediators of telomerase access. Science *286*, 117-120.

Falck, J., Coates, J., and Jackson, S. P. (2005). Conserved modes of recruitment of ATM, ATR and DNA-PKcs to sites of DNA damage. Nature *434*, 605-611.

Feng, J., Funk, W. D., Wang, S. S., Weinrich, S. L., Avilion, A. A., Chiu, C. P., Adams, R. R., Chang, E., Allsopp, R. C., Yu, J., and et al. (1995). The RNA component of human telomerase. Science *269*, 1236-1241.

Fiorentini, P., Huang, K., Tishkoff, D., Kolodner, R., and Symington, L. (1997). Exonuclease I of Saccharomyces cerevisiae functions in mitotic recombination in vivo and in vitro. Mol Cell Biol *17*, 2764-2773.

Firmenich, A. A., Elias-Arnanz, M., and Berg, P. (1995). A novel allele of *Saccharomyces cerevisiae RFA1* that is deficient in recombination and repair and suppressible by *RAD52*. Mol Cell Biol *15*, 1620-1631.

Flint, J., Craddock, C. F., Villegas, A., Bentley, D. P., Williams, H. J., Galanello, R., Cao, A., Wood, W. G., Ayyub, H., and Higgs, D. R. (1994). Healing of broken human chromosomes by the addition of telomeric repeats. Am J Hum Genet *55*, 505-512.

Formosa, T., and Alberts, B. M. (1986). DNA synthesis dependent on genetic recombination: characterization of a reaction catalyzed by purified bacteriophage T4 proteins. Cell *47*, 793-806.

Forney, J. D., and Blackburn, E. H. (1988). Developmentally controlled telomere addition in wild-type and mutant paramecia. Mol Cell Biol *8*, 251-258.

Fortin, G. S., and Symington, L. S. (2002). Mutations in yeast Rad51 that partially bypass the requirement for Rad55 and Rad57 in DNA repair by increasing the stability of Rad51-DNA complexes. EMBO J *21*, 3160-3170.

Frank-Vaillant, M., and Marcand, S. (2002). Transient stability of DNA ends allows nonhomologous end joining to precede homologous recombination. Mol Cell *10*, 1189-1199.

Futreal, P. A., Liu, Q., Shattuck-Eidens, D., Cochran, C., Harshman, K., Tavtigian, S., Bennett, L. M., Haugen-Strano, A., Swensen, J., Miki, Y., *et al.* (1994). BRCA1 mutations in primary breast and ovarian carcinomas. Science *266*, 120-2.

Gaillard, P. H., Noguchi, E., Shanahan, P., and Russell, P. (2003). The endogenous Mus81-Eme1 complex resolves Holliday junctions by a nick and counternick mechanism. Mol Cell *12*, 747-759.

Game, J. C., and Mortimer, R. K. (1974). A genetic study of x-ray sensitive mutants in yeast. Mutat Res *24*, 281-292.

Gangloff, S., Soustelle, C., and Fabre, F. (2000). Homologous recombination is responsible for cell death in the absence of the Sgs1 and Srs2 helicases. Nat Genet *25*, 192-194.

Gellert, M. (2002). V(D)J recombination: rag proteins, repair factors, and regulation. Annual Review of Biochemistry *71*, 101-132.

Golin, J. E., and Esposito, M. S. (1984). Coincident gene conversion during mitosis in saccharomyces. Genetics *107*, 355-365.

Goodhead, D. T. (1994). Initial Events in the Cellular Effects of Ionizing Radiations: Clustered Damage in DNA. International Journal of Radiation Biology *65*, 7-17.

Goudsouzian, L. K., Tuzon, C. T., and Zakian, V. A. (2006). *S. cerevisiae* Tel1p and Mre11p are required for normal levels of Est1p and Est2p telomere association. Mol Cell *24*, 603-610.

Gravel, S., and Wellinger, R. J. (2002). Maintenance of double-stranded telomeric repeats as the critical determinant for cell viability in yeast cells lacking Ku. Mol Cell Biol *22*, 2182-2193.

Greider, C. W., and Blackburn, E. H. (1985). Identification of a specific telomere terminal transferase activity in Tetrahymena extracts. Cell *43*, 405-413.

Griffith, J. D., Comeau, L., Rosenfield, S., Stansel, R. M., Bianchi, A., Moss, H., and de Lange, T. (1999). Mammalian telomeres end in a large duplex loop. Cell *97*, 503-514.

Griffiths, D. J., Barbet, N. C., McCready, S., Lehmann, A. R., Carr, A. M. (1995). Fission yeast rad17: a homologue of budding yeast RAD24 that shares regions of sequence similarity with DNA polymerase accessory proteins. EMBO J. *14*, 5812-23.

Gu, Y., Jin, S., Gao, Y., Weaver, D. T., and Alt, F. W. (1997). Ku70-deficient embryonic stem cells have increased ionizing radiosensitivity, defective DNA end-binding activity, and inability to support V(D)J recombination. Proc Natl Acad Sci U.S.A. *94*, 8076-8081.

Haber, J. E. (1998). Mating-type gene switching in *saccharomyces cerevisiae.* Annual Review of Genetics *32*, 561-599.

Harrington, L. (2004). Those dam-aged telomeres! Curr Opin Genet Dev *14*, 22-28.

Hartsuiker, E., Vaessen, E., Carr, A. M., and Kohli, J. (2001). Fission yeast Rad50 stimulates sister chromatid recombination and links cohesion with repair. EMBO J *20*, 6660-6671.

Hayatu Raji, E. H. (2006). Double-strand break repair and homologous recombination in *Schizosaccharomyces pombe.* Yeast *23*, 963-976.

Hays, S. L., Firmenich, A. A., and Berg, P. (1995). Complex formation in yeast double-strand break repair: participation of Rad51, Rad52, Rad55, and Rad57 proteins. Proc Natl Acad Sci U.S.A. *92*, 6925-6929.

Hefferin, M. L., and Tomkinson, A. E. (2005). Mechanism of DNA double-strand break repair by non-homologous end joining. DNA Repair (Amst) *4*, 639-648.

Herrmann, G., Lindahl, T., and Schar, P. (1998). Saccharomyces cerevisiae LIF1: a function involved in DNA double-strand break repair related to mammalian XRCC4. EMBO J *17*, 4188-4198.

Herzberg, K., Bashkirov, V. I., Rolfsmeier, M., Haghnazari, E., McDonald, W. H., Anderson, S., Bashkirova, E. V., Yates, J. R. 3rd, Heyer, W. D. (2006). Phosphorylation of Rad55 on serines 2, 8, and 14 is required for efficient homologous recombination in the recovery of stalled replication forks. Mol Cell Biol. *26*, 8396-409.

Heyer, W. D., Rao, M. R., Erdile, L. F., Kelly, T. J., and Kolodner, R. D. (1990). An essential Saccharomyces cerevisiae single-stranded DNA binding protein is homologous to the large subunit of human RP-A. EMBOJ *9*, 2321-2329.

Hiraoka, M., Watanabe, K.-i., Umezu, K., and Maki, H. (2000). Spontaneous Loss of Heterozygosity in Diploid Saccharomyces cerevisiae Cells. Genetics *156*, 1531-1548.

Hope, J. C., Maftahi, M., and Freyer, G. A. (2005). A postsynaptic role for Rhp55/57 that is responsible for cell death in Deltarqh1 mutants following replication arrest in Schizosaccharomyces pombe. Genetics *170*, 519-531.

Hopfner, K. P., Craig, L., Moncalian, G., Zinkel, R. A., Usui, T., Owen, B. A., Karcher, A., Henderson, B., Bodmer, J. L., McMurray, C. T., *et al.* (2002). The Rad50 zinc-hook is a structure joining Mre11 complexes in DNA recombination and repair. Nature *418*, 562-566.

Hopfner, K. P., Karcher, A., Craig, L., Woo, T. T., Carney, J. P., and Tainer, J. A. (2001). Structural biochemistry and interaction architecture of the DNA double-strand break repair Mre11 nuclease and Rad50-ATPase. Cell *105*, 473-485.

Hsiang, Y., Hertzberg, R., Hecht, S., and Liu, L. (1985). Camptothecin induces protein-linked DNA breaks via mammalian DNA topoisomerase I. J Biol Chem *260*, 14873-14878.

Hsiang, Y.-H., Lihou, M. G., and Liu, L. F. (1989). Arrest of Replication Forks by Drug-stabilized Topoisomerase I-DNA Cleavable Complexes as a Mechanism of Cell Killing by Camptothecin. Cancer Res *49*, 5077-5082.

Hsiang, Y.-H., and Liu, L. F. (1988). Identification of Mammalian DNA Topoisomerase I as an Intracellular Target of the Anticancer Drug Camptothecin. Cancer Res *48*, 1722-1726.

Huang, J., and Dynan, W. S. (2002). Reconstitution of the mammalian DNA double-strand break end-joining reaction reveals a requirement for an Mre11/Rad50/NBS1-containing fraction. Nucleic Acids Res *30*, 667-674.

Hughes, T. R., Evans, S. K., Weilbaecher, R. G., and Lundblad, V. (2000). The Est3 protein is a subunit of yeast telomerase. Curr Biol *10*, 809-812.

Hussey, S. P. (2003). Investigating the mechanisms of DNA double-strand break repair and loss of heterozygosity in fission yeast. D. Phil Thesis. Wolfson College. University of Oxford.

Iijima, K., Komatsu, K., Matsuura, S., and Tauchi, H. (2004). The Nijmegen breakage syndrome gene and its role in genome stability. Chromosoma *113*, 53-61.

Inbar, O., and Kupiec, M. (1999). Homology Search and Choice of Homologous Partner during Mitotic Recombination. Mol Cell Biol *19*, 4134-4142.

Inbar, O., Liefshitz, B., Bitan, G., and Kupiec, M. (2000). The Relationship between Homology Length and Crossing Over during the Repair of a Broken Chromosome. J Biol Chem *275*, 30833-30838.

Ira, G., Malkova, A., Liberi, G., Foiani, M., and Haber, J. E. (2003). Srs2 and Sgs1-Top3 suppress crossovers during double-strand break repair in yeast. Cell *115*, 401-411.

Ira, G., Pellicioli, A., Balijja, A., Wang, X., Fiorani, S., Carotenuto, W., Liberi, G., Bressan, D., Wan, L., Hollingsworth, N. M., *et al.* (2004). DNA end resection, homologous recombination and DNA damage checkpoint activation require CDK1. Nature *431*, 1011-1017.

Ira, G., Satory, D., and Haber, J. E. (2006). Conservative Inheritance of Newly Synthesized DNA in Double-Strand Break-Induced Gene Conversion. Mol Cell Biol *26*, 9424-9429.

Ivanov, E., and Haber, J. (1995). RAD1 and RAD10, but not other excision repair genes, are required for double-strand break-induced recombination in Saccharomyces cerevisiae. Mol Cell Biol *15*, 2245-2251.

Ivanov, E. L., Sugawara, N., White, C. I., Fabre, F., and Haber, J. E. (1994). Mutations in XRS2 and RAD50 delay but do not prevent mating-type switching in Saccharomyces cerevisiae. Mol Cell Biol *14*, 3414-3425.

Jaco, I., Munoz, P., Goytisolo, F., Wesoly, J., Bailey, S., Taccioli, G., and Blasco, M. A. (2003). Role of mammalian Rad54 in telomere length maintenance. Mol Cell Biol *23*, 5572-5580.

Jasin, M. (2000). LOH and mitotic recombination. In DNA alterations in Cancer, M. Ehrlich, ed. (Natick, MA, USA, Eaton Publishing), pp. 191-209.

Jeggo, P. A. (1990). Studies on mammalian mutants defective in rejoining double-strand breaks in DNA. Mutat Res *239*, 1-16.

Jeggo, P. A. (1997). DNA-PK: at the cross-roads of biochemistry and genetics. Mutat Res *384*, 1-14.

Jeggo, P. A. (1998). DNA breakage and repair. Adv Genet *38*, 185-218.

Johnson, R. D., and Jasin, M. (2001). Double-strand-break-induced homologous recombination in mammalian cells. Biochem Soc Trans *29*, 196-201.

Johnson, R. D., Liu, N., and Jasin, M. (1999). Mammalian XRCC2 promotes the repair of DNA double-strand breaks by homologous recombination. *401*, 397-399.

Johnson, R. D., and Symington, L. S. (1995). Functional differences and interactions among the putative RecA homologs Rad51, Rad55, and Rad57. Mol Cell Biol *15*, 4843-4850.

Kadyk, L. C., Hartwell, L. H. (1992) Sister chromatids are preffered over homologs as substrates for recombinational repair in *S. cerevisiae*. Genetics *132*

Kagawa, W., Kurumizaka, H., Ikawa, S., Yokoyama, S., and Shibata, T. (2001). Homologous pairing promoted by the human Rad52 protein. J Biol Chem *276*, 35201-35208.

Kai, M., Boddy, M. N., Russell, P., and Wang, T. S.-F. (2005). Replication checkpoint kinase Cds1 regulates Mus81 to preserve genome integrity during replication stress 10.1101/gad.1304305. Genes Dev *19*, 919-932.

Kanaar, R., Hoeijmakers, J. H., and van Gent, D. C. (1998). Molecular mechanisms of DNA double strand break repair. Trends Cell Biol *8*, 483-489.

Kans, J. A., and Mortimer, R. K. (1991). Nucleotide sequence of the RAD57 gene of Saccharomyces cerevisiae. Gene *105*, 139-140.

Karow, J. K., Wu, L., and Hickson, I. D. (2000). RecQ family helicases: roles in cancer and aging. Curr Opin Genet Dev *10*, 32-38.

Kaye, J. A., Melo, J. A., Cheung, S. K., Vaze, M. B., Haber, J. E., and Toczyski, D. P. (2004). DNA breaks promote genomic instability by impeding proper chromosome segregation. Curr Biol *14*, 2096-2106.

Khanna, K. K., and Jackson, S. P. (2001). DNA double-strand breaks: signaling, repair and the cancer connection. Nat Genet *27*, 247-254.

Khasanov, F. K., Salakhova, A. F., Chepurnaja, O. V., Korolev, V. G., and Bashkirov, V. I. (2004). Identification and characterization of the rlp1+, the novel Rad51 paralog in the fission yeast Schizosaccharomyces pombe. DNA Repair (Amst) *3*, 1363-1374.

Khasanov, F. K., Savchenko, G. V., Bashkirova, E. V., Korolev, V. G., Heyer, W.-D., and Bashkirov, V. I. (1999). A New Recombinational DNA Repair Gene From Schizosaccharomyces pombe With Homology to Escherichia coli RecA. Genetics *152*, 1557-1572.

Kinzler, K. W., and Vogelstein, B. (1997). Cancer-susceptibility genes. Gatekeepers and caretakers. Nature *386*, 761, 763.

Kitao, S., Shimamoto, A., Goto, M., Miller, R. W., Smithson, W. A., Lindor, N. M., Furuichi, Y. (1999). Mutations in RECQL4 cause a subset of cases of Rothmund-Thomson syndrome. Nat Genet *22*, 82-4.

Klein, H. L. (1997). RDH54, a RAD54 homologue in Saccharomyces cerevisiae, is required for mitotic diploid-specific recombination and repair and for meiosis. Genetics *147*, 1533-1543.

Knudson, A. G. (1993). Antioncogenes and human cancer. Proc Natl Acad Sci U.S.A. *90*, 10914-10921.

Knudson, A. G., Jr. (1971). Mutation and cancer: statistical study of retinoblastoma. Proc Natl Acad Sci U S A *68*, 820-823.

Kobayashi, J., Antoccia, A., Tauchi, H., Matsuura, S., and Komatsu, K. (2004). NBS1 and its functional role in the DNA damage response. DNA Repair (Amst) *3*, 855-861.

Kolodner, R. D., Putnam, C. D., and Myung, K. (2002). Maintenance of genome stability in Saccharomyces cerevisiae. Science *297*, 552-557.

Kramer, K. M., and Haber, J. E. (1993). New telomeres in yeast are initiated with a highly selected subset of TG1-3 repeats. Genes Dev *7*, 2345-2356.

Krejci, L., Song, B., Bussen, W., Rothstein, R., Mortensen, U. H., and Sung, P. (2002). Interaction with Rad51 is indispensable for recombination mediator function of Rad52. J Biol Chem *277*, 40132-40141.

Krejci, L., Van Komen, S., Li, Y., Villemain, J., Reddy, M. S., Klein, H., Ellenberger, T., and Sung, P. (2003). DNA helicase Srs2 disrupts the Rad51 presynaptic filament. Nature *423*, 305-309.

Krishna, S., Wagener, B. M., Liu, H. P., Lo, Y. C., Sterk, R., Petrini, J. H., and Nickoloff, J. A. (2007). Mre11 and Ku regulation of double-strand break repair by gene conversion and break-induced replication. DNA Repair (Amst) *6*, 797-808.

Krogh, B. O., and Symington, L. S. (2004). Recombination proteins in yeast. Annu Rev Genet *38*, 233-271.

Kuhne, C., Tjornhammar, M. L., Pongor, S., Banks, L., and Simoncsits, A. (2003). Repair of a minimal DNA double-strand break by NHEJ requires DNA-PKcs and is controlled by the ATM/ATR checkpoint. Nucleic Acids Res *31*, 7227-7237.

Larrivee, M., LeBel, C., and Wellinger, R. J. (2004). The generation of proper constitutive G-tails on yeast telomeres is dependent on the MRX complex. Genes Dev *18*, 1391-1396.

Lasko, D., Cavenee, W., and Nordenskjold, M. (1991). Loss of Constitutional Heterozygosity in Human Cancer. Annual Review of Genetics *25*, 281-314.

Lavin, M. F., and Shiloh, Y. (1997). The genetic defect in ataxia-telangiectasia. Annu Rev Immunol *15*, 177-202.

Le, S., Moore, J. K., Haber, J. E., and Greider, C. W. (1999). RAD50 and RAD51 define two pathways that collaborate to maintain telomeres in the absence of telomerase. Genetics *152*, 143-152.

LeBel, C., and Wellinger, R. J. (2005). Telomeres: what's new at your end? J Cell Sci *118*, 2785-2788.

Lee, K. J., Huang, J., Takeda, Y., and Dynan, W. S. (2000). DNA ligase IV and XRCC4 form a stable mixed tetramer that functions synergistically with other repair factors in a cell-free end-joining system. J Biol Chem *275*, 34787-34796.

Lee, M. S., Gallagher, R. C., Bradley, J., and Blackburn, E. H. (1993). In vivo and in vitro studies of telomeres and telomerase. Cold Spring Harb Symp Quant Biol *58*, 707-718.

Lee, S. E., Bressan, D. A., Petrini, J. H., and Haber, J. E. (2002). Complementation between N-terminal Saccharomyces cerevisiae mre11 alleles in DNA repair and telomere length maintenance. DNA Repair (Amst) *1*, 27-40.

Lee, S. E., Mitchell, R. A., Cheng, A., and Hendrickson, E. A. (1997). Evidence for DNA-PK-dependent and -independent DNA double-strand break repair pathways in mammalian cells as a function of the cell cycle. Mol Cell Biol *17*, 1425-1433.

Lee, S. E., Moore, J. K., Holmes, A., Umezu, K., Kolodner, R. D., and Haber, J. E. (1998). Saccharomyces Ku70, mre11/rad50 and RPA proteins regulate adaptation to G2/M arrest after DNA damage. Cell *94*, 399-409.

Lemoine, F. J., Degtyareva, N. P., Lobachev, K., and Petes, T. D. (2005). Chromosomal translocations in yeast induced by low levels of DNA polymerase a model for chromosome fragile sites. Cell *120*, 587-598.

Lendvay, T. S., Morris, D. K., Sah, J., Balasubramanian, B., and Lundblad, V. (1996). Senescence mutants of Saccharomyces cerevisiae with a defect in telomere replication identify three additional EST genes. Genetics *144*, 1399-1412.

Lengauer, C., Kinzler, K. W., and Vogelstein, B. (1998). Genetic instabilities in human cancers. Nature *396*, 643-649.

Lettier, G. l., Feng, Q., de Mayolo, A. A. n., Erdeniz, N., Reid, R. J. D., Lisby, M., Mortensen, U. H., and Rothstein, R. (2006). The Role of DNA Double-Strand Breaks in Spontaneous Homologous Recombination in S. cerevisiae. PLoS Genetics *2*, e194.

Leupold, U., and Gutz, H. (1964). *Genetics Today: Proceedings of the XIth International Congress on Genetics* (The Hague, The Netherlands, Pergamon Press, Oxford, U.K.).

Lewis, L. K., Karthikeyan, G., Westmoreland, J. W., and Resnick, M. A. (2002). Differential Suppression of DNA Repair Deficiencies of Yeast rad50, mre11 and xrs2 Mutants by EXO1 and TLC1 (the RNA Component of Telomerase). Genetics *160*, 49-62.

Lewis, L. K., Kirchner, J. M., and Resnick, M. A. (1998). Requirement for End-Joining and Checkpoint Functions, but Not RAD52-Mediated Recombination, after EcoRI Endonuclease Cleavage of Saccharomyces cerevisiae DNA. Mol Cell Biol *18*, 1891-1902.

Liang, F., Han, M., Romanienko, P. J., and Jasin, M. (1998a). Homology-directed repair is a major double-strand break repair pathway in mammalian cells. Proc Natl Acad Sci U.S.A. *95*, 5172-5177.

Liang, F., Han, M., Romanienko, P. J., and Jasin, M. (1998b). Homology-directed repair is a major double-strand break repair pathway in mammalian cells. Proc Natl Acad Sci U.S.A *95*, 5172-5177.

Lindsay, H. D., Griffiths, D. J. F., Edwards, R. J., Christensen, P. U., Murray, J. M., Osman, F., Walworth, N., and Carr, A. M. (1998). S-phase-specific activation of Cds1 kinase defines a subpathway of the checkpoint response in *Schizosaccharomyces pombe*. Genes Dev *12*, 382-395.

Lingner, J., Cech, T. R., Hughes, T. R., and Lundblad, V. (1997a). Three Ever Shorter Telomere (EST) genes are dispensable for in vitro yeast telomerase activity. Proc Natl Acad Sci U.S.A. *94*, 11190-11195.

Lingner, J., Hughes, T. R., Shevchenko, A., Mann, M., Lundblad, V., and Cech, T. R. (1997b). Reverse transcriptase motifs in the catalytic subunit of telomerase. Science *276*, 561-567.

Lisby, M., Barlow, J. H., Burgess, R. C., and Rothstein, R. (2004). Choreography of the DNA damage response: spatiotemporal relationships among checkpoint and repair proteins. Cell *118*, 699-713.

Liu, T. X., Becker, M. W., Jelinek, J., Wu, W.-S., Deng, M., Mikhalkevich, N., Hsu, K., Bloomfield, C. D., Stone, R. M., DeAngelo, D. J., *et al.* (2007). Chromosome 5q deletion and epigenetic suppression of the gene encoding [alpha]-catenin (CTNNA1) in myeloid cell transformation. Nat Med *13*, 78-83.

Liu, Y., Masson, J. Y., Shah, R., O'Regan, P., and West, S. C. (2004). RAD51C is required for Holliday junction processing in mammalian cells. Science *303*, 243-246.

Llorente, B., and Symington, L. S. (2004). The Mre11 Nuclease Is Not Required for 5' to 3' Resection at Multiple HO-Induced Double-Strand Breaks. Mol Cell Biol *24*, 9682-9694.

Loayza, D., and de Lange, T. (2004). Telomerase regulation at the telomere: a binary switch. Cell *117*, 279-280.

Lobachev, K., Vitriol, E., Stemple, J., Resnick, M. A., and Bloom, K. (2004). Chromosome fragmentation after induction of a double-strand break is an active process prevented by the RMX repair complex. Curr Biol *14*, 2107-2112.

Loeb, L. A. (2001). A Mutator Phenotype in Cancer. Cancer Res *61*, 3230-3239.

Lorenz, A., and Whitby, M. C. (2006). Crossover promotion and prevention. Biochem Soc Trans *34*, 537-541.

Louis, E. J. (1995). The chromosome ends of *Saccharomyces cerevisiae*. Yeast *11*, 1553-1573.

Lovett, S. T. (1994). Sequence of the RAD55 gene of *Saccharomyces cerevisiae*: similarity of RAD55 to prokaryotic RecA and other RecA-like proteins. Gene *142*, 103-106.

Lundblad, V., and Blackburn, E. H. (1993). An alternative pathway for yeast telomere maintenance rescues est1- senescence. Cell *73*, 347-360.

Lundin, C., North, M., Erixon, K., Walters, K., Jenssen, D., Goldman, A. S. H., and Helleday, T. (2005). Methyl methanesulfonate (MMS) produces heat-labile DNA damage but no detectable in vivo DNA double-strand breaks. Nucl Acids Res *33*, 3799-3811.

Lydall, D. (2003). Hiding at the ends of yeast chromosomes: telomeres, nucleases and checkpoint pathways. J Cell Sci *116*, 4057-4065.

Lydall, D., Weinert, T. (1995). Yeast checkpoint genes in DNA damage processing: implications for repair and arrest. Science. *270*, 1488-91.

Malkova, A., Ivanov, E. L., and Haber, J. E. (1996). Double-strand break repair in the absence of RAD51 in yeast: a possible role for break-induced DNA replication. Proc Natl Acad Sci U S A *93*, 7131-7136.

Malkova, A., Naylor, M. L., Yamaguchi, M., Ira, G., and Haber, J. E. (2005). RAD51-Dependent Break-Induced Replication Differs in Kinetics and Checkpoint Responses from RAD51-Mediated Gene Conversion. Mol Cell Biol *25*, 933-944.

Malkova, A., Signon, L., Schaefer, C. B., Naylor, M. L., Theis, J. F., Newlon, C. S., and Haber, J. E. (2001). RAD51-independent break-induced replication to repair a broken chromosome depends on a distant enhancer site. Genes Dev *15*, 1055-1060.

Mangahas, J. L., Alexander, M. K., Sandell, L. L., and Zakian, V. A. (2001). Repair of chromosome ends after telomere loss in Saccharomyces. Mol Biol Cell *12*, 4078-4089.

Manolis, K. G., Nimmo, E. R., Hartsuiker, E., Carr, A. M., Jeggo, P. A., and Allshire, R. C. (2001). Novel functional requirements for non-homologous DNA end joining in *Schizosaccharomyces pombe*. EMBOJ *20*, 210-221.

Martin, S. G., Laroche, T., Suka, N., Grunstein, M., and Gasser, S. M. (1999). Relocalization of telomeric Ku and SIR proteins in response to DNA strand breaks in yeast. Cell *97*, 621-633.

Martin, V., Chahwan, C., Gao, H., Blais, V., Wohlschlegel, J., Yates, J. R., 3rd, McGowan, C. H., and Russell, P. (2006). Sws1 is a conserved regulator of homologous recombination in eukaryotic cells. EMBOJ *25*, 2564-2574.

Matsumoto, T., Fukui, K., Niwa, O., Sugawara, N., Szostak, J. W., and Yanagida, M. (1987). Identification of healed terminal DNA fragments in linear minichromosomes of Schizosaccharomyces pombe. Mol Cell Biol *7*, 4424-4430.

Matsuura, S., Tauchi, H., Nakamura, A., Kondo, N., Sakamoto, S., Endo, S., Smeets, D., Solder, B., Belohradsky, B. H., Der Kaloustian, V. M., *et al.* (1998). Positional cloning of the gene for Nijmegen breakage syndrome. Nat Genet *19*, 179-181.

Maundrell, K. (1993). Thiamine-repressible expression vectors pREP and pRIP for fission yeast. Gene *123*, 127-130.

Mazin, A. V., Alexeev, A. A., and Kowalczykowski, S. C. (2003). A novel function of Rad54 protein. Stabilization of the Rad51 nucleoprotein filament. J Biol Chem *278*, 14029-14036.

Mazin, A. V., Bornarth, C. J., Solinger, J. A., Heyer, W. D., and Kowalczykowski, S. C. (2000a). Rad54 protein is targeted to pairing loci by the Rad51 nucleoprotein filament. Mol Cell *6*, 583-592.

Mazin, A. V., Zaitseva, E., Sung, P., and Kowalczykowski, S. C. (2000b). Tailed duplex DNA is the preferred substrate for Rad51 protein-mediated homologous pairing. EMBOJ *19*, 1148-1156.

Mazina, O. M., and Mazin, A. V. (2004). Human Rad54 protein stimulates DNA strand exchange activity of hRad51 protein in the presence of Ca2+. J Biol Chem *279*, 52042-52051.

McEachern, M. J., and Haber, J. E. (2006). Break-induced replication and recombinational telomere elongation in yeast. Annual Review of Biochemistry *75*, 111-135.

McGill, C., Shafer, B., and Strathern, J. (1989). Coconversion of flanking sequences with homothallic switching. Cell *57*, 459-467.

McGlynn, P., and Lloyd, R. G. (2002). Recombinational repair and restart of damaged replication forks. Nat Rev Mol Cell Biol *3*, 859-870.

Melo, J., and Toczyski, D. (2002). A unified view of the DNA-damage checkpoint. Curr Opin Cell Biol *14*, 237-245.

Mendenhall, M. D., and Hodge, A. E. (1998). Regulation of Cdc28 Cyclin-Dependent Protein Kinase Activity during the Cell Cycle of the Yeast *Saccharomyces cerevisiae*. Microbiol Mol Biol Rev *62*, 1191-1243.

Meyerson, M., Counter, C. M., Eaton, E. N., Ellisen, L. W., Steiner, P., Caddle, S. D., Ziaugra, L., Beijersbergen, R. L., Davidoff, M. J., Liu, Q., *et al.* (1997). hEST2, the putative human telomerase catalytic subunit gene, is up-regulated in tumor cells and during immortalization. Cell *90*, 785-795.

Mills, K. D., Sinclair, D. A., and Guarente, L. (1999). MEC1-dependent redistribution of the Sir3 silencing protein from telomeres to DNA double-strand breaks. Cell *97*, 609-620.

Miyazaki, T., Bressan, D. A., Shinohara, M., Haber, J. E., and Shinohara, A. (2004). In vivo assembly and disassembly of Rad51 and Rad52 complexes during double-strand break repair. EMBOJ *23*, 939-949.

Mohaghegh, P., Hickson, I. D. DNA helicase deficiencies associated with cancer predisposition and premature ageing disorders. (2001). Hum Mol Genet *10*, 741-6.

Moreau, S., Ferguson, J. R., and Symington, L. S. (1999). The nuclease activity of Mre11 is required for meiosis but not for mating type switching, end joining, or telomere maintenance. Mol Cell Biol *19*, 556-566.

Moreau, S., Morgan, E. A., and Symington, L. S. (2001). Overlapping Functions of the Saccharomyces cerevisiae Mre11, Exo1 and Rad27 Nucleases in DNA Metabolism. Genetics *159*, 1423-1433.

Moreno, S., Klar, A., and Nurse, P. (1991). Molecular genetic analysis of fission yeast *Schizosaccharomyces pombe*. Methods Enzymol *194*, 795-823.

Morgan, W. F., Day, J. P., Kaplan, M. I., McGhee, E. M., and Limoli, C. L. (1996). Genomic instability induced by ionizing radiation. Radiat Res *146*, 247-258.

Morrow, D. M., Connelly, C., and Hieter, P. (1997). "Break copy" duplication: a model for chromosome fragment formation in Saccharomyces cerevisiae. Genetics *147*, 371-382.

Mortensen, U. H., Bendixen, C., Sunjevaric, I., and Rothstein, R. (1996). DNA strand annealing is promoted by the yeast Rad52 protein. Proc Natl Acad Sci U.S.A. *93*, 10729-10734.

Moshous, D., Callebaut, I., de Chasseval, R., Corneo, B., Cavazzana-Calvo, M., Le Deist, F., Tezcan, I., Sanal, O., Bertrand, Y., Philippe, N., *et al.* (2001). Artemis, a novel DNA double-strand break repair/V(D)J recombination protein, is mutated in human severe combined immune deficiency. Cell *105*, 177-186.

Moynahan, M. E., and Jasin, M. (1997). Loss of heterozygosity induced by a chromosomal double-strand break. Proc Natl Acad Sci U.S.A *94*, 8988-8993.

Muris, D. F., Vreeken, K., Carr, A. M., Murray, J. M., Smit, C., Lohman, P. H., and Pastink, A. (1996). Isolation of the *Schizosaccharomyces pombe RAD54* homologue, *rhp54+*, a gene involved in the repair of radiation damage and replication fidelity. J Cell Sci *109 ( Pt 1)*, 73-81.

Muris, D. F., Vreeken, K., Schmidt, H., Ostermann, K., Clever, B., Lohman, P. H., and Pastink, A. (1997). Homologous recombination in the fission yeast Schizosaccharomyces pombe: different requirements for the *rhp51+*, *rhp54+* and *rad22+* genes. Curr Genet *31*, 248-254.

Muris, D. F. R., vreeken, K., Carr, A. M., Broghton, B. C., Lehmann, A. R., Lohman, P. H. M., and Pastink, A. (1993). Cloning the *RAD51* homologue of *Schizosaccharomyces* pombe. Nucl Acids Res *21*, 4586-4591.

Myung, K., Chen, C., and Kolodner, R. D. (2001). Multiple pathways cooperate in the suppression of genome instability in *Saccharomyces cerevisiae*. Nature *411*, 1073-1076.

Myung, K., and Kolodner, R. D. (2003). Induction of genome instability by DNA damage in *Saccharomyces cerevisiae*. DNA Repair (Amst) *2*, 243-258.

Nadège Presneau, K. D., Vince Forgetta, Diane Provencher, Anne-Marie Mes-Masson, Patricia N. Tonin, (2005). Loss of heterozygosity and transcriptome analyses of a 1.2 Mb candidate ovarian cancer tumor suppressor locus region at 17q25.1-q25.2. Molecular Carcinogenesis *43*, 141-154.

Naito, T., Matsuura, A., and Ishikawa, F. (1998). Circular chromosome formation in a fission yeast mutant defective in two ATM homologues. Nat Genet *20*, 203-206.

Nakamura, T. M., Morin, G. B., Chapman, K. B., Weinrich, S. L., Andrews, W. H., Lingner, J., Harley, C. B., and Cech, T. R. (1997). Telomerase Catalytic Subunit Homologs from Fission Yeast and Human Science *277*, 955-959.

Niwa, O., Matsumoto, T., and Yanagida, M. (1986). Construction of a mini-chromosome by deletion and its mitotic and meiotic behaviour in fission yeast. Molecular and General Genetics *203*, 397-405.

Nussenzweig, A., Sokol, K., Burgman, P., Li, L., and Li, G. C. (1997). Hypersensitivity of Ku80-deficient cell lines and mice to DNA damage: the effects of ionizing radiation on growth, survival, and development. Proc Natl Acad Sci U.S.A. *94*, 13588-13593.

Obaya, A. J., and Sedivy, J. M. (2002). Regulation of cyclin-Cdk activity in mammalian cells. Cell Mol Life Sci *59*, 126-142.

Olive, P. L. (1998). The role of DNA single- and double-strand breaks in cell killing by ionizing radiation. Radiat Res *150*, S42-S51.

Ono, Y., Tomita, K., Matsuura, A., Nakagawa, T., Masukata, H., Uritani, M., Ushimaru, T., and Ueno, M. (2003). A novel allele of fission yeast rad11 that causes defects in DNA repair and telomere length regulation. Nucleic Acids Res *31*, 7141-7149.

Onoda, F., Seki, M., Miyajima, A., and Enomoto, T. (2001). Involvement of SGS1 in DNA damage-induced heteroallelic recombination that requires RAD52 in Saccharomyces cerevisiae. Mol Gen Genet *264*, 702-708.

Orren, D. K., Theodore, S., and Machwe, A. (2002). The Werner syndrome helicase/exonuclease (WRN) disrupts and degrades D-loops in vitro. Biochemistry *41*, 13483-13488.

Osman, F., Dixon, J., Barr, A. R., and Whitby, M. C. (2005). The F-Box DNA Helicase Fbh1 Prevents Rhp51-Dependent Recombination without Mediator Proteins. Mol Cell Biol *25*, 8084-8096.

Osman, F., Dixon, J., Doe, C. L., and Whitby, M. C. (2003). Generating crossovers by resolution of nicked Holliday junctions: a role for Mus81-Eme1 in meiosis. Mol Cell *12*, 761-774.

Osman, F., Fortunato, E. A., and Subramani, S. (1996). Double-strand break-induced mitotic intrachromosomal recombination in the fission yeast *Schizosaccharomyces pombe*. Genetics *142*, 341-357.

Paffett, K. S., Clikeman, J. A., Palmer, S., and Nickoloff, J. A. (2005). Overexpression of Rad51 inhibits double-strand break-induced homologous recombination but does not affect gene conversion tract lengths. DNA Repair (Amst) *4*, 687-698.

Palladino, F., and Klein, H. L. (1992). Analysis of mitotic and meiotic defects in *Saccharomyces cerevisiae SRS2* DNA helicase mutants. Genetics *132*, 23-37.

Pandita, R. K., Sharma, G. G., Laszlo, A., Hopkins, K. M., Davey, S., Chakhparonian, M., Gupta, A., Wellinger, R. J., Zhang, J., Powell, S. N., *et al.* (2006). Mammalian Rad9 plays a role in telomere stability, S- and G2-phase-specific cell survival, and homologous recombinational repair. Mol Cell Biol *26*, 1850-1864.

Paques, F., and Haber, J. E. (1999). Multiple Pathways of Recombination Induced by Double-Strand Breaks in *Saccharomyces cerevisiae*. Microbiol Mol Biol Rev *63*, 349-404.

Parket, A., Inbar, O., and Kupiec, M. (1995). Recombination of Ty elements in yeast can be induced by a double-strand break. Genetics *140*, 67-77.

Pascucci, B., Russo, M. T., Crescenzi, M., Bignami, M., and Dogliotti, E. (2005). The accumulation of MMS-induced single strand breaks in G1 phase is recombinogenic in DNA polymerase {beta} defective mammalian cells. Nucl Acids Res *33*, 280-288.

Pennaneach, V., Putnam, C. D., and Kolodner, R. D. (2006). Chromosome healing by de novo telomere addition in *Saccharomyces cerevisiae*. Mol Microbiol *59*, 1357-1368.

Petukhova, G., Stratton, S., and Sung, P. (1998). Catalysis of homologous DNA pairing by yeast Rad51 and Rad54 proteins. Nature *393*, 91-94.

Petukhova, G., Stratton, S. A., and Sung, P. (1999a). Single strand DNA binding and annealing activities in the yeast recombination factor Rad59. J Biol Chem *274*, 33839-33842.

Petukhova, G., Van Komen, S., Vergano, S., Klein, H., and Sung, P. (1999b). Yeast Rad54 promotes Rad51-dependent homologous DNA pairing via ATP hydrolysis-driven change in DNA double helix conformation. J Biol Chem *274*, 29453-29462.

Pfeiffer, P., Thode, S., Hancke, J., Keohavong, P., and Thilly, W. G. (1994). Resolution and conservation of mismatches in DNA end joining. Mutagenesis *9*, 527-535.

Povirk, L. F. (1996). DNA damage and mutagenesis by radiomimetic DNA-cleaving agents: bleomycin, neocarzinostatin and other enediynes. Mutat Res *355*, 71-89.

Povirk, L. F., Wubker, W., Kohnlein, W., and Hutchinson, F. (1977). DNA double-strand breaks and alkali-labile bonds produced by bleomycin. Nucl Acids Res *4*, 3573-3580.

Prado, F., and Aguilera, A. (2003). Control of cross-over by single-strand DNA resection. Trends Genet *19*, 428-431.

Prince, P. R., Emond, M. J., and Monnat, R. J., Jr. (2001). Loss of Werner syndrome protein function promotes aberrant mitotic recombination. Genes Dev *15*, 933-938.

Prudden, J., Evans, J. S., Hussey, S. P., Deans, B., O'Neill, P., Thacker, J., and Humphrey, T. (2003). Pathway utilization in response to a site-specific DNA double-strand break in fission yeast. EMBO J *22*, 1419-1430.

Putnam, C. D., Pennaneach, V., and Kolodner, R. D. (2004). Chromosome healing through terminal deletions generated by de novo telomere additions in *Saccharomyces cerevisiae*. Proc Natl Acad Sci U.S.A. *101*, 13262-13267.

Qi, H., and Zakian, V. A. (2000). The *Saccharomyces* telomere-binding protein Cdc13p interacts with both the catalytic subunit of DNA polymerase alpha and the telomerase-associated est1 protein. Genes Dev *14*, 1777-1788.

Rajagopalan, H., Nowak, M. A., Vogelstein, B., and Lengauer, C. (2003). The significance of unstable chromosomes in colorectal cancer. Nat Rev Cancer *3*, 695-701.

Raji, H., and Hartsuiker, E. (2006). Double-strand break repair and homologous recombination in *Schizosaccharomyces pombe*. Yeast *23*, 963-976.

Ralf, C., Hickson, I. D., and Wu, L. (2006). The Bloom's syndrome helicase can promote the regression of a model replication fork. J Biol Chem *281*, 22839-22846.

Ranatunga, W., Jackson, D., Lloyd, J. A., Forget, A. L., Knight, K. L., and Borgstahl, G. E. (2001). Human RAD52 exhibits two modes of self-association. J Biol Chem *276*, 15876-15880.

Rapp, A., and Greulich, K. O. (2004). After double-strand break induction by UV-A, homologous recombination and nonhomologous end joining cooperate at the same DSB if both systems are available. J Cell Sci *117*, 4935-4945.

Rattray, A. J., and Symington, L. S. (1994). Use of a chromosomal inverted repeat to demonstrate that the RAD51 and RAD52 genes of *Saccharomyces cerevisiae* have different roles in mitotic recombination. Genetics *138*, 587-595.

Raveh, D., Hughes, S. H., Shafer, B. K., and Strathern, J. N. (1989). Analysis of the HO-cleaved MAT DNA intermediate generated during the mating type switch in the yeast *Saccharomyces cerevisiae*. Mol Gen Genet *220*, 33-42.

Richard L. Momparler, V. B. (2000). DNA methylation and cancer. Journal of Cellular Physiology *183*, 145-154.

Richardson, C., Horikoshi, N., and Pandita, T. K. (2004). The role of the DNA double-strand break response network in meiosis. DNA Repair (Amst) *3*, 1149-1164.

Richardson, C., Moynahan, M. E., and Jasin, M. (1998). Double-strand break repair by interchromosomal recombination: suppression of chromosomal translocations. Genes Dev *12*, 3831-3842.

Rijkers, T., Van Den Ouweland, J., Morolli, B., Rolink, A. G., Baarends, W. M., Van Sloun, P. P., Lohman, P. H., and Pastink, A. (1998). Targeted inactivation of mouse *RAD52* reduces homologous recombination but not resistance to ionizing radiation. Mol Cell Biol *18*, 6423-6429.

Santocanale, C., and Diffley, J. F. (1998). A Mec1- and Rad53-dependent checkpoint controls late-firing origins of DNA replication. Nature *395*, 615-618.

Sattler, M., and Griffin, J. D. (2001). Mechanisms of transformation by the BCR/ABL oncogene. Int J Hematol *73*, 278-291.

Savitsky, K., Bar-Shira, A., Gilad, S., Rotman, G., Ziv, Y., Vanagaite, L., Tagle, D. A., Smith, S., Uziel, T., Sfez, S., Ashkenazi, M., Pecker, I., Frydman, M., Harnik, R., Patanjali, S. R., Simmons, A., Clines, G. A., Sartiel, A., Gatti, R. A., Chessa, L., Sanal, O., Lavin, M. F., Jaspers, N. G., Taylor, A. M., Arlett, C. F., Miki, T., Weissman, S. M., Lovett, M., Collins, F. S., Shiloh, Y. (1995). A single ataxia telangiectasia gene with a product similar to PI-3 kinase. Science *268*, 1700-1.

Schramke, V., Luciano, P., Brevet, V., Guillot, S., Corda, Y., Longhese, M. P., Gilson, E., and Geli, V. (2004). RPA regulates telomerase action by providing Est1p access to chromosome ends. Nat Genet *36*, 46-54.

Schulz, V. P., and Zakian, V. A. (1994). The *Saccharomyces PIF1* DNA helicase inhibits telomere elongation and *de novo* telomere formation. Cell *76*, 145-155.

Shinohara, A., Ogawa, H., and Ogawa, T. (1992). Rad51 protein involved in repair and recombination in *S. cerevisiae* is a RecA-like protein. Cell *69*, 457-470.

Shinohara, A., Shinohara, M., Ohta, T., Matsuda, S., and Ogawa, T. (1998). Rad52 forms ring structures and co-operates with RPA in single-strand DNA annealing. Genes Cells *3*, 145-156.

Shu, Z., Smith, S., Wang, L., Rice, M. C., and Kmiec, E. B. (1999). Disruption of muREC2/RAD51L1 in mice results in early embryonic lethality which can Be partially rescued in a p53(-/-) background. Mol Cell Biol *19*, 8686-8693.

Sieber, O. M., Heinimann, K., and Tomlinson, I. P. (2003). Genomic instability--the engine of tumorigenesis? Nat Rev Cancer *3*, 701-708.

Signon, L., Malkova, A., Naylor, M. L., Klein, H., and Haber, J. E. (2001). Genetic requirements for *RAD51*- and *RAD54*-independent break-induced replication repair of a chromosomal double-strand break. Mol Cell Biol *21*, 2048-2056.

Sigurdsson, S., Van Komen, S., Petukhova, G., and Sung, P. (2002). Homologous DNA pairing by human recombination factors Rad51 and Rad54. J Biol Chem *277*, 42790-42794.

Singer, M. S., and Gottschling, D. E. (1994). TLC1: template RNA component of *Saccharomyces cerevisiae* telomerase. Science *266*, 404-409.

Sinha, R. P., and Hader, D. P. (2002). UV-induced DNA damage and repair: a review. Photochem Photobiol Sci *1*, 225-236.

Smeets, M. F., Francesconi, S., and Baldacci, G. (2003). High dosage Rhp51 suppression of the MMS sensitivity of DNA structure checkpoint mutants reveals a relationship between Crb2 and Rhp51. Genes Cells *8*, 573-586.

Smith, C. E., Llorente, B., and Symington, L. S. (2007). Template switching during break-induced replication. Nature *447*, 102-105.

Smith, G. C., Divecha, N., Lakin, N. D., and Jackson, S. P. (1999). DNA-dependent protein kinase and related proteins. Biochem Soc Symp *64*, 91-104.

Smith, S., Gupta, A., Kolodner, R. D., and Myung, K. (2005). Suppression of gross chromosomal rearrangements by the multiple functions of the Mre11-Rad50-Xrs2 complex in *Saccharomyces cerevisiae*. DNA Repair (Amst) *4*, 606-617.

Sobol, R. W., Kartalou, M., Almeida, K. H., Joyce, D. F., Engelward, B. P., Horton, J. K., Prasad, R., Samson, L. D., and Wilson, S. H. (2003). Base Excision Repair Intermediates Induce p53-independent Cytotoxic and Genotoxic Responses. J Biol Chem *278*, 39951-39959.

Solinger, J. A., Kiianitsa, K., and Heyer, W. D. (2002). Rad54, a Swi2/Snf2-like recombinational repair protein, disassembles Rad51:dsDNA filaments. Mol Cell *10*, 1175-1188.

Song, B., and Sung, P. (2000). Functional interactions among yeast Rad51 recombinase, Rad52 mediator, and replication protein A in DNA strand exchange. J Biol Chem *275*, 15895-15904.

Sonoda, E., Sasaki, M. S., Buerstedde, J. M., Bezzubova, O., Shinohara, A., Ogawa, H., Takata, M., Yamaguchi-Iwai, Y., and Takeda, S. (1998). Rad51-deficient vertebrate cells accumulate chromosomal breaks prior to cell death. EMBO J *17*, 598-608.

Sorensen, C. S., Hansen, L. T., Dziegielewski, J., Syljuasen, R. G., Lundin, C., Bartek, J., and Helleday, T. (2005). The cell-cycle checkpoint kinase Chk1 is required for mammalian homologous recombination repair. Nat Cell Biol *7*, 195-201.

Spangler, E. A., Ryan, T., and Blackburn, E. H. (1988). Developmentally regulated telomere addition in Tetrahymena thermophila. Nucleic Acids Res *16*, 5569-5585.

Stark, J. M., and Jasin, M. (2003). Extensive Loss of Heterozygosity Is Suppressed during Homologous Repair of Chromosomal Breaks. Mol Cell Biol *23*, 733-743.

Stellwagen, A. E., Haimberger, Z. W., Veatch, J. R., and Gottschling, D. E. (2003). Ku interacts with telomerase RNA to promote telomere addition at native and broken chromosome ends. Genes Dev *17*, 2384-2395.

Stewart, E., Chapman, C. R., Al-Khodairy, F., Carr, A. M., and Enoch, T. (1997). rqh1+, a fission yeast gene related to the Bloom's and Werner's syndrome genes, is required for reversible S phase arrest. EMBO J *16*, 2682-2692.

Stewart, G. S., Maser, R. S., Stankovic, T., Bressan, D. A., Kaplan, M. I., Jaspers, N. G., Raams, A., Byrd, P. J., Petrini, J. H., and Taylor, A. M. (1999). The DNA double-strand break repair gene hMRE11 is mutated in individuals with an ataxia-telangiectasia-like disorder. Cell *99*, 577-587.

Storici, F., Durham, C. L., Gordenin, D. A., and Resnick, M. A. (2003). Chromosomal site-specific double-strand breaks are efficiently targeted for repair by oligonucleotides in yeast. Proc Natl Acad Sci U.S.A *100*, 14994-14999.

Strathern, J. N., Klar, A. J., Hicks, J. B., Abraham, J., Ivy, J. M., Nasmyth, K. A., and McGill, C. (1982). Homothallic switching of yeast mating type cassettes is initiated by a double-stranded cut in the MAT locus. Cell *31*, 183-192.

Su, T. T. (2006). Cellular Responses to DNA Damage: One Signal, Multiple Choices. Ann. Rev. Genet. *40*, 187-208.

Sugawara, N. (1989) DNA sequence at telomeres of the fission yeast Schizosaccharomyces pombe., Harvard University, Cambridge, MA. P. hD thesis.

Sugawara, N., and Haber, J. E. (1992). Characterization of double-strand break-induced recombination: homology requirements and single-stranded DNA formation. Mol Cell Biol *12*, 563-575.

Sugawara, N., Ira, G., and Haber, J. E. (2000). DNA Length Dependence of the Single-Strand Annealing Pathway and the Role of Saccharomyces cerevisiae RAD59 in Double-Strand Break Repair. Mol Cell Biol *20*, 5300-5309.

Sugawara, N., Paques, F., Colaiacovo, M., and Haber, J. E. (1997). Role of *Saccharomyces cerevisiae* Msh2 and Msh3 repair proteins in double-strand break-induced recombination. Proc Natl Acad Sci U.S.A *94*, 9214-9219.

Sugiyama, T., Kantake, N., Wu, Y., and Kowalczykowski, S. C. (2006). Rad52-mediated DNA annealing after Rad51-mediated DNA strand exchange promotes second ssDNA capture. EMBO J *25*, 5539-5548.

Sugiyama, T., Zaitseva, E. M., and Kowalczykowski, S. C. (1997). A single-stranded DNA-binding protein is needed for efficient presynaptic complex formation by the Saccharomyces cerevisiae Rad51 protein. J Biol Chem *272*, 7940-7945.

Sung, P. (1994). Catalysis of ATP-dependent homologous DNA pairing and strand exchange by yeast RAD51 protein. Science *265*, 1241-1243.

Sung, P. (1997a). Function of yeast Rad52 protein as a mediator between replication protein A and the Rad51 recombinase. J Biol Chem *272*, 28194-28197.

Sung, P. (1997b). Yeast Rad55 and Rad57 proteins form a heterodimer that functions with replication protein A to promote DNA strand exchange by Rad51 recombinase. Genes Dev *11*, 1111-1121.

Swagemakers, S. M., Essers, J., de Wit, J., Hoeijmakers, J. H., and Kanaar, R. (1998). The human RAD54 recombinational DNA repair protein is a double-stranded DNA-dependent ATPase. J Biol Chem *273*, 28292-28297.

Symington, L. S. (2002). Role of *RAD52* epistasis group genes in homologous recombination and double-strand break repair. Microbiol Mol Biol Rev *66*, 630-670.

Symington, L. S., and Heyer, W. D. (2006). Some disassembly required: role of DNA translocases in the disruption of recombination intermediates and dead-end complexes. Genes Dev *20*, 2479-2486.

Symington, L. S., Kang, L. E., and Moreau, S. (2000). Alteration of gene conversion tract length and associated crossing over during plasmid gap repair in nuclease-deficient strains of *Saccharomyces cerevisiae*. Nucl Acids Res *28*, 4649-4656.

Takata, M., Sasaki, M. S., Sonoda, E., Morrison, C., Hashimoto, M., Utsumi, H., Yamaguchi-Iwai, Y., Shinohara, A., and Takeda, S. (1998). Homologous recombination and non-homologous end-joining pathways of DNA double-strand break repair have overlapping roles in the maintenance of chromosomal integrity in vertebrate cells. EMBO J *17*, 5497-5508.

Thacker, J. (1994). The Study of Responses to 'Model' DNA Breaks Induced by Restriction Endonucleases in Cells and Cell-free Systems: Achievements and Difficulties. International Journal of Radiation Biology *66*, 591-596.

Thacker, J., and Zdzienicka, M. Z. (2003). The mammalian XRCC genes: their roles in DNA repair and genetic stability. DNA Repair (Amst) *2*, 655-672.

Ting, N. S., Yu, Y., Pohorelic, B., Lees-Miller, S. P., and Beattie, T. L. (2005). Human Ku70/80 interacts directly with hTR, the RNA component of human telomerase. Nucleic Acids Res *33*, 2090-2098.

Tishkoff, D. X., Boerger, A. L., Bertrand, P., Filosi, N., Gaida, G. M., Kane, M. F., and Kolodner, R. D. (1997). Identification and characterization of Saccharomyces cerevisiae EXO1, a gene encoding an exonuclease that interacts with MSH2. Proc Natl Acad Sci U.S.A *94*, 7487-7492.

Tomita, K., Matsuura, A., Caspari, T., Carr, A. M., Akamatsu, Y., Iwasaki, H., Mizuno, K., Ohta, K., Uritani, M., Ushimaru, T., *et al.* (2003). Competition between the Rad50 complex and the Ku heterodimer reveals a role for Exo1 in processing double-strand breaks but not telomeres. Mol Cell Biol *23*, 5186-5197.

Trujillo, K. M., and Sung, P. (2001). DNA Structure-specific Nuclease Activities in the *Saccharomyces cerevisiae* Rad50-Mre11 Complex. J Biol Chem *276*, 35458-35464.

Tseng, S. F., Lin, J. J., and Teng, S. C. (2006). The telomerase-recruitment domain of the telomere binding protein Cdc13 is regulated by Mec1p/Tel1p-dependent phosphorylation. Nucleic Acids Res *34*, 6327-6336.

Tsubouchi, H., and Ogawa, H. (1998). A Novel mre11 Mutation Impairs Processing of Double-Strand Breaks of DNA during Both Mitosis and Meiosis. Mol Cell Biol *18*, 260-268.

Tsutsui, Y., Khasanov, F. K., Shinagawa, H., Iwasaki, H., and Bashkirov, V. I. (2001). Multiple interactions among the components of the recombinational DNA repair system in *Schizosaccharomyces pombe*. Genetics *159*, 91-105.

Tsuzuki, T., Fujii, Y., Sakumi, K., Tominaga, Y., Nakao, K., Sekiguchi, M., Matsushiro, A., Yoshimura, Y., and Morita, T. (1996). Targeted disruption of the Rad51 gene leads to lethality in embryonic mice. Proc Natl Acad Sci U.S.A *93*, 6236-6240.

Ueno, M., Nakazaki, T., Akamatsu, Y., Watanabe, K., Tomita, K., Lindsay, H. D., Shinagawa, H., and Iwasaki, H. (2003). Molecular Characterization of the *Schizosaccharomyces pombe nbs1+* Gene Involved in DNA Repair and Telomere Maintenance. Mol Cell Biol *23*, 6553-6563.

Valencia, M., Bentele, M., Vaze, M. B., Herrmann, G., Kraus, E., Lee, S. E., Schar, P., and Haber, J. E. (2001). NEJ1 controls non-homologous end joining in *Saccharomyces cerevisiae*. Nature *414*, 666-669.

van Brabant, A. J., Ye, T., Sanz, M., German, I. J., Ellis, N. A., and Holloman, W. K. (2000). Binding and melting of D-loops by the Bloom syndrome helicase. Biochemistry *39*, 14617-14625.

van den Bosch, M., Bree, R. T., and Lowndes, N. F. (2003). The MRN complex: coordinating and mediating the response to broken chromosomes. EMBO Rep *4*, 844-849.

van den Bosch, M., Vreeken, K., Zonneveld, J. B., Brandsma, J. A., Lombaerts, M., Murray, J. M., Lohman, P. H., and Pastink, A. (2001). Characterization of *RAD52* homologs in the fission yeast Schizosaccharomyces pombe. Mutat Res *461*, 311-323.

Van Komen, S., Petukhova, G., Sigurdsson, S., Stratton, S., and Sung, P. (2000). Superhelicity-driven homologous DNA pairing by yeast recombination factors Rad51 and Rad54. Mol Cell *6*, 563-572.

Varon, R., Vissinga, C., Platzer, M., Cerosaletti, K. M., Chrzanowska, K. H., Saar, K., Beckmann, G., Seemanova, E., Cooper, P. R., Nowak, N. J., *et al.* (1998). Nibrin, a novel DNA double-strand break repair protein, is mutated in Nijmegen breakage syndrome. Cell *93*, 467-476.

Veaute, X., Jeusset, J., Soustelle, C., Kowalczykowski, S. C., Le Cam, E., and Fabre, F. (2003). The Srs2 helicase prevents recombination by disrupting Rad51 nucleoprotein filaments. Nature *423*, 309-312.

Verdun, R. E., and Karlseder, J. (2006). The DNA damage machinery and homologous recombination pathway act consecutively to protect human telomeres. Cell *127*, 709-720.

Viscardi, V., Clerici, M., Cartagena-Lirola, H., and Longhese, M. P. (2005). Telomeres and DNA damage checkpoints. Biochimie *87*, 613-624.

Wallace, S. S. (1998). Enzymatic processing of radiation-induced free radical damage in DNA. Radiat Res *150*, S60-79.

Wang, S.-W., Goodwin, A., Hickson, I. D., and Norbury, C. J. (2001). Involvement of Schizosaccharomyces pombe Srs2 in cellular responses to DNA damage. Nucl Acids Res *29*, 2963-2972.

Wang, X., and Haber, J. E. (2004). Role of Saccharomyces single-stranded DNA-binding protein RPA in the strand invasion step of double-strand break repair. PLoS Biol *2*, E21.

Wang, X., Ira, G., Tercero, J. A., Holmes, A. M., Diffley, J. F. X., and Haber, J. E. (2004). Role of DNA Replication Proteins in Double-Strand Break-Induced Recombination in *Saccharomyces cerevisiae*. Mol Cell Biol *24*, 6891-6899.

Wellinger, R. J., and Sen, D. (1997). The DNA structures at the ends of eukaryotic chromosomes. Eur J Cancer *33*, 735-749.

West, R. B., Yaneva, M., and Lieber, M. R. (1998). Productive and nonproductive complexes of Ku and DNA-dependent protein kinase at DNA termini. Mol Cell Biol *18*, 5908-5920.

Weterings, E., and van Gent, D. C. (2004). The mechanism of non-homologous end-joining: a synopsis of synapsis. DNA Repair (Amst) *3*, 1425-1435.

White, C. I., and Haber, J. E. (1990). Intermediates of recombination during mating type switching in *Saccharomyces cerevisiae*. EMBOJ *9*, 663-673.

Wilkie, A. O., Lamb, J., Harris, P. C., Finney, R. D., and Higgs, D. R. (1990). A truncated human chromosome 16 associated with alpha thalassaemia is stabilized by addition of telomeric repeat (TTAGGG)n. Nature *346*, 868-871.

Wong, A. C., Ning, Y., Flint, J., Clark, K., Dumanski, J. P., Ledbetter, D. H., and McDermid, H. E. (1997). Molecular characterization of a 130-kb terminal microdeletion at 22q in a child with mild mental retardation. Am J Hum Genet *60*, 113-120.

Wooster, R., Bignell, G., Lancaster, J., Swift, S., Seal, S., Mangion, J., Collins, N., Gregory, S., Gumbs, C., Micklem, G. (1995). Identification of the breast cancer susceptibility gene BRCA2. Nature *378*, 789-92.

Wu, L., Bachrati, C. Z., Ou, J., Xu, C., Yin, J., Chang, M., Wang, W., Li, L., Brown, G. W., and Hickson, I. D. (2006). BLAP75/RMI1 promotes the BLM-dependent dissolution of homologous recombination intermediates. Proc Natl Acad Sci U S A *103*, 4068-4073.

Wu, L., and Hickson, I. D. (2003). The Bloom's syndrome helicase suppresses crossing over during homologous recombination. Nature *426*, 870-874.

Yu, C. E., Oshima, J., Fu, Y. H., Wijsman, E. M., Hisama, F., Alisch, R., Matthews, S., Nakura, J., Miki, T., Ouais, S., Martin, G. M., Mulligan, J., Schellenberg, G. D. (1996). Positional cloning of the Werner's syndrome gene. Science *272*, 258-62.

Yu-Wee, B. (2006) Investigating chromosome restoration in response to a site-specific DNA double-strand break. D. Phil Thesis. Wolfson College. University of Oxford. U.K.

# 8. APPENDICIES.

# Appendix I. Protocols for DNA extraction and isolation.

## Qiagen® buffers provided in QIAprep mini-prep and QIAfilter maxi-prep kits.

**Buffer P1** (Resuspension buffer) 50mM Tris-HCl (pH8.0), 10mM EDTA, 100mg/mL RNase A.

**Buffer P2** (Lysis buffer) 200mM NaOH, 1% SDS.

**Buffer N3** (Neutralisation buffer) 3M potassium acetate (pH5.5).

**Buffer QBT** (Equilibration buffer) 750mM NaCl, 50mM MOPS (pH7.0), 15% isopropanol, 0.15% triton X-100.

**Buffer PE/Buffer QC** (Wash buffer in Mini/Maxi kits, respectively) 1M NaCl, 50mM MOPS (pH7.0), 15% isopropanol.

**Buffer QF** (Elution buffer, Maxi-prep kit) 1.25M NaCl, 50mM Tris-HCl (pH8.5), 15% isopropanol.

**Buffer EB** (Elution and storage buffer, Mini-prep kit) 10mM Tris-HCl pH8.5.

## Mini-prep protocol.

The bacterial pellet of cells was resuspended in 150µl Buffer P1 and transferred to a 1.5mL micro-centrifuge tube. 250µl of Buffer P2 was added, the sample incubated for 2mins at room temperature and Buffer P3 then added to precipitate lipid and protein. The resultant mix was centrifuged at 13,000rpm for 10mins during which a QIAprep spin column was placed into a 2mL collection tube. The supernatant from this was then decanted into the spin column and centrifuged at 13,000rpm for 1min to bind DNA. After the flow-through was removed, the column was washed by adding 750µl of Buffer PE and then centrifuging the column at 13,000rpm for 1min. The flow-through was again discarded and the column centrifuged for an additional minute to remove residual wash buffer. The column was placed into a fresh 1.5mL micro-centrifuge tube and 50µl of Buffer EB added to the column. After 1min incubation at

room temperature, DNA was eluted by centrifugation at 13,000rpm for 1min. Mini-prep plasmid DNA samples were stored at -20°C until use.

**Maxi-prep protocol.**

The bacterial cell pellet was resuspended in 10mL of Buffer P1 and transferred to a 50mL polypropylene spin tube. 10mL of Buffer P2 was added and the mixture incubated for 5mins at room temperature. 10mL of Buffer P3 was then added and the resultant suspension transferred to a QIAfilter syringe. After 10mins incubation at room temperature, the plunger was inserted into the syringe and liquid expelled into a QIAGEN 500$^{TM}$ column that had been pre-equilibrated with 15mL of Buffer QBT. The DNA was allowed to pass through the column by gravity flow, after which the column was washed with 60mL Buffer QC. DNA was then eluted into a 50mL polypropylene spin tube with 15mL of Buffer QF and 10.5mL of isopropanol added. The sample was centrifuged at 15,000xg for 10mins (4°C), the supernatant discarded and the DNA pellet rinsed in 5mL 70% ethanol. After another centrifugation cycle (as above) the supernatant was removed and the pellet allowed to air dry. The pellet was then resuspended in 1mL TE buffer (Table 2.1) and stored at -20°C.

**Gel extraction protocol.**

The DNA fragment was first excised from the gel with a clean, sharp scalpel, minimising the size of the slice by removing excess agarose. The gel slice was subsequently weighed in a colourless tube, and 3 volumes of Buffer QG added to 1 volume of gel (100mg ~ 100µl). The resultant tube was incubated at 50°C for 10mins or until the gel slice had dissolved. Care was taken to ensure the solution remained yellow. 1 gel volume of isopropanol was then added to the sample and mixed. To bind DNA the sample was added to a QIAquick spin column, centrifuged for 1min at

13,000rpm and the flow through discarded. For sample volumes greater than that of the spin column, the sample was simply loaded and spun again. All flow through was discarded. 750µl Buffer PE was then added to the column and centrifuged at 13,000rpm for 1min. The flow-through was again discarded and the column centrifuged for an additional minute to remove residual wash buffer. The column was then placed into a fresh 1.5mL micro-centrifuge tube and 50µl of Buffer EB added. After 1min incubation at room temperature, DNA was eluted by centrifugation at 13,000rpm for 1min. DNA fragments were stored at -20°C until use.

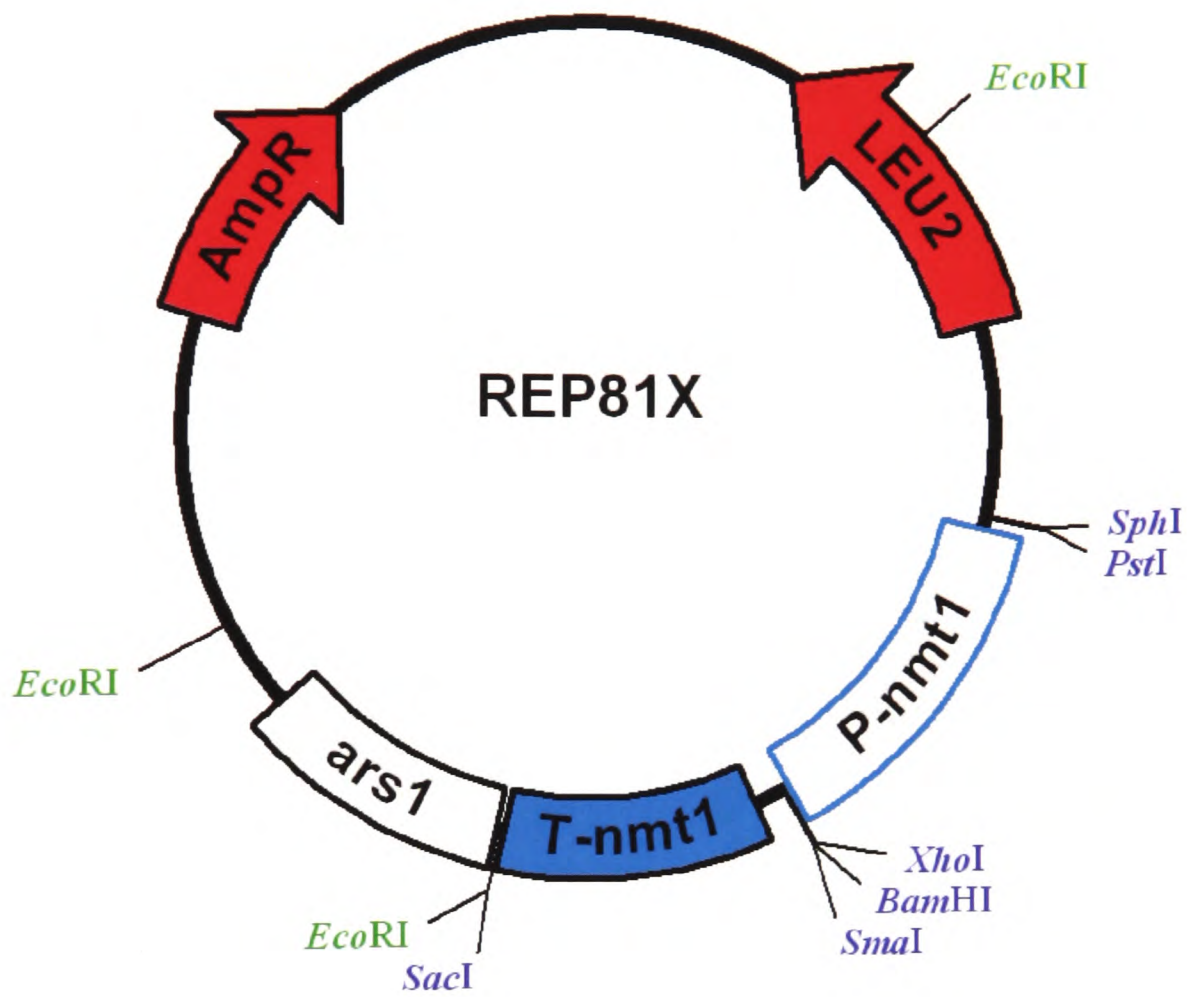
**PCR purification protocol.**

250µl of Buffer PB was first added to the PCR sample (50µl) which was then placed into a QIAquick spin column and centrifuged at 13,000rpm for 1min to bind DNA. The flow through was removed and the DNA washed with 750µl Buffer PE using centrifugation as described above. The flow-through was again discarded and the column centrifuged for an additional minute to remove residual wash buffer. The column was then placed into a fresh 1.5mL micro-centrifuge tube and 50µl of Buffer EB added. After 1min incubation at room temperature, DNA was eluted by centrifugation at 13,000rpm for 1min. Purified and isolation PCR products were stored at -20°C until use.

## Appendix II. Oligonucleotide primers used during this study.

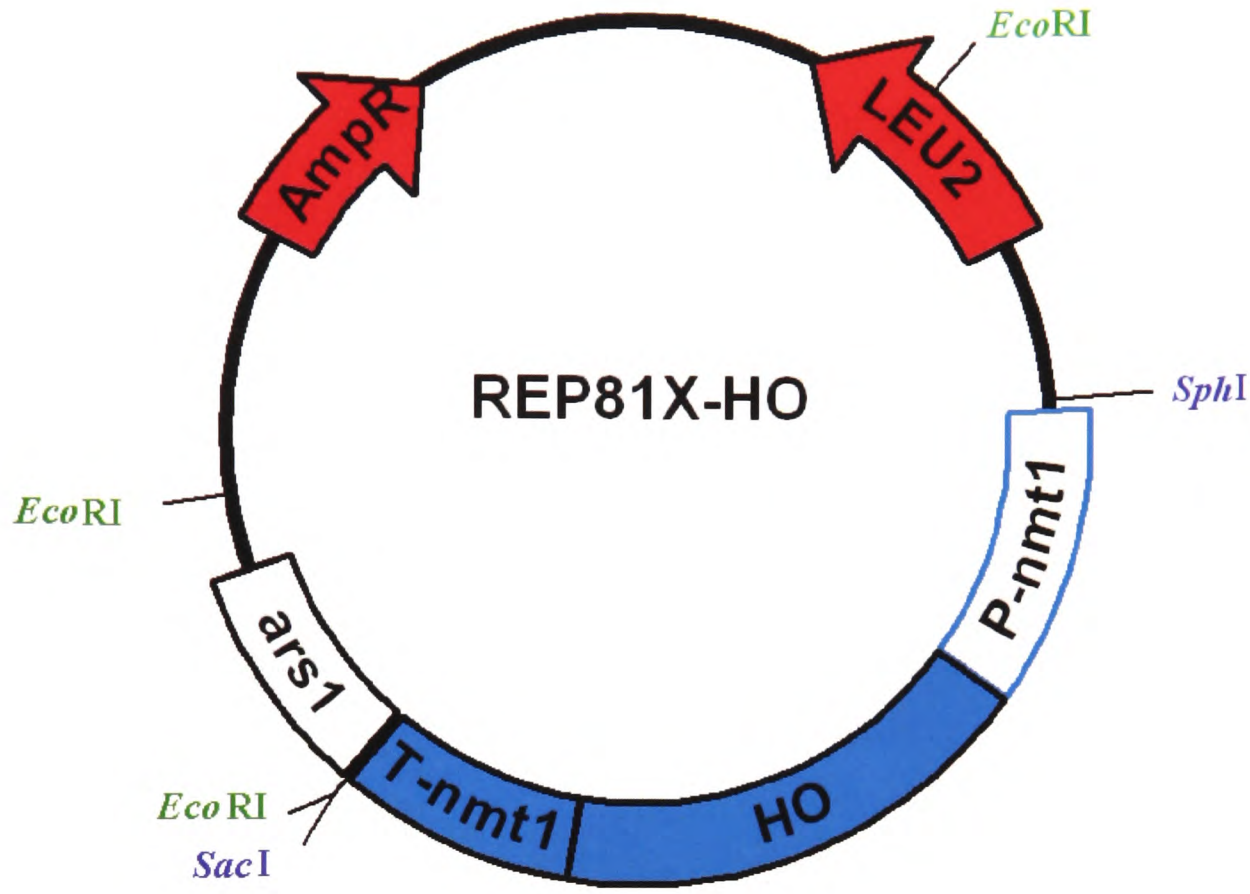
| Name | Sequence (5'-3') | Source |
|---|---|---|
| R1 (RAD21-5B) | GATTTAAACCTGGATTTGGGC | Lab stock |
| T1 (TELO-SENSE) | CTGTAACCGTGTAACCGTAAC | Dr. B. Wee, DPhil thesis. |
| DM11F | ACTTTGTTTTGCTCATCACT | This study |
| DM11R | TTCTTGAATTCCGATAAAAC | This study |
| RAD21-5 | TATCTGAGGCCCTTCC | Lab stock |

**Appendix III. DNA plasmids.**



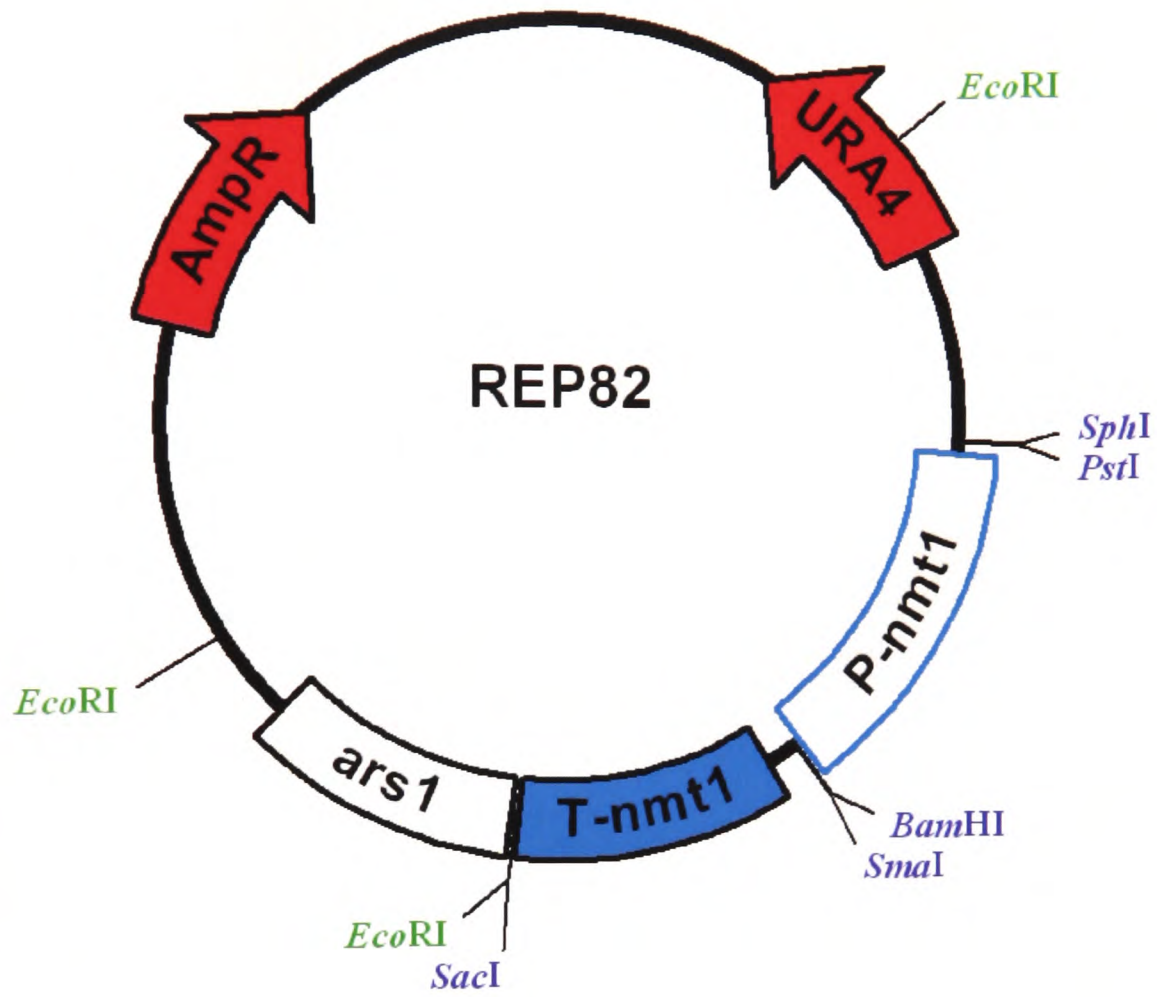

Provided by Fekret Osman (Osman *et al.*, 1996). A *LEU2* multi-copy plasmid containing the thiamine repressible *nmt1* promoter. This promoter is the weaker rep81X derivative (Forsburg *et al.*, 1993).

**Appendix III. continued.**



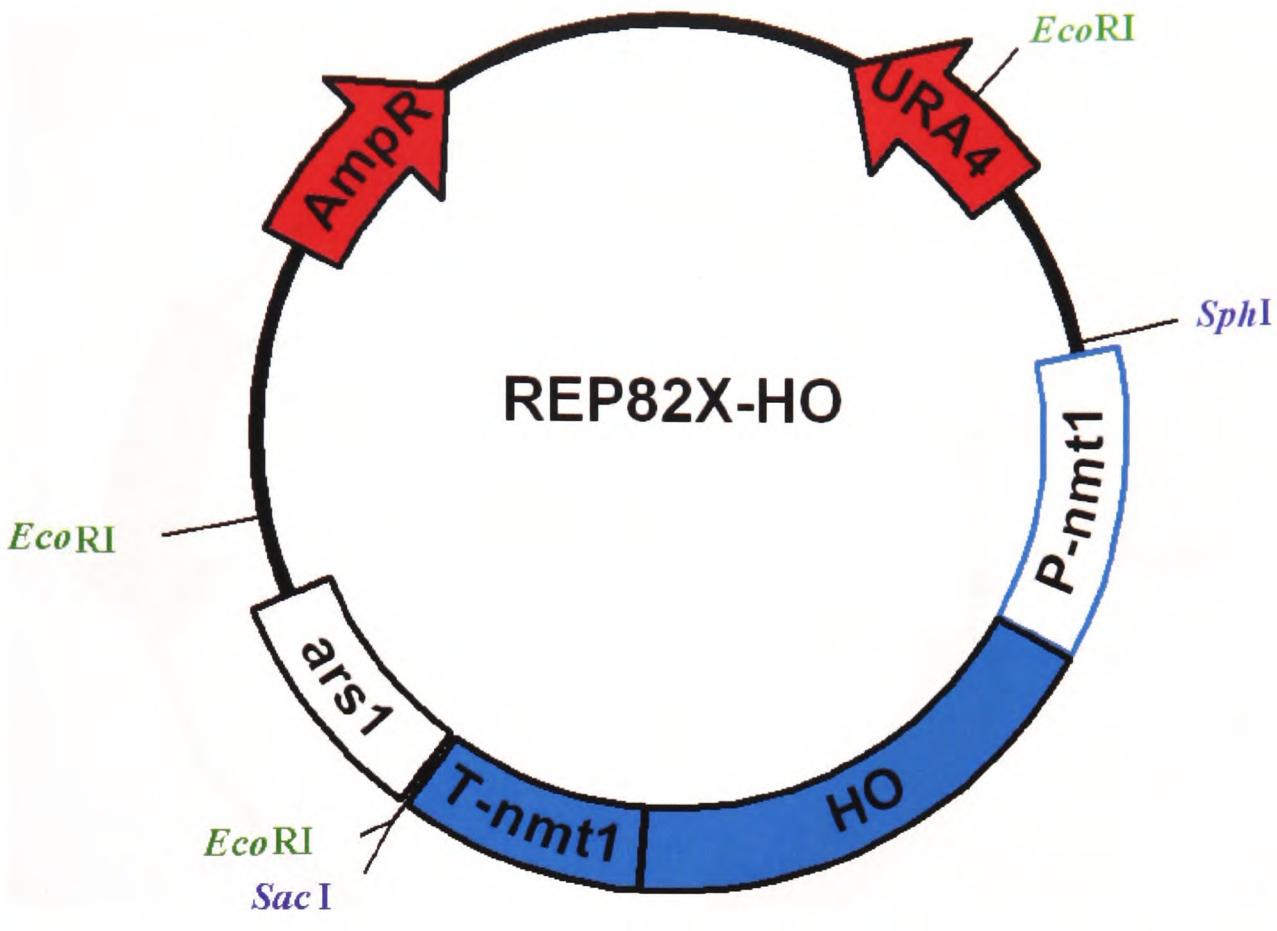

Provided by Fekeret Osman (Osman *et al.*, 1996). pREP81X containing the *S. cerevisiae* HO-endonuclease ORF under control of the thiamine repressible *nmt1* promoter.

**Appendix III. continued.**



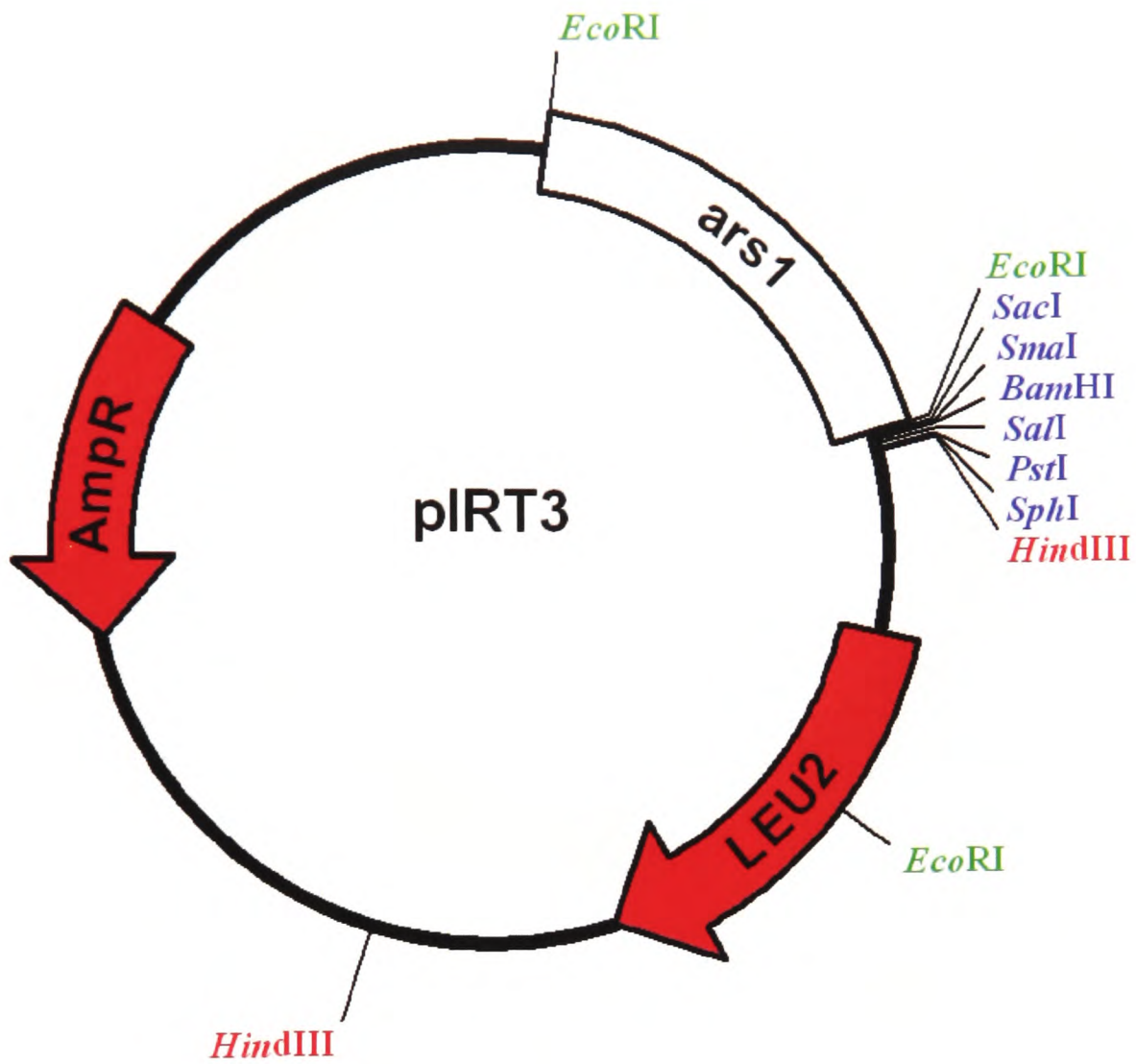

A *ura4*$^{+}$ multi-copy plasmid containing the thiamine repressible *nmt1* promoter, similar in strength to pREP81X (Maundrell *et al.*, 1993).

**Appendix III. continued.**



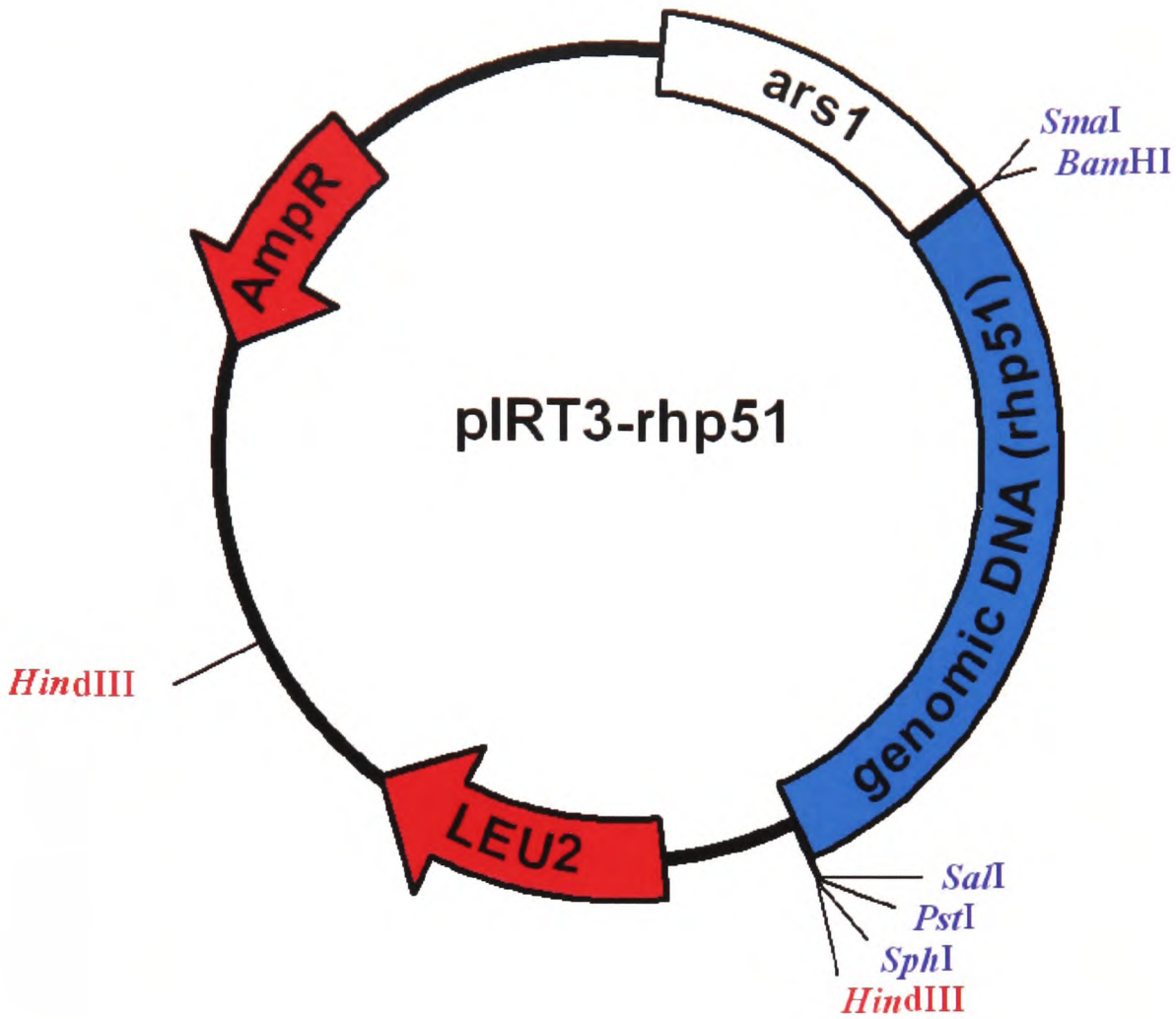

Constructed by Jason Cullen. See Section 2.5.8.1.

**Appendix III. continued.**




Provided by Stefania Francesconi (Smeets *et al.*, 2003). A *LEU2* multi-copy plasmid.

**Appendix III. continued.**




Provided by Stefania Francesconi (Smeets *et al.*, 2003). A *LEU2* multi-copy plasmid into which genomic DNA was inserted to identify high dosage suppressors of *crb2Δ*. 4-10Kb fragments, purified from a partial *Sau*3A digest of *S. pombe* DNA, were cloned into the *Bam*HI site of pIRT3.

# Appendix IV. Genetic determinants of site-specific DSB-induced marker loss in wt and HR mutants.

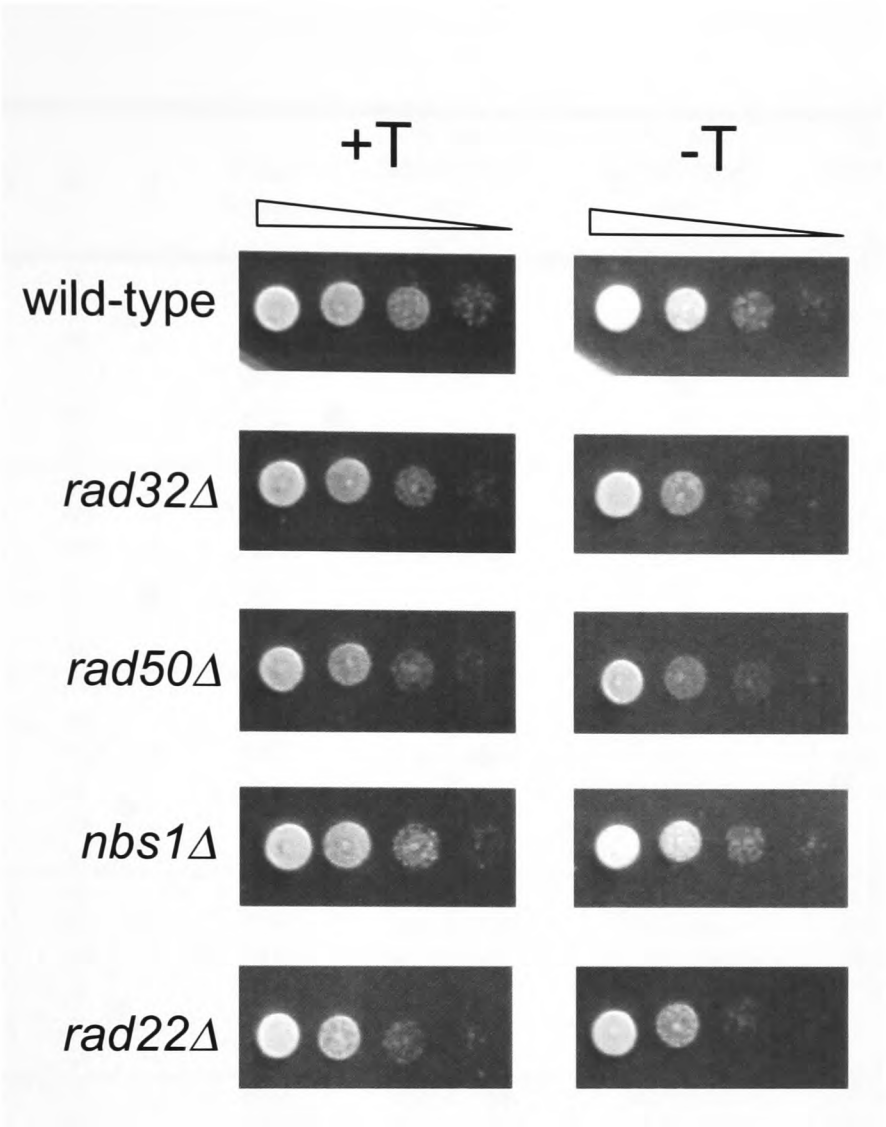
| Genetic background | ± HO | h | T | Total scored | % *ade*$^+$ G418$^S$/Hyg$^S$ *his*$^+$ (GC) | %*ade*$^+$ G418$^R$/Hyg$^R$ *his*$^+$ (EJ/SCR) | % *ade*$^-$ G418$^S$/Hyg$^S$ *his*$^-$ (Ch$^{16}$ loss) | % *ade*$^+$ G418$^S$/Hyg$^S$ *his*$^-$ (LOH) | % *ade*$^-$ G418$^S$/Hyg$^S$ *his*$^+$ (LOH) |
|---|---|---|---|---|---|---|---|---|---|
| *wild-type* | + | 0 | | 4300 | 8.0 ± 1.4 | 91.6 ± 1.4 | 0.3 ± 0.1 | 0 | 0 |
| | | 48 | - | 1375 | 49.7 ± 2.6 | 25.0 ± 1.4 | 23.7 ± 1.7 | 1.71 ± 0.27 | 0 |
| | | 48 | + | 1771 | 8.1 ± 0.7 | 88.7 ± 0.9 | 3.2 ± 1.1 | 0 | 0 |
| | - | 0 | | 877 | 0 | 100 | 0 | 0 | 0 |
| | | 48 | - | 672 | 0 | 100 | 0 | 0 | 0 |
| | | 48 | + | 1094 | 0 | 100 | 0 | 0 | 0 |
| *rad32Δ* | + | 0 | | 3947 | 1.1 ± 0.3 | 94.2 ± 1.5 | 4.7 ± 1.3 | 0 | 0 |
| | | 48 | - | 3868 | 30.8 ± 2.1 | 25.6 ± 5.1 | 42.9 ± 5.8 | 0.59 ± 0.16 | 0 |
| | | 48 | + | 3783 | 1.2 ± 0.4 | 88.6 ± 2.4 | 10.2 ± 2.0 | 0 | 0 |
| | - | 0 | | 482 | 0 | 97.5 | 2.5 | 0 | 0 |
| | | 48 | - | 454 | 0 | 92.7 | 7.3 | 0 | 0 |
| | | 48 | + | 641 | 0 | 95.8 | 4.2 | 0 | 0 |
| *rad50Δ* | + | 0 | | 3489 | 1.1 ± 0.5 | 95.2 ± 0.5 | 3.6 ± 0.1 | 0 | 0 |
| | | 48 | - | 3099 | 18.3 ± 1.8 | 23.9 ± 0.6 | 57.2 ± 2.0 | 0.57 ± 0.16 | 0 |
| | | 48 | + | 3070 | 1.5 ± 3.4 | 87.4 ± 1.5 | 11.1 ± 1.4 | 0 | 0 |
| | - | 0 | | 673 | 0 | 96.6 | 3.4 | 0 | 0 |
| | | 48 | - | 361 | 0 | 92.3 | 7.5 | 0.23 | 0 |
| | | 48 | + | 424 | 0 | 92.9 | 7.1 | 0 | 0 |
| *nbs1Δ* | + | 0 | | 1259 | 0.8 ± 0.2 | 94.1 ± 0.9 | 4.9 ± 0.7 | 0.12 ± 0.12 | 0 |
| | | 48 | - | 1442 | 15.6 ± 0.7 | 30.9 ± 2.6 | 52.0 ± 3.3 | 1.43 ± 0.2 | 0 |
| | | 48 | + | 2448 | 1.3 ± 0.3 | 91.5 ± 0.7 | 7.2 ± 1.5 | 0 | 0 |
| | - | 0 | | 443 | 0 | 96.6 | 3.4 | 0 | 0 |
| | | 48 | - | 347 | 0 | 91.6 | 8.4 | 0 | 0 |
| | | 48 | + | 514 | 0 | 91.4 | 8.6 | 0 | 0 |
| *exo1Δ* | + | 0 | | 6186 | 3.2 ± 0.6 | 96.5 ± 0.6 | 0.3 ± 0.1 | 0 | 0 |
| | | 48 | - | 2583 | 52.8 ± 1.0 | 33.1 ± 0.7 | 13.2 ± 0.8 | 1.06 ± 0.48 | 0.09± 0.05 |
| | | 48 | + | 6502 | 5.4 ± 0.6 | 94.2 ± 0.6 | 0.4 ± 0.1 | 0 | 0 |
| | - | 0 | | 1005 | 0 | 100 | 0 | 0 | 0 |
| | | 48 | - | 985 | 0 | 99.8 | 0.2 | 0 | 0 |
| | | 48 | + | 1042 | 0 | 99.9 | 0.1 | 0 | 0 |
| *rad11D223Y* | + | 0 | | 2937 | 0.5 ± 0.3 | 97.3 ± 0.3 | 2.1 ± 0.2 | 0.02 ± 0.02 | 0 |
| | | 48 | - | 1079 | 20.5 ± 1.5 | 27.1 ± 1.3 | 49.5 ± 1.7 | 2.93 ± 0.99 | 0 |
| | | 48 | + | 2878 | 0.7 ± 0.1 | 93.0 ± 1.0 | 6.3 ± 0.6 | 0.05 ± 0.05 | 0 |
| | - | 0 | | | | | | | |
| | | 48 | - | N.D. | N.D. | N.D. | N.D. | N.D. | N.D. |
| | | 48 | + | | | | | | |
| *rad22Δ* | + | 0 | | 2016 | 0.06 ± 0.06 | 90.1 ± 2.3 | 9.9 ± 2.2 | 0 | 0 |
| | | 48 | - | 2518 | 0 | 22.3 ± 1.1 | 75.5 ± 1.7 | 2.29 ± 0.62 | 0 |
| | | 48 | + | 3053 | 0 | 81.0 ± 0.9 | 18.9 ± 0.9 | 0 | 0 |
| | - | 0 | | 256 | 0 | 94.7 | 5.3 | 0 | 0 |
| | | 48 | - | 505 | 0 | 93.3 | 6.7 | 0 | 0 |
| | | 48 | + | 519 | 0 | 90.2 | 9.8 | 0 | 0 |
| *rhp55Δ* | + | 0 | | 2213 | 0.04± 0.04 | 98.2 ± 0.4 | 1.6 ± 0.5 | 0.04 ± 0.04 | 0 |
| | | 48 | - | 2646 | 2.3 ± 0.6 | 54.7 ± 9.8 | 42.3 ± 8.9 | 0.76 ± 0.28 | 0 |
| | | 48 | + | 3901 | 0.02 ± 0.02 | 97.0 ± 0.1 | 2.9 ± 0.1 | 0 | 0 |
| | - | 0 | | 582 | 0 | 99.3 | 0.7 | 0 | 0 |
| | | 48 | - | 617 | 0 | 97.9 | 2.1 | 0 | 0 |
| | | 48 | + | 521 | 0 | 97.3 | 2.7 | 0 | 0 |
| *rhp51Δ* | + | 0 | | 2777 | 0 | 91.5 ± 4.4 | 8.5 ± 4.4 | 0 | 0 |
| | | 48 | - | 5097 | 1.0 ± 0.5 | 35.9 ± 2.9 | 62.4 ± 2.9 | 0.76 ± 0.33 | 0 |
| | | 48 | + | 3845 | 0.6 ± 0.4 | 80.4 ± 6.2 | 19.0 ± 5.8 | 0 | 0 |
| | - | 0 | | 534 | 0 | 98.1 | 1.9 | 0 | 0 |
| | | 48 | - | 670 | 0 | 94.6 | 5.4 | 0 | 0 |
| | | 48 | + | 625 | 0 | 96.0 | 4.0 | 0 | 0 |

# Appendix IV. continued.

| | | | | | | | | | |
|---|---|---|---|---|---|---|---|---|---|
| *rhp54Δ* | | 0 | | 5274 | 0.3 ± 0.2 | 89.9 ± 0.8 | 9.8 ± 0.8 | 0 | 0 |
| | + | 48 | - | 10798 | 3.2 ± 1.9 | 36.8 ± 3.3 | 60.0 ± 4.5 | 0.40 ± 0.20 | 0 |
| | | 48 | + | 4708 | 0.7 ± 0.7 | 74.4 ± 0.9 | 24.8 ± 1.3 | 0 | 0 |
| | | 0 | | 160 | 0 | 85.6 | 14.4 | 0 | 0 |
| | - | 48 | - | 186 | 0 | 72.6 | 27.4 | 0 | 0 |
| | | 48 | + | 237 | 0 | 74.7 | 25.3 | 0 | 0 |
| *mus81Δ* | | 0 | | 6068 | 1.0 ± 0.3 | 97.0 ± 0.4 | 1.9 ± 0.2 | 0 | 0 |
| | + | 48 | - | 11267 | 29.2 ± 2.9 | 28.1 ± 3.4 | 42.7 ± 4.4 | 0.20 ± 0.05 | 0 |
| | | 48 | + | 5735 | 1.0 ± 0.4 | 91.7 ± 0.4 | 0.9 ± 0.4 | 0 | 0 |
| | | 0 | | 497 | 0 | 97.9 | 2.0 | 0 | 0 |
| | - | 48 | - | 415 | 0 | 95.4 | 4.6 | 0 | 0 |
| | | 48 | + | 146 | 0 | 93.8 | 6.2 | 0 | 0 |

For each genetic background with HO (+), the genetic assay was independently repeated at least three times (with independent isolates), such that >1000 colonies were scored at each timepoint. The average value for each timepoint and the standard errors between the independent experiments are shown. A single strain control with blank vector only (- HO) was also performed for each background tested. N.D. Not determined.

**Appendix V. Analysis of break-induced loss of viability in wt and HR mutants.**




Serial 10-fold dilutions of wild-type, *rad32Δ*, *rad50Δ*, *nbs1Δ* and *rad22Δ* $Ch^{16}$-MGH/MHH strains containing pREP81X-HO were performed as described in Section 2.5.7.3. None of the mutants tested displayed a significant change in viability with (+T) or without (-T) thiamine. Viability assays of other mutants used in this study were performed by J. Prudden (D. Phil thesis) and S. Hussey (D. Phil thesis).

# Appendix VI. Genetic determinants of site-specific DSB-induced marker loss in WT and various *rhp55Δ* derived mutants.

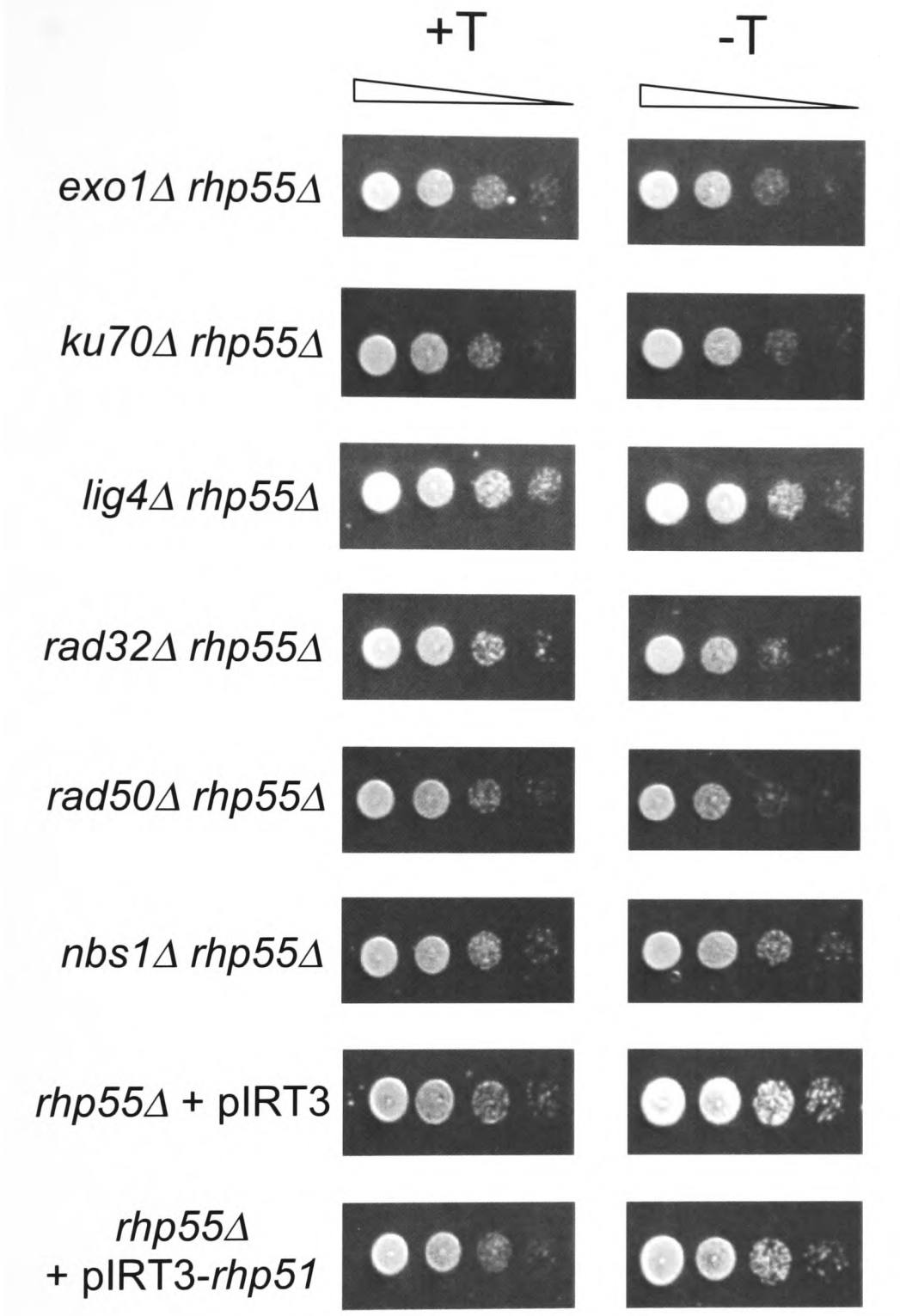
| Genetic background | ± HO | h | T | Total scored | % *ade*$^+$ G418$^S$/Hyg$^S$ *his*$^+$ (GC) | %*ade*$^+$ G418$^R$/Hyg$^R$ *his*$^+$ (EJ/SCR) | % *ade*$^-$ G418$^S$/Hyg$^S$ *his*$^-$ (Ch$^{16}$ loss) | % *ade*$^+$ G418$^S$/Hyg$^S$ *his*$^-$ (LOH) | % *ade*$^-$ G418$^S$/Hyg$^S$ *his*$^+$ (LOH) |
|---|---|---|---|---|---|---|---|---|---|
| *wild-type* | + | 0 | | 4300 | 8.0 ± 1.4 | 91.6 ± 1.4 | 0.3 ± 0.1 | 0 | 0 |
| | | 48 | - | 1375 | 49.7 ± 2.6 | 25.0 ± 1.4 | 23.7 ± 1.7 | 1.71 ± 0.27 | 0 |
| | | 48 | + | 1771 | 8.1 ± 0.7 | 88.7 ± 0.9 | 3.2 ± 1.1 | 0 | 0 |
| | - | 0 | | 877 | 0 | 100 | 0 | 0 | 0 |
| | | 48 | - | 672 | 0 | 100 | 0 | 0 | 0 |
| | | 48 | + | 1094 | 0 | 100 | 0 | 0 | 0 |
| *rhp55Δ* | + | 0 | | 2213 | 0.04± 0.04 | 98.2 ± 0.4 | 1.6 ± 0.5 | 0.04 ± 0.04 | 0 |
| | | 48 | - | 2646 | 2.3 ± 0.6 | 54.7 ± 9.8 | 42.3 ± 8.9 | 0.76 ± 0.28 | 0 |
| | | 48 | + | 3901 | 0.02 ± 0.02 | 97.0 ± 0.1 | 2.9 ± 0.1 | 0 | 0 |
| | - | 0 | | 582 | 0 | 99.3 | 0.7 | 0 | 0 |
| | | 48 | - | 617 | 0 | 97.9 | 2.1 | 0 | 0 |
| | | 48 | + | 521 | 0 | 97.3 | 2.7 | 0 | 0 |
| *rad32Δrhp55Δ* | + | 0 | | 1381 | 0.29 ± 0.01 | 84.7 ± 1.5 | 13.8 ± 0.9 | 1.19 ± 0.65 | 0 |
| | | 48 | - | 1866 | 0.64 ± 0.36 | 20.1 ± 0.2 | 72.7 ± 0.1 | 6.56 ± 0.20 | 0 |
| | | 48 | + | 1737 | 0.87 ± 0.76 | 76.8 ± 1.3 | 21.5 ± 0.6 | 0.86 ± 0.04 | 0 |
| | - | 0 | | 780 | 0 | 94.5 | 5.5 | 0 | 0 |
| | | 48 | - | 1152 | 0 | 88.9 | 11.0 | 0 | 0 |
| | | 48 | + | 1112 | 0 | 89.8 | 10.2 | 0 | 0 |
| *rad50Δrhp55Δ* | + | 0 | | 1513 | 0.08 ± 0.08 | 90.7 ± 1.1 | 9.2 ± 0.9 | 0.08 ± 0.08 | 0 |
| | | 48 | - | 1738 | 0.86 ± 0.28 | 29.2 ± 6.3 | 64.9 ± 5.3 | 5.08 ± 0.65 | 0 |
| | | 48 | + | 2032 | 0.58 ± 0.17 | 85.5 ± 0.8 | 13.9 ± 0.6 | 0 | 0 |
| | - | 0 | | 490 | 0 | 89.2 | 10.8 | 0 | 0 |
| | | 48 | - | 1161 | 0 | 88.9 | 10.9 | 0.17 | 0 |
| | | 48 | + | 823 | 0 | 87.0 | 12.9 | 0.12 | 0 |
| *nbs1Δrhp55Δ* | + | 0 | | 1623 | 0.06 ± 0.06 | 92.8 ± 1.0 | 7.1 ± 1.0 | 0 | 0 |
| | | 48 | - | 1769 | 0.05 ± 0.05 | 23.4 ± 1.9 | 73.9 ± 1.6 | 2.64 ± 0.46 | 0 |
| | | 48 | + | 2461 | 0.08 ± 0.08 | 89.1 ± 0.6 | 10.8 ± 0.6 | 0.05 ± 0.05 | 0 |
| | - | 0 | | 452 | 0 | 93.4 | 6.6 | 0 | 0 |
| | | 48 | - | 782 | 0 | 87.9 | 12.0 | 0 | 0 |
| | | 48 | + | 716 | 0 | 89.9 | 10.1 | 0 | 0 |
| *ku70Δ* | + | 0 | | 3918 | 1.1 ± 0.3 | 98.7 ± 0.3 | 0.1 ± 0.03 | 0 | 0 |
| | | 48 | - | 2590 | 53.4 ± 2.8 | 38.5 ± 2.2 | 6.3 ± 1.0 | 1.47 ± 0.07 | 0.39 ± 0.14 |
| | | 48 | + | 4867 | 1.8 ± 0.3 | 97.9 ± 0.3 | 0.3 ± 0.01 | 0 | 0 |
| | - | 0 | | 608 | 0 | 100 | 0 | 0 | 0 |
| | | 48 | - | 1210 | 0 | 100 | 0 | 0 | 0 |
| | | 48 | + | 1161 | 0 | 99.8 | 0.2 | 0 | 0 |
| *lig4Δ* | + | 0 | | 6395 | 12.3 ± 3.4 | 85.4 ± 3.8 | 2.3 ± 0.6 | 0 | 0 |
| | | 48 | - | 6612 | 47.2 ± 3.6 | 39.1 ± 3.1 | 12.9 ± 0.5 | 0.73 ± 1.1 | 0.19 ± 0.09 |
| | | 48 | + | 5055 | 13.7 ± 3.3 | 83.5 ± 3.9 | 2.7 ± 0.9 | 0.09±0.05 | 0 |
| | - | 0 | | 1164 | 0 | 100 | 0 | 0 | 0 |
| | | 48 | - | 1070 | 0 | 99.9 | 0.1 | 0 | 0 |
| | | 48 | + | 1160 | 0 | 99.9 | 0.1 | 0 | 0 |
| *ku70Δrhp55Δ* | + | 0 | | 3411 | 1.7 ± 0.3 | 95.2 ± 0.2 | 2.9 ± 0.1 | 0.37 ± 0.12 | 0 |
| | | 48 | - | 4257 | 15.4 ± 0.9 | 46.7 ± 4.1 | 30.2± 2.1 | 7.61 ± 0.69 | 0 |
| | | 48 | + | 4321 | 2.0 ± 0.6 | 93.4 ± 1.3 | 4.1 ± 0.5 | 0.48 ± 0.19 | 0 |
| | - | 0 | | 441 | 0 | 97.7 | 2.3 | 0 | 0 |
| | | 48 | - | 1024 | 0 | 97.0 | 3.0 | 0 | 0 |
| | | 48 | + | 551 | 0 | 94.6 | 5.4 | 0 | 0 |
| *lig4Δrhp55Δ* | + | 0 | | 2395 | 0.11 ± 0.07 | 97.5 ± 0.4 | 2.3 ± 0.3 | 0.07 ± 0.04 | 0 |
| | | 48 | - | 1862 | 3.6 ± 1.3 | 58.8 ± 6.2 | 35.3± 5.7 | 2.27 ± 0.20 | 0 |
| | | 48 | + | 2229 | 0.06 ± 0.06 | 93.4 ± 0.8 | 6.5 ± 0.5 | 0.06 ± 0.06 | 0 |
| | - | 0 | | 466 | 0 | 98.3 | 1.7 | 0 | 0 |
| | | 48 | - | 758 | 0 | 97.2 | 2.8 | 0 | 0 |
| | | 48 | + | 775 | 0 | 97.8 | 2.2 | 0 | 0 |

# Appendix VI. continued.

| | | | | | | | | | |
|---|---|---|---|---|---|---|---|---|---|
| *rhp55Δexo1Δ* | + | 0 | - | 4394 | 0.05 ± 0.05 | 98.9 ± 0.3 | 1.0 ± 0.3 | 0 | 0 |
| | | 48 | | 2693 | 5.8 ± 2.4 | 54.4 ± 7.3 | 38.8 ± 5.8 | 1.02 ± 0.35 | 0 |
| | | 48 | + | 3598 | 0 | 95.5 ± 0.8 | 4.4 ± 0.8 | 0.03 ± 0.03 | 0 |
| | - | 0 | | 439 | 0 | 98.4 | 1.6 | 0 | 0 |
| | | 48 | - | 623 | 0 | 98.4 | 1.6 | 0 | 0 |
| | | 48 | + | 602 | 0 | 96.9 | 3.2 | 0 | 0 |
| *rhp55Δ* + pIRT3 | + | 0 | | 2258 | 0 | 98.6 ± 0.2 | 1.4 ± 0.2 | 0 | 0 |
| | | 48 | - | 1861 | 3.1 ± 1.1 | 46.2 ± 3.5 | 49.6 ± 4.4 | 1.07 ± 0.27 | 0 |
| | | 48 | + | 1869 | 0.4 ± 0.2 | 95.2 ± 0.9 | 4.3 ± 0.8 | 0.06 ± 0.06 | 0 |
| | - | 0 | | | | | | | |
| | | 48 | - | N.D. | N.D. | N.D. | N.D. | N.D. | N.D. |
| | | 48 | + | | | | | | |
| *rhp55Δ* + pIRT3-*rhp51* | + | 0 | | 3655 | 0.4 ± 0.1 | 99.4 ± 0.1 | 0.16 ± 0.01 | 0 | 0 |
| | | 48 | - | 2887 | 12.2 ± 0.2 | 71.5 ± 0.4 | 15.8 ± 0.4 | 0.51 ± 0.09 | 0 |
| | | 48 | + | 3288 | 0.7 ± 0.1 | 98.9 ± 0.1 | 0.39 ± 0.05 | 0 | 0 |
| | - | 0 | | | | | | | |
| | | 48 | - | N.D. | N.D. | N.D. | N.D. | N.D. | N.D. |
| | | 48 | + | | | | | | |

For each genetic background with HO (+), the genetic assay was independently repeated at least three times (with independent isolates), such that >1000 colonies were scored at each timepoint. The average value for each timepoint and the standard errors between the independent experiments are shown. A single strain control with vector only (- HO) was also performed for each background tested. N.D. Not determined.

**Appendix VII. Analysis of break-induced loss of viability in various *rhp55Δ* double mutants.**




Serial 10-fold dilutions of *exo1Δrhp55Δ*, *ku70Δrhp55Δ*, *lig4Δrhp55Δ*, *rad32Δrhp55Δ*, *rad50Δrhp55Δ* and *nbs1Δrhp55Δ* $Ch^{16}$-MGH/MHH strains containing pREP81X-HO, and *rhp55Δ* $Ch^{16}$-MGH cells containing pIRT3/pIRT3-*rhp51* were performed as described in Section 2.5.7.3. None of the mutants tested displayed a significant change in viability with (+T) or without (-T) thiamine.